

Formula SAE Hybrid Carbon Fiber Monocoque/  
Steel Tube Frame Chassis  
for the Cal Poly Formula SAE Team

**CAL POLY** *Racing*  
**FORMULA CHASSIS WORKS**



**Formula Chassis Works**  
**Senior Project**

**Matthew Hagan**  
hagan.matt.r@gmail.com

**John Rappolt**  
john.rappolt@gmail.com

**John Waldrop**  
johnwwaldrop@gmail.com

California Polytechnic State University  
Mechanical Engineering Department  
Advisor: Dr. Joseph D. Mello

Formula Chassis Works would like to extend a special thanks to the following people and companies. Without their contributions, this project would not have been possible. Thank you for believing in us!

**CAL POLY** *Racing*  
**FORMULA SAE**

 **Mechanical  
Engineering**  
CAL POLY

**ZODIAC  
AEROSPACE** 

 **Quatro**  
COMPOSITES™

**Dr. Joseph D. Mello**

**John Fabijanic**

**Simon Rowe**

**ME Student Fee Allocation Committee**

**AERO Student Fee Committee**

**The Waldrop Family**

**Tabak Law**

**Texas Almet**

# Table of Contents

- Executive Summary..... 12
- 1. Introduction ..... 13
  - Problem Statement..... 13
  - Recent Team History..... 13
  - Recent Chassis History ..... 15
  - Team Goals..... 16
  - Project Goals ..... 18
  - Initial Project Direction ..... 18
- 2. Project Management ..... 19
- 3. Formula SAE Rules ..... 22
  - Structures..... 22
  - Front Protection..... 23
  - Templates..... 24
  - Harness ..... 24
  - Miscellaneous ..... 25
- 4. Requirements..... 25
  - Safety ..... 26
    - Impact ..... 27
    - Intrusion..... 29
  - Torsional Stiffness..... 29
  - Miscellaneous ..... 31
- 5. Vehicle Design..... 31
- 6. Full Monocoque Chassis Design and Analysis..... 34
  - Initial Material Selection..... 34
  - Manufacturing Concept ..... 35
  - Geometry and Packaging Development ..... 35
  - Analysis ..... 37
    - Mechanical..... 37
    - Thermal..... 37
  - Issues and Switch to Hybrid Chassis ..... 38
- 7. Hybrid Chassis Design and Analysis ..... 41
  - Loading Sources ..... 41
  - Monocoque..... 42
    - Geometry ..... 42

Laminate Development.....	43
Attachments.....	51
Bond .....	53
Frame and Front Hoop.....	54
Attachments.....	54
Initial Design.....	55
Torsional Stiffness .....	58
Final Construction .....	64
Nose Cone/Impact Attenuator .....	67
8. Laminate Testing and Data Analysis .....	69
Material Properties Testing .....	69
SAE Laminate Testing.....	72
Suspension Attachment/Balsa Core .....	79
Impact Attenuator Testing.....	80
Conclusions .....	83
9. Manufacturing and Vehicle Integration.....	84
Monocoque.....	85
Buck and Mold .....	85
Layup and Cure .....	88
Bond and Lap Joint.....	96
Closeouts.....	99
Inserts.....	100
Fit and Finish .....	101
Frame and Attachments .....	103
Jig .....	103
Bulkhead and Box.....	104
Main Hoop .....	105
Longitudinal Members .....	106
Monocoque Attachment.....	107
Suspension Attachment .....	108
Fit and Finish .....	108
Front Hoop.....	109
Tubing .....	109
Monocoque Attachment.....	110
Cockpit Controls.....	111

Fit and Finish .....	111
Nose Cone/Impact Attenuator .....	112
Buck and Mold .....	112
Layup .....	113
Fit and Finish .....	113
Inserts.....	114
Anti-Intrusion Plate .....	115
Design.....	115
Manufacturing .....	115
Harness Mounting.....	115
Head Rest/Firewall.....	117
Electronics Cover.....	118
Seat .....	119
10. Mass Properties .....	120
11. Vehicle Performance.....	123
Vehicle Testing .....	123
Competition .....	123
12. Budget, Funding, and Sponsorship .....	127
13. Conclusions .....	128
Requirements.....	128
Vehicle.....	129
Components.....	130
Monocoque and Attachments .....	130
Frame .....	132
Nose Cone .....	132
Material Procurement .....	134
Analysis .....	135
Structural Equivalency .....	135
Finite Element Analysis .....	135
Dynamic Loading.....	136
Bolted Connections.....	136
14. Final Recommendations and Future Work .....	137
Appendices.....	138
Appendix A: Section Writers .....	138
Appendix B: Additional Photos .....	141

Appendix C: CLT Script ..... 149  
Appendix D: Cockpit Opening Stiffness Analysis..... 161  
Appendix E: Impact Attenuator Data..... 182  
Appendix F: Accounting ..... 188  
Appendix G: References..... 194

## List of Figures

Figure 1.1 – The 2003 car.....	14
Figure 1.2 – The 2004 car.....	14
Figure 1.3 – The 2006 car utilizing a solid rear axle.....	14
Figure 1.4 – The 2008 car.....	14
Figure 1.5 – The 2009 car.....	15
Figure 1.6 – The 2012 car, utilizing a steel tube frame.....	15
Figure 2.1 – Project flow chart.....	19
Figure 2.2 – Team Gantt chart, incorporating chassis schedule.....	20
Figure 2.3 – Project action log.....	21
Figure 2.4 – Team critical path.....	21
Figure 2.5 – Team tasks.....	22
Figure 3.1 – The “Percy” Template.....	24
Figure 3.2 - Roll hoop line clearances from the 2013 Formula SAE Rules.....	24
Figure 4.1 – A bead seat from Bald Spot Sports.....	27
Figure 4.2 – An OMP harness with a Camlok quick release.....	27
Figure 4.3 - Histogram of speed for a FSAE Autocross course, with speed in ft/s.....	28
Figure 4.4 - System stiffness as a function of chassis stiffness, with ratio to system stiffness with a rigid chassis on the vertical axis and chassis stiffness over roll stiffnesses in series on the horizontal.....	30
Figure 5.1 - Drawings were used in SolidWorks to determine effect of wheelbase on corner geometry.....	32
Figure 5.2 - Lap time as a function of wheelbase.....	32
Figure 5.3 – Hagan in the mock cockpit.....	33
Figure 5.4 – Wally in the mock cockpit.....	33
Figure 5.5 – The developed vehicle layout.....	34
Figure 6.1 – Basic component and SAE template layout in relation to the driver.....	36
Figure 6.2 – Rear chassis geometry to meet suspension attachment points.....	36
Figure 7.1 – The chassis assembly solid model.....	41
Figure 7.2 - 45-degree transformation of shear load on a stress block.....	45
Figure 7.3 - Unrestrained tube with open cross section under torsion. Note the axial deformation in the top view at right.....	45
Figure 7.4 - Tube restrained at one end.....	46
Figure 7.5 - Shear flow in a composite laminate with core.....	46
Figure 7.6 - Laminate regions of the monocoque.....	48
Figure 7.7 - SAE’s monocoque front bulkhead model, from the SES (view is looking down edge of bulkhead).....	51
Figure 7.8 – Tension failure mode.....	51
Figure 7.9 – Shear failure mode.....	51
Figure 7.10 – Line loads associated with failure modes shown above. (source: <a href="http://www.structsource.com">www.structsource.com</a> ).....	52
Figure 7.11 - Lap joint loading model, showing the two sets of lap joint plies and a single part.....	53
Figure 7.12 - Front hoop attachment brackets (gussets not yet incorporated).....	54
Figure 7.13 – Front hoop baking plates.....	54
Figure 7.14 - Main hoop attachment brackets, at 90 degrees to each other.....	54
Figure 7.15 - Main hoop attachment bracket gussets.....	54
Figure 7.16 - Attachment point reactions. Vertical loading at left and lateral loading at right.....	55
Figure 7.17 - Main hoop bracing options in side view.....	56
Figure 7.18 - Options for frame triangulation in side view.....	56
Figure 7.19 - The main hoop geometry.....	56

Figure 7.20 - Shoulder harness bar with gussets. ....	56
Figure 7.21 - Front view of the frame bulkhead. ....	57
Figure 7.22 - Rear rocker and shock mounting at rear of frame. ....	58
Figure 7.23 - The frame structure in SolidWorks. ....	58
Figure 7.24 - Vehicle assembly in Abaqus. ....	59
Figure 7.25 - Frame with rear triangulation options. ....	60
Figure 7.26 - Loads and constraints in finite element model. ....	60
Figure 7.27 - Frame member identifications. ....	61
Figure 7.28 - Deformed shapes from torsional stiffness finite element model. Color graph represents node rotation about the longitudinal axis. ....	62
Figure 7.29 - Frame with chosen rear triangulation. ....	62
Figure 7.30 – Jacking point detail. ....	64
Figure 7.31 – Adjustments made to frame sketch in SolidWorks. ....	64
Figure 7.32 - Bulkhead and box notch detail. ....	65
Figure 7.33 - Notches at upper node of bulkhead with unfinished tube hidden. ....	65
Figure 7.34 – Frame solid model in its final form. ....	65
Figure 7.35 - Rear assembly. ....	66
Figure 7.36 - Front hoop. ....	66
Figure 7.37 - Side section view of the top of the front hoop and monocoque from the SES submission. .	67
Figure 7.38 - Front hoop bracing brackets. ....	67
Figure 7.39 - Side view of nose cone construction, cut from extension of monocoque loft. ....	68
Figure 7.40 - Front view of material removal for mounting fasteners. ....	68
Figure 7.41 - Nose cone solid model. ....	68
Figure 8.1 – ASTM 3518 45 degree tensile test set up. ....	69
Figure 8.2 – Stress strain curve for unidirectional carbon fiber specimen from ASTM 3518 test. ....	70
Figure 8.3 – Stress strain curve for cloth carbon fiber specimen from ASTM 3518 test. ....	70
Figure 8.4 – ASTM 790 flex test setup. ....	71
Figure 8.5 – Test setup picture for SAE three point bend test in accordance to rule T3.31. The rig had a span of 20 inches and could accommodate a specimen up to 8 inches in width. ....	72
Figure 8.6 – Load versus deflection curve for three point bend test piece with core ribbon direction oriented perpendicular to span. ....	73
Figure 8.7 – Initial test piece “S” shape failure due to core shear. ....	73
Figure 8.8 – Load vs. Deflection plot of a specimen of the Side Impact Structure with 8 inch width and 20 inch span. Core ribbon direction was oriented in the span direction. ....	74
Figure 8.9 – Steel tube compliance test setup. ....	75
Figure 8.10 – Load vs. deflection plot of two 1018 steel tubes (1 in diameter, 0.065 in wall) subjected to three point bending over a 20 in span. ....	75
Figure 8.11 – Perimeter shear test setup ....	76
Figure 8.12 – Load versus displacement plot for perimeter shear test, ....	76
Figure 8.13 – Harness attachment point test rig with overall dimensions. ....	77
Figure 8.14 – Harness attachment point test setup. ....	78
Figure 8.15 – Load deflection curve for harness attachment test. ....	78
Figure 8.16 – Drawing of test setup for balsa core testing. ....	79
Figure 8.17 – Load deflection curve of lower suspension attachment test. ....	80
Figure 8.18 – Load versus deflection for the balsa splice, three point bend test. ....	80
Figure 8.19 – Test setup for nosecone quasi-static crush test. ....	81
Figure 8.20 – Load versus displacement curve for quasi-static crush test for nose cone. ....	82



Figure 8.21 – Energy absorbed versus displacement of the impact attenuator during the quasi-static crush test. ....	82
Figure 9.1 - Completed chassis with subsystems installed. ....	84
Figure 9.2 - Completed chassis with subsystems installed. ....	85
Figure 9.3 - A buck covered in guide coat and ready for sanding. ....	86
Figure 9.4 - The buck with the sealer applied and scribe lines scratched into the surface. ....	86
Figure 9.5 - Resin, plaster and chopped fiberglass applied to the buck. ....	86
Figure 9.6 - The main support structure added to the mold. Hemp, plaster and a tubular steel framework. ....	86
Figure 9.7 - The finished mold undergoing a final cleaning before the release agent it applied. ....	87
Figure 9.8 - Machining the front bulkhead plug from the MDF stock on the TM1. ....	87
Figure 9.9 - The completed front bulkhead plug glued into the mold with the silicone fillet applied. ....	87
Figure 9.10 - The experimental “blob” layup that was used to validate the cure cycle and see how the materials behaved while handling them. ....	88
Figure 9.11 - Using fabric store remnants to make patterns for cutting the carbon. ....	89
Figure 9.12 - Using a sharp scribe to clean out the scribe lines in the mold. ....	89
Figure 9.13 - Using high temperature double sided stick tape to place the two inch wide nylon strap for the lap joint step into the molds. ....	89
Figure 9.14 - Placing the first layer of carbon into the first mold. ....	90
Figure 9.15 - The premade front bulkhead skins. ....	91
Figure 9.16 - Installing the front bulkhead sub-assembly. ....	91
Figure 9.17 - The part under vacuum for one of the many debulking periods. ....	91
Figure 9.18 - The completed outer skin after an overnight debulk. ....	91
Figure 9.19 - Placing the film adhesive in the mold before the core goes in. ....	92
Figure 9.20 - Placing the core in the mold. The white seams are film adhesive used to splice sections of core together. ....	92
Figure 9.21 - Placing the end grain balsa inserts in for the lower front suspension mount and the pedal box. ....	92
Figure 9.22 - The layer of film adhesive that was laid on the core in preparation for the inner skin. ....	93
Figure 9.23 - The final layers of the inner skin going into the mold. ....	93
Figure 9.24 - The edge dams that had to be installed to prevent the core from being crushed under vacuum. ....	94
Figure 9.25 - The parts under vacuum and ready for the cure cycle to start. ....	94
Figure 9.26 - The cured part after taking the vacuum bag off. ....	95
Figure 9.27 - The first part to be taken out of the mold. ....	95
Figure 9.28 - The two completed monocoque halves and four happy team members. ....	96
Figure 9.29 - Rough cutting the parts to prepare to bond the two halves together. ....	97
Figure 9.30 - Sanding the mating surfaces flat using a frame table. ....	97
Figure 9.31 - Bonding and clamping the two halves together. ....	97
Figure 9.32 - The top lap joint lay up under vacuum. ....	98
Figure 9.33 - The completed top lap joint. ....	98
Figure 9.34 - The steering shaft cut out on the bottom of the tub. ....	99
Figure 9.35 - Front bulkhead cut out after it was filled with microballoons. ....	99
Figure 9.36 - Making the cockpit opening closeouts. ....	99
Figure 9.37 - The finished cockpit opening closeouts. ....	99
Figure 9.38 – Using a guide to drill a hole in the monocoque. ....	100
Figure 9.39 - Aluminum insert in the monocoque. ....	101

Figure 9.40 - The microballoon and resin surface (in white) and the glazing putty used to fill the pinholes. ....	102
Figure 9.41 - The tub after it had been primed. ....	102
Figure 9.42 - The finished green paint and gold pinstripe. There is a satin finish on the exposed carbon and all of the sponsor stickers have been placed. ....	103
Figure 9.43 - The first layout line on the frame table representing the car centerline. ....	103
Figure 9.44 - Using a frame jig to make and weld the bulkhead together. ....	104
Figure 9.45 - The bulkhead on the mill for final post machining after welding. ....	104
Figure 9.46 - Welding the box in its frame jig. ....	105
Figure 9.47 - Getting ready to bend the main roll hoop. Both the one inch and 1.25 inch tubes can be seen. ....	106
Figure 9.48 - Placing the completed main roll hoop onto the frame table in the correct position. ....	106
Figure 9.49 - Welding in the longitudinal members. The completed rear box can be seen. ....	106
Figure 9.50 - Making the attachment plates to mount the monocoque to the rear frame. ....	107
Figure 9.51 - Using the suspension jig to locate the holes for mounting the front suspension mounts. ....	108
Figure 9.52 - Using the suspension jig to locate the rear suspension mounting tabs. ....	108
Figure 9.53 - Using the tubing bender to bend one half of the front roll hoop. ....	109
Figure 9.54 - The front roll hoop fit into the tub and tack welded into place. ....	110
Figure 9.55 - The fully welded front roll hoop halves and steering mount. ....	110
Figure 9.56 - Showing how the front roll hoop attaches to the sides of the monocoque. There is an equally sized plate on the outside of the tub to spread the load out over a larger area. ....	110
Figure 9.57 - The starter button and kill switch at the side of the front hoop. ....	111
Figure 9.58 - Engine switches in place near the top of the front hoop. ....	111
Figure 9.59 - Front hoop with component mounting brackets. ....	111
Figure 9.60 - The raw high density foam stock the nose buck was machined from. ....	112
Figure 9.61 - The first operation in machining the nose cone buck. ....	112
Figure 9.62 - The two nose cone buck halves getting test fit together. ....	113
Figure 9.63 - Completed nosecone installed on the car. Anti-intrusion plate visible along base of the nosecone. ....	114
Figure 9.64 - Potted insert in front bulkhead. ....	114
Figure 9.65 - The anti-intrusion plate ready to mount to the car. ....	115
Figure 9.66 - Lower monocoque attachment backing plate. ....	116
Figure 9.67 - Solid model of block for lap belt mounting tabs. ....	116
Figure 9.68 - Lap belt mounting tabs being welded in place. ....	116
Figure 9.69 - Completed lap belt mounting brackets. ....	116
Figure 9.70 - Side view of head rest mount construction. ....	117
Figure 9.71 - Edge view of the plane for final shaping of the head rest mount boss. Material was removed to the left as shown. ....	117
Figure 9.72 - Completed solid model of head rest mount. ....	117
Figure 9.73 - Bending the head rest mount. ....	118
Figure 9.74 - Welding the head rest mount. ....	118
Figure 9.75 - Head rest as assembled on the car. ....	118
Figure 9.76 - Electronics cover undergoing cut and fold bend. ....	119
Figure 9.77 - The electronics cover seated in the car. ....	119
Figure 9.78 - Mixing the resin with the beads. ....	120
Figure 9.79 - Working the beads down into the shoulder area. ....	120
Figure 9.80 - The cured bead seat before trimming. ....	120
Figure 11.1 - The car being driven during dynamic testing. ....	123

Figure 11.2 - The Cal Poly Formula SAE Team, Formula Electric team members, and advisor John Fabijanac at FSAE Lincoln..... 124

## List of Tables

Table 1.1 – Cal Poly FSAE’s team leads since 2002.....	15
Table 1.2 - Properties of the Top-10 cars in Autocross at Formula SAE West 2011.....	17
Table 2.1 – Basic project responsibilities.....	19
Table 2.2 - Initial project schedule, working backwards from the team’s “driving car” date.....	20
Table 4.1 – Safety requirements for the chassis subsystem.....	26
Table 4.2 - Crash tests from the 2012 Formula One Technical Regulations.....	27
Table 4.3 – Additional chassis requirements.....	31
Table 7.1 – Material properties used in analysis.....	44
Table 7.2 - Cockpit opening finite element models.....	46
Table 7.3 - Requirements for the laminate regions.....	48
Table 7.4 – Requirement details.....	48
Table 7.5 - Results of laminate analysis, with minimum SES passing margins and loading failure indices (maximum/fiber only).....	50
Table 7.6 – Layups and failure indices for in-plane loading of suspension attachment points.....	52
Table 7.7 – FEA results for torsional stiffness.....	61
Table 7.8 - Sensitivity of torsional stiffness to sizing of various frame members.....	63
Table 8.1 – ASTM 3518 test results.....	70
Table 8.2 – ASTM 790 test results for unidirectional and cloth carbon fiber laminates.....	71
Table 8.3 – Properties used is SES for carbon fiber sandwich material.....	77
Table 10.1 - Mass properties of the 2013 chassis subsystem, in comparison to the 2012 subsystem. ...	120
Table 10.2 - Mass properties of the 2012 chassis subsystem components. Estimated weights are in parentheses, and are +/- 1 lb or +/- 10%, whichever is lower.....	121
Table 10.3 - Mass properties of the 2013 chassis subsystem components. Estimated weights are in parentheses, and are +/- 1 lb or +/- 10%, whichever is lower. “H+BP” stands for “hardware and backing plates”.....	121
Table 10.4 - Relevant vehicle mass properties.....	122
Table 12.1 - Chassis subsystem costs.....	127
Table 12.2 - Project sponsors with their contributions and their approximate values.....	128

## Executive Summary

The Formula SAE Hybrid Carbon Fiber Monocoque/Steel Tube Frame Chassis project was sponsored by the Cal Poly Formula SAE Team in San Luis Obispo, California, and completed by the Formula Chassis Works senior project group in 2013. The team proposed this project in order to design and fabricate a high-performance, safe chassis which would be competitive at the 2013 Formula SAE (FSAE) Lincoln competition, and to document the process so that future teams could more easily design and manufacture a chassis. The 2012 chassis subsystem weighed 143 lbs. This project aimed to reduce the weight of the chassis subsystem to approximately 70 lb while achieving a torsional stiffness of 1700 lb\*ft/degree, and to develop composites analysis and manufacturing techniques in the process.

The team initially considered a full monocoque design utilizing a pre-impregnated carbon-fiber sandwich structure. It was believed that this design would have the best specific stiffness compared to a steel space frame or hybrid front monocoque/steel tube rear frame design. During the design process major issues with engine accessibility, rear component packaging, and engine heat management forced the design to move toward a hybrid design. This decision had little effect on weight through the elimination of some monocoque attachment structures.

The front geometry of the monocoque was carried over to the hybrid design and a rear steel tube space frame was designed to attach to the monocoque. Classical Lamination Theory was used to develop the monocoque layup schedule. The monocoque and frame were modeled in Abaqus for torsional stiffness analysis, and layups, tube geometry, and tube sizing were investigated to achieve maximum specific stiffness. A torsional stiffness of 1725 lb\*ft/deg. was predicted from this investigation.

During the final stages of design, a series of tests were run to make sure the laminates chosen would meet the structural equivalency of a standard steel tube frame as outline in the 2013 FSAE Rules. These tests included a 3-point bend test of the side impact structure, penetration test of the side impact structure, and harness attachment loading test. Additionally, core splice, suspension attachment, and basic material properties tests were performed.

In addition to laminate testing, the custom nose cone/impact attenuator was tested for impact requirements. The team set impact goals greater than those established by SAE, but meeting those goals proved to be difficult so only the SAE requirements were met. During quasi-static testing, the nose cone absorbed 7350 J of energy with average and peak accelerations of 17.0 G and 31.3 G, respectively.

The frame, monocoque, and accessories were then manufactured. The frame was constructed from 4130 steel tubing that was aligned using a custom jig. The front monocoque was made by laying up pre-impregnated carbon fiber into two molds constructed by C&D Zodiac that produced the left and right halves. These halves were bonded using a wet-layup carbon fiber strap joint. The monocoque and frame were aligned and married using the team's suspension alignment tooling.

The completed chassis subsystem weighed 94.5 lb, approximately 50 lb less than the 2012 chassis. This was significantly over the 2013 weight requirement, which was found to be unrealistic. Additionally, many options for potential weight reductions were identified, which could add up to approximately 15 lb. Future work for this project includes validating the torsional stiffness finite element model and exercising the suggestions for saving weight. We believe that with further development of the hybrid chassis solution, a high specific stiffness can be achieved which rivals that of well-designed steel tube chassis while maintaining the intrusion safety benefits of a monocoque structure. Additionally, following SAE's Alternative Frame rules to create a chassis using the knowledge from this project may produce even better results.

# 1. Introduction

## Problem Statement

Cal Poly's Formula SAE Team produces a prototype, formula-style race car for the weekend autocrosser designed, built, and tested by its students. Every year, they take part in a competition with schools from around the world in events centered on design, cost, business, performance, and reliability. In 2013 they will compete in the Formula SAE Lincoln competition, organized by SAE International. The team aims to finish toward the top of the competition using a car which is engineered from the ground up with high attention to integration and detail, and tested to prove designs and reliability. Through good engineering practices and extensive documentation, this year will serve as an example for the team in the future and provide a base on which to iterate and improve.

The car's chassis has been identified as an area of high potential, and need, for improvement. The team competed in 2012 with a heavy, under-developed chassis, which resulted in compromised performance due to a high car weight (450 lb total, with 122 lb in the chassis itself and 143 lb in the entire chassis subsystem) and poor representation of the team's engineering abilities. The Formula Chassis Works senior project group will supply Cal Poly Formula SAE with a chassis subsystem which will help the team to achieve its goals for 2013. This will include the chassis structure, mounting for other subsystems, driver restraints, and impact structures. The chassis and its accessories will meet the team's requirements, comply with SAE's rules for the Formula SAE competitions, and lead advancement of the team's engineering practices. They will also be developed with a mind toward composite materials in the interests of low weight and driver safety. The project will be strengthened by the rigor and accountability inherent of a senior project in the Cal Poly Mechanical Engineering Department, in comparison to completing the project independently as part of the Formula SAE Team.

This endeavor will provide a base for engineering the 2013 car as a whole and documentation for future chassis development. Our process and product will not only serve the team in 2013, but also help to ensure the continued advancement of Cal Poly Formula SAE.

## Recent Team History

The team has been developing cars for Formula SAE competitions since the 1980s. In 2002, the team created Cal Poly's first monocoque using carbon fiber pre-impregnated plies with honeycomb core for the cockpit and attaching a steel tube frame for the rear of the chassis. This base, consisting of a carbon-fiber monocoque, carbon-fiber brake discs, 4-cylinder engine, and independent rear suspension, was also used for the 2003 and 2004 cars, shown in Figures 1.1 and 1.2. During this time the team proved to be competitive as long as things went to plan at the competition.



Figure 1.1 – The 2003 car.



Figure 1.2 – The 2004 car.

After the 2004 car it was determined that the best way to place well in the competition was to produce as lightweight a car as possible. The 2006 car in Figure 1.3 had the carbon-fiber component concepts maintained, but the 4-cylinder engine was replaced with a single-cylinder and independent rear suspension dropped in favor of a solid, live rear axle, similar to a kart but with suspension travel as defined in the SAE rules (defined in order to keep kart-like suspensions from being used). This setup proved successful and was continued into 2008, exhibited in Figure 1.4, with an iteration including tires for carbon-fiber 13” wheels, a fuel-injection system to increase engine power, and front and rear aero devices. Potential wasn’t realized at the competition, and with a large number of experienced members the ground-up lightweight design in Figure 1.5 was produced for 2009. This potential also wasn’t realized, and the car wasn’t able to compete in dynamic events.



Figure 1.3 – The 2006 car utilizing a solid rear axle.



Figure 1.4 – The 2008 car.

Going into 2010 a less-experienced team planned to fulfill the 2009 setup and take an issues-free car to the competition. However, significant damage to the monocoque was discovered, so plans were abandoned. At the same time, a senior project working with the 2008 car concluded that an independent rear suspension could perform as well as a solid-axle setup but with better driveability (Formula SAE Interchangeable Independent Rear Suspension Design, 2009). The team began design on a ground-up car incorporating independent rear suspension for 2011. Well into the design process, the monocoque was abandoned in favor of a full frame due to a lack of composites knowledge within the team, and the realization that previous teams had taken shortcuts with composites which the team wasn’t willing to take again. Design and manufacturing weren’t sufficiently progressed, and at the end of 2011 just a partial frame and some components lay on the table.



Figure 1.5 – The 2009 car.



Figure 1.6 – The 2012 car, utilizing a steel tube frame.

The team was mostly new again for 2012. It was realized that the only way to avoid repeating recent failures was to focus on simply getting a car to the competition, with the sole ambition being to compete in every dynamic event. A new approach was taken with engine tuning in order to increase reliability. The 2011 car was finished, becoming the 2012 car shown in Figure 1.6, and the competition goal was accomplished. With high motivation and experienced team members, it was planned to develop the 2013 car as an iteration of the 2012 car, designed and built from the ground up to allow for good vehicle-level integration. Following the learning from 2012, and incorporation of improved engineering and documentation processes, the 2013 car would provide a base for future teams so little team-member experience would be needed to achieve success.

This has been a brief summary. The names of team leads from this time period are included in Table 1.1, so that they may be contacted in case more information is needed.

Table 1.1 – Cal Poly FSAE’s team leads since 2002.

Year	Team Lead
2002	Adam Brinkman
2003	Brian Wares
2004	David Hu
2006	Jason Schulberg
2008	Aaron Bailey
2009	Matthew Ales
2010	Joshua Roepke
2011	Johnathon Gorski
2012	Matthew Hagan
2013	John Waldrop

### Recent Chassis History

The 2004 chassis was an iteration of 2003’s. Due to a need for driver protection, need for engine serviceability, and existence of a large number of hard points at the rear, a hybrid chassis with a front monocoque and rear frame was continued from 2003. Four plies of unidirectional Toray T700 pre-preg were used with .5” nomex honeycomb core. 4130 chromoly steel was used for the frame and roll hoops. Finite element analysis (FEA) was used to design the monocoque’s laminates.

For 2006, the goal of creating a 300-lb car dominated design. Hard point quantity was reduced, and a front monocoque chosen for its high specific stiffness. A rear tube frame was used for ease of engine

access and main roll hoop integration. It was concluded that a monocoque would be easier to manufacture than a full tube frame once tooling existed, despite the fact that a tube frame was being used as part of the chassis. It was also claimed that a monocoque would absorb approximately 100 times the energy of a steel tube frame in front and side impact. Cytec 5225 3K-70P woven cloth was used with .572" and .460" Nomex honeycomb core, weight 3 lb and cell size 1/8". FEA was used to design the chassis' laminates and geometry, and used to find a torsional stiffness of 1320 lb\*ft/deg. The laminates were quasi-isotropic, with face sheets mostly made up of two plies, and four only in high-stress areas. The total car weight came out to 315 lb, with 16 lb in the tub and 19 lb in the frame (believed to be before inserts and attachments).

The 2008 chassis stuck closely to that of 2006. Manufacturability and accessibility were claimed to be improved. FEA was used to evaluate torsional stiffness as in 2006, but now reasoning was given for the number, with the statement that the chassis must be an order of magnitude stiffer than the suspension in order to make the car sensitive to suspension changes. The weight of the monocoque, with inserts and attachments, was 26 lb. It was claimed that the low weight of the monocoque as compared to a tube frame, saving 15 lb, resulted in 1.5% lower lap times. Materials, laminates, and energy absorption numbers were the same as in 2006. The Structural Equivalency Form (SEF) created in 2006 was modified for submission to SAE.

In 2009 there was a push to improve manufacturability of the car as a whole. The hybrid chassis concept was chosen after a comparison with a full monocoque and full tube frame (same weight and lap time numbers from 2008 were claimed). It was decided that a monocoque was as manufacturable as a tube frame due to its greater familiarity, although the team was familiar with tube frames (rear frames) as well as monocoques from previous cars. Front roll hoop weight was decreased, as it was designed to be fully enclosed by the monocoque for the first time. Insert weight was decreased by a claimed 7 lb, due to a change from steel to plastic. It was claimed that the frame was lighter and more accessible than in 2008. The monocoque geometry was significantly different from that of the previous two versions, due to the introduction of strict template rules (for further information, see the Templates section). Unlike with previous monocoques, this one was given a horizontal split such that all suspension points could be located on a single part, with bonding not interfering with location. The same materials and laminates were used as in 2006 and 2008, and the SEF was modified again for submission. When the chassis was being considered for use in 2010, delamination was discovered and frame and pedal assembly mounting positions, pointing toward poor face sheet bonding.

The 2012 chassis, conceptualized in 2011, was originally going to be an improvement of its predecessor. However, it was discovered that beyond copying the previous year's SEF, much composites knowledge was necessary to perform analysis. This knowledge didn't exist within the team, and designs were changed to accommodate a full steel tube frame. Total weight (including the chassis and all its accessories) came out to 145 lb. It was decided to focus efforts on incorporation of composites so the team could return to a lightweight chassis for 2013.

To summarize, past monocoques showed great potential for low weight, but other reasoning behind them exhibited poor consistency, lacked evidence, and was sometimes misleading or wrong.

## Team Goals

The over-arching goal for 2013 was to set a new standard for the team and ensure consistent success in the future. A large number of members were returning with much experience from 2012, and they were highly motivated following the year's success. Everyone recognized that a combination of inconsistency year-to-year, poor knowledge transfer, and poor engineering practices were largely to blame for past



teams' failures, and they were willing to do the work required to continue the team's new start and convert it into long-term success. Very few compromises would be afforded throughout the recruitment, design, manufacturing, and testing processes in order for 2013 to be a lesson to future teams in Formula SAE team operation. The idea that future teams would look back to us as a model was ever-present in our minds. Good documentation would be the key to fulfilling this goal.

The team aimed for a Top-10 finish at the Formula SAE Lincoln competition, to be achieved with a high-performance car (i.e. low weight, high power). Analysis of previous competition results from Table 1.2 was performed to determine the car properties (weight and power) required to achieve this goal. Autocross Event results were decided to be the most relevant, due to complex factors affecting results in events such as Endurance and Design. Each value in the table was obtained using the best method possible, including referencing the Event Program and teams' websites. Engine powers were estimated based on engine package, if not specified explicitly.

**Table 1.2 - Properties of the Top-10 cars in Autocross at Formula SAE West 2011.**

<b>Pos.</b>	<b>School</b>	<b>Weight, with driver (lb)</b>	<b>Weight, car only (lb)</b>	<b>Power (hp)</b>	<b>Weight/power, w/ driver (lb/hp)</b>
1	Oregon State Univ	495	345	50	9.9
2	Univ of Kansas - Lawrence			90	
3	Univ of Maryland - College Park	625	475	90	6.9
4	Ecole De Technologie Superieure	470	320	50	9.4
5	Missouri University of Science and Tech	590	440	90	6.6
6	Univ of Oklahoma	490	340	65	7.5
7	Univ of Wisconsin - Madison	492	342	70	7.0
8	Univ of Illinois - Urbana Champaign	630	480	90	7.0
9	Univ of New Mexico	590	440	55	10.7
10	Univ of Washington	570	420	89	6.4

The team expected to achieve 65 hp with the 2013 engine package. With an average weight/power value of 7.8 lb/hp between these teams, the car weight would need to be around 360 lb. Schools with similar engine power (Oklahoma and Wisconsin) were around 340 lb. From this information, the team aimed for a 350-lb car with 65 hp to achieve a Top-10 finish.

A lap simulator was created to evaluate further decisions based on Autocross Event lap time, which gave a good overall performance indication and was directly relevant to Autocross and Endurance. Conceptual development was focused on the chassis and engine, which would give the greatest improvements from 2012 in the context of meeting these numbers. Appropriate concepts were carried over from 2012, including the tires (Hoosiers for 13" wheels), suspension geometry, brake rotor type (ductile iron), and differential type (Torsen T1).

Following the 2012 experience, high testing time was identified as a necessity in meeting the goal of finishing in the Top 10. Testing lasted 7 weeks in 2012, and gave just enough time to work through the major problems, so an ideal 15 weeks of testing time was used to determine the car's schedule - time to work out problems, prepare the car, and train the drivers. To accommodate this schedule, conceptualization and early design began 15 months before the 2013 competition.

Driver protection against impact and intrusion was chosen as a focal point. The team wanted to show the competition officials that we went beyond the minimum requirements in the name of safety, which would be valuable to the weekend autocrosser. The safety of the teams' drivers was also a concern, largely due to poor testing venues. In addition to being sensible, the goal of high safety was used to support a monocoque chassis, which we desired to create.

When possible, the car was designed around 50 hours of life, which would give a safe margin on 2 years of running. This would allow the 2014 team to confidently take the 2013 car to the Michigan competition if they suffered resource restriction, foreseen to be lack of experience due to many team members graduating or moving on at the end of 2013.

## **Project Goals**

In addition to the team's goals, we set a goal to do more with this chassis project than simply create something to be used for the 2013 car. Given the team's inconsistent history, of the team as a whole and the chassis specifically, we saw a need to develop the team's vehicle design process and composites knowledge, and produce documentation to be passed down to future team members.

With the team's main leaders in our project group, and the responsibility of the broad subsystem which is the chassis, we aimed to set a high standard for engineering design within the team. This would extend from vehicle-level design and integration to detailed component design, including problem development, mechanical analysis techniques, and manufacturing planning.

The aerospace and automotive industries, as well as other Formula SAE teams, have increasingly incorporated composite structures into their products. Fiber composites specifically, consisting of a fiber reinforcement in a resin matrix, have been shown to achieve very high specific strengths and stiffnesses as compared to metal structures. These materials are only increasing in usage and are still being developed for better performance and wider application. Bringing knowledge of these materials and their processes to our team would allow current and future team members to better evaluate material choices for the chassis and other subsystems, and gain exposure to engineering processes which would make them better prepared for their roles in industry.

This report will serve as documentation to help in continuing improvement of the team's engineering practices and ensuring that our project can be used as a reference for the future. For the chassis subsystem specifically, future team members will be able to investigate our process and recommendations, and decide whether to continue our work or use it as evidence to support another direction.

## **Initial Project Direction**

At the beginning of the project we identified our options for chassis type as being steel tube frame, full monocoque, and hybrid (front monocoque with rear steel tube frame). These were the general types of chassis we were familiar with from our team and others.

During development of the overall vehicle design we decided to proceed with a full carbon-fiber monocoque chassis. The information at hand suggested that a monocoque chassis would have higher specific strength and stiffness (lower weight) and provide better driver protection than a steel tube frame. It would also satisfy our goal of improving the team's composites knowledge. We concluded that its disadvantages as compared to a steel tube frame, being longer and more expensive manufacturing, less flexibility during manufacturing, and lower serviceability, would be accounted for by our planning and approach. An estimated chassis manufacturing schedule fit into the team's schedule, we had begun

speaking with sponsors for molds and materials, and our systematic and early start to design would allow us to better plan integration with the rest of the car’s subsystems. Additionally, a full monocoque would require no tube frame construction and no bodywork separate from the chassis’ structure. A full monocoque was chosen over a hybrid largely in order to capitalize on the weight-savings potential we saw in composites over steel tubes, and to introduce a new type of chassis to the team.

This decision was made early in the design process to allow us to focus our efforts. With the time required to develop the full monocoque design, we did not want to spend time generating alternative hybrid and steel tube frame designs which we were confident would prove to be inferior. However, the direction of the project was eventually changed in favor of a hybrid chassis. This transition is discussed in the Issues and Switch to Hybrid Chassis section.

## 2. Project Management

We began the project by performing research and setting requirements. As these actions developed, we created the flow chart in Figure 2.1 to help us schedule the remainder of the project and assign duties. We used this to identify the areas requiring responsibility, and assigned them in Table 2.1.

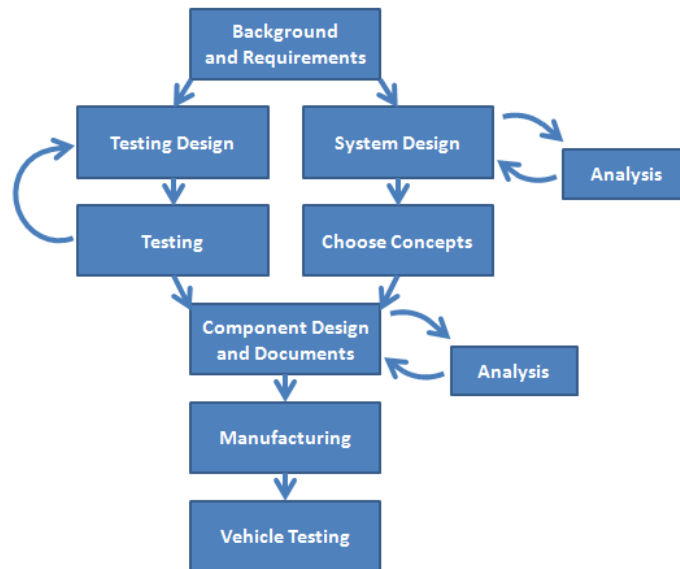


Figure 2.1 – Project flow chart.

Table 2.1 – Basic project responsibilities.

Project Member	Responsibilities
Nick Henderson	Design
John Waldrop	Analysis, Documentation
John Rappolt	Testing
Matt Hagan	Manufacturing

Additionally, an initial schedule was crafted in Table 2.2. This schedule was incorporated into the team’s Gantt chart, made using Microsoft Project and displayed in Figure 2.2. This chart served as an initial plan for the team, and was presented at the team’s CDR in October 2012. A dynamic, wall-mounted schedule

was created for the team to help communicate the Gantt chart. However, neither the Gantt chart nor its physical representation proved to be useful once the team’s pace picked up and design and manufacturing increased in complexity.

**Table 2.2** - Initial project schedule, working backwards from the team’s “driving car” date.

Dates	Work to be completed
Feb. 28, 2013	By this date: driving car
Feb. 17 – 28	Car assembly
Feb. 10 – 17	Static chassis testing
Jan. 21 – Feb. 10	Monocoque fit and finish
Jan. 18 – 21	Monocoque layup
Jan. 14 – 18	Monocoque mold prep
Dec. 8 – Jan. 13	Monocoque tooling
Dec. 8, 2012	By this date: analysis, testing, shape
Summer	Testing plan

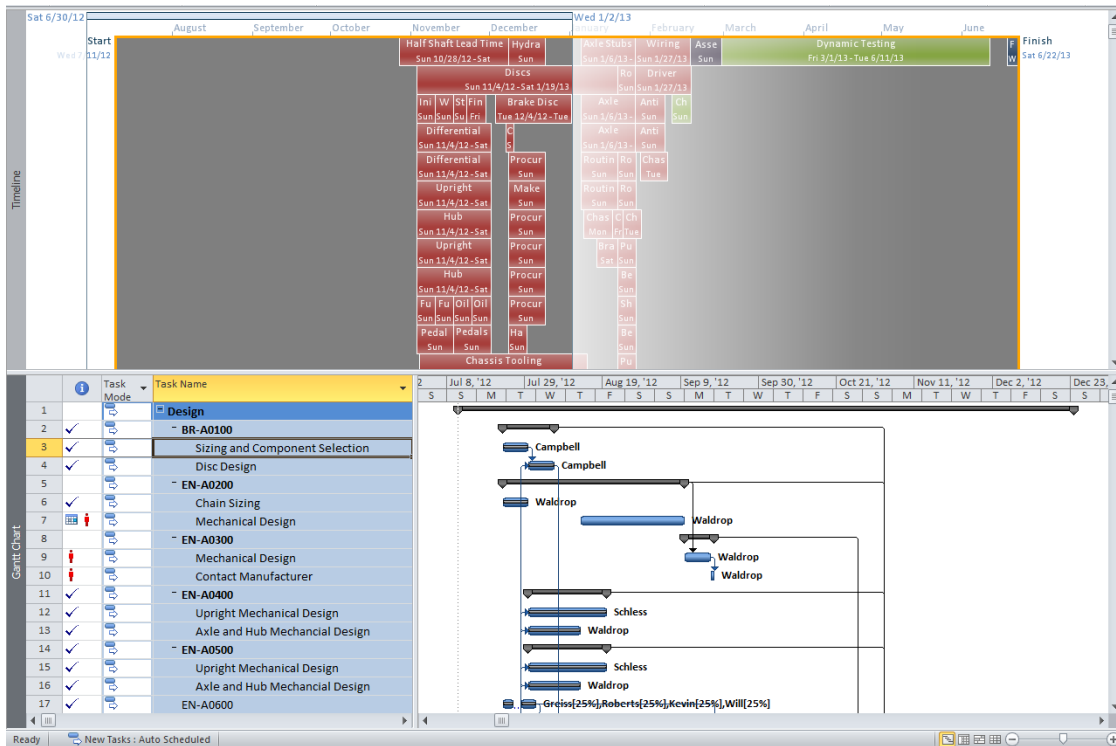


**Figure 2.2** – Team Gantt chart, incorporating chassis schedule.

As the chassis project advanced, we developed an action log in Microsoft Excel which kept track of tasks and their progress, shown in Figure 2.3. This was used in Fall 2012 as ideas were developed and varied investigations were required, but was abandoned as the project gained direction and intensity.

Number	Date the action was Planned	Action (What)	Comments (How)	Accountability (Who)	Begin Date (Planned)	End Date (Planned)	Begin Date (Actual)	End Date (Actual)	Status
6	06-Nov-12	Nose Cone manufacture	Design tooling for shop bot, obtain tooling material, cut mold, finish mold, make several design concepts to test	Matt Hagan	6-Nov-12	19-Nov-12			In progress
7	06-Nov-12	Sidepod attachment	Determine how sidepods mount to chassis, model in CAD, strength calcs.	Nick Henderson	6-Nov-12	15-Nov-12			In progress
8	06-Nov-12	Sidepod manufacture	Design tooling for shop bot, obtain tooling material, cut mold, finish mold, layup and cure	Matt Hagan	6-Nov-12	19-Nov-12			In progress
9	06-Nov-12	Test layups	Make layups for testing. Short beam shear test, side impact structure test, penetration test, suspension pickup test.	John Rappolt	8-Nov-12	12-Nov-12	9-Nov-12		Completed
10	06-Nov-12	Global Layup	Determine the overall global layup in the front, middle, and rear section of the chassis. Use FEA to determine if layup meets stiffness requirements of chassis	John Waldrop	6-Nov-12	9-Nov-12	6-Nov-12	17-Nov-12	Completed
11	06-Nov-12	Suspension Reinforcement/Inserts	Design local layup to accommodate suspension loads. Account for all failure modes. FOS between 2-3	John Rappolt	6-Nov-12	8-Nov-12	6-Nov-12	7-Nov-12	Completed
12	06-Nov-12	Civil Engineering Department Instron Usage	Contact civil engineering department regarding use of their heavy duty instron test machine for nosecone quasi-static testing	Matt Hagan	6-Nov-12	16-Nov-12		4-Jan-13	To be started
13	06-Nov-12	Chassis Mock Up	Manufacture chassis mock up from wood and cardboard. Determine access panel locations, serviceability issues. Allow subteams to plumb and wire as necessary.	John Rappolt	10-Nov-12	17-Nov-12			Cancelled
14	06-Nov-12	Review Date set up	Set up design review date	John Waldrop	6-Nov-12	6-Nov-12	6-Nov-12	6-Nov-12	Completed

Figure 2.3 – Project action log.

The critical path schedule in Figure 2.4 was created in Google Docs toward the middle of the team’s manufacturing phase. This allowed for easy visualization of tasks and projects, which was especially useful for the chassis subsystem given its high quantity of tasks and their interactions.

A	B	C	D	E	F	G	H	I	J	K	L
Tub after layup	Flange inserts	Design	Obtain	Manual lathe	Pot-known-inserts						
	Sleeve inserts	Determine lengths	Manual lathe								
	Tub halves	Tub - Trim	Drill-holes	Sand			Lay up lap joint	Glue bulkhead		Drill holes in bulkhead and nose cones	Pot inserts
	Resin	Obtain									
	Lap joint	Design									
	Front bulkhead	Develop nose attachment	Design	Manufacture							
	Nose cone		Finalize laminate								
	Nose cone buck	Tub halves - CNC mill						Lay up/cure nose cones			
	Nose cone mold	Design	Lay up mold	Cure							
	Impact attenuator	Develop test plan							Test	Submit IA Data	
	Side pod structure	Develop-test-plan	Lay up	Cure	Test						
	Frame and roll hoops	Side pod skin	Design				Lay up/cure structure	Glue, tub - Glue structure	Paint	Attach skin	
Side pod bucks		CNC mill bucks	Lay up molds	Cure							
Side pod molds		Design					Lay up/cure skin				
Side pod skin attachment		Design									
Frame connection tabs		Cut sheet			Suspension jig, tub - Form and weld tabs	Drill holes in tub	Pot inserts				
Frame		Notch tubes		Weld frame							
Seats		Tub - Set seats	Bend bar	Weld bar		Powdercoat frame					
Shoulder harness bar		Tub - Cut									
Front roll hoop	Bend/weld			Drill holes	Pot inserts						
Front roll hoop tabs	Cut sheet	Tub - form and weld tabs		Powdercoat							
Harness brackets	Seats - Cut sheet	Weld brackets	Drill holes	Pot-inserts							
Head rest/firewall	Design	Obtain	Manufacture								

Figure 2.4 – Team critical path.

During the testing phase, the schedule was changed to a simple task list, exhibited in Figure 2.5. This allowed the team to keep track of tasks despite their variety and spontaneity of occurrence.

## Chassis

- Install rub strips
- Prepare tub for transponder mounting - TECH
- Modify seat for Endurance drivers
- Sand tub
- Enlarge wire harness hole in head rest
- Manufacture, test, and mount nose cones - TECH
- Write your god-damn report
- Trim belts
- Drill drain holes in tub for water
- Paint tub
- Manufacture radiator mounts
- Apply resin to nose cones
- Scotch-brite head rest
- Install harder material for frame protection from chain
- Paint backing plates
- Manufacture new chain guard front mount
- Manufacture new chain guard, mount with 1/4-inch bolts - TECH
- Fix hole for one front hoop bolt
- Paint front hoop
- Paint frame (jacking bar must be orange) - TECH
- Check Percy angle and determine whether changes to harness are required
- Weld front hoop gussets - TECH
- Sort out nose hitting a cone on track
- Trim main hoop down tubes
- Install temperature stickers

Figure 2.5 – Team tasks.

Maintaining a dynamic scheduling method throughout the year, for the team and specifically for our project, allowed us to maximize productivity by adapting to the situation at hand. Once a certain scheduling method was no longer viable, it was ditched in favor of a more appropriate one.

In order to keep to the schedule, team meetings were held often. The team held general meetings once a week for the purpose of updating the entire team and retaining new members, but stopped these meetings once things got really busy in March 2013. Meetings were held weekly among the team's leads as well, which covered more detailed technical information. In Fall 2012, the meetings were structured as workshops during which the leads worked on design in a single location. This format accommodated easy information transfer while design mostly involved integration between subsystems, and kept everyone on the same page. These meetings were especially important for the chassis subsystem, which had to connect and package all the other subsystems. Once design was sufficiently progressed and manufacturing begun, meetings were shortened and consisted of giving updates and discussing logistics regarding design and manufacturing. Around March 2013 these meetings became unnecessary due to the high frequency of communication between leads during many long nights in the machine shop.

Chassis meetings were held weekly with our faculty advisor, Dr. Joseph Mello, during Fall 2012 as design options were being investigated. They were then held during Winter 2013 only as manufacturing issues or concerns arose. Since the project group members often communicated and worked together, these meetings were mainly for the purpose of updating Dr. Mello and obtaining his input when assistance was required in developing discussions.

### 3. Formula SAE Rules

The following section is a summary of SAE's 2013 Formula SAE Rules (the rules), in the context of the chassis subsystem. It should only be treated as an introduction to the rules, and doesn't make up for reading the rule book and tech inspection sheet.

#### Structures

The structural rules found in Part T Article 3 of the rules are intended to govern vehicle safety. Their purpose is to guide the creation of a safe vehicle in a way which is easy for teams to follow and requires

minimal student analysis. This also makes evaluation easy for officials at the competition. The structural rules can be considered as three distinct sections: steel tube frame, monocoque, and alternate frame.

The rules regarding steel tube frames define tubing geometry and sizing. The foundations of the primary structure are the Main Hoop and Front Hoop, which are located by the driver's head and legs, respectively. These have cross sections of 1"x.095" and are designed to protect the driver in roll-over. These hoops are connected on both sides by the Side Impact Structure, consisting of three 1"x.065" tubes. The lower tube connects the lower-most points of the hoops, while the upper tube connects the hoops within a window 11.8-13.8" above the ground. The third tube provides triangulation. At the front of the car is the Bulkhead, forward of the driver's feet and other objects and constructed of 1"x.065" tubing. The Front Bulkhead Support runs on both sides from the Bulkhead back to the Front Hoop; one 1"x.049" tube connects the lower points, the second connects the top of the Bulkhead to within 2" of the top of the Front Hoop, and the third triangulates. The Front Hoop Bracing consists of two 1x.065" tubes which run forward from within 2" of the top of the front hoop to the Bulkhead or other structure forward of the driver's feet. The Main Hoop Bracing is made of two 1"x.065" tubes which extend down from within 6" of the top of the Main Hoop, making no less than a 30-degree angle with the hoop. They can go forward or rearward, depending on main hoop geometry. Connecting from the lower end of the Main Hoop Bracing on both sides is the Main Hoop Bracing Support. This consists of two 1"x.049" tubes, one which connects to the bottom of the Main Hoop and another which connects to the Main Hoop at the upper tube of the Side Impact Structure. Finally, the Shoulder Harness Mounting Bar must be of 1"x.095" tubing and span across the Main Hoop. It is allowed to be bent if calculations are shown and proper gusseting is used. The Structural Equivalency Spreadsheet (SES) must be submitted to SAE to prove that all of these requirements are met.

The monocoque rules (T3.28 through T3.41) are intended to allow for easy incorporation of laminate structures into the frame. All structures except for the Main Hoop, Front Hoop, and Main Hoop Bracing are allowed to be constructed of a laminate. These structures must meet the same requirements as their steel-tube counterparts, through proving equivalency in the beam properties of stiffness, yield strength, tensile strength, maximum load at mid-span, maximum deflection, and energy absorbed up to failure. These requirements are met through simply-supported beam calculations in the SES. Additionally, there are intrusion requirements for the Side Impact Structure and Front Bulkhead Support. The design process in the context of laminate structures will be detailed in the Laminate Development section. Monocoque attachments to other parts of the primary structure must incorporate brackets and backing plates of sufficient shear perimeter, as verified in the SES, and be fastened with at least two 5/16" Grade 5 fasteners or equivalent (T3.40.3).

Finally, the structural rules for steel tube frames and monocoques as defined in Part T Article 3 may be foregone for an alternate frame. This option allows teams to take an alternative to the simple definitions and create a frame with unique geometry and materials, proven to be structurally sound through use of FEA. Due to the conservative nature of SAE's structural rules for the sake of simplicity, it is possible to achieve a lighter frame by this way. The free-form nature of this option requires close communication with SAE throughout the design process.

## Front Protection

An Anti-Intrusion Plate (AI plate) must be attached to the front bulkhead, either welded or fastened as specified in T3.21.5. The material must meet the perimeter shear strength of .060" steel. In front impact, the AI Plate must not permanent deform more than 1" (T3.22.9).

For front impact protection, an Impact Attenuator (IA) must be attached to either the Bulkhead or AI plate (if sufficiently supported, as referenced in T3.22.9). The IA must be proven to meet deceleration and energy absorption requirements as specified in T3.22.1. This requires testing and submission of a report to SAE. Another option is to purchase the standard foam-block IA from SAE, which requires no testing. Either way, SAE accepts four 5/16" Grade 5 bolts in the axial orientation as a simple fastening solution.

## Templates

There are two requirements which define cockpit size. These both involve templates of a specified cross section defined in T4.1 and T4.2. One must pass through the cockpit opening to a specified height from the ground, while the other must pass through the cockpit from the Front Hoop to the pedals. These templates ensure that the cockpit can fit a 95th-percentile male.

One more template rule involves "Percy". Percy is a set of circles shown in Figure 3.1, connected by rods representing a 95th-percentile male's heads, shoulders, and hips. The hips are placed a specified distance from the pedals, as described in T3.10.4, and the head is checked for at least 2" of clearance to lines from Main Hoop to Front Hoop and Main Hoop to Main Hoop Bracing, as shown in Figure 3.2. This same requirement applies to the team's drivers. Additionally, Percy's back angle in this position defines whether the car's driver position is "reclined" or not (to affect harness options).

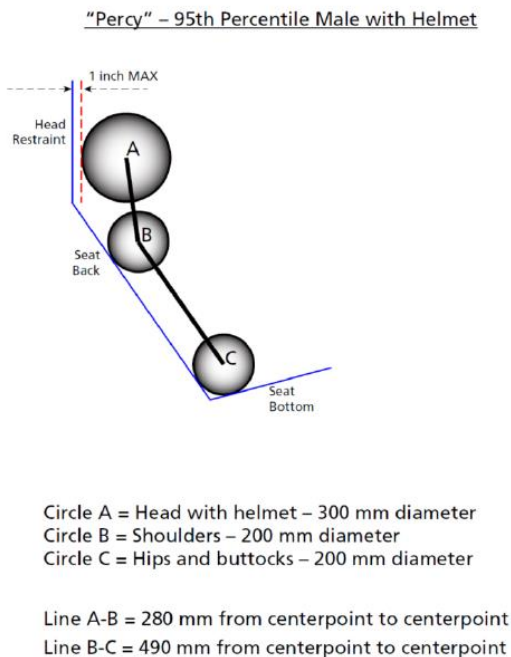


Figure 3.1 – The "Percy" Template

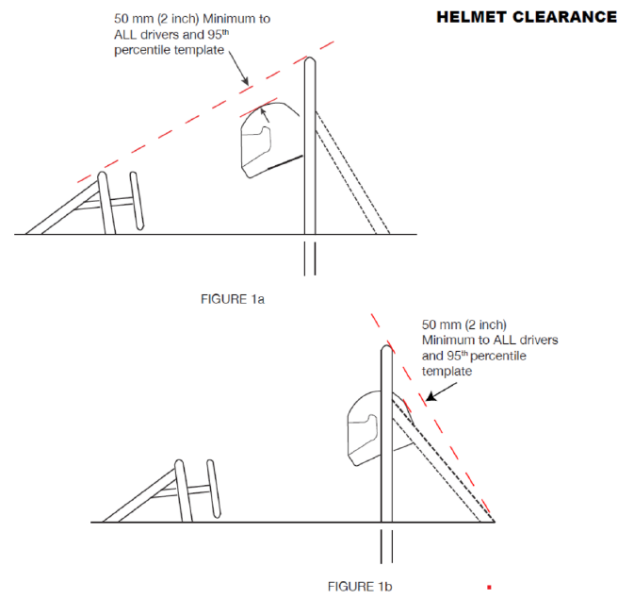


Figure 3.2 - Roll hoop line clearances from the 2013 Formula SAE Rules.

## Harness

Harness rules are defined in T5.1 through T5.5. For every car, the shoulder belts must be mounted to the Shoulder Harness Mounting Bar or equivalent structure, spaced apart a specified distance. All harnesses must have two shoulder belts and two lap belts, both with quick adjusters and 3"-wide belts; this restriction greatly limits harness options. These belts must attach to a quick-release buckle. If the car's driver position isn't reclined, a 5-, 6-, or 7-point harness may be used. This is a difference between 1, 2,



and 3 anti-submarine (anti-sub) belts of 2" width connecting to the quick-release. Typically, these are mounted to the floor through the driver's groin and around the legs. If the driver position is reclined, a 6- or 7-point harness must be used, and the anti-sub belts must have quick adjusters or there must be two sets of anti-sub belts.

For 6-point harnesses, the anti-sub belts may be mounted to the lap belt points, essentially creating a 4-point harness with anti-sub belts. Harnesses mounted to monocoques (tabs not welded to frame) have slightly more stringent rules. The lap belt points must be shown to support a certain load through testing, per SES. There is a lower load, which is the minimum requirement and does not allow mounting anti-sub belts to the lap belt points. If a higher load is met, the anti-sub belts may be mounted to the same points. There are no requirements for 6-point anti-sub mounting beyond a simple spacing rule and this monocoque-specific rule.

There are belt orientation requirements for the team's range of drivers; these angles are difficult to plan for and measure, and are mainly provided as guidelines. Finally, all pins for belt connections when a belt buckle is present (typically only used for lap and anti-sub belts) must be 5/16" Grade 5 fasteners or equivalent, mounted in a way which allows the belt buckle to pivot to be in line with the belt when a driver is strapped in. This typically requires double-shear mounting, with two tabs spaced sufficiently apart. These tabs must be of .063" steel for lap belts.

### Miscellaneous

The driver must be protected by heat transfer from the engine area (T4.3.2). This requires spacing of hot components from the seat back, and use of insulation and radiation shielding. Additionally, there must be a firewall between the driver and the fuel, oil, and cooling systems, which seals the cockpit from the engine area and prevents line-of-sight to the driver's body from any of these systems (T4.5).

A head restraint (head rest) must support the back of the driver's head in order to protect against rear impact (T5.6). It must be made of 2"-thick foam padding and be of certain dimensions, depending on whether its position is adjustable. The point of the helmet which contacts the head rest must be at least 2" away from the edge of the head rest for all drivers. The head rest mounting must be able to support a 200-lb load in the rearward direction, but there is no proof of this required. Additionally, roll bar padding must be used on the Main Hoop to prevent hard contact with the driver's head.

The driver must be able to egress from their belted-in driving position within 5 seconds in the case of an emergency (T4.8). The driver must begin with hands on the steering wheel and actuate the kill switch before unbuckling.

Bodywork is required for the car, and must cover the entire chassis forward of the Main Hoop, except for the cockpit opening. There is no material requirement for the bodywork – it must simply provide a physical barrier between the driver and the environment.

A jacking point must be provided at the rear of the car to allow quick-jacks to be used (T6.6). This is a tube which supports the car's weight during jacking, and can be integrated in a variety of ways into the rear of the chassis.

## 4. Requirements

Requirements were used to guide the design of the chassis in addition to the rules. The team also defined requirements for the car's other subsystems, which provided vehicle-level oversight and

ensured that designs were kept in line with the big picture. Chassis requirements were determined as a part of the project instead of being defined beforehand.

A number of requirements were set for the whole vehicle which were relevant to the chassis. Weight distribution was required to be between 45 and 48% front, and CG height was required to be no higher than 10" with a 6'-tall driver; these values were decided using the team's lap simulator. When possible, systems and components were to be designed for a safety factor of 1.5-1.8 on 50 hours of life. Structural components would be fastened with aircraft-grade (AN) fasteners to ensure reliability, with locking mechanisms such as nyloc nuts, jet nuts, or safety wire.

## Safety

Driver safety was a large concern for the team. While the SAE rules were meant to cover this subject, we examined them for omissions and shortcomings. This allowed us to develop a set of safety requirements to supplement the rule book. These requirements are shown in Table 4.1, and are developed throughout this section.

Table 4.1 – Safety requirements for the chassis subsystem.

Description	Requirement
Front impact average acceleration for 35-ft/s impact with rigid structure	20 G, maximum
Front impact peak acceleration for 35-ft/s impact with rigid structure	40 G, maximum
Front impact of 35 ft/s energy absorption	13 kJ, minimum
Side impact average acceleration for 25-ft/s impact with rigid structure	20 G, maximum
Side impact peak acceleration for 25-ft/s impact with rigid structure	40 G, maximum
Side impact of 25 ft/s energy absorption	7 kJ, minimum
Penetration load for sides of primary structure for intruding device of 1" diameter	1700 lb, minimum
Penetration load for 3.5" diameter surrounding front upper suspension points for intruding device of 1" diameter	3500 lb, minimum
Intrusion protection	Entire primary structure, fuel tank, cockpit from engine
Height of side of primary structure at cockpit opening	Driver's shoulder height, minimum
Location of driver's ankles	At or behind forward-most point of front wheels
Seat type	Bead seat, 1" thickness at spine
Harness quick release type	Camlok

It was determined that a couple of subjects were missing from the rules. First was the position of the driver. Beyond the location of the front bulkhead and implications of the roll hoop rules, there is no specification for locating the driver in the car. Longitudinally speaking, the driver can be anywhere relative to the car's axles. It is important to provide as much energy-absorbing material as possible ahead of the driver in the case of an accident. For Formula 1 (F1), the governing body (FIA) requires the

front axle centerline to be ahead of the driver’s feet, such that the car’s suspension may assist in absorbing energy in impact. For a Formula SAE car, the wheelbase is so short that this requirement is unreasonable while maintaining an acceptable weight distribution. As a compromise, we required the forward-most point of the front wheels to be ahead of the driver’s ankles, which still ensures that an impactor must go through the front suspension before harming the driver.

The second subject missing was seat type. While the rules cover the harness which protects in front impact, there is nothing which protects the driver from acceleration in rear impact. We chose to require the use of a bead seat, which is made of many foam beads cured with resin into a shape as exemplified in Figure 4.1. In impact, these beads deform and absorb energy. This type of seat is used in Formula 1 and IndyCar. It is recommended to maintain 1” of seat thickness along the spine for sufficient protection. The seat can also provide good side support, and is easy to manufacture since the only tooling required is the chassis and driver.

Additionally, we decided to use a harness with a Camlok quick release for quick driver egress, like the one in Figure 4.2.



Figure 4.1 – A bead seat from Bald Spot Sports.



Figure 4.2 – An OMP harness with a Camlok quick release.

## Impact

SAE considers a single impact scenario in its rules. This is a head-on front impact with a rigid structure, with the car traveling at 23 ft/s (16 mph). Under this scenario, the IA must absorb the car’s kinetic energy and keep average acceleration under 20 G and peak acceleration under 40 G.

We developed possible impact scenarios, suspecting that more than just front impact would matter and that the impact speed defined by SAE would be too low. The safety regulations for F1 were investigated, considering their high development in the last two decades and their race-proven success. The 2012 Formula One Technical Regulations required the crash tests in Table 4.2 to be conducted, with the car at full weight and impacting a rigid structure:

Table 4.2 - Crash tests from the 2012 Formula One Technical Regulations.

Impact	Speed
Front	15 m/s (34 mph)
Side	10 m/s (22 mph)
Rear	11 m/s (25 mph)

F1 circuits see average speeds of 100 to 150 mph and peak speeds of around 200 mph, so these numbers were surprisingly low. This highlighted a number of things regarding impacts in F1. First, cars typically slow before an impact occurs, due to driver action and features such as gravel traps. Second, impacts are most likely to occur with a non-rigid structure such as a tire barrier or another car. Third, a head-on impact is less likely to occur than an impact at some amount of angle. Finally, since a front impact likely doesn't involve the car sliding or spinning, its speed is higher than a side or rear impact. All these notes but the second directly apply to Formula SAE; this is because in our parking-lot testing venue, impacts are likely to occur with a rigid structure such as a light post or large vehicle. As a result, our "baseline" speed wouldn't be reduced for testing with a rigid structure, as F1's speeds were. In determining our baseline speed, we considered the speeds encountered on-track. A histogram of speed from our lap simulator in Figure 4.3 showed that approximately 75% of time on-track is spent under the 50 ft/s (34 mph) mark. This mark would be our baseline. Considering an impact at a 45-degree angle to be likely, this speed was adjusted to 35 ft/s (24 mph). Therefore, our front impact speed was set to 35 ft/s and our side impact speed to 25 ft/s (17 mph), scaled similarly to F1's speeds. Ensuring safety in these conditions would give high confidence of driver safety in general. Rear impact was ignored; the driver receives support in rear impact from the seat and head rest, and there is significant structure between the driver and the impactor to absorb energy.

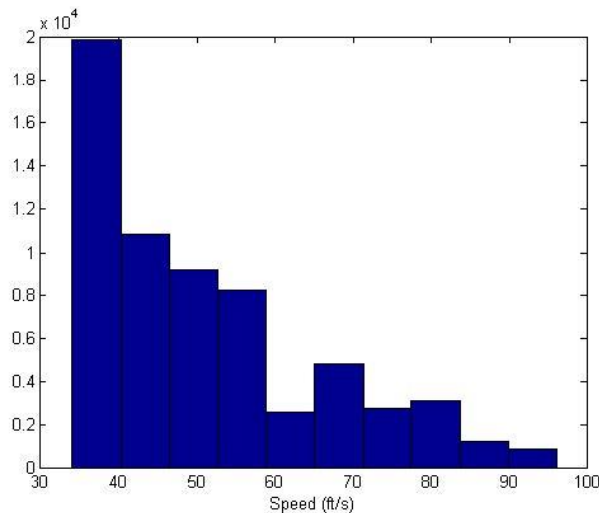


Figure 4.3 - Histogram of speed for a FSAE Autocross course, with speed in ft/s.

We also investigated impact accelerations. SAE requires accelerations in its front-impact scenario to be under 20 G average and 40 G peak; it was questioned whether these values were sufficient. The work of the U.S. Air Force and Col. John Paul Stapp was researched. In the 1950s, Col. Stapp acted as a human test dummy during research on aircraft pilot safety systems. From the results of his tests, we concluded that approximately 20-G acceleration was the limit for front impact resulting in minor harm to the driver. Also, above approximately 40-G acceleration significant harm would be likely to occur, including damage to the driver's organs (Col. Stapp underwent 46-G acceleration in front impact and ruptured his retinas). We decided that the SAE acceleration requirements were appropriate for front impact, and extended them to side impact in which the driver has similar support.

## Intrusion

Intrusion was considered in the case of an impact. For steel tube frames the rules are extremely lenient: the only intrusion protection required is that some form of bodywork must be used for the cockpit. For monocoques, there are stricter intrusion requirements: the Side Impact Structure must resist intrusion from a 1" diameter intruder forced at least 1700 lb (540 lb/inch), and the Front Bulkhead Support 880 lb. We determined that the most likely object to intrude a Formula SAE car was the bulkhead of another car. Assuming a car weight of 600 lb, acceleration of 40 G, and perimeter of 55", the applied shear load was calculated to be 440 lb/inch. This load was less than the load required by SAE for the Side Impact Structure, so the SAE load was used. We defined a "primary structure" as a survival cell, extending from 2" ahead of the driver's feet to 2" behind the driver's shoulders. SAE's 1700-lb requirement was applied to the entire side of the primary structure to ensure driver safety. To ensure that the suspension members would absorb energy in impact instead of intrude the primary structure, their maximum load capacity was calculated and translated into a shear load on the primary structure to set a shear strength requirement. This maximum load would be either the buckling load of the A-arm member or shear failure load of its mounting bolt. For an upper A-arm the buckling load of 5800 lb was greatest, and was applied over the bracket perimeter to give 1200 lb/inch of shear load. This was equivalent to 3500 lb applied to a 1" intruder. This requirement was applied to a 3.5" diameter surrounding the upper suspension points; at this diameter the shear load from the 5800 lb was equivalent to the 540 lb/inch required for the entire side of the primary structure, so this ensured that the buckling load wouldn't cause shear failure of the area around the bracket. Finally, the side of the primary structure at the cockpit opening was required to meet the shoulder height of the driver, and basic intrusion protection was required for the top and bottom of the primary structure, the structure around the fuel tank, and the structure between the driver and the engine.

## Torsional Stiffness

There are many characteristics of chassis and suspension stiffness and many situations in which they come into play. We focused on chassis torsional stiffness for its high influence on transient cornering behavior. This behavior is one of the most important aspects of a car's driveability, especially in autocross conditions with frequent direction changes. Development of our chassis torsional stiffness requirement follows.

In order for the suspension to distribute load onto the tires in transient cornering, as a function of front and rear lateral accelerations and steering input, the connection between the front and rear of the car must be stiff. The car's balance depends on the tires' load distribution, and the rear of the car must respond to the driver's steering of the front tires (slip angle and jacking). Consistent, predictable behavior is very important for the driver's feel in corner entry and exit – without good driver feel, a car can be very difficult to drive and tune.

While a chassis must be stiff, there comes a point when it is stiff enough; stiffness is related to the amount of material in the structure, which is proportional to weight. We want to achieve a certain stiffness value without going beyond, for the purpose of minimizing weight. For chassis torsional stiffness, the chassis must be stiff enough such that it doesn't reduce the effect of changes to the suspension's springs. This concept was confirmed in Milliken's Race Car Vehicle Dynamics. This can be compared to the stiffness of linear springs in series, represented in (1) – the less stiff a spring, the more it affects the system stiffness.

$$k = \frac{1}{\frac{1}{k_1} + \frac{1}{k_2}} \quad (1)$$

For example, if two springs are in series and one has a stiffness of 1 lb/inch and the other has a stiffness of 3 lb/inch, the system stiffness is 0.75 lb/inch. If the stiffness of the first spring is doubled, the system stiffness is 1.2 lb/inch – 1.6 times the initial system stiffness. Now, if the second spring’s stiffness is reduced to 2 lb/inch, this result is 1.5 times the initial system stiffness – less than with the 3 lb/inch spring. With the stiffer second spring, the change of the first spring rate had a larger effect on the system.

We examined the stiffnesses of the front suspension, chassis, and rear suspension in series. Specifically, the front roll stiffness, chassis torsional stiffness, and rear roll stiffness. The system stiffness (as a ratio of system stiffness with a rigid chassis) was plotted as a function of chassis stiffness (as a ratio of chassis stiffness over front and rear roll stiffnesses in series) in Figure 4.4. It was found that with a ratio of chassis stiffness to roll stiffness around the 20-times mark, system stiffness was affected very little by changes in chassis stiffness, and was approximately 95% the value with a rigid chassis. With front and rear roll stiffnesses of 250 lb\*ft/deg and 135 lb\*ft/deg, respectively, our chassis torsional stiffness requirement was set to 1700 lb\*ft/deg.

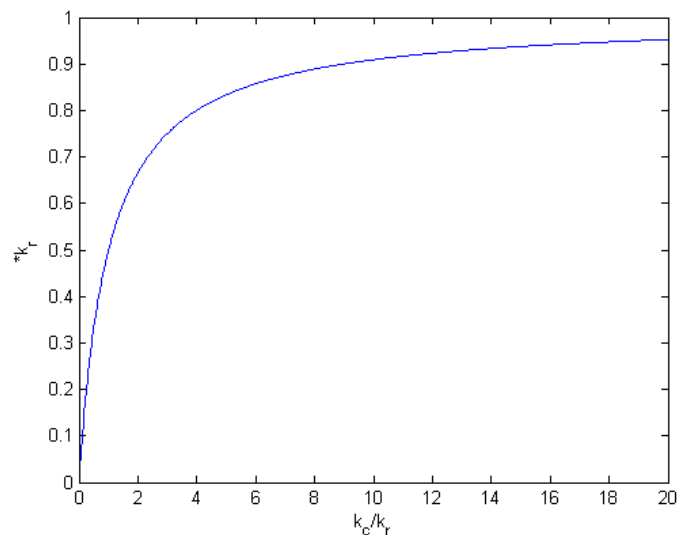


**Figure 4.4** - System stiffness as a function of chassis stiffness, with ratio to system stiffness with a rigid chassis on the vertical axis and chassis stiffness over roll stiffnesses in series on the horizontal.

The front and rear stiffness distribution of the chassis was also investigated for its effect on the front and rear stiffness distribution of the car as a whole. This distribution determines the car’s steady-state balance in cornering, and is usually calculated by comparing the front and rear roll stiffnesses alone. With a non-rigid chassis, we wanted to ensure that the chassis wouldn’t affect this distribution and cause issues during tuning. Using a simple point-mass approximation of the car’s mass concentrated at its center of gravity (CG), it was found that changing roll stiffness distribution by 1% could be achieved through a 5% change in front roll stiffness or a 50% change in front chassis stiffness (chassis ahead of the CG). With such a small effect on roll stiffness distribution coming from the chassis, it being very stiff relative to the suspension, chassis stiffness distribution was ignored.

## Miscellaneous

Additional requirements for the chassis subsystem are shown in Table 4.3. Most of these requirements were developed for the purpose of ensuring easy servicing. The weight requirements were set based on the weight goal for the entire car and estimations from previous cars. In total, the chassis subsystem weight requirement was 69 lb (50 lb in chassis and 19 lb in accessories). Loading requirements are detailed in the Loading and Structural Equivalency section.

Table 4.3 – Additional chassis requirements.

Description	Requirement
Chassis assembly weight	50 lb, maximum
Firewall, head rest, seat, etc. assembly weight	19 lb, maximum
Engine installation time with 2 people	15 minutes, maximum
Support for driver's thighs	
Comfortable driving position for all drivers with no more than 2 seats and 2 pedal assembly positions	
Quarter-turn fasteners for non-structural bodywork	
Mounting for suspension alignment and ride-height tools	
Skid protection for low points of chassis	
Engine components (except exhaust) not visible from side and top views	

## 5. Vehicle Design

The design of the vehicle as a whole began with the wheelbase. Early in the design phase, it was decided to increase the wheelbase of the car from the 2012 car's 60 inches. In 2012, 60" was chosen because it was the minimum wheelbase allowed by SAE and it was hypothesized that a shorter wheelbase would be faster on a tight autocross course due to the ability to take larger radii around corners and through slaloms. Its effect on the greater vehicle design was ignored, resulting in a few major issues.

The first issue was that the driver's feet sat well ahead of the front axle. This made the driver's lower extremities vulnerable in an impact, reducing both safety and driver confidence. Such positioning wouldn't meet our 2013 safety requirements.

Second, the driver's hands were so close longitudinally to the steering box that a complicated shaft system with two U-joints was required to get the shaft down from the steering wheel to the steering box at the floor while maintaining an acceptable steering wheel orientation. The system was difficult to manufacture and had significant play once assembled. This used up valuable time, made the system's safety questionable, and reduced driver confidence.

Third, even with a single brake disc at the rear of the car, significantly larger calipers were required at the front of the car since the front did approximately 80% of the braking work. Different disc diameters were required front and rear to give a balanced system with the calipers and master cylinders available. This resulted in a complex system and reduced serviceability because the team couldn't afford to have spares for such a large number of different components. Additionally, with 40% of braking energy going into a front disc and 20% into the rear, the brakes heated unevenly. Even heating is extremely important for Autocross to maintain consistent braking behavior throughout a run, because friction values can be highly dependent on temperature.

Seeing many downsides to a 60" wheelbase, we analyzed the short-wheelbase hypothesis using the team's lap simulator, which ran the car around an autocross course and modified the racing line to account for changes in wheelbase. The geometric model in Figure 5.1 was used with a number of similar models to develop equations describing corner geometry as a function of wheelbase, dependent on corner angle and radius. We determined that the short-wheelbase hypothesis was true, but found through the plot in Figure 5.2 that increasing the wheelbase had a very small effect on lap time.

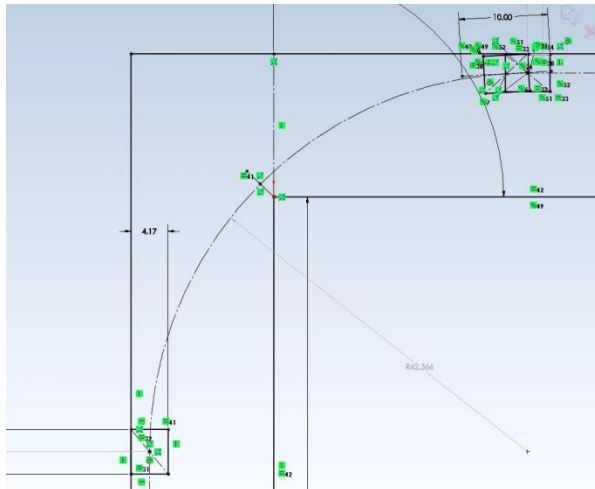


Figure 5.1 - Drawings were used in SolidWorks to determine effect of wheelbase on corner geometry.

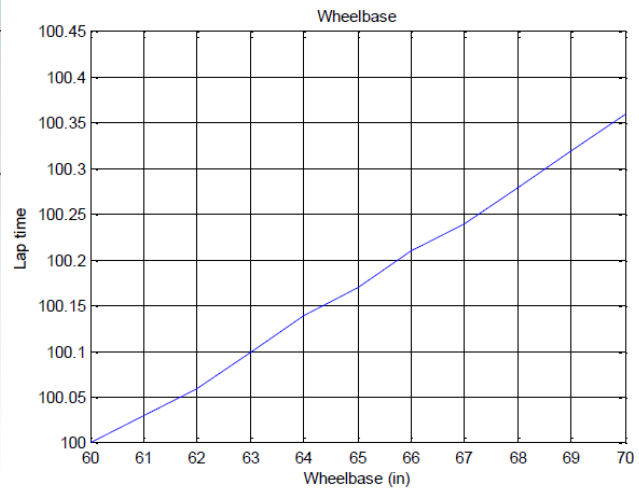


Figure 5.2 - Lap time as a function of wheelbase.

This finding gave us the freedom to increase the wheelbase to 64" and gain a number of advantages:

- Driver safety requirement regarding position relative to front axle could be met while maintaining an acceptable weight distribution.
- Steering system options were expanded by increasing longitudinal distance from the driver's hands to the steering box, allowing for a straight steering shaft.
- Brakes sizing was made easier by decreasing forward weight transfer under braking, allowing for common brake components and near-equal brake disc energy inputs when using a single rear rotor.
- Weight distribution sensitivity to changes in driver and fuel weights was reduced, increasing consistency of vehicle balance in different conditions.

These points were the main drivers behind improving vehicle-level integration, and were planned to be a focus during Design. The value of 64 inches was initially determined using a rough vehicle layout with driver solid models from 2006, named "Jeff" and "Jason". Jeff was a 95th-percentile 190-lb male, and Jason was a small 120-lb male.

From here, the vehicle-level design of the car was centered on the driver. For the 2012 car the cockpit was designed around Jeff, because the rules stated that a cockpit must accommodate a person of his size and the team saw that as a requirement which would be enforced at the competition. Little focus was placed during design on accommodating the team's drivers as compared to Jeff, which contributed to the car being uncomfortable for drivers of normal size. At the competition, beyond the scrutineers checking Percy's fitment, the only time that cockpit size came into question was when design judges sat



in the car. Following the 2012 experience, we decided to focus on designing the car around our tallest and shortest drivers, and to ignore fitting a 95th-percentile male beyond meeting the Percy rule. We concluded that the gains from our drivers being as comfortable as possible during testing and the competition would outweigh the potential loss of points in Design.

We prepared to design around the team's tallest and shortest potential 2013 drivers, who were Matt Hagan ("Hagan") and John Waldrop ("Wally"). This would ensure achieving good driver comfort and car mass properties. They were placed in a mock cockpit for a single-seater race car, constructed by John Fabijanic, and measurements and photos in Figures 5.3 and 5.4 were taken. These were used to create a model for each driver in SolidWorks, with accurate body member shapes and dimensions, angles between body members for a comfortable driving position, weight, and CG location. Hagan and Wally were placed in a SolidWorks assembly with a sketch of the wheelbase with wheels and tires, engine solid model, and point mass representing the "rest of the car". The "rest of the car" was all but the driver and engine, with a weight distribution of 49% front found by weighing the 2012 car without driver and removing the engine mass through calculation.



Figure 5.3 – Hagan in the mock cockpit.



Figure 5.4 – Wally in the mock cockpit.

The drivers' torsos were placed in the same location, and the front axle located to satisfy our safety requirements. They were placed as low as possible, the driver being the most massive component of the car, while keeping the floor from bottoming out with suspension in full bump. Additionally, the driver models were modified to be seated more upright than in a typical single-seater. This accommodated a higher steering shaft angle (acceptable driver comfort up to 30 degrees from horizontal, which could be met with a straight steering shaft), increased flexibility of engine positioning, and helped to avoid a "reclined" driver position. To further ease engine packaging, the car's electronics were planned to be positioned under the driver's thighs, where there was free space which wasn't affected by the template rules. Seat back position was determined considering a 1" bead seat, and the engine was positioned as close to the seat back as possible considering the 1" clearance required for the exhaust, and size of the fuel tank. With the massive components in place relative to the front axle, the planned 64" wheelbase was shown to place the rear axle such that weight distribution with either Hagan or Wally met our requirement. 45-46% front weight distribution was expected, depending on the driver. These placements also allowed the pedal assembly positions, steering wheel location, and differential location to be determined. This layout is shown in Figure 5.5.

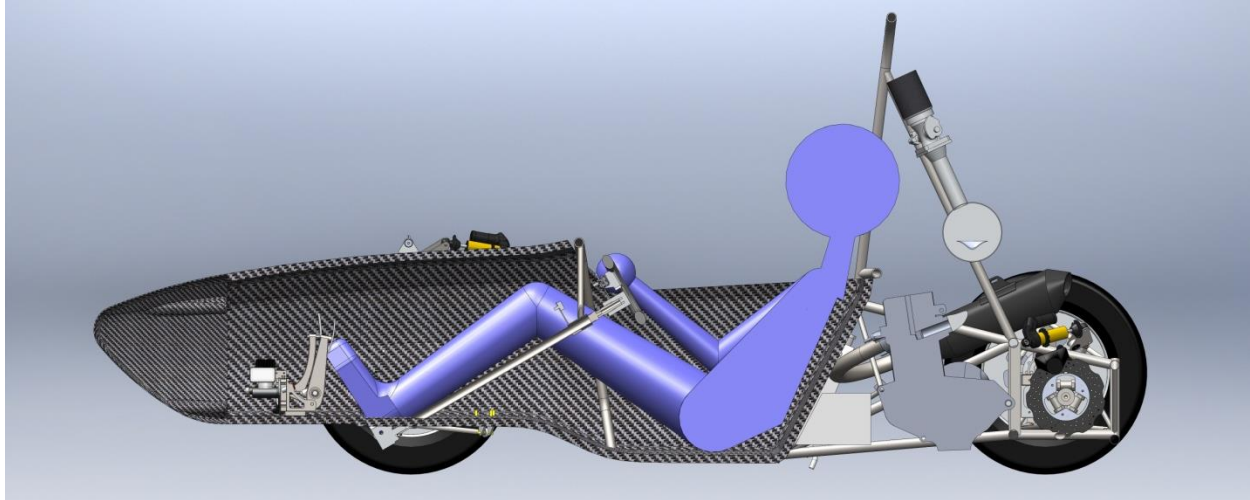


Figure 5.5 – The developed vehicle layout.

This vehicle-level design was referenced throughout the car's entire design process, and was planned to ensure development of well-grounded designs which contributed to the big picture.

## 6. Full Monocoque Chassis Design and Analysis

### Initial Material Selection

The monocoque chassis design was planned to be manufactured using a carbon fiber sandwich structure. The sandwich structure was to be constructed out of pre-impregnated (prepreg) carbon fiber skins bonded to a honeycomb core with film adhesive. This was chosen so that the laminate would have good specific stiffness. Additionally, with the use of prepreg the layup can be done over the course of a few days due to the long out-time of the resin.

The carbon fiber skins would utilize both woven and unidirectional varieties so as to optimize the weight of the structure. The material that was obtained was manufactured by Aldila Composite Materials in San Diego, California. The cloth was Aldila's 3K2X2-AX021610G-204/36, a 2X2 weave fabric with a 250 F cure temperature epoxy resin system. The unidirectional prepreg was Aldila's X534-AF254-150/35, a 50K tow fiber with a 250 F cure temperature epoxy resin system. Note that it was important that the two resin systems be compatible with one another since they were to be co-cured.

The core material that was selected to be used was Hexcel's HRH-10 series honeycomb core. The HRH10 series is made from Nomex, a aramid material that is commonly used in non-metallic composite structures due to its high strength to weigh ratio. A cell size of 1/8 inch was selected so complex curvatures could be achieved without excessive manufacturing difficulty. A core density of 3 lb/ft<sup>3</sup> was chosen in an effort to minimize weight and still achieve the required strength needed to carry the various loads the chassis is subjected to.

Initially, a core thickness of 0.450 inches was chosen. This was done based on past laminates done by the team as well as composite insert availability. Since composite inserts are manufactured in standard sizes, the thickness of the laminate had to match that of the inserts. Later it was determined that this core was not stiff enough to meet structural equivalency. This is outlined in the Loading and Structural Equivalency section under Laminate Development.

To bond the skins to the honeycomb core, a structural film adhesive was selected. The film adhesive was manufactured by 3M under the brand ScotchWeld. It was selected due to its compatibility with the above mentioned resin systems and availability to the team.

## **Manufacturing Concept**

We had to design the monocoque and plan its manufacturing around the mold's geometry. A two-part mold would be required so that the monocoque could be laid up on a positive draft and thereby be removed. A two-part monocoque was selected, with two stand-alone molds, as opposed to a one-part monocoque with molds bolted together. The latter option would greatly complicate the layup process, because a single person would have to go up into the bolted molds to do the layup; with a two-part monocoque, many hands could be performing the layup at one time. The team was familiar with the bonding required for the two-parts. We had the option to part the monocoque vertically or horizontally. The horizontal parting method was done in 2009 for the advantage of locating all suspension points on the bottom half of the monocoque, which reduced the need for accurate bonding. Despite this, we chose to part the monocoque vertically. Because of the monocoque's lateral symmetry, this would result in mirrored tools, mirrored layups, and mirrored parts. From mold manufacturing, to the layup, to finishing the parts, the process would be straightforward and efficient.

The molds were planned to be made at C&D Zodiac's facilities in Santa Maria. The company manufactures tooling for aircraft interiors, and provided tool manufacturing services to the team in 2009. Their method is to machine male bucks on which female molds are laid up, for making male parts. The male buck allows for easy machining, because there's room for the 5-axis mill's head to orient itself to machine highly angled surfaces. This buck is machined from foam, which is easy to machine but wouldn't be able to serve as a mold due to its inability to withstand multiple high-temperature cures. To make the mold, a special resin is laid up on the buck with support from plaster with hemp and steel reinforcement. This structure can withstand typical curing temperatures and produce multiple parts.

## **Geometry and Packaging Development**

After the driver was located in the SolidWorks, other subsystems were located before the chassis could take shape. These subsystems included the suspension components, engine, differential, and driver controls. Since the purpose of the chassis was to connect all these components, it was necessary to locate these components prior to designing the chassis geometry

The suspension components that mounted directly to the chassis included control arms, rockers, shocks, and the front anti-roll bar (ARB). The chassis was to come within 1 inch of the points of these components to allow adequate clearance for mounting brackets. This also gave the suspension team some flexibility in bracket design to connect the suspension members to the chassis.

The engine placement was determined by taking into consideration a fully enclosed structure in the rear of the car. The bottom of the engine was placed 1.75 inches above the ground plane. Longitudinally, it was placed such the head of the engine was a minimum distance of 1 inch from the firewall, as per SAE rules. The engine was to be equipped with a turbocharger, so adequate space for packaging and heat shielding needed to be considered when designing the shape of the chassis. Additionally, space was left between the engine and driver to accommodate a fuel tank.

The differential, which mounted a brake disc and drive sprocket, was placed with sufficient space to the engine ahead of it to allow for adjustment of differential position and sprocket and brake disc sizes. The engine and differential sprockets were placed in the same longitudinal plane. Additionally, half-shaft angles were minimized as much as was easy, and kept below 22 degrees.

Once these subsystems were in place, the chassis could now begin to take shape. To begin, the SAE templates were constructed and placed in a SolidWorks assembly along with the driver model, engine, differential, driver controls, and suspension geometry, as shown In Figure 6.1 below. Next, flat points where the front suspension mounted to the chassis were drawn in to ensure a flush mounting surface. From these sketches, the shape was lofted forward to house the pedal assembly. In a similar fashion, the shape was lofted rearward to the driver seat back, making sure to leave room for the SAE template.

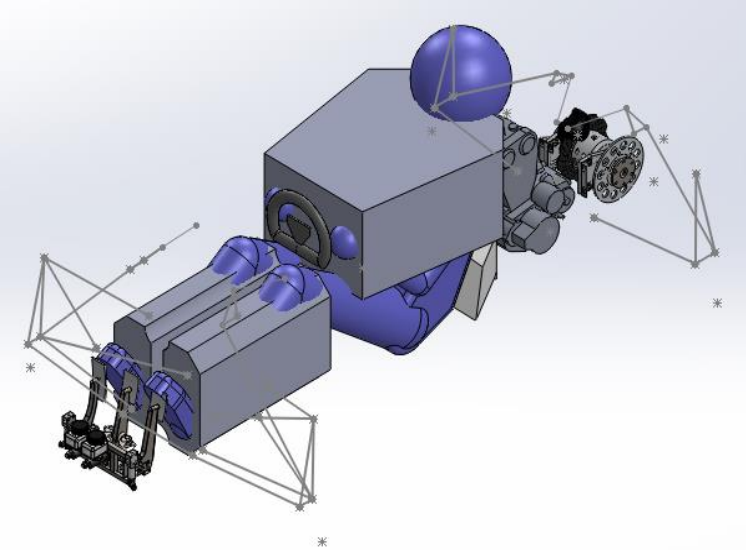


Figure 6.1 – Basic component and SAE template layout in relation to the driver.

The rear chassis shape was designed to accommodate all of the subsystems at the back of the car. The suspension was the main driver for the shape, as the mounting points to achieve the desired kinematics made the very rear of the chassis very narrow. This presented challenges in the design as space for the engine was low. However, angled sides to meet the suspension mounting points were incorporated into the chassis which didn't interfere with the engine, as illustrated in Figure 6.2.

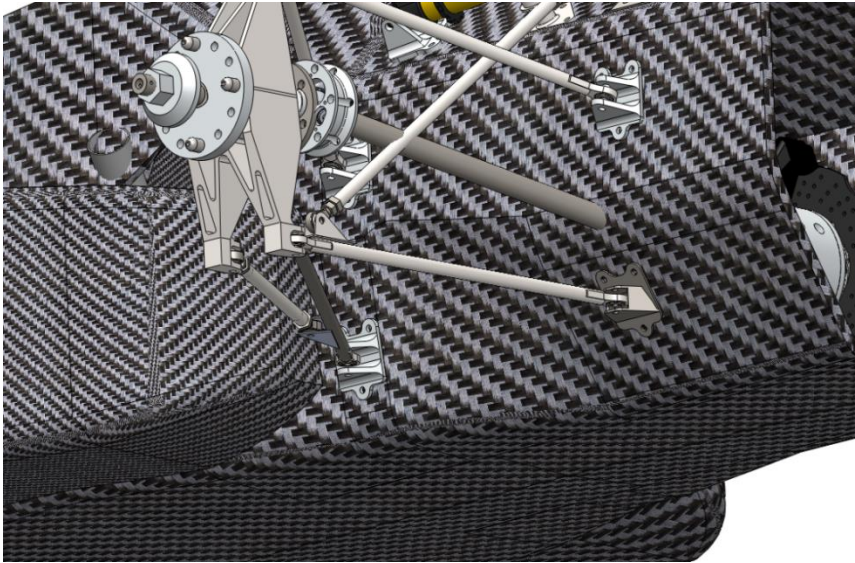


Figure 6.2 – Rear chassis geometry to meet suspension attachment points.

Next, the transition area from the driver cell to the engine cell was considered. To install and remove the engine, a removable firewall was designed. The section of the chassis around the firewall had a hump so that the head of the engine could pass through. To make the firewall removable, and to increase torsional stiffness, a bulkhead was incorporated into the transition area. Additionally, a flat spot was made on the top of the chassis to accommodate harness mounting.

## Analysis

### Mechanical

To ensure structural integrity, analysis was planned to be done on the attachment points of the chassis. This included the front suspension mounting points, the rear suspension mounting points, engine mounting points, and pedal assembly mounting points. Due to the late and major change in design, discussed in the Issues and Switch to Hybrid Chassis section, the only composite mechanical analysis which carried over to the final product included just the front suspension mounting points and pedal assembly mounting. This analysis is covered in the Hybrid Chassis Design and Analysis section.

### Thermal

Since the engine and turbocharger were to be housed inside the monocoque structure, structural integrity had to be insured under operating temperatures. The design case was chosen to be analysis was the heat soak condition. This is when the vehicle has been operating for an extended period of time, such that the engine and turbocharger have reached a steady state temperature, and the car is brought to a stop and shut off. To prevent the chassis from heating up excessively, the inner surface was proposed to be lined with a layer of ethylene propylene diene monomer (EPDM) rubber. To determine the thickness of the EPDM lining, the following analysis was performed.

The goal for insulating the engine bay was to keep the carbon fiber temperature at or below 90 F. For the purpose of this analysis, the following assumptions were made:

- The turbo inlet temperature was 1200 F (922 K)
- The turbo outlet temperature was 600 F (589 K)
- The turbo housing was made of iron with a thermal conductivity of 53.3 W/m\*K (370 BTU\*in/hr\*ft<sup>2</sup>\*F)
- Air gap experiences natural convection
- EPDM rubber has a thermal conductivity of 0.0648 W/m\*k (0.450 BTU\*in/hr\*ft<sup>2</sup>\*F)
- The surface of the turbo housing was the average of the inlet and outlet temperatures, 900 F (755 K)

A simple energy balance was applied, with the turbo charger supplying energy into the system and the air and EPDM rubber dissipating it. (1a) and (1b) below show this in mathematical form.

$$\sum \dot{Q}_{out} = \sum \dot{Q}_{in} \quad (1a)$$

$$\dot{Q}_{EPDM} + \dot{Q}_{AIR} = \dot{Q}_{TURBO} \quad (1b)$$

The energy that the turbocharger inputted into the system was found to be approximately 13 kW, as determined by equation (2) below, where  $h$  is the enthalpy and  $\dot{m}$  is the mass flow rate of the exhaust.

$$\dot{Q}_{TURBO} = (h_{in} - h_{out}) * \dot{m} \quad (2)$$

Next, the energy of the air needed to be calculated. This was done by exercising the assumption of natural or free convection. First the Rayleigh number had to be calculated using (3) below, where  $\beta$  is the thermal expansion coefficient,  $\nu$  is the kinematic viscosity,  $\alpha$  is the thermal diffusivity, and  $D$  is the length of the air gap between the turbocharger housing and chassis.

$$Ra_D = \frac{g\beta(T_s - T_i)D^3}{\alpha\nu} \quad (3)$$

Then, the Nusselt number was calculated using (4) below, where  $Pr$  is the Prandtl number evaluated at the average temperature of the surface and air (550 K)

$$\overline{Nu}_D = 2 + \frac{0.589Ra_D^{1/4}}{[1 + (0.469/Pr)^{9/16}]^{4/9}} \quad (4)$$

Then, the convection coefficient was calculated using (5) below.

$$\bar{h} = \frac{\overline{Nu}_D k}{D} \quad (5)$$

Finally, the heat energy absorbed by the air was determined to be 55.36 W using (6) below.

$$\dot{Q}_{AIR} = \bar{h}A(\Delta T) \quad (6)$$

Now (1b) can be solved for the energy absorbed by the EPDM rubber, which equates to (7) below.

$$\dot{Q}_{EPDM} = kA \frac{\Delta T}{d} \sim 13.5 \text{ kW} \quad (7)$$

Solving for  $d$ , the thickness of the EPDM, in 7 gave a result of 0.0075 inches. After incorporating a safety factor, the thickness of the EPDM rubber insulation was chosen to be 0.125 inches.

## Issues and Switch to Hybrid Chassis

At this point in the design process, in mid-November 2012, there were a number of major issues which either hadn't been addressed or were proving difficult to solve. These arose naturally through the design process, and were points of concern during the project's PDR and team's CDR, both in late October. These issues were all related to the engine and its systems.

First and foremost was engine accessibility. We had planned to address this through designing holes in the rear of the chassis, but it wasn't guaranteed that we would achieve a sufficient level of accessibility. Easy access was required for smooth manufacturing, due to the largely free-form routing and mounting of engine systems which would take place once the chassis was on the table. More importantly, accessibility would have a direct impact on time available for testing, considering getting components in and out of the chassis and having to work on systems on-car. If the chassis' rear accessibility was poor, it would have a hugely negative effect on testing time. This time was considered to be the most important influence on our competition result. Additionally, we were worried that unforeseen modifications to the chassis would be required during manufacturing or testing to access the engine's systems, namely in the form of swiss-cheesing the rear, which would compromise the chassis' structure.

Second, heat from the engine had been included in analysis but was not fully understood. Due to the high complexity of heat transfer calculations, and unknowns regarding exhaust and turbo temperatures, the answers to heat questions would only come from testing. There especially were concerns regarding temperatures in the confines of the rear of the chassis after the car would come to a stop, with little to no ventilation. There was no time to make laminates and get the engine running well enough on the dyno to test this in controlled conditions before running the car. Finding out the answers with the car running was not an option - damage to the composite structure of the chassis could be a showstopper.

Third, the composite's ability to withstand vibration from a single-cylinder engine was unknown. The testing and analysis needed to determine this would require significant time and require highly-developed methods. The main concern was delamination of the face sheet from the core at mounting points, which could be a showstopper.

Finally, initial designs of engine mounting were proving to be complex, and interfere with engine installation. Tube frame and composite structures were being conceptualized, which required mounting to the chassis and proper analysis to determine loading. These structures would partially exist ahead of the engine, in the installation path, meaning they would need to be removable. It was doubtful that we could develop a strong mounting structure without creating a heavy tube frame within the rear of the chassis; we estimated that the hybrid chassis would reduce weight by 2 lb, largely due to more efficient engine mounting.

A switch to a hybrid chassis, with a front monocoque and rear tube frame, was considered to be a simple solution to these issues. The front monocoque maintained driver safety, while the tube frame's open, metal structure, with high potential for modification and ease of meeting hard points, fit the needs of the engine. A list of pros and cons for the switch was created:

Pros:

- Improved engine accessibility
- Improved heat dissipation
- Greater strength in vibration due to steel's ductility
- Simpler engine mounting
- Easier modification due to ability to weld
- Easier engine leak identification
- Less carbon pre-preg and core required
- Smaller tool size for monocoque
- No bulkheads for seat back or rear
- Fewer, less various inserts
- Less FEA due to no re-meshing to evaluate access holes
- Estimated 2-lb weight reduction

Cons:

- Redesign of rear suspension attachment
- Change of manufacturing plans with C&D Zodiac
- Need for stand-alone jig to locate suspension front/rear
- Scrapping of much work up to this point

In addition to these pros, which we believed greatly outweighed the cons, the team's big-picture goals would be much better satisfied by a hybrid chassis. The monocoque was mainly required to meet the goal of high driver safety, which only applied to the front, and the rear could be left a simple tube frame. Testing time would be maximized by avoiding the potential issues caused by a full monocoque and its interaction with the engine and its systems. Our project's goal of improving the team's composites knowledge would be preserved. We easily made the choice to change the project's direction and proceeded with a hybrid design.

A full-monocoque design had been initially chosen with insufficient problem development and poor judgment. If we had known at the beginning what we discovered through the full monocoque design we would have designed a hybrid from the beginning, but we were slightly blinded by the desire to do something different and challenging. A switch to a hybrid appeared to be inevitable following the full-monocoque investigation, and simply came later in the game than we would have liked. Despite the fact that we had "committed" to a full monocoque, we discovered that it was not the optimal choice for what we were trying to achieve and we changed our direction accordingly. We viewed this change as a good engineering decision, supported by developed evidence and made with a mind toward better ensuring the team's success.

Later in the design phase, the team decided to abandon the turbocharger due to reliability concerns with its oiling system. As with the chassis decision, this greatly improved chance of success, although the car would no longer meet the power requirement which we believed would allow us to place in the Top 10 at FSAE Lincoln. As a result of this decision, the remaining processes for the chassis subsystem do not include the turbocharger.



## 7. Hybrid Chassis Design and Analysis

Images of the final chassis assembly design, including its interaction with other subsystems, are included in Figure 7.1.



Figure 7.1 – The chassis assembly solid model.

### Loading Sources

The chassis is subjected to many loads when the car is in operation. As such, it is important to identify these loads so that the structure can be designed to withstand the resulting stresses. The main loading of the chassis comes from the suspension system. The suspension system loads the chassis in cornering, braking, acceleration, and general bump, the most severe of which for our geometry are cornering and bump. During bump, the loading comes from the wheel being subject to a sudden vertical displacement whereas during cornering, the reaction of the tires and the road surface causes the loading in the suspension system.

Additional loading sources include impact loads, engine loads, and driver induced loads. During impact, the chassis is loaded dynamically by means of the vehicle being decelerated rapidly by an object. These loads are usually large impulse loads and should be considered when evaluating the integrity of the chassis in the event of a crash. The engine loads the chassis due to its reciprocating parts and the torque applied on the chain. Driver induced loads become significant when considering egress and operation of the car. When the driver egresses the car quickly (i.e. in the event of a fire), the floor is subjected to a significant load and must be accounted for. During operation of the vehicle, the large reaction arm of the brake pedal creates a substantial moment that is carried by the chassis.

For the purpose of our design, it was determined that the main loading condition would be the bump condition as it loaded the suspension the greatest of the four conditions mentioned above. Additionally, engine dynamic loads were not entirely considered however a healthy safety factor was applied to the members supporting the engine. Finally, vehicle impact loads and driver induced loads were considered. All considerations are detailed in the subsequent Monocoque section.

## Monocoque

### Geometry

The composite tub for the hybrid chassis was an exercise in iterative shape design. After it was discovered that the full monocoque was no longer an option, to stay on track and not lose our sponsorship with C&D Zodiac through being late with our design, we had about 3 days to design and shape the tub. We designed the tub using multiple sketch planes (approximately 12) to get the basic outside shape finalized. The curves and transitions between sections were made as smooth as possible with fairly large radii; the goal being to keep the fibers from having to go around a sharp corner.

The tub shape was governed mainly by the following things: templates (as defined by rules), front suspension points, keeping the driver's feet behind the front of the wheels, accommodating the engine and finally a sketch drawn on a whiteboard that we all seemed to like. First the basic templates and driver models were located in space and a rough shape was taken from a crude scale of the whiteboard sketch. The driver models were built based on our shortest and tallest drivers and is described in the Vehicle Design section. As stated above, about 12 points on the sketch were chosen and corresponding planes were set up in SolidWorks and cross sectional sketches were drawn and lofted together. First, the area where the front suspension and template were located was made. Next the part surrounding the driver's torso and cockpit opening template was designed. After this basic shape was formed, the section joining the two was made and room was left so that the front roll hoop could be installed and have the chassis still meet template. The last lofted section to be designed was the front of the chassis in front of the driver's feet. All the while an effort was made to constantly keep a three dimensional surface on the side of the tub to minimize the amount of "flat plate" sections to help with out of plane loads in the event of a side impact. Curvatures were changed, the model was narrowed and widened, the openings and cross sections were modified, and the driver position (knee angle, seat back angle, head height - for visibility) were all changed many times until we were left with a shape that not only met rules, located suspension points, and fit the driver, but was also smooth and pleasing to look at.

After the lofting was taken care of, a few cut planes and extrusions were made for the sections that needed flat mounting. Cut planes were used to make small flat spots where the mounts for the front suspension needed to be as it is much easier to make mounts that have a flat mounting surface than a curved one. Another two were used to make the seat back angle and ground clearance plane. The seat back was chosen in an effort to not need to use a 6 point harness by having the driver in a more upright position. This negatively affected our center of gravity, but also allowed us a shorter car as a more

upright driver takes up less longitudinal space. Having a more upright driver also allowed the top of the tub to be higher while minimally affecting visibility yet allowing for more clearance for the front template and a higher steering wheel letting us use a solid steering shaft. Ground clearance was chosen to allow for a full one inch of suspension compression with a small safety factor in an effort to keep the tub from scraping the ground. The final two cut planes were chamfers where the seat back met the sides of the tub. These were 45 degree cuts to allow the main roll hoop tube to nest inside both the outer side face and the outer rear face making it easier to make our mounting plates that attached the tub to the main roll hoop. By doing this we were able to have the mounting plates transfer load into the chassis in the fiber direction instead of an out of plane punch load as was done in previous years. The only extrusions needed were for the front bulkhead and floor to facilitate mounting of the pedal assembly.

To give space for the electrical mounting, the floor of the tub - specifically the cockpit floor - was extended forward to provide a cavity underneath the driver's thighs to allow room for the ECU and data acquisition system. The cover panel for the electronics served both to cover the electronics and provide the needed support for the driver's legs that was lost when the floor was extended forward.

One of the last things that were modified was the top of the tub. We extended the cockpit opening forward and brought the front lip of the cockpit opening up until there was enough room to fit the steering wheel. We went with a straight steering shaft this year and needed to make sure that the front roll hoop was tall enough to meet rules. But, having the top of the tub come over the top of the front roll hoop impacted visibility. So, it was decided to end the tub at the forward edge of the roll hoop and at the same level. This made visibility over the top of the car better, and gave us a simple way to mount the top of the front roll hoop so that we could also use the top of the tub as the front roll hoop support - rules state the front roll hoop has to have bracing between it and the front bulkhead.

Also, one item that we wanted to look at but ran out of time due to the tight time table was possibly extruding flat bosses from the side of the tub instead of doing a flat cut plane for things such as suspension pick-ups, ARB mounting, and rocker mounting. Not only was there not enough time to experiment with the solid model, but using a flat cut plane was more advantageous as we were able to use end grain balsa wood as core since we needed a higher shear strength in the core in those areas. Had they been extruded bosses, fixing the core would have been much harder and probably much heavier as well.

Once all of the above was done, the final thing to do was to fillet all the sharp edges. The fillet was determined by how tight a radii we thought we could manage with the .700 core we were using. After that the chassis was sent off to C&D Zodiac for final critiques. C&D Zodiac added the three degree draft on the bottom of the tub to facilitate removal from the molds (a draft had already been built into the top) and fixed one surface blend up near the front suspension mounting area that SolidWorks kept faulting on, both using CATIA. After the draft was added and the surface was fixed, C&D Zodiac sent the model back to us to inspect and validate that nothing was lost in transferring the model between SolidWorks and CATIA. After the external dimensions were checked, the model was shelled to an approximate thickness and templates and driver fitment were checked before the final approval was given for C&D Zodiac to begin cutting the tooling.

### **Laminate Development**

The laminates of the monocoque had to meet a number of stiffness and strength requirements, which were prioritized to ease the design process. Weight minimization would be the central focus, followed by manufacturability in the context of the layup.

The laminates would first be designed in the context of our torsional stiffness requirement. Next, the laminates would be checked against expected loading situations for strength, using Euler-Bernoulli Beam Theory and Classical Lamination Theory (CLT), an extension of Kirchhoff-Love Plate Theory. These situations would include suspension, impact, and driver loads. The MATLAB script used for this analysis is included in Appendix C: CLT Script. Finally, SAE’s Structural Equivalency requirements would be met. Most of these analyses were originally done in the context of the full monocoque design, but were able to be translated to the hybrid chassis due to its similar loading.

In general, fibers would be placed in the direction of load to make the best use of the composite. Core would be used as a shear mechanism to increase beam strength and stiffness. Only balanced and symmetrical laminates were considered, to ensure isotropic mechanical behaviors for the expected loading and to avoid warping due to cooling from the cure temperature. The laminates developed would later be optimized locally for loading at attachment points.

Material properties and the strain failure theory used for laminate development are detailed in Table 7.1. Typical carbon pre-preg values were used (AS4/3501-6 was used as a reference).

**Table 7.1 – Material properties used in analysis.**

Material	Carbon pre-preg uni	Carbon pre-preg cloth	Core
<b>Thickness (in)</b>	0.0052	0.010	0.700
<b>E<sub>11</sub> (psi)</b>	20.0e6	9.4e6	1
<b>E<sub>22</sub> (psi)</b>	1.4e6	9.4e6	1
<b>ν<sub>12</sub></b>	0.30	0.05	0.01
<b>G<sub>12</sub> (psi)</b>	0.93e6	0.77e6	1
<b>G<sub>13</sub> (psi)</b>	0.93e6	0.77e6	2000
<b>G<sub>23</sub> (psi)</b>	0.93e6	0.77e6	2000
<b>α<sub>11</sub></b>	-0.5e-6	-0.3e-6	0
<b>α<sub>22</sub></b>	15e-6	-0.3e-6	0
<b>α<sub>12</sub></b>	0	0	0
<b>ε<sub>11</sub> tensile fail.</b>	0.014	0.010	
<b>ε<sub>11</sub> comp. fail.</b>	0.007	0.010	
<b>ε<sub>22</sub> tensile fail.</b>	0.012	0.010	
<b>ε<sub>22</sub> comp. fail.</b>	0.031	0.010	
<b>ε<sub>12</sub> fail.</b>	0.030	0.025	

### ***Torsional Stiffness***

For a closed cross section, torsional loads create shear stresses in the axial and hoop directions. This loading is represented in Figure 7.2 on a stress block. To transform the shear into normal loading, the stress block must be rotated by 45 degrees, as shown. Therefore, to best support loading due to torsion, fibers should be oriented in the plus- and minus-45-degree directions. This would be used to form the basis of the majority of laminates across the tub, considering it to be a long tube. However, this theory breaks down at the cockpit opening, where the chassis is no longer a closed cross section. Due to the large opening required by the rules we expected this region to be significantly less stiff than the rest of the chassis, and therefore be the governing compliance of the system. We would focus our efforts on this region to design the monocoque to best meet our torsional stiffness requirement.

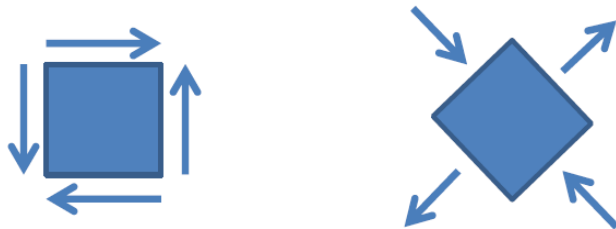


Figure 7.2 - 45-degree transformation of shear load on a stress block.

Methods for calculating the stiffness of a tube of open cross section were investigated. First, (1) was found for angular deformation of a closed cross section in Shigley’s Mechanical Engineering Design, Chapter 3. It was reworked with the open cross section approximation in (2) from Roark’s Formulas for Stress and Strain, in which  $t$  is material thickness and  $L_m$  is cross-sectional perimeter. (1) was then modified to work with our composite material using (3), in which  $A_{66}$  is the laminate shear stiffness from CLT.

$$\varphi = \frac{TL}{GJ} \tag{1}$$

$$J = \frac{L_m t^3}{3} \tag{2}$$

$$G = \frac{A_{66}}{t} \tag{3}$$

Initial calculations yielded very low stiffness numbers. We discovered that the equation was for a structure unrestrained at either end, providing axial freedom which greatly reduced torsional stiffness, as demonstrated in Figure 7.3. This was unlike the chassis, in which the cockpit opening had closed cross sections at either end to restrain it.

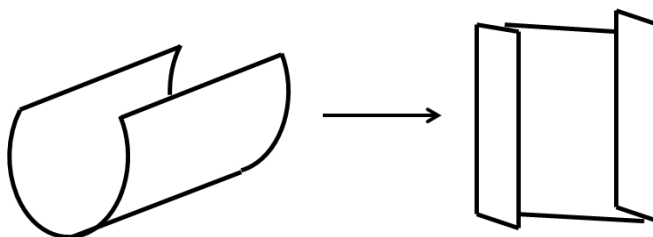


Figure 7.3 - Unrestrained tube with open cross section under torsion. Note the axial deformation in the top view at right.

An improved model which had the structure restrained at one end as shown in Figure 7.4 was found in Cook & Young’s Advanced Mechanics of Materials, Chapter 9 as developed by Timoshenko, and modified to work with our composite material. By halving the length of the structure and doubling the deformation, both ends were mathematically restrained (essentially, two structures with their unrestrained ends connected). However, this too gave very low stiffness values. After some further investigation, we discovered that both models were poor representations of our composite structure because they were developed for thin-walled, isotropic structures. This explained why the thickness

terms in the equations were so prominent, and difficult to apply to our thick composite laminate which has completely different properties and shear-flow characteristics, exhibited in Figure 7.5. This discovery showed the importance of using edge close-outs around the cockpit opening, something which wasn't done on recent Cal Poly chassis.

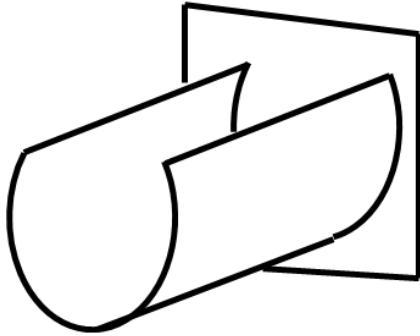


Figure 7.4 - Tube restrained at one end.

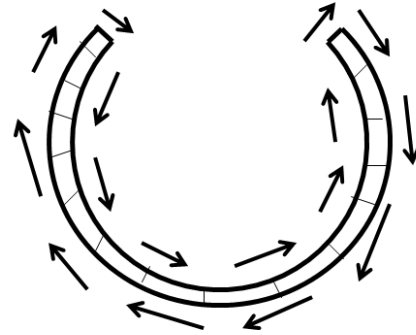
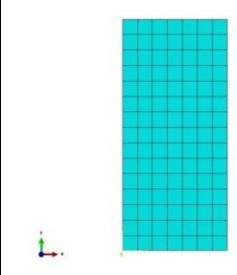
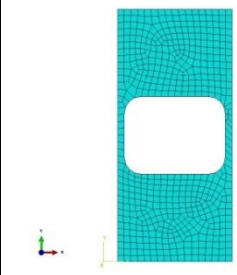
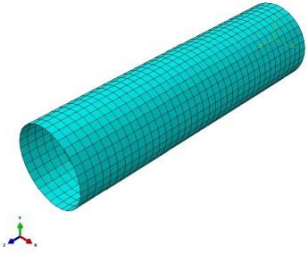
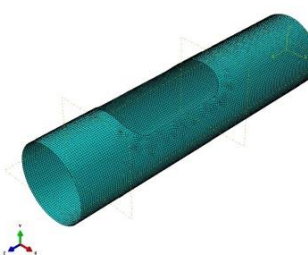



Figure 7.5 - Shear flow in a composite laminate with core.

We switched our focus to FEA using Abaqus/Standard, with linear-quadrilateral shell elements and the Composite Layup feature. Five models were created in the development of the analysis, shown in Table 7.2. The first two represent the entire circumference of the section of the monocoque around the cockpit opening, unwrapped to create flat geometry. A full report is included in Appendix B: Cockpit Opening Stiffness Analysis.

Table 7.2 - Cockpit opening finite element models.

Model	Image	Structure	Details
1		2D rectangle	Used to validate FEA results against CLT. Element size was arbitrary. Car longitudinal axis is horizontal as shown.
2		2D rectangle with cutout	Used to begin development of the laminate in a simple model and compare to subsequent 3D results. The two extreme edges were maintained parallel to each other to represent both ends being restrained by the rest of the chassis. A mesh convergence study was required due to the complex geometry.

3		3D round tube	Used to validate the FEA results against CLT. A mesh convergence study was required due to the complex geometry.
4		3D round tube with cutout	Used to determine element size for Model 5 through a mesh convergence study.
5		3D round tube with cutout and partitions	Used to finish development of the laminate and experiment with different laminates immediately fore and aft of the cockpit opening.

For Models 1 and 3, which were of simple geometry, FEA results were shown to match those of CLT. A comparison between results from Model 1 and Model 2 showed that the cockpit opening reduced stiffness of that section of chassis by 89%, confirming our suspicion that it would be the governing compliance of the system.

The first results influencing the laminate design came from Model 2. The laminate with highest specific stiffness was one made up of 45-degree cloth and 90-degree unidirectional plies. This suggested that the best laminate was one which provided a solid connection around the circumference of the chassis, complementing the torsional support from the 45-degree fibers. This laminate also performed best in Model 5, showing the ability to accurately represent 3D geometry with a simpler 2D model. The runner-up laminate for the 3D geometry, at 90% the specific stiffness of the 45/90 laminate, was purely quasi-isotropic with 45- and 0-degree cloth plies. This simpler and more versatile laminate, with exclusively cloth plies and fibers in every direction, could be used to obtain similar performance.

The high performance of these two laminates suggested that limiting radial deformation near the cockpit opening was a large factor in maximizing torsional stiffness. We decided to proceed with the quasi-isotropic laminate from the standpoint of manufacturability. Its ability to be easily blended with laminates meeting other requirements around the chassis would make the layup process simpler.

### Loading and Structural Equivalency

The monocoque was split into six regions with unique requirements, shown in Figure 7.6 with requirements specified in Table 7.3. In addition to plies for torsional stiffness, these regions' laminates would incorporate fiber directions which best met the loads they would see during car operation. Some laminates had to meet Structural Equivalency rules.

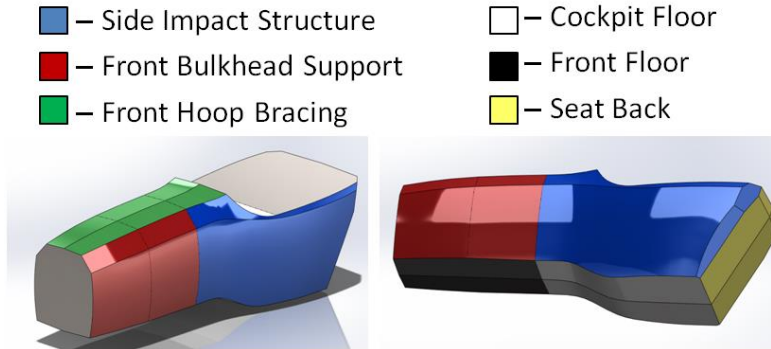


Figure 7.6 - Laminate regions of the monocoque.

Table 7.3 - Requirements for the laminate regions.

Region	Requirements
Side Impact Structure	Structural Equivalency
Front Bulkhead Support	Structural Equivalency, Front Impact, Front Upper Suspension Load
Front Hoop Bracing	Structural Equivalency, Front Impact
Cockpit Floor	Driver Launch
Front Floor	Brake Pedal Effort, Front Lower Suspension Load
Seat Back	Rear Impact

Requirements are detailed in Table 7.4.

Table 7.4 – Requirement details.

Requirement	Description	Load	Geometry
Front Impact	Front supports Impact Attenuator under 40-G front impact	20000 lb, in-plane	Width: 45"
Rear Impact	Back supports driver under 40-G rear impact	$7000 * \cos(30 \text{ deg.})$ lb, bending	Width: 18", Span: 15"
Front Upper Suspension Load	Side supports maximum upper suspension loads under normal conditions	300 lb, bending	Width: 14", Span: 12"
Front Lower Suspension Load	Floor supports maximum lower suspension loads under normal conditions	900 lb, offset from plane	Width: 15", Ecc.: 1.3"



Brake Pedal Effort	Floor supports maximum brake pedal effort from human	450 lb, offset from plane	Width: 6", Ecc.: 8"
Driver Launch	Floor supports driver when jumping out of car	500 lb, bending	Width: 20", Span: 30"
Structural Equivalency: Side Impact Structure	Laminate has properties equivalent to three 1"x.065" steel tubes		
Structural Equivalency: Front Bulkhead Support	Laminate has properties equivalent to three 1"x.049" steel tubes		
Structural Equivalency: Front Hoop Bracing	Laminate has properties equivalent to one 1"x.065" steel tube		

The "Structural Equivalency" requirements were evaluated using Beam Theory through SAE's Structural Equivalency Spreadsheet (SES), while the other requirements were evaluated using CLT and Beam Theory in a MATLAB script. Out-of-plane shear was ignored. For all bending requirements, each laminate was modeled as a simply-supported beam with load distributed across its width at mid-span (in side view, a concentrated load at mid-span). This model was conservative, because the laminates of the monocoque typically had support from all sides including moment reaction, and out-of-plane geometry.

In the early stages of analysis for these requirements, the chosen core thickness of .450" was questioned. This thickness was selected based on previous years' monocoques, assuming that it would allow us to meet bending requirements while maintaining a low ply count, and thereby low weight. However, since the last monocoque had been made, the Structural Equivalency rules had switched from using a "Form" (SEF) to using the aforementioned "Spreadsheet" (SES). Instead of showing calculations in a custom-formatted report, calculations now took place in a controlled Excel spreadsheet. It was discovered that in previous years the team had run very lightweight monocoques because the laminates had not met requirements; SAE's difficulty in evaluating the free-form reports allowed them to sneak by. Now, high numbers of plies were needed to meet requirements, resulting in high weight. This would have a large effect on the car's final weight as compared to our goal.

Alternatives were considered to the .450" option, and analyzed for difference in carbon and core weights. Thickness of .575" gave a total weight reduction of 1.9 lb (2.8 lb less carbon, 0.9 lb more core), and .700" 3.2 lb (5.0 lb less carbon, 1.8 lb more core). A thickness of .700" provided close to the minimum weight - a minimum face-sheet ply count was required to provide fiber orientations to meet requirements for a number of laminates, so increasing core thickness beyond this just added core weight. Because ply count was reduced from the .450" core, less carbon pre-preg material and processing time would be needed for the layup. We proceeded with .700" core for the remainder of analysis.

Laminates were first designed to maximize specific strength using CLT with a strain failure theory, keeping the torsional stiffness analysis results in mind. Only matrix and fiber failure were considered. They were then analyzed in the SES: testing results were used to define an elastic modulus and strength for an isotropic face sheet, which were used with face sheet thickness and core thickness to determine whether requirements were met. From the laminate designs developed using CLT, face sheet thicknesses were increased just enough to meet strength, stiffness, and energy requirements in the SES. Final laminate designs with failure indices for their appropriate loading cases (maximum failure index and fiber failure index) and SES passing margins are shown in Table 7.5.

Table 7.5 - Results of laminate analysis, with minimum SES passing margins and loading failure indices (maximum/fiber only).

Region	Laminate Design	SES	Front Imp.	Rear Imp.	F.U. Susp. Load	F.L. Susp. Load	Brake Pedal Effort	Driver Launch
Side Impact Structure	[45c,0c,0,0c,45c,core]s	14%						
Front Bulkhead Support	[45c,0c,0,0c,45c,core]s	16%	0.51/ 0.07		0.53/ 0.02			
Front Hoop Bracing	[45c,0c,0,core]s	13%	0.52/ 0.11					
Cockpit Floor	[45c,0c,45c,core]s							0.19/ 0.19
Front Floor	[45c,0c,0,0,core]s		0.48/ 0.08			0.54/ 0.06	0.59/ 0.32	
Seat Back	[0c,90,90,45c,core]s			0.71/ 0.53				

SES passing margins were minimized, while failure indices were conservative to make up for lack of load and analysis validation. Failure indices for suspension loads were especially conservative, to ensure performance under repeated and higher-than-expected loading. For the most part, only fiber failure indices were considered. Most of the maximum failure indices represented matrix failure; while these failure indices were high, their magnitudes mostly came from hygrothermal effects due to the laminate cooling from the cure temperature to ambient. Mechanical loading changed the matrix failure indices very little, so the designs were conservative with respect to matrix failure. These findings made sense due to the high elongation at failure of the matrix relative to the fibers. Additionally, analysis with reduced material properties due to matrix failure showed that fiber failure was minorly affected by the matrix having failed.

SES passing margins for the specified laminates were limited by bending strength. This was because the core of the test piece failed in compression at the loading device, as opposed to load increasing up to fiber failure. If the core hadn't failed, SES passing margins would have been limited by stiffness due to laminate shear deformation. See the Structural Equivalency section under Conclusions for further discussion on SAE's Structural Equivalency rules. This testing result suggested a very different failure mode from that assumed in the CLT analysis. See the SAE Laminate Testing section for further conclusions.

Mechanical compromises were made in the laminate design to increase manufacturability. The laminates would have to be blended where they met in the layout to maintain consistent monocoque thickness, so the more similar the laminates the easier the layout process would be. Similar laminates would allow more freedom to lay ply sections spanning multiple regions, making cutting pieces to shape less critical. The entire monocoque had 45-degree cloth at the top of each face sheet (this turned into 0-degree when it hit the seat-back angle). All laminates but the Seat Back had 0-degree cloth for the next ply in. The front half of the monocoque then had 0-degree uni. The Side Impact Structure and Front Bulkhead Support laminates were made exactly the same due to their similar requirements, giving the entire side of the monocoque the same layout schedule. Finally, the Cockpit Floor had a 45-degree cloth

ply which was extended up into the Seat Back. Designing the laminates with manufacturing in mind gave a good combination of performance and manufacturability.

The design of the Front Bulkhead shown in Figure 7.7 was defined in the SES as essentially a stand-alone sandwich structure at the front of the vehicle. A rectangular cutout of 9" width and 7.5" height was made for pedal assembly access, and the face sheets were sized to be .115" thick to just meet requirements, limited by strength.

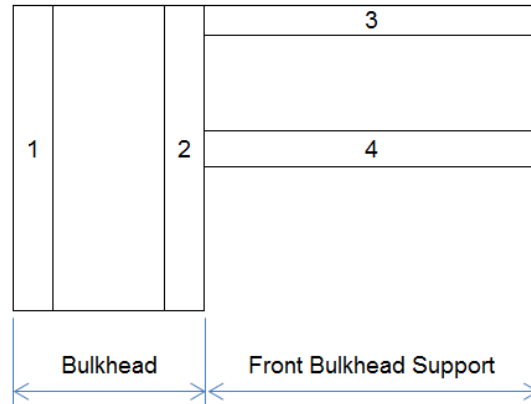


Figure 7.7 - SAE's monocoque front bulkhead model, from the SES (view is looking down edge of bulkhead).

### Attachments

As mentioned in the Monocoque section under Hybrid Chassis Design and Analysis, the attachment points of the suspension into the monocoque structure needed to be analyzed to ensure mechanical integrity. This was done to identify the different failure modes, develop the proper line loads, and apply classical lamination theory to determine the failure indices. Additionally, core shear strength and deflection was analyzed for the upper suspension mounts due to the out of plane nature of the loading.

The attachment holes that were to be drilled into the chassis could fail in two main modes. The first mode was a tension failure mode. This is where the laminate fails at the diameter of the drilled hole, perpendicular to the load applied. Note that this load also has a stress concentration factor associated with it. The second mode is a shear out failure mode. This is where the bolt shears the laminate parallel to the load applied. Figures 7.8 and 7.9 below illustrate these failure modes.

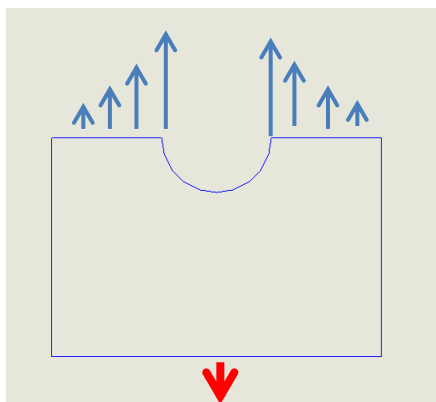


Figure 7.8 – Tension failure mode.

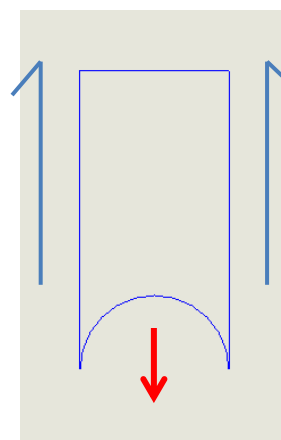


Figure 7.9 – Shear failure mode.

The line loads that are associated with these failure modes are shown below in Figure 7.10. Line loads  $N_x$  and  $N_y$  are associated with tension mode failures, where the line load  $N_{xy}$  is associated with the shear failure mode. Additionally, there are line moments  $M_x$  and  $M_y$  generated due to the eccentricity of the mounting. Each attachment point was analyzed using a 3.5 inch square element around the attachment. (1), (2), (3), (4), and (5) show the line loads and moments used.

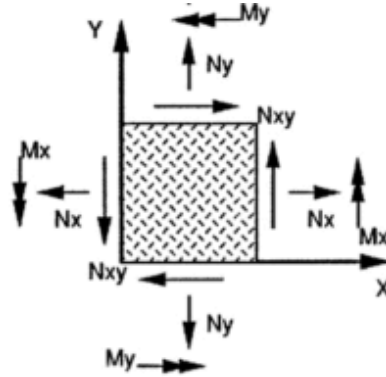


Figure 7.10 – Line loads associated with failure modes shown above. (source: [www.structsource.com](http://www.structsource.com))

$$N_x = \frac{SCF * F_x}{w} \quad (1)$$

$$N_y = \frac{SCF * F_y}{w} \quad (2)$$

$$N_{xy} = \frac{F_x + F_y}{w} \quad (3)$$

$$M_x = \frac{F_x * e}{w} \quad (4)$$

$$M_y = \frac{F_y * e}{w} \quad (5)$$

Table 7.6 below shows the results from the analysis. Only the worst case for each of the upper and lower attachments was analyzed. Note that the failure indices for all the attachment points are all well below 1, meaning that the laminates do not need further reinforcement for in-plane loads.

Table 7.6 – Layups and failure indices for in-plane loading of suspension attachment points.

Attachment Point	Layup	Failure Index	1 <sup>st</sup> Ply Failure, mode
Upper	[45c/0c/0/0c/45/core] <sub>s</sub>	0.34	0 uni, matrix
Lower	[45c/0c/0 <sub>2</sub> /core] <sub>s</sub>	0.41	0 uni, matrix

Next the core strength was checked for compression and shear failure for the upper suspension mounts as the loading was mainly out of plane. Using (6) below (where A is the contact area of the mount), the compression stress was compared with the compressive strength of the core. The stress was found to be 13.75 psi, which was well under the compressive strength of 270 psi. For shear stress, (7) was utilized where b is the thickness of the laminate and h is the width of the element. The shear stress was found to

be 32 psi, resulting in a factor of safety of 2.6. Due to the uncertainty of the loading in this area, the core in this section was replaced with end grain balsa wood that has shear strength of 427 psi. This resulted in a factor of safety of 13.3, providing extra insurance in the integrity of the chassis.

$$\sigma = \frac{F_z}{A} \tag{6}$$

$$\tau = \frac{F_z}{bh} \tag{7}$$

In addition to the strength of the core at the upper suspension members, the stiffness of the laminate is also important to consider. The loading model used was taken from the Hexcel Design Manual assuming simply supported plate and all four sides, for a conservative estimate. Using the balsa core inserts, the core shear deflection was estimated to be 0.002 inches. This was deemed acceptable as it did not affect the dynamics of the suspension in a significant way.

### Bond

The bond design for the two parts consisted of a butt joint which located the parts relative to each other and then a lap joint both inside and outside for strength. The lap joint greatly increased the bond area between the two parts, and provided a shear connection in a second plane (butt joint bond and lap joint bond were at 90 degrees to each other). It was assumed that all load was taken by the lap joint. The plies of the lap joint would be of lower strength and approximately same thickness of the monocoque's face sheets, and the adhesion between the lap joint and monocoque would be stronger than the monocoque's face sheets; this meant that the lap joint plies would be the failure point. In-plane failure load was calculated using CLT for the weakest face sheet being bonded, found to be 3000 lb/inch. Using the model in Figure 7.11 to develop (1), and assuming a resin shear strength of 2000 lb/inch<sup>2</sup>, a bond width of 1.5" would give the resin the equivalent strength of the face sheet in that direction. The bond lap joint was made a total of 4" wide (a conservative 2" of bond with the face sheet of each part).

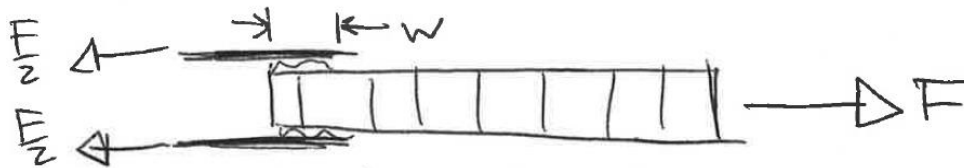


Figure 7.11 - Lap joint loading model, showing the two sets of lap joint plies and a single part.

$$w = \frac{F}{2\tau} \tag{1}$$

## Frame and Front Hoop

### Attachments

The main and front hoops were both required by the rules to be connected to both sides of the monocoque at lower and upper points. For the front hoop, which wasn't a load-bearing structure, brackets with gussets shown in Figure 7.12 and backing plates shown in Figure 7.13 were designed to satisfy the SES.



Figure 7.12 - Front hoop attachment brackets (gussets not yet incorporated).



Figure 7.13 – Front hoop backing plates.

For the main hoop, the same was done for four brackets on the monocoque's sides. However, additional brackets extended from the main hoop to the back of the monocoque as shown in Figure 7.14 (in a plane 90 degrees from the side brackets). With this arrangement, in any loading condition, loads would be transferred in the planes of the brackets and laminates. This maximized strength and stiffness by avoiding bending loads in the relatively thin brackets. In the end, they were incorporated into SES calculations to prove compliance with attachment strength requirements. Gussets between the brackets and main hoop were required due to bends in the brackets, detailed in Figure 7.15. The upper and lower attachment points were located as high and low as possible, respectively, to maximize usage of the monocoque cross section for torsional stiffness.



Figure 7.14 - Main hoop attachment brackets, at 90 degrees to each other.

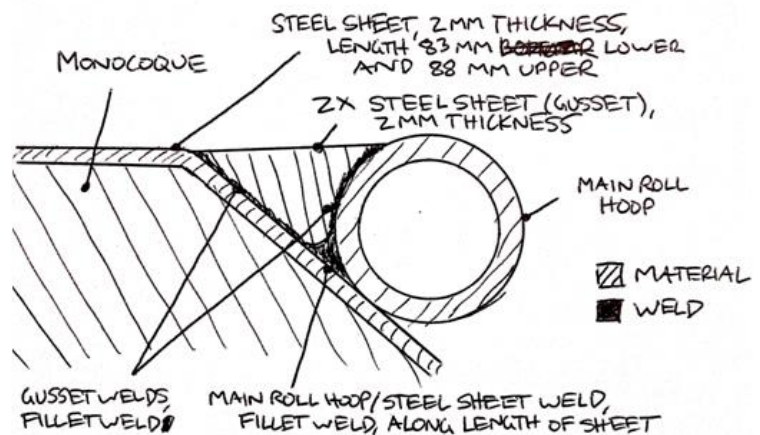


Figure 7.15 - Main hoop attachment bracket gussets.

To determine fastener count at each main hoop attachment point, a 3-G load was considered acting at the car's CG, first vertically and then laterally. Treating the car as a beam with simple supports at the front and rear axles, moment and shear were calculated at the cross-section at the main hoop; moment was reacted by the side mounts, and shear was assumed to be reacted solely by the back mounts. Loading of the attachment points is included in Figure 7.16.

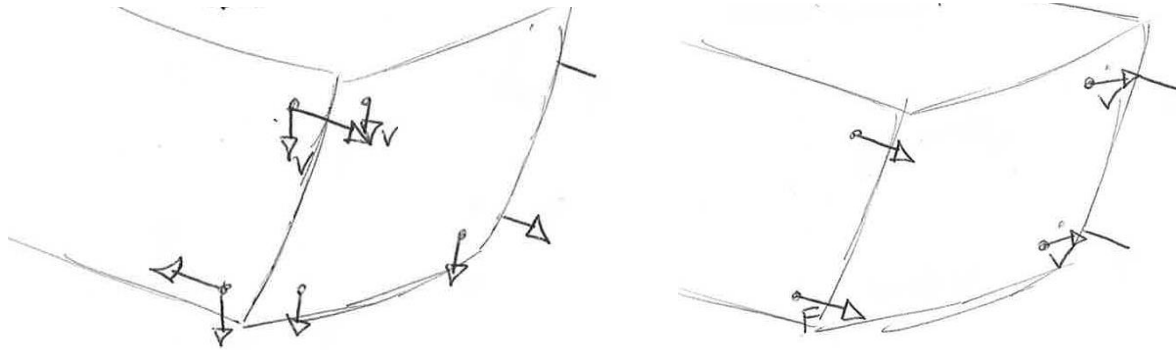


Figure 7.16 - Attachment point reactions. Vertical loading at left and lateral loading at right.

Maximum shear load was calculated to be 900 lb at the side attachments and 200 lb at the back attachments. The minimum requirement of two 5/16" Grade 5 fasteners for the four side brackets was determined to be sufficient to withstand these loading conditions; the back brackets used a single 5/16" fastener each. Considering other factors, the fastener count at the lower side brackets was increased to three to better react out-of-plane loads in the case that the backing plates inside the monocoque were used as harness attachment points. Harness mounting is detailed in the Harness Mounting section.

### Initial Design

The frame had to attach to the monocoque, mount the engine, mount the differential, mount the suspension, mount the shoulder belts, and provide a jacking point. It was initially conceptualized as a main hoop with a box at the rear which mounted the suspension and differential, with space between for the engine. The box was connected to the main hoop in a way which met the structural rules, with triangulated connections to the two monocoque attachment points and the top of the hoop.

As with the monocoque, the frame was designed around torsional stiffness and weight. Approximate geometry was defined in SolidWorks (largely influenced by the 2012 chassis), with a number of options for triangulation methods between the main hoop and box, and a rear suspension. This model was imported into Abaqus; the main hoop was constrained in all three directions at the four monocoque attachment points, and loads were applied to the pushrods at each upright to create a moment. This model would serve as a basic guide to influence geometry, before more detailed and accurate torsional stiffness analysis with the whole vehicle (see the Torsional Stiffness section under Frame and Front Hoop for this analysis). First, the main hoop bracing and its triangulation were analyzed for the options shown in Figure 7.17. Option 1 was the method used in 2012. All options yielded approximately the same specific stiffness, but Option 3 was 3 lb lighter than the others (28 lb as compared to 31 lb for 1 and 2) so it was chosen. With this decided, the triangulating member at the side of the frame was analyzed for two geometries shown in Figure 7.18. Option A weighed 0.5 lb more than B, but its specific stiffness was 20% higher. We proceeded with Option A, deciding that the stiffness gains outweighed the weight gain. Additionally, Option B would have increased the number of members in the main hoop bracing support structure, reducing sizing options.

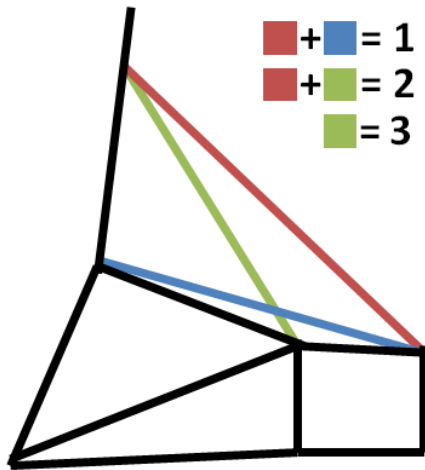


Figure 7.17 - Main hoop bracing options in side view.

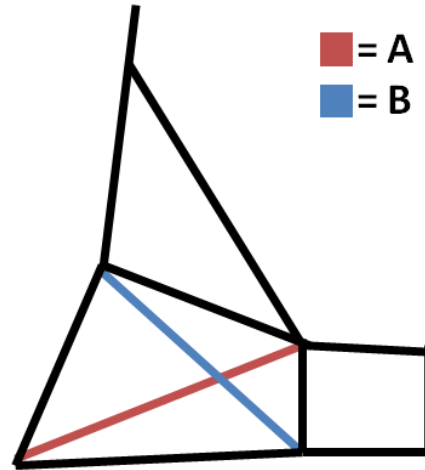


Figure 7.18 - Options for frame triangulation in side view.

With basic geometry settled, the frame was constructed from the ground up to meet hard points. A 3D sketch was created in SolidWorks and lines were drawn which would serve as the base of the frame. Points were defined with dimensions in all three directions in the car's coordinate system to allow for easy location.

First, the main roll hoop geometry was set to incorporate large, 6" bend radii at the lower bends to allow the hoop to closely follow the tub's curvature, and at the top bend to give sufficient room for the driver's head (and look better than the pointy 3" radius at the top of the 2012 hoop). As shown in Figure 7.19, the hoop matched the seat back angle along the monocoque and was angled at 7 degrees from vertical above the upper monocoque attachment point to meet hoop/driver clearance and hoop bracing angle rules while minimizing height. The shoulder harness bar spanned the main hoop at a height which satisfied rules for the team's drivers, and was bent toward the rear to give sufficient shoulder clearance. Gussets in Figure 7.20 were used for support because it was bent; calculations necessitating the gussets were included in the SES submission.

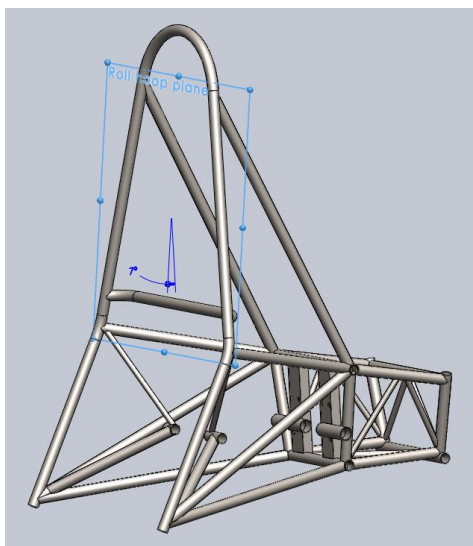


Figure 7.19 - The main hoop geometry.



Figure 7.20 - Shoulder harness bar with gussets.



Moving rearward, a bulkhead was conceptualized which would mount the rear of the engine, differential, rear fore suspension points, and shocks. The engine was located laterally such that its CG was near the car centerline and the chain was able to run to the differential without interference. In the front view of Figure 7.21, the bulkhead had angled sides to meet suspension points, and flat, wide surfaces (rectangular tubes) to mount the differential and allow chain tensioning with the use of shims. Tubes with drilled caps were run across to allow fastening of the rear engine mount, and the shocks would connect to the upper member. This solid structure would serve as the focal point of loads in the frame, thereby minimizing frame weight through using material efficiently and providing simple load paths. For one, the highest load applied to the car, the chain tension load, would transfer directly between the differential and engine through this bulkhead. With the bulkhead locating the rear engine mount, the engine's orientation was set to locate the front engine mounts, which connected to the main hoop at the monocoque attachment points.

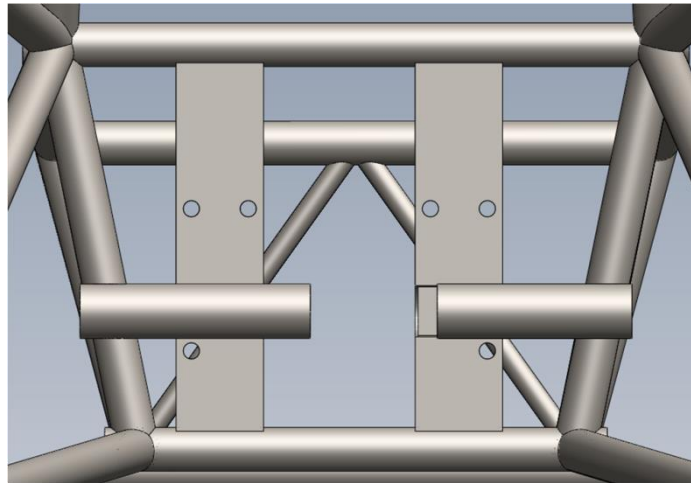


Figure 7.21 - Front view of the frame bulkhead.

Next, at the back of the frame, a simple box in front view was used to mount the aft suspension points. Fore and aft suspension points were moved longitudinally to best meet the bulkhead and box, and the bulkhead's upper member was placed higher than the box's to provide angled members between to mount the rockers in a plane which met the shock mounting point. The rocker mounting concept is shown in Figure 7.22. With the three main structures in place - the main hoop, bulkhead, and box - frame members were placed to connect the dots, resulting in the geometry in Figure 7.23.

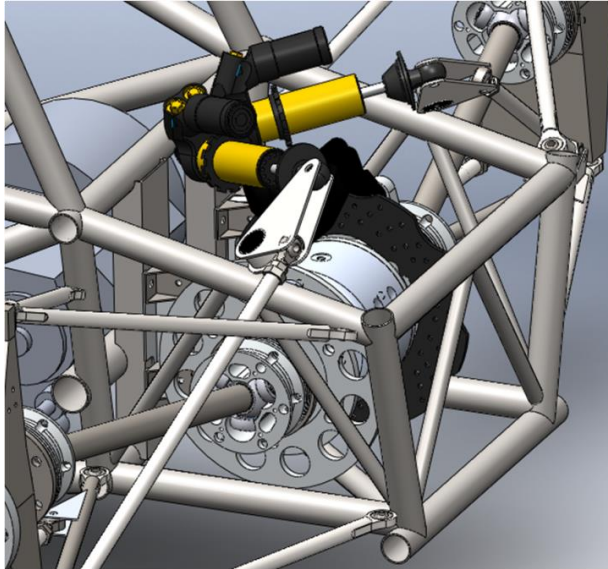


Figure 7.22 - Rear rocker and shock mounting at rear of frame.

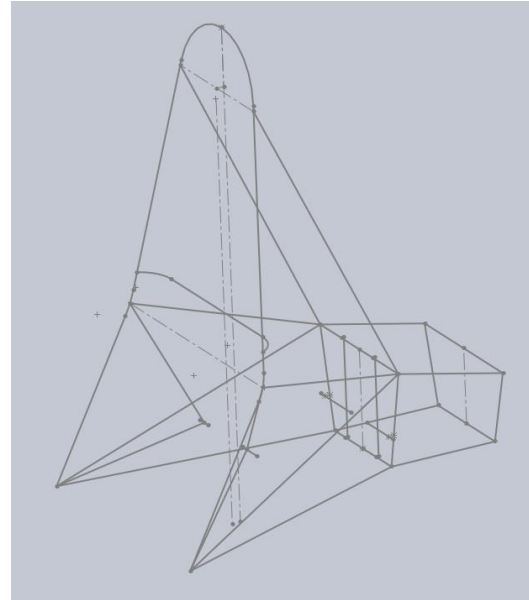


Figure 7.23 - The frame structure in SolidWorks.

All members defined by rules would be constructed of round tubes of 1" outer diameter and defined wall thicknesses. Because of the high specific strength and stiffness of 1" tubing with a thin wall thickness, similar sizing would be used for the other structural members. Members in addition to the base structure, which would triangulate the frame around the suspension, were considered for their possible contribution to specific torsional stiffness. Sizing frame members which weren't defined by the rules in a way which maximized specific torsional stiffness would require FEA.

### Torsional Stiffness

The frame was designed using FEA to maximize specific stiffness and verify that the torsional stiffness target had been met. Loading conditions and results would only be accurate with a vehicle-level model. Specifically, the suspension, monocoque, frame, front hoop, and engine would be modeled with interactions. Loading and constraint would exist at the tire contact patches, and the frame design would be evaluated for its contribution to total system compliance. The monocoque design was left static following its previous development.

The monocoque and engine would be made of 3D shell elements. The suspension, frame, and front hoop would be beam elements. In SolidWorks, the monocoque model was simplified to a solid structure with no fillets or complex edges, and the engine was modeled as a basic solid structure. Their surfaces were selected and saved as .SAT v7 files for easy importing with Abaqus. The suspension and frame were modeled as sketches which were saved as IGES Wireframe files. The suspension geometry was modified at each corner to consist of three members representing the upright, providing the three points to which the six control arms connected. A point at the tire contact patch was connected by members to those three points on the upright as well, providing a point at each corner of the car for accurate loading and constraining. The front hoop was not designed at this stage, so it was created with simple lines and curves in Abaqus. All the modeling in SolidWorks was done in the car's coordinate system, so components were in their correct positions when imported.

Connections between components were required to make them a single system, and were made with rigid beam connectors. These had to connect one node to another, which was easy to do with the

wireframes. The engine also had sufficient nodes, but the monocoque lacked nodes for the suspension, frame, and front hoop. To solve this, the monocoque was brought into Abaqus as a separate part, and meshed based on findings during the laminate development of the Torsional Stiffness section under Laminate Development. The mesh was then written to an Abaqus input file. When the vehicle components were brought into Abaqus from their SolidWorks outputs, this version of the monocoque was imported instead of the .SAT v7 file, now with many nodes. The assembled components are shown in Figure 7.24.

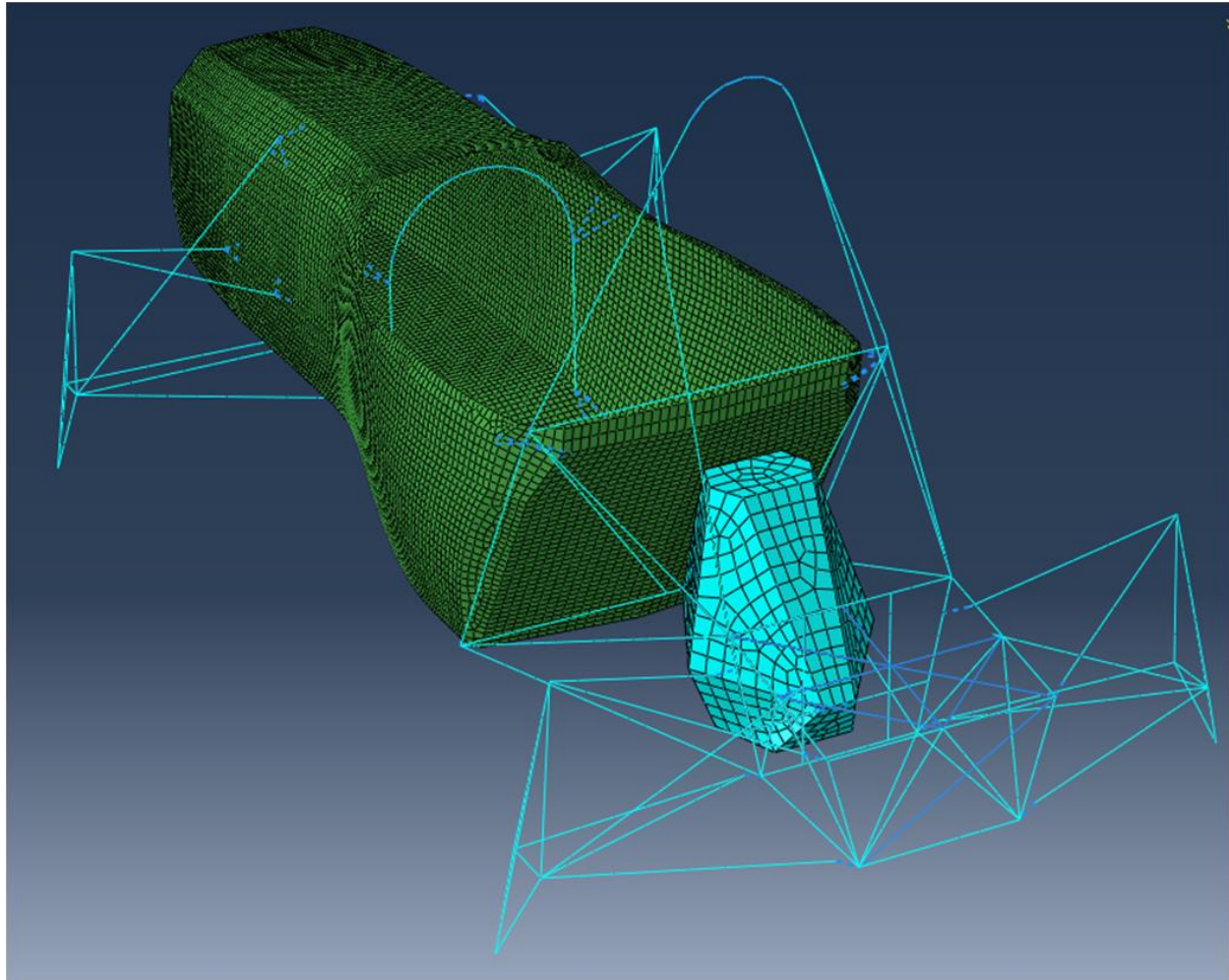


Figure 7.24 - Vehicle assembly in Abaqus.

Different areas of the monocoque were assigned different layup schedules based on the results of the laminate development. The engine was assigned aluminum material properties with a 3/8" thickness. The suspension members were assigned a material named "super steel", which was very stiff. All steel tubes were assigned basic steel material properties. In order to investigate different triangulation options for the rear of the frame, without importing and meshing different versions of the frame over and over again, all possible members were included in the imported frame model in Figure 7.25. A material called "air" was defined, with very low stiffness. Members were turned "off" by assigning this material to them, allowing many different options to be quickly evaluated.

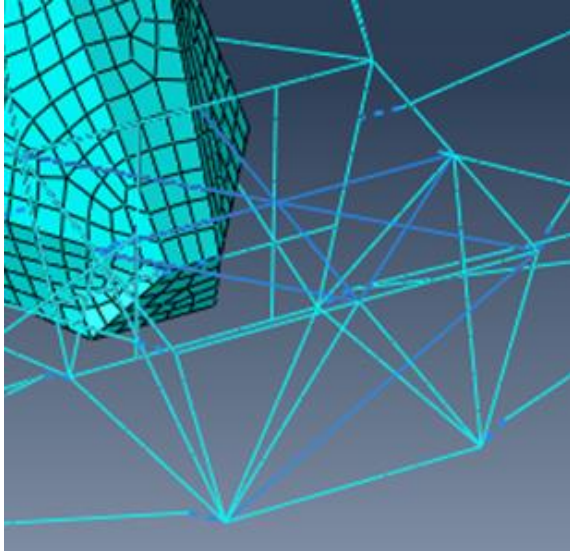


Figure 7.25 - Frame with rear triangulation options.

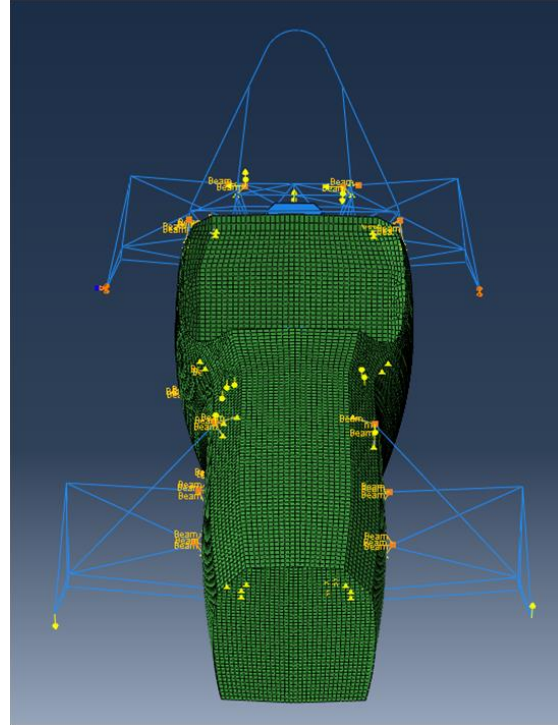


Figure 7.26 - Loads and constraints in finite element model.

To test the torsional stiffness, each tire contact patch was assigned appropriate loads or constraints, represented in Figure 7.26. Each rear contact patch was constrained in the vertical and longitudinal directions, and one of the rears was constrained in the lateral direction. This lack of constraint on the other rear avoided over-constraining the system; however, it was found that constraining both rears in all three directions had little effect on results. This finding may bode well for simpler real-life testing, but was ignored for the time being. Five degrees of freedom were now constrained at the rear. The two options for proceeding from here were to constrain one of the fronts vertically and apply vertical load to the other, or to constrain the rear from rotating about the lateral axis and apply equal and opposite vertical loads to the fronts. The latter option was chosen, but the two produced identical results. A 1-lb load was applied to each front contact patch in opposite directions, and the resulting moment calculated. This in combination with the angular displacement of the front, calculated by measuring the difference in vertical deflection  $\delta$  of the contact patches and considering track width  $T$ , gave the torsional stiffness in (4).

$$K = \frac{FT^2}{\delta} \quad (4)$$

Additionally, loads to represent the shocks were applied, which were calculated using a MATLAB script which output suspension member loads as functions of loads at the tire contact patch. This method was easier than representing the rockers in Abaqus, which would require revolute features as opposed to simple rigid beam connectors to result the pushrods into the chassis.

Results of the triangulation analysis are shown in Table 7.7, with frame member identifications included in Figure 7.27. Figure 7.28 includes deformed shapes.

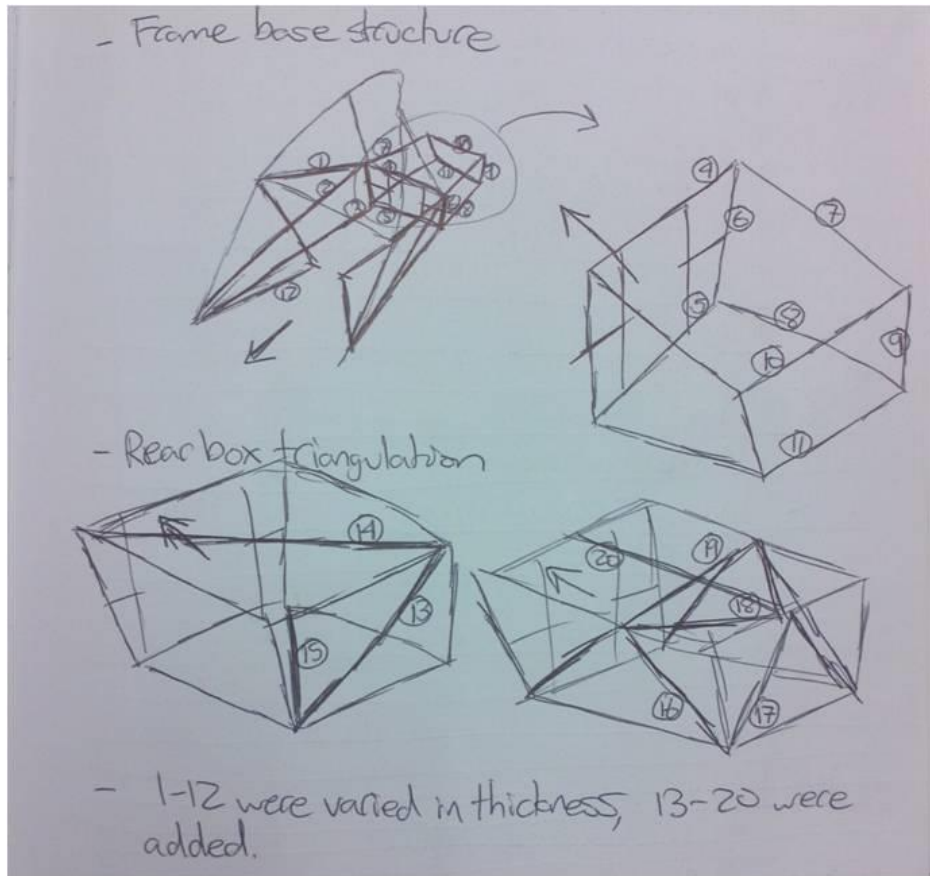


Figure 7.27 - Frame member identifications.

Table 7.7 – FEA results for torsional stiffness.

Members Used	Frame weight (lb)	Disp. for 1-lb corner load (in)	Stiffness (lb*ft/deg)	Norm. specific stiffness
Baseline	48.00	0.002143	1499	89.70
13	48.42	0.002096	1533	90.94
14	48.53	0.002068	1554	91.98
15	48.44	0.002002	1605	95.18
16	48.77	0.002116	1518	89.41
17	48.34	0.002092	1536	91.27
18	48.53	0.002118	1517	89.79
13, 14	48.95	0.002024	1587	93.13
13, 15	48.86	0.001943	1654	97.24
16, 17	49.11	0.002007	1601	93.64
16, 13	49.19	0.002016	1594	93.08
18, 20	48.85	0.002108	1524	89.61
16, 13, 14	49.72	0.001982	1621	93.65
16, 13, 15	49.63	0.001866	1722	99.67
16, 17, 15	49.55	0.001863	1725	100.00

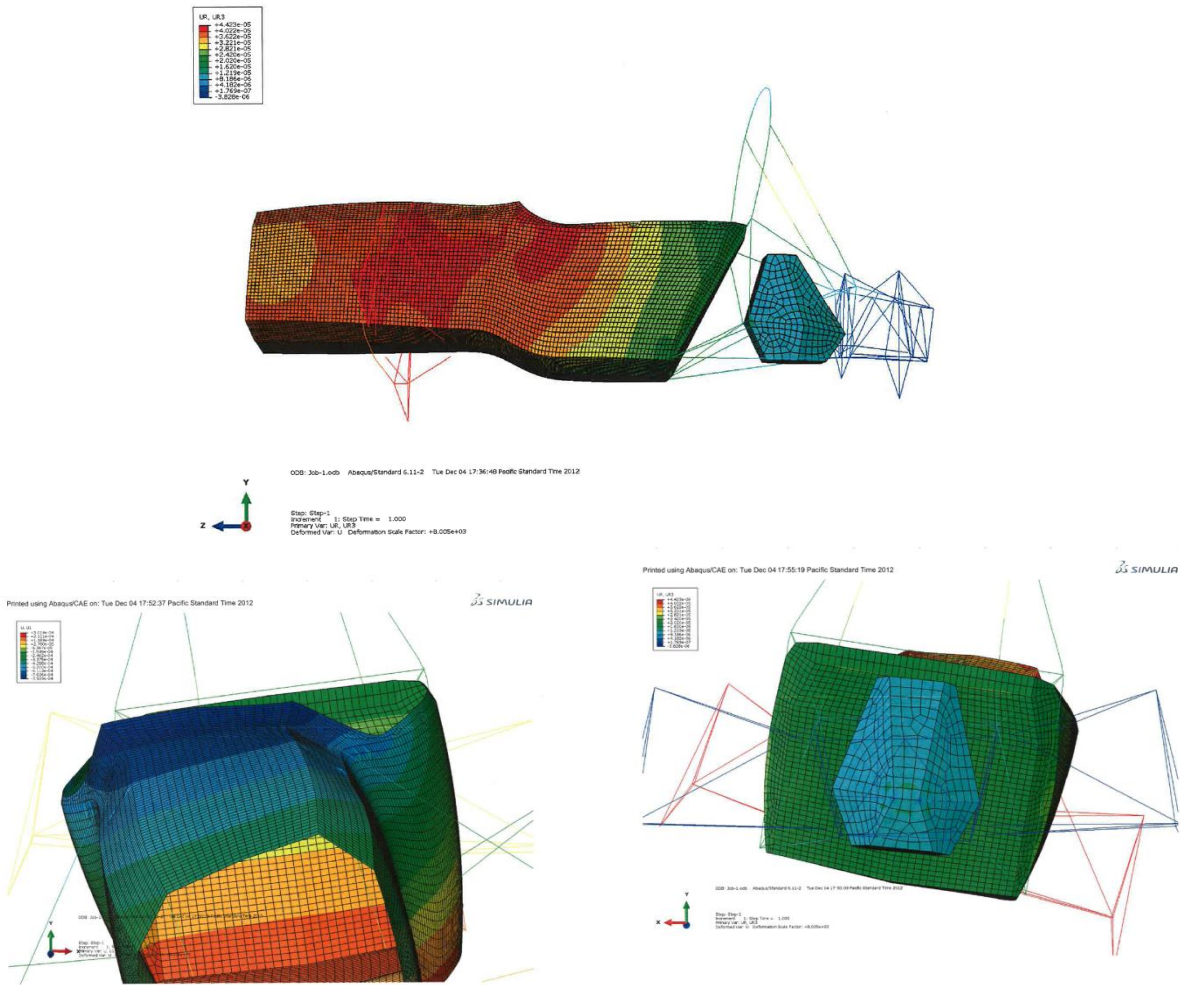


Figure 7.28 - Deformed shapes from torsional stiffness finite element model. Color graph represents node rotation about the longitudinal axis.

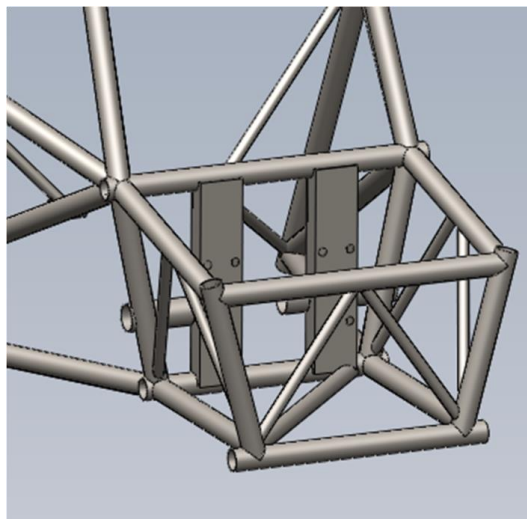


Figure 7.29 - Frame with chosen rear triangulation.

The frame with Members 16, 17, and 15, shown in Figure 7.29, not only gave the highest specific stiffness, but also met our torsional stiffness requirement of 1700 lb\*ft/deg. Proceeding with this combination, we experimented with increasing the wall thicknesses (or diameters, if less than 1”) of the base frame members to see if further gains could be had. Results of the stiffness sensitivity study are shown in Table 7.8.

**Table 7.8 - Sensitivity of torsional stiffness to sizing of various frame members.**

<b>Members Modified</b>	<b>Frame weight (lb)</b>	<b>Disp. for 1-lb corner load (in)</b>	<b>Stiffness (lb*ft/deg)</b>	<b>Norm. specific stiffness</b>
Baseline	49.55	0.001863	1725	100.00
1	49.97	0.001855	1732	99.56
2	50.22	0.001846	1740	99.52
3	50.17	0.001823	1762	100.88
4	49.73	0.001845	1741	100.56
5	49.68	0.001851	1736	100.37
6	49.79	0.001843	1743	100.56
7	49.81	0.001855	1732	99.88
8	49.81	0.001860	1727	99.59
9	49.73	0.001862	1725	99.64
10	49.73	0.001858	1729	99.87
11	49.68	0.001861	1726	99.80
12	50.19	0.001858	1729	98.95

A few members were able to increase specific stiffness, but since the stiffness goal was already met we decided to not increase wall thicknesses in the interest of minimizing weight. However, these members were now identified as the most important for the front/rear connection. If stiffness needed to be increased in the future, good ways to do it were now obvious.

The FEA model could be improved to produce more accurate results. First, through experiment, better connection methods than rigid beam connectors could be developed. Also, revolute features could be used to represent the rockers; with a member running from each rocker to the chassis to represent the shock, stiffness in addition to load would be represented. For the suspension, members with realistic stiffness values may provide better insight into actual hub-to-hub stiffness. As an improved analysis method, better understanding of each component’s contribution to the system stiffness could be easily developed and used in the design process. Also, analysis of stiffness distribution along the chassis’ length could provide insight into behaviors during transient cornering.

Not only was the frame geometry advanced by this analysis, but also a few behaviors were discovered. The stiffness of the front of the chassis was 3210 lb\*ft/deg, and the rear was 3720 lb\*ft/deg. With the monocoque/frame connection at about 39” behind the front axle, this meant that the monocoque had a stiffness of 125000 lb\*ft/deg/inch, and the frame 93000. The composite monocoque structure was approximately 35% stiffer in torsion than the steel-tube frame, which was expected due to the tube-like geometry of the monocoque. Also, removing the front hoop reduced system stiffness by 12%, and monocoque stiffness by 20%. This agreed with the finding from the laminate development that limiting radial deformation was the key to stiffness at the cockpit opening. While the front hoop had a large effect on stiffness, removing the engine reduced stiffness by only 2.5%. This suggested that engine mounting was not important from the perspective of torsional stiffness.

## Final Construction

The geometry was next modified to increase manufacturability and best meet hard points. The simple geometry was good for FEA, but had to be improved for the final frame construction. A new 3D sketch was created in SolidWorks, which referenced the base frame sketch and incorporated adjustments to point locations. First, the box's lower member was placed as shown in Figure 7.30 to meet rules to serve as the car's jacking point; its bottom half was now fully exposed, and it extended to the 12" length defined by the rules. The triangulating tubes at the rear of the frame were offset from nodes and the differential mounting tubes were adjusted longitudinally, both to simplify notching. See Figure 7.31 for the sketch with all adjustments. The base and adjustment sketches were used with the Weldments tools (Structural Members and Trim/Extend) to form the frame solid model. Using these tools as opposed to generating individual extrusions allowed member cross sections to be easily defined, and simplified reconstruction of the solid model through editing the sketch.

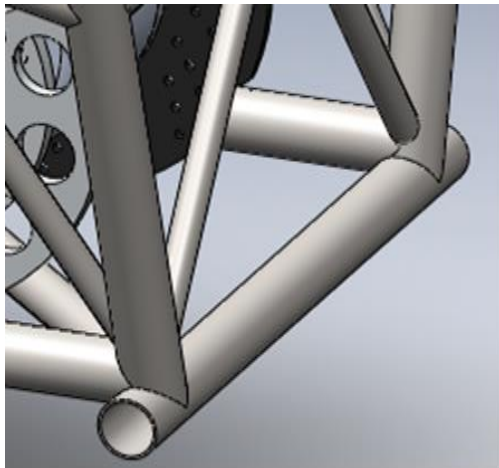


Figure 7.30 – Jacking point detail.

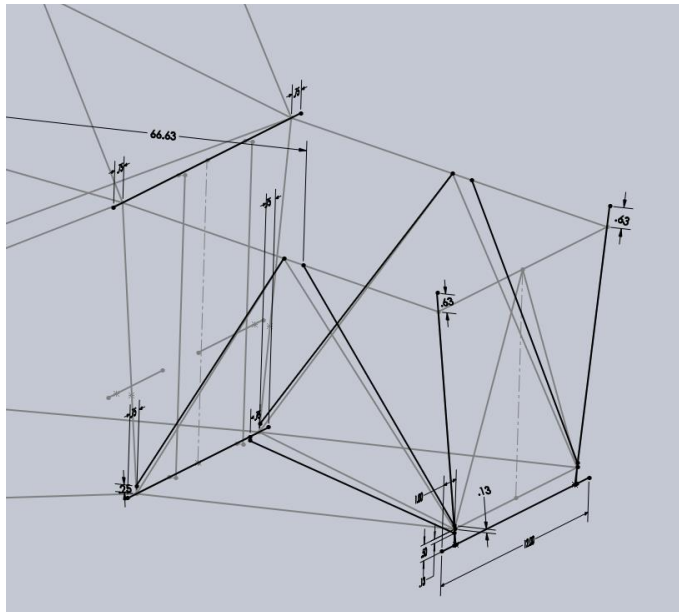


Figure 7.31 – Adjustments made to frame sketch in SolidWorks.

The Trim/Extend tool could be used to notch tubes in SolidWorks. By exporting a notched tube to a new part, making a cut to discontinue the circumference, and then using the Sheet Metal tools to “unwrap” the tube, the outline of the notched tube was created. This could be printed as a drawing at 1:1 scale, and then wrapped around a real-life tube for guided notching. To make manufacturing easiest while using this method, notches were planned such that each tube end was notched for no more than 2 other tubes at each node, which minimized notch complexity. The lateral members of the bulkhead and box were left with unfinished ends, and the vertical tubes were notched for the single tube at each of their ends (simpler than a miter notch). This strategy was modified for the box, with the upper ends of the vertical tubes left unfinished to allow suspension tabs to be easily welded. Images of these notches are shown in Figure 7.32. The unfinished ends of the tubes had to be extended beyond their nodes in the sketch to allow for full mating with the notched tubes, as shown in Figure 7.31. The longitudinal tubes connecting the bulkhead and box were notched for the 2 tubes at each end. The remaining planning dealt with connecting from the upper nodes of the bulkhead to the three points on the main hoop. The tubes were notched in ascending order as shown in Figure 7.33, keeping the notches simple and easing assembly of the members.



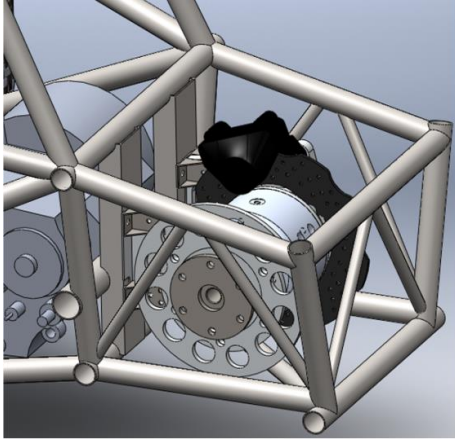


Figure 7.32 - Bulkhead and box notch detail.

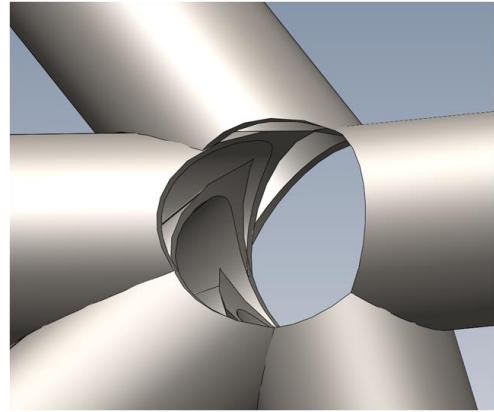


Figure 7.33 - Notches at upper node of bulkhead with unfinished tube hidden.

The final frame solid model is shown in Figure 7.34. Detail of mounting of other components at the rear is shown in Figure 7.35. Because of an inaccurate engine solid model, the left-hand rectangular tube for mounting the differential was modified during manufacturing to clear the engine case and chain. Also, the front engine mounting tubes were changed from the 1/2" outer diameter shown to 7/8" to increase strength and stiffness.

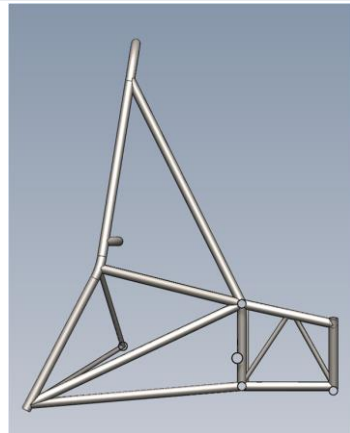
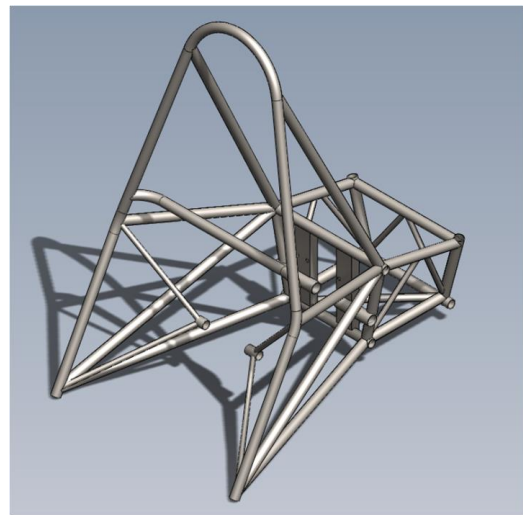
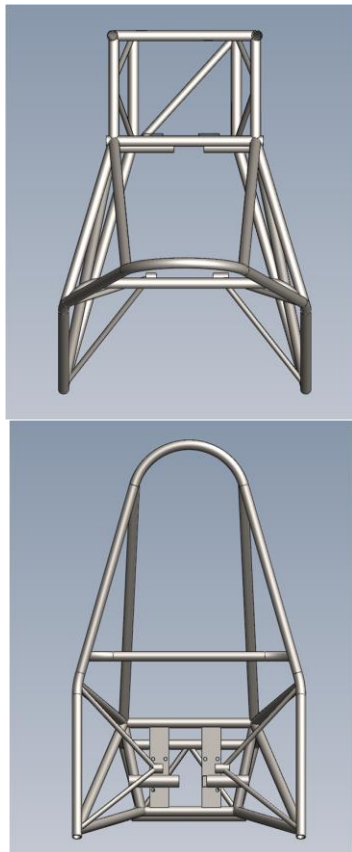


Figure 7.34 – Frame solid model in its final form.

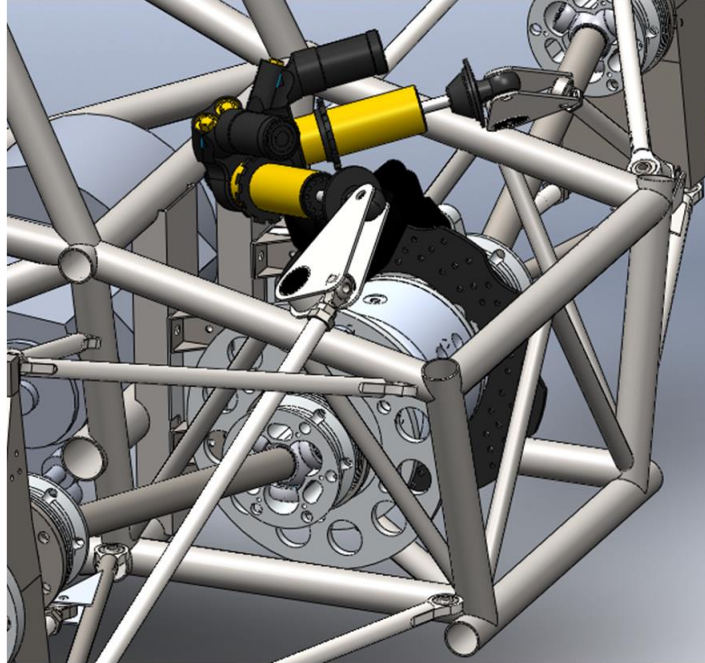


Figure 7.35 - Rear assembly.

The front hoop in Figure 7.36 was designed to follow the cross-sectional profile of the monocoque at the front of the cockpit opening and exceed the height of the steering wheel (as specified in the rules). Its attachment points would be at the top and bottom of the monocoque's sides, and an attachment point at its top would allow the top of the monocoque to serve as the front hoop bracing. The front hoop was level with the laminate at this point so that the laminate could be fastened between brackets extending from the top and bottom of the front hoop tube, as detailed in Figure 7.37 and shown on the car in Figure 7.38.



Figure 7.36 - Front hoop.

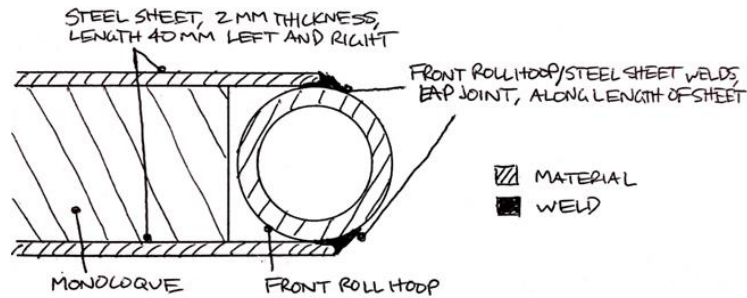


Figure 7.37 - Side section view of the top of the front hoop and monocoque from the SES submission.

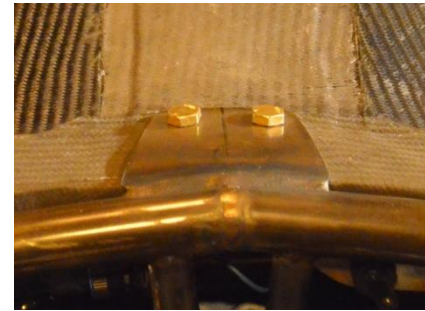


Figure 7.38 - Front hoop bracing brackets.

## Nose Cone/Impact Attenuator

We decided to manufacture a custom Impact Attenuator (IA) as opposed to using SAE's standard IA. A composite-skin nose cone which acted as the IA would weigh approximately 2.2 lb with fasteners, while using the standard IA would require a similar 2-lb nose cone for aesthetics plus the 2.2-lb foam attenuator (including fasteners). Also, the nose cone would transfer load directly into the monocoque's skin, avoiding bending loading on the Anti-Intrusion Plate or front bulkhead which could require extra support. Finally, the standard attenuator was not designed to meet the team's impact requirements.

For the nose cone to act as the IA, it would have to be designed to meet our energy absorption and acceleration requirements. For a front impact at a speed of 35 ft/s, bringing the car to a stop without exceeding 20 G would require at least 11.4" of usable length, calculated using (1).

$$L = \frac{v^2}{2a} \quad (1)$$

The nose cone was designed to be 13.4" long to provide a safety margin on this requirement. The shape was envisioned to be of decreasing cross-sectional area moving from the front bulkhead forward, to ensure that maximum line load was always as forward as possible. This way, failure would theoretically occur at the position of the impactor and not farther down the nose cone which could result in an unstable failure mode.

The laminate was designed with plies of unidirectional fibers placed at alternating perpendicular directions (0 and 90 degrees) to provoke delamination under normal loading. This delamination in combination with fiber failures would absorb the impact energy. The forward 3" of the nose cone (cap) was made of far fewer plies than the main structure, such that it was essentially non-existent. This exposed the edges of the laminate of the main structure to the impactor and initiated failure in fiber breakage and delamination. The cap would likely fold into the nose cone under loading, and if it was strong there was a risk of it bringing the rest of the structure with it, resulting in less-powerful failure modes.

To create the part in SolidWorks, the loft feature of the monocoque was extended ahead of the front bulkhead. In the side view of Figure 7.39, material was removed to shape the profile of the nose cone, define its length, and ensure that the radius of the forward edge met the 1.5" required by the rules. The dimensional requirements from the rules for the IA were easily met. Fillets were used to finish the general shape before a cut was made at each of the four corners for mounting to the front bulkhead

using fasteners. Draft angles were included longitudinally and vertically in the profile of the cut, shown in Figure 7.40, which was extruded forward with a draft angle. This geometry would ease machining and mold manufacturing.

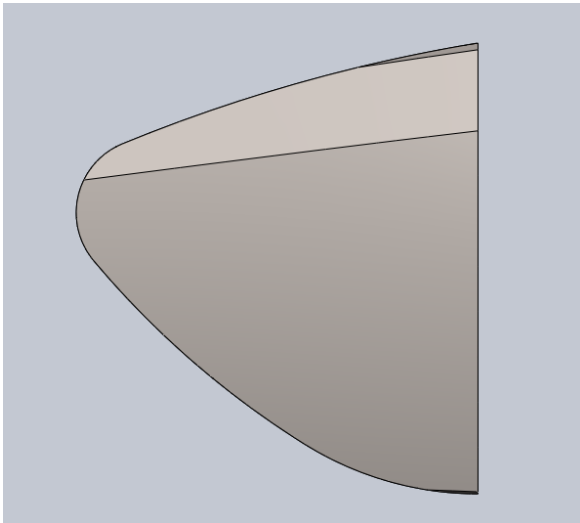


Figure 7.39 - Side view of nose cone construction, cut from extension of monocoque loft.

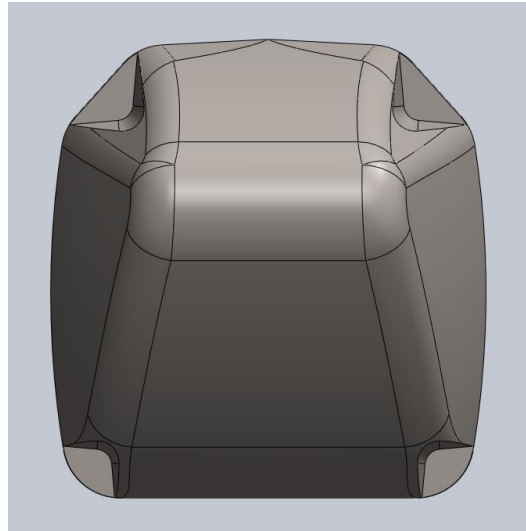


Figure 7.40 - Front view of material removal for mounting fasteners.

Edges created by the material removal were filleted. The holes for the axial mounting fasteners were located inward of the edges by a comfortable margin to avoid non-flat surfaces near the edges of the front bulkhead, and clearance was given for the head of an M8 socket head cap screw and its washer. Images of the final nose cone model, with a shell feature, are shown in Figure 7.41.

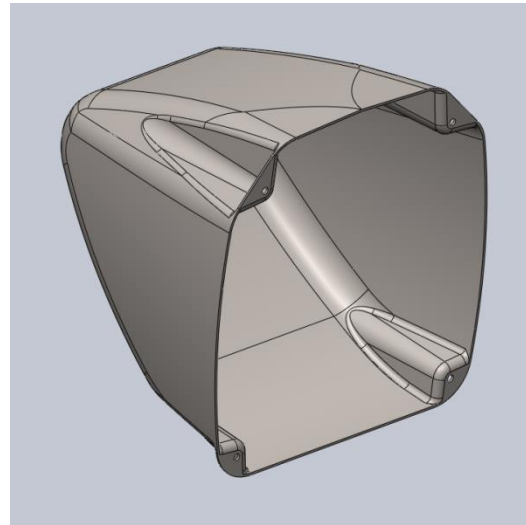
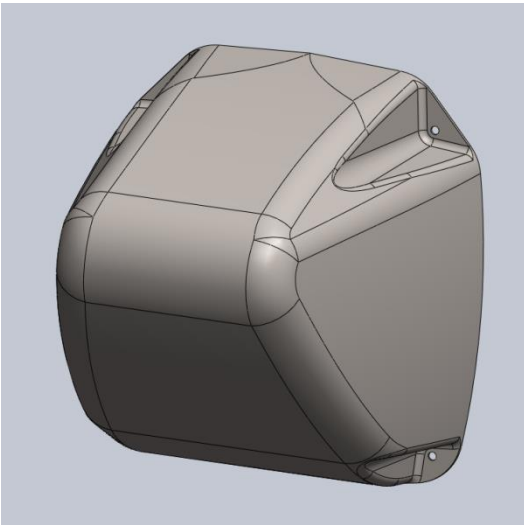


Figure 7.41 - Nose cone solid model.

## 8. Laminate Testing and Data Analysis

Given the carbon fiber composite structure that was chosen for the chassis, various tests needed to be conducted to ensure structural integrity. These tests included verifying designs for layup schedules, core materials, attachments solutions, and impact structures. In addition to proving structural integrity, the tests conducted also proved equivalency to the standard steel tube space frame set forth by SAE, a necessary step in getting approval to compete in the Formula SAE Collegiate Design Series. All of the following tests were performed in the Cal Poly Composites Lab in room temperature on the Instron Test Machine unless noted otherwise.

### Material Properties Testing

The first series of tests were done to verify the materials that were donated to FCW by Quatro Composites in San Diego, CA. The carbon fiber donated was considered expired for aerospace use since it was more than one year old. Therefore, to ensure resin integrity, material property tests were conducted.

The tests selected for verifying material properties were the ASTM 3518 45 degree tensile test and the ASTM 790 flex test. These tests were to be initially conducted on two rolls material: a roll Torayca T800H-6k PW/3900-2D carbon fiber cloth and a roll of Aldila X534-AF254-150/35 unidirectional carbon fiber. All test pieces were cured for one hour at 250°F with 5°F/min ramps. All tests were done at room temperature.

The ASTM 3518 45 degree tensile test was done on the unidirectional and cloth test specimens to determine the shear properties. These properties were not reported in the material data sheets, so these values will be used in the design and analysis. Figure 8.1 below shows the test setup. Table 8.1 below shows the results from the tests.



Figure 8.1 – ASTM 3518 45 degree tensile test set up.

Table 8.1 – ASTM 3518 test results.

Specimen	Layup Schedule	Shear Modulus (MSI)
Unidirectional Tape	[+45/-45] <sub>8s</sub>	0.723
Cloth	[±45] <sub>8s</sub>	0.0619

Figures 8.2 and 8.3 below show the stress strain curves for the unidirectional and cloth specimens respectfully. Note the extremely low shear modulus for the cloth specimen. This is consistent with the results from the ASTM 790 test discussed later in this memo.

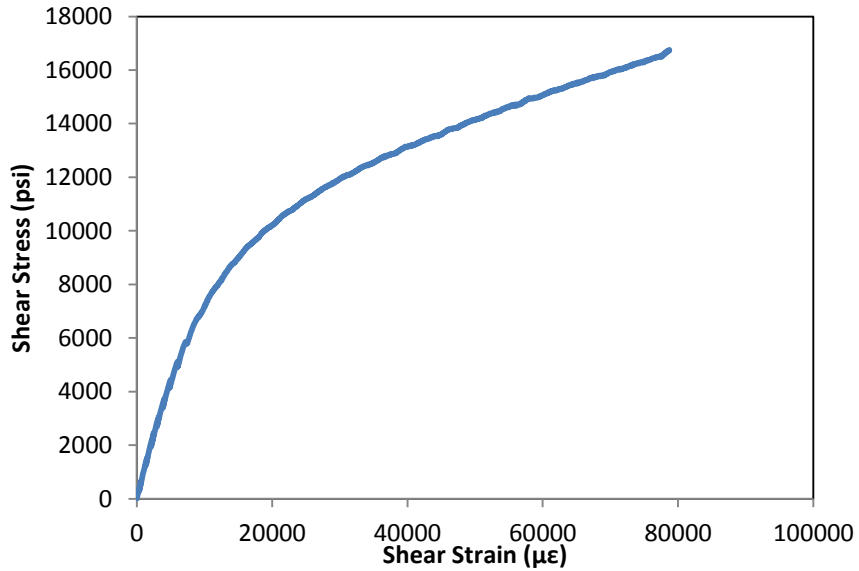


Figure 8.2 – Stress strain curve for unidirectional carbon fiber specimen from ASTM 3518 test.

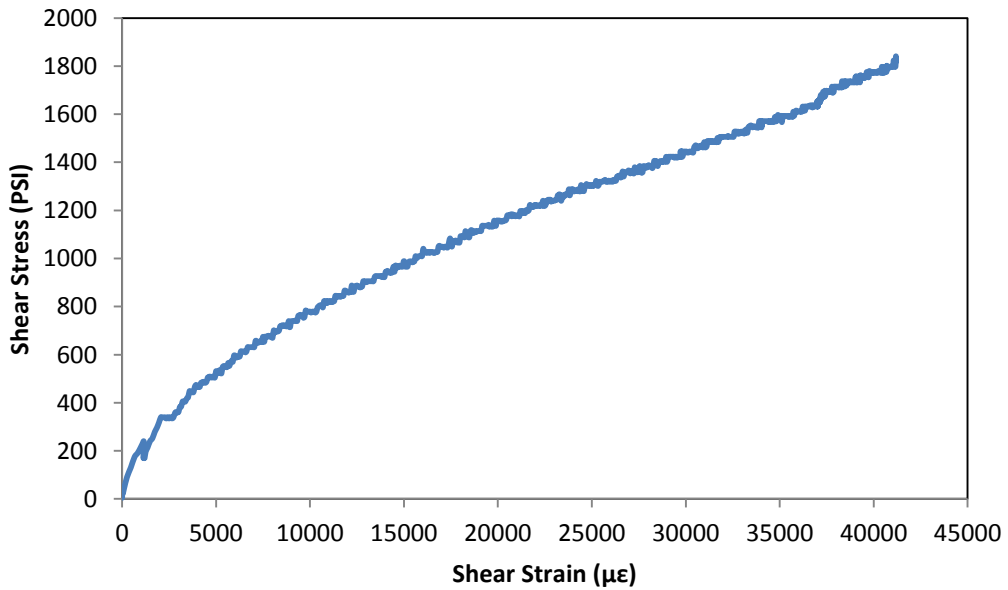


Figure 8.3 – Stress strain curve for cloth carbon fiber specimen from ASTM 3518 test.

Next, the ASTM 790 flex test was done on 3 samples of cloth and unidirectional tape each. Figure 8.4 below shows the test setup. Table 8.2 below summarizes the average results.



Figure 8.4 – ASTM 790 flex test setup.

Table 8.2 – ASTM 790 test results for unidirectional and cloth carbon fiber laminates.

Specimen	Layup	Average Flex Modulus (MSI)	Reported Flex Modulus (MSI)
Cloth	[0] <sub>4</sub>	4.175	22
Unidirectional	[0] <sub>8</sub>	17.356	19

The unidirectional tape's flex modulus was within 10% (actual 8.6%) of the reported value. We can conclude that the matrix still holds its integrity and the reported values can be used for design.

On the other hand, the tested value of the cloth was found to be only about 20% of the reported value (81% actual error). This shows that something with the matrix of the pre-preg is off. Either the matrix has been compromised with too much out-time, the manufacturing process was incorrect, or the test method was not followed properly.

One mistake noted with the test results was that the cloth span to depth ratio was a little high. On average it was about 24:1, which is higher than the ASTM specified 16:1. This could've contributed to the unusual results.

However, the big mistake was that the wrong cure temperature was used for the cloth. After some investigation after the test, it was found that the Torayca 3900 series epoxy is a 350°F cure. In short, the cloth pieces used in these tests were not fully cured and so they did not behave as predicted.

This presented a dilemma to the team since the two materials were incompatible with one another due to the different cure temperatures. Carbon fiber cloth that was compatible with the unidirectional tape was obtained from Quatro Composites. However, since this material was obtained so late in the timeline of the project, it was decided that the SAE laminate tests would be conducted without explicitly testing the integrity of the matrix.

## SAE Laminate Testing

The Formula SAE competition requires a series of composite material tests to prove that the proposed structure meets the same energy absorption as that of the baseline steel tube space frame defined by SAE. These tests include a three-point bend test on the side impact structure, a penetration test, and a harness attachment test. For all of these tests, the material that was used was the same carbon fiber prepreg that would be used to construct the chassis. The unidirectional material was the same from the previous tests (Aldila X534-AF254-150/35) and the cloth was the new material donated by Quatro Composites (Aldila 3K2X2-AX021610G-024/36). All of the test pieces were cured at 250 °F for one hour with 5 °F/min ramps.

The first test performed was the three point bend test in accordance with Formula SAE Rule T3.31. The panel was constructed using the lay-up schedule of  $[45_c, 0_c, 0_c, 0_c, 45_c, \text{core}]_s$  and had dimensions of 24 inches long by 8 inches wide. The testing rig was constructed out of steel and had a span of 20 inches, as per Formula SAE rules. A picture of the test set up is shown below in Figure 8.5.



**Figure 8.5** – Test setup picture for SAE three point bend test in accordance to rule T3.31. The rig had a span of 20 inches and could accommodate a specimen up to 8 inches in width.

The initial test piece failed as it was not stiff enough and did not absorb enough energy to meet the baseline steel equivalent. Figure 8.6 below shows the load vs. deflection curve for the initial test piece. The specimen failed in shear, as noted by the “S” shape it formed depicted in Figure 8.7. Also note that the face sheet completely debonded from the core despite the application of sheet resin. This is indicative that the inter-laminar shear stress between the face sheet and core was too high and caused the specimen to fail prematurely. It was determined that the core was oriented in the “wrong” direction, meaning that the ribbon direction of the core was placed perpendicular to the span of the specimen. This caused the core to be too flexible when introduced to shear loading and thus built up too much inter-laminar shear stress with the face sheet.



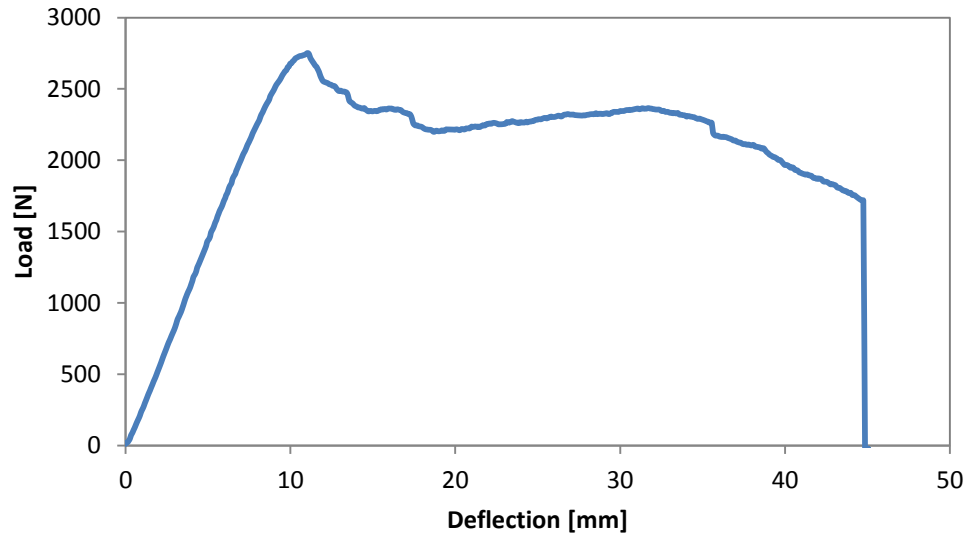
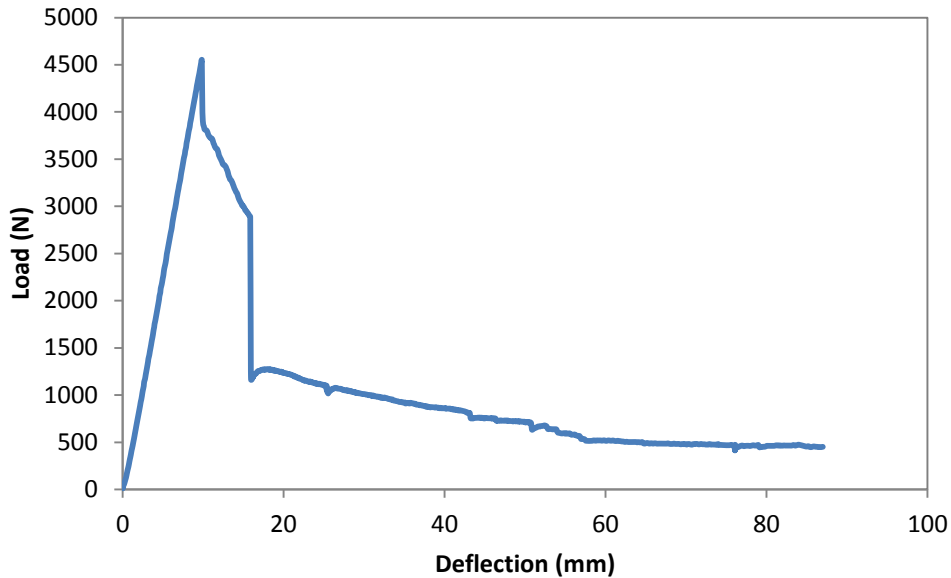


Figure 8.6 – Load versus deflection curve for three point bend test piece with core ribbon direction oriented perpendicular to span.



Figure 8.7 – Initial test piece “S” shape failure due to core shear

To correct this, a new piece with the same dimensions and layup schedule was constructed, this time orienting the ribbon direction of the core parallel to the span. The same test was run and the results were much more promising. Figure 8.8 below shows the load vs. deflection curve of the test with this specimen.



**Figure 8.8** – Load vs. Deflection plot of a specimen of the Side Impact Structure with 8 inch width and 20 inch span. Core ribbon direction was oriented in the span direction.

The specimen sees first ply failure on the top face sheet at approximately 10 mm of deflection with complete failure at approximately 15 mm of deflection. The piece initially failed at 4450 N of force. Note that the initial failure was in out of plane compression of the face sheet, followed quickly by core compression. After the face sheet fails, the core is progressively crushed as seen by the long “tail” seen from approximately 15mm of deflection to 90 mm of deflection. The piece was not completely failed. This failure mode was different compared to the mode predicted by CLT (in plane compression in the face sheet). This can be attributed to the stress concentration caused by the test fixture. The diameter of the tube used to apply the load was too small, resulting in a pseudo point load condition causing premature failure. In the future, a bearing plate could be utilized to avoid this.

The theoretical bending and shear stiffness’s of the laminates were determined to be 997 N/mm and 1190 N/mm respectively. This results in a total laminate stiffness of 532 N/mm. The actual stiffness of the laminate was 463 N/mm, resulting in a 15% error. The error could be from the fact that the material was expired and resin properties could have been compromised. Additionally, AS4/3501-6 properties were used to determine theoretical values as true material properties were unavailable. Finally, ply thicknesses were based on AS4/3501-6 and could have varied from the true material properties.

Initially, the stiffness of the laminate was too low, but a compliance test was done to reveal any compliance in the rig. Two 1018 steel tubes measuring 1 inch in diameter and 0.065 in wall were subjected to the same test on the same rig. Figures 8.9 and 8.10 below show the test setup and load vs. deflection curves respectively.

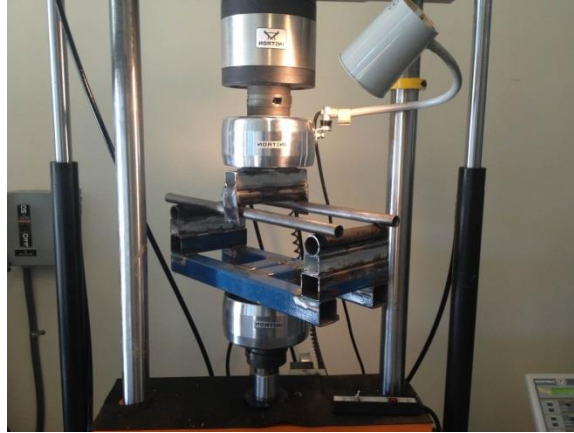


Figure 8.9 – Steel tube compliance test setup.

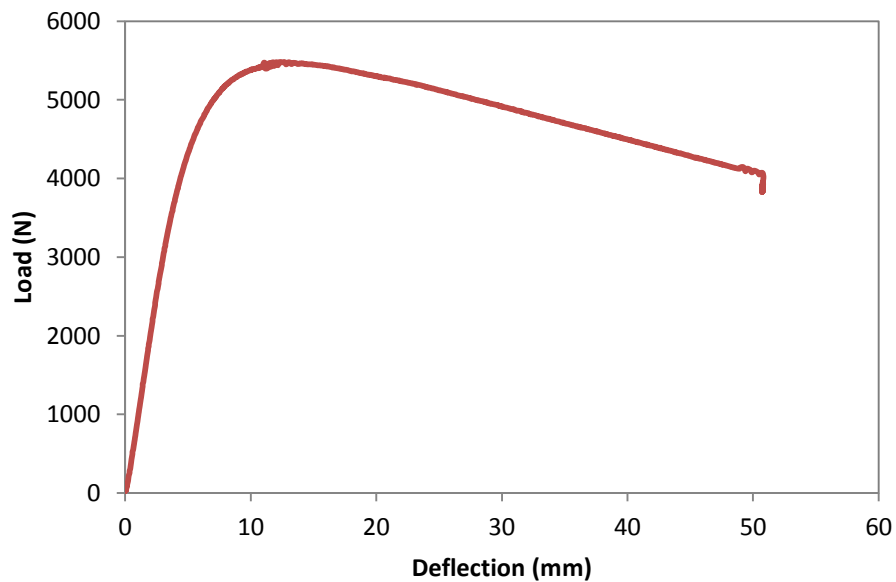


Figure 8.10 – Load vs. deflection plot of two 1018 steel tubes (1 in diameter, 0.065 in wall) subjected to three point bending over a 20 in span.

The tests shows the ductile qualities of steel; as it moves past its yield point, the tubes start to plastically deform. The test was stopped when the tubes started to kink. The area that is of concern of this test is the linear elastic region from 0mm to approximately 6.6 mm of deflection. The theoretical EI value of the tubes was  $3.49 \times 10^9 \text{ N}\cdot\text{mm}^2$ . The tested value based on SAE's calculations shows that the EI value of the tubes was  $2.03 \times 10^9 \text{ N}\cdot\text{mm}^2$ , a 42% error. This, according to SAE, attributed to 534 N/mm of rig compliance. Upon further investigation, we found that there was an error in the calculations done by SAE. They assumed that all of the deflection was attributed to bending and did not take into account any shear deflection. This explains the false rig compliance. Despite this fact, this test proved that the laminate designed for the Side Impact Structure passed SAE's requirements.

The second SAE test performed was the perimeter shear test on the front bulkhead support and side impact structure as per Formula SAE rules T3.33.3 and T3.34.3 respectively. This test consists of penetrating a sample laminate with a one inch diameter impactor. The test results are used to

determine perimeter shear strength to be used when designing attachment points and the penetration load of the laminate. Figure 8.11 below shows the test set up.

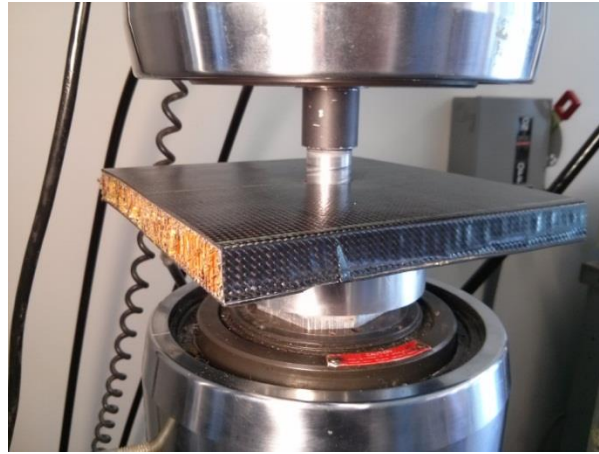


Figure 8.11 – Perimeter shear test setup

Figure 8.12 shows the load deflection curve of the specimen. The two large peaks at approximately 4mm and 17 mm of deflection correspond to the failures of the top and bottom face sheets respectively. The trough between the two peaks shows the compression of the core which is relatively constant. The notch at 7 mm of deflection is from resetting the Instron machine during the test. The top sheet failed at approximately 6500 N while the bottom face sheet the failed at approximately 7750 N. The perimeter shear strength of the laminate was determined to be 57.6 MPa using (1) where  $F$  is the peak load of the first skin,  $d$  is the diameter of the impactor, and  $t$  is the thickness of one face sheet. If the attachment utilizes a backing plate,  $t$  is the total thickness of both face sheets since both are now captured by the attachment. Finally, the penetration load was 7736 N and met structural equivalency.

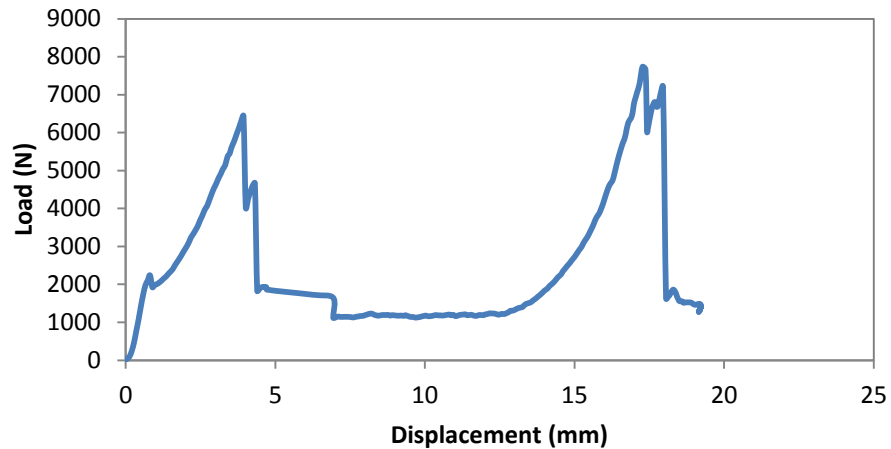


Figure 8.12 – Load versus displacement plot for perimeter shear test,

$$\sigma_{shear} = \frac{F_{peak}}{(\pi d) * t_{skin}} \quad (1)$$

With these tests, the material is now characterized and can be used throughout SES to determine the equivalency of the composite structures compared to the baseline steel frame. Table 8.3 below shows the properties used in SES.

**Table 8.3** – Properties used in SES for carbon fiber sandwich material.

Property	Value
Young's Modulus	51.1 GPa
Strength	112 MPa
Perimeter Shear Strength	57.6 MPa

The last test performed for SAE was the harness attachment test according to rule T3.41. This test simulates the combined loading situation that the harness attachment point would experience and tests its ultimate strength. A rig was designed out of steel to accommodate a test sample 7.75 in x 7.75 in. The pull tabs were oriented at 30 degrees off of the plane of the face sheets. Figure 8.13 below shows a drawing of the test rig. Figure 8.14 below shows the actual test setup in the Instron.

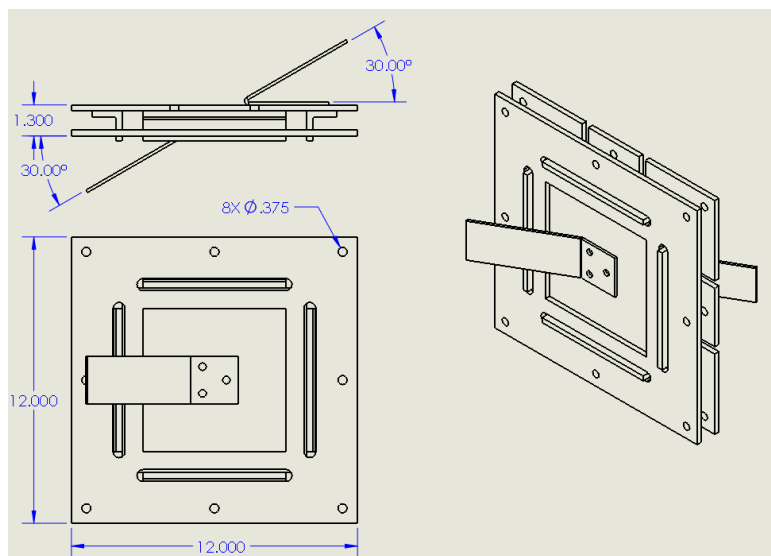


**Figure 8.13** – Harness attachment point test rig with overall dimensions.

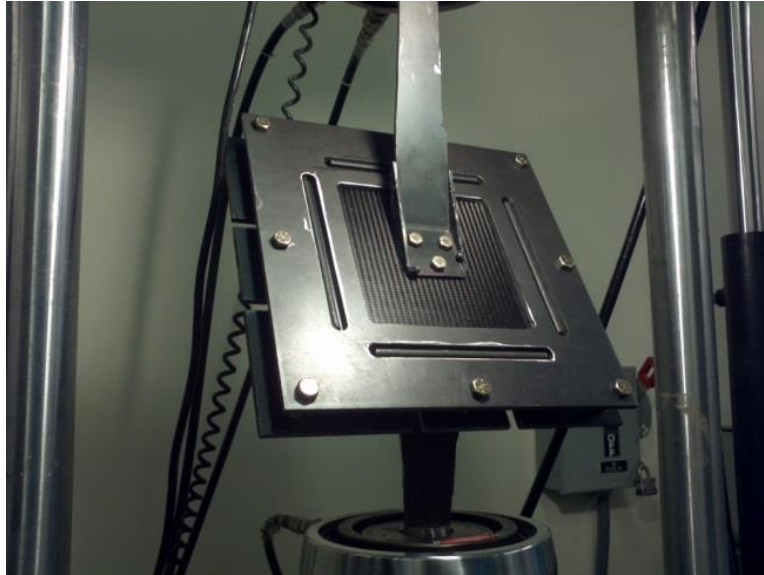


Figure 8.14 – Harness attachment point test setup.

Figure 8.15 below shows the load deflection curve from the test. Initially the slope of the curve is very linear. At about 3.7 mm of deflection, the curve bends slightly which shows evidence of yielding in the steel pull tabs. The test piece experiences its first failure at 7.4 mm of deflection and 15800 N of load. This failure appears to be a matrix cracking because the piece is able to build load back up to 16770 N at 8.9 mm of deflection. At this point, the test piece appears to have experienced first ply fiber failure thus the failure load was determined to be 16770 N.

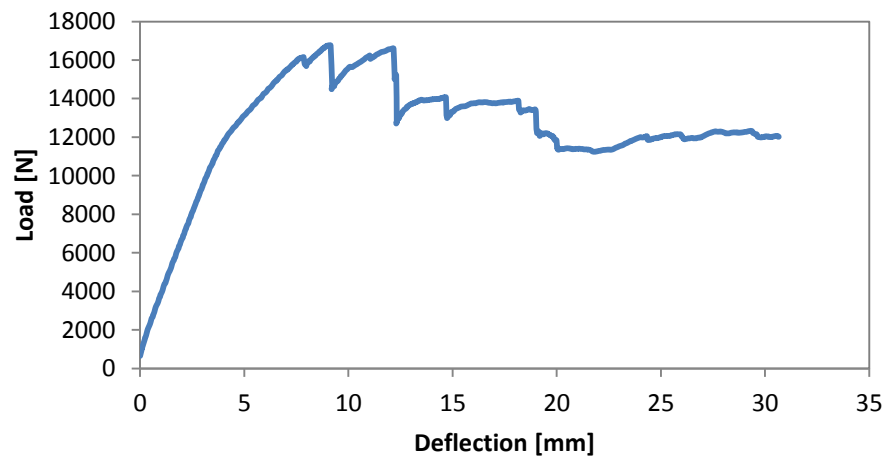


Figure 8.15 – Load deflection curve for harness attachment test.

Two important conclusions can be determined from this. First, if assuming a 150 lb driver and there are four harness attachment points, this load corresponds to an approximately 100 g impact. At the speeds and venues that this car will potentially drive at, a 100 g impact is highly unlikely and therefore the attachment solution can be concluded as overbuilt and therefore will not fail in a typical collision. Second, even if such an impact was to occur and the driver survived the G forces, the attachment point

will not fail catastrophically, but rather progressively. This progressive failure ensures that the driver remain within the driver cell for the entirety of the crash thus minimizing his or her chances of injury.

### Suspension Attachment/Balsa Core

The loads seen through the suspension members put both shear and compression stress on the carbon monocoque. The core material selected had relatively low shear strength of 85 psi (586 kPa). In key areas, such as the rocker stud and pedal assembly attachment, the Nomex honeycomb core was replaced with medium density end grain balsa in order to accommodate the shear loads. The test to prove that these solutions were acceptable consisted of a laminate coupon 12 in in length and 6 in in width, mock suspension mounting tabs, backing plates, and grip tabs. This would simulate the attachment point as it would appear on the car. Figure 8.16 below shows a drawing of the test set up, the red arrows indicating the pull direction when loaded into the Instron Test Machine.

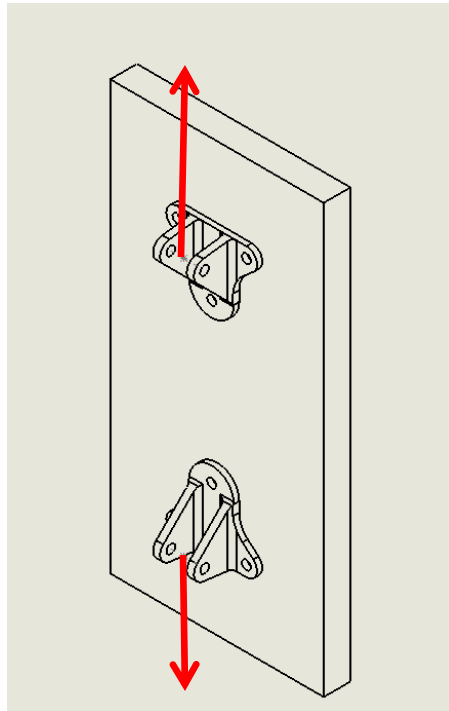


Figure 8.16 – Drawing of test setup for balsa core testing.

Figure 8.17 below shows the load vs. deflection curve from the test. Note that initially the laminate behaves very linearly under this loading case. At approximately 5300 N (1200 lb), the specimen experiences fiber failure, however the specimen is able to build some load back up at a reduced rate. The specimen built up nearly 5000 N before the test was terminated. Although the ultimate load was far below that of the expected peak suspension load on the lower members (650 lb worse case), this demonstrates that should there be a catastrophic failure, the car will more than like be able to stop without putting the driver in a considerable amount of danger.

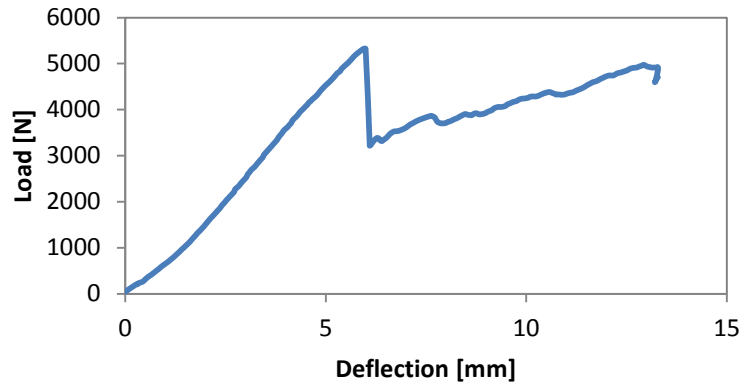


Figure 8.17 – Load deflection curve of lower suspension attachment test.

Next, the technique for splicing the Hexcel and balsa cores was tested using a three-point bend test with a span of 9 inches. The test specimen was 11 inches in length by 4 inches in depth. The core was cut and spliced using film adhesive in two locations, each 2 inches away from the overhanging edge of the specimen. The specimen was then placed into the fixture and loaded until failure. Figure 8.18 below shows the load vs. deflection curve for the splice test.

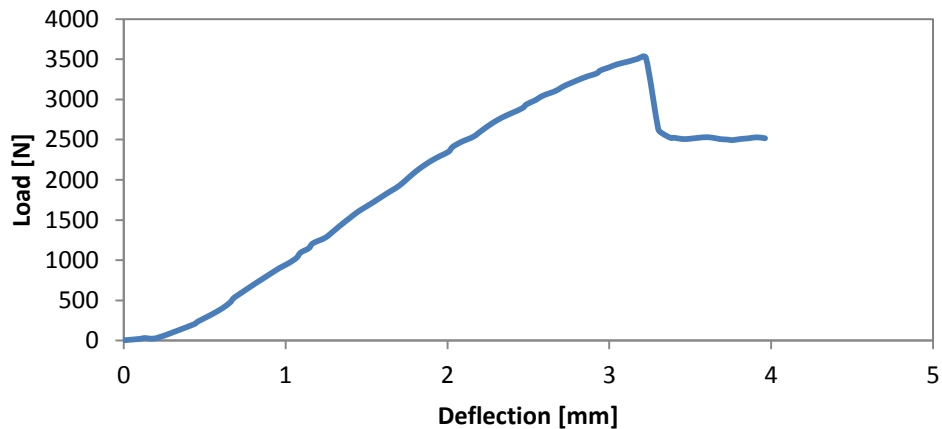


Figure 8.18 – Load versus deflection for the balsa splice, three point bend test.

The specimen failed at a load of 3517 N (790 lb) and most importantly the failure did not occur at the bond line of the splice. This indicates that the failure of the laminate is not dependent on the strength of the splice bond, but rather the shear strength of the core itself. Thus, it was determined that the film adhesive that was to be used to splice the balsa and honeycomb cores was strong enough for our application.

### Impact Attenuator Testing

In order to compete in the FSAE competition, the car must be outfitted with a frontal crush structure designed to attenuate the impact energy in the event of a crash. Rule T3.22.1 states that the impact attenuator must be able to stop a 300 kg (661 lb) vehicle running into a solid, non-yielding barrier with a velocity impact of 7 meters/second (23 ft/s) with an average deceleration not exceeding 20 g's and a



peak deceleration not exceeding 40 g's. In all, the total energy absorbed must meet or exceed 7350 J. The full report submitted to SAE to prove compliance is found in Appendix E: Impact Attenuator Data.

The desired primary mode of failure in the nosecone was delamination. This was designed into the nosecone in an effort to produce a constant force during impact, much like what occurs when crushing honeycomb core. A constant decelerating force produces a smoother deceleration which in turn reduces injuries to the driver due to high g loading. The delamination failure mode was designed into the laminate by alternating the layers of unidirectional carbon fiber by 90 degrees. When this is done, the interlaminar shear stresses are very high resulting in delamination failures. Additionally, the middle layers of the nose cone were extended to the tip in order to promote the delamination failure mode.

The tip of the nosecone was made with 3 plies of unidirectional carbon fiber. This was done to create a trigger zone for the nosecone. A trigger zone is a feature built into an impact attenuator that forces a certain failure mode and shape. It also reduces the peak load from impact and thus peak decelerations. The thin cap on the FSAE nose was designed to crush easily during the event of an impact and force delaminations in the sidewalls.

In order to demonstrate the performance of the composite nosecone/impact attenuator, a quasi-static crush test was performed at the Cal Poly Civil Engineering Department. The Civil Engineering Department's MTS test machine was utilized to perform the test. The MTS test machine is capable of applying loads of up to 100 kips and has a head travel length of 145 mm.

Figure 8.19 below shows the test setup. A base fixture was constructed out of 2 inch steel square stock to constrain the nosecone and simulate the attachment to the front bulkhead. Since the MTS test machine's head travel was less than the overall length of the nosecone, a spacer was made from steel I-Beam sections to perform the crush test in two steps. Additionally, sections of all-thread were used to secure the deformed shape of the nosecone in between the first and second steps. A crosshead feed of 0.016 in/sec was used to perform the test, in which the first step utilized 145 mm of travel and the second step utilized the remaining 40 mm. Figure 8.20 below shows the load versus displacement curve for the quasi-static crush test.



Figure 8.19 – Test setup for nosecone quasi-static crush test.

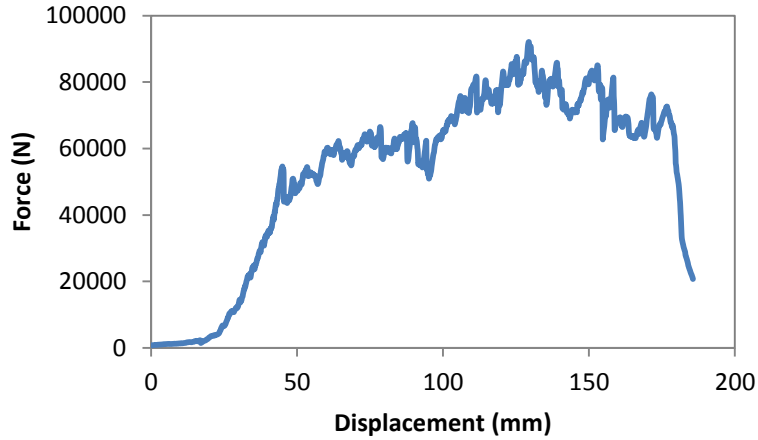


Figure 8.20 – Load versus displacement curve for quasi-static crush test for nose cone.

To calculate the energy absorbed, (2) below was used where  $F$  is the applied force and  $x$  is the displacement. Figure 8.21 below shows the energy absorbed by the nosecone with respect to displacement.

$$E = \sum_{i=2}^N F_i(x_i - x_{i-1}) \quad (2)$$

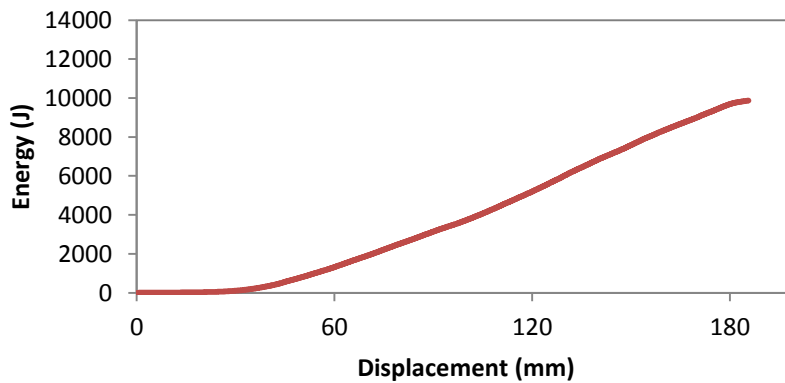


Figure 8.21 – Energy absorbed versus displacement of the impact attenuator during the quasi-static crush test.

To calculate the instantaneous deceleration of the vehicle, (3) was utilized and a mass of 300 kg was assumed as per rule T3.22.1. An average of all instantaneous acceleration points was used to determine the average deceleration of the vehicle.

$$a = \frac{F}{m} \quad (3)$$

Before discussion of the results, it should be noted that a 300 kg vehicle travelling at 7 m/s has 7350 J of kinetic energy. Therefore, once 7350 J of energy is absorbed, the vehicle has come to a stop. Any additional energy absorbed as a result of this test would not be absorbed in the impact event prescribed by SAE.

When the impact attenuator absorbed 7350 J of energy, the resulting peak and average decelerations were 31.3 g's and 17.0 g's respectively. These values were within SAE requirements for the impact attenuator, so no further iterations of the nosecone design were done in the interest of time.

In the load versus displacement curve above (Figure 8.20) the effect of the trigger zone is clearly shown. The initiation force is quite low compared to the impact reaction forces. Additionally, the delamination failures provided steady energy absorption, which results in a safer crash.

While the impact attenuator did not meet the team's requirement of 13 kJ of energy absorbed (equivalent to a crash at 10.7 m/s), the structure did pass the SAE requirement. It was decided to relax the team's requirements and use this design that passed SAE regulations in the interest of time. In the future, new geometries and layup schedules should be investigated to improve the impact performance of the nosecone. With the aid of finite element analysis, many iterations of geometry and layups can be investigated relatively quickly resulting in a more optimized design. With these improvements, it is possible to meet the team's original energy absorption requirement of 13 kJ.

## Conclusions

Testing provided very important insight into the performance of the materials chosen for the chassis before the chassis was actually built. Most importantly, it showed how carbon and steel structures fail differently, how relative shear and bending strength effects the failure mode, and how stress concentrations in test fixtures influence results.

First, steel tubes absorb energy very well when compared to a carbon fiber sandwich structure. Since the steel is ductile, it continues to build load past yield. This results in a large area under the load deflection curve which in turn results in a large amount of energy absorbed. Carbon epoxy composite sandwich structures, on the other hand, have a high specific stiffness and are very brittle compared to steel. This means that when a carbon epoxy composite sandwich structure fails, it fails "catastrophically" and does not maintain a large load past failure. It should be noted that carbon fiber sandwich structures can fail progressively and, if designed correctly, can absorb a comparable amount of energy as a steel tube structure.

Second, it was shown that the relative shear and bending strength of the test specimen as a large effect on failure mode. For isotropic materials, shear strength increases linearly and bending strength increases squared with respect to the thickness of the specimen. This results in beams with large aspect ratios (low thickness compared to span) failing in bending whereas beams with low aspect ratios failing in shear. For composite sandwich panels, the anisotropy of the core and skin materials must be accounted for. For example, when the core's weak direction was placed in the direction of the span, the sandwich structure failed prematurely due to a shear failure at the core-skin interface. It should be noted that the University of Manitoba's FSAE team experienced a similar failure during testing and reduced the number of plies in the skin to reduce the bending strength. This eliminated the shear failure mode as bending failure was now the prevailing mode. Additionally, it is desired to have bending failure over shear failure when designing the layup for a FSAE chassis. This is because bending failure allows more progressive damage; if the bending strength of the laminated is exceeded, the part still has some load capacity. If the dominate failure mode is shear, the failure is catastrophic and the laminate has very little load capacity after failure.

Third, stress concentrations due to test fixturing have a high influence on the subsequent failure mode the part experiences during a test. During the three point bend test, a bear plate had to be utilized in order to reduce the stress concentrations developed by the crosshead. These stress concentrations can

cause premature local compression in the part and artificially low failure loads. There is no SAE guidance as to the specifics of the three point bend test so the size of the bearing plate must be such that the specimen still behaves as if it were subjected to said test. If the bearing plate were too large, then the test is no longer a three point bend test. Additionally, corners of loading brackets (i.e. harness pull tab) can cause high stress which initiate cracks in the test specimen. It is important to develop and manufacture test fixturing such that this does not alter test results by means of premature failure.

## 9. Manufacturing and Vehicle Integration

Images of the manufactured chassis subsystem as part of the complete car are included in Figures 9.1 and 9.2. This section includes details of component manufacturing.



Figure 9.1 - Completed chassis with subsystems installed.



Figure 9.2 - Completed chassis with subsystems installed.

## Monocoque

### Buck and Mold

After the model was turned over to C&D Zodiac, they glued together 4" thick pieces of foam until they had a rough block to machine the final shape out of. Once the stock was made, it was loaded onto a 5 axis gantry mill for final machining. After the roughing and finishing passes, scribe lines were scratched into the part surface to serve as reference marks for mounts and as trim lines on the final parts. When that was completed the bucks were removed and prepped for sanding. Sanding, sanding, sanding; then more sanding. During sanding, the surface was constantly coated with a guide coat – a blue colored powder shown in Figure 9.3 that will show high and low spots when sanded - and once the surface was smooth and level, with no low spots, it was ready for sealer. The reason there can be no low spots is that low spots in the buck will become high spots in the mold make it difficult or impossible to remove the part from the mold. Once the sealer is applied - the foam is porous - it is sanded again. This time the sanding is not to remove low spots, but rather to make as smooth a surface as possible. The surface finish of the sealer will be transferred to the mold and hence to the finished part. Once the sealer is sanded to the desired surface finish and scribe lines are cleaned out as seen in Figure 9.4 below, mold release is applied and the buck is complete.



Figure 9.3 - A buck covered in guide coat and ready for sanding.



Figure 9.4 - The buck with the sealer applied and scribe lines scratched into the surface.

To get a mold from a buck, the buck is cleaned of all debris, and another layer of mold release is applied. Once the release is dry, it is cleaned one more time to remove any debris and a 2 part hard resin coating is applied to the surface. Once the resin starts to harden, a thin layer of plaster is applied to give the resin layer a study base. Figure 9.5 below shows that as the plaster starts to harden, chopped fiberglass is thrown onto the plaster to give a rough and textured surface. Next, hemp rope is mixed with plaster to provide a strong casting material. The hemp and plaster is laid over the resin and plastered buck with the chopped fiberglass giving the hemp and plaster something to grab on too. As the hemp and plaster mixture is drying, a frame is erected around the molds and is used to hold up a steel tube framework that can be seen in Figure 9.6 below. This framework is attached to the mold using more plaster and hemp. The plaster and hemp acts like legs holding up the steel framework. Once the plaster is dry, the supporting frame is removed and the physical mold is completed. After curing for a few days, the mold is separated from the buck and is ready for final prep. Final prep consists of more sanding. The molds are wet sanded to 600 grit sandpaper. After sanding is completed, the scribe lines we mentioned earlier are cleaned out and it is made sure that they will imprint on the final part by running over them again with a sharp scribe by hand. Great care is taken to not scratch the surface of the mold. Once the final sanding is completed the mold is cleaned which can be seen in Figure 9.7 and is coated with a release agent - in our case Frekote. It was given 10 coats and one final scribe line clean out before being covered with plastic and stored until needed for the layup.



Figure 9.5 - Resin, plaster and chopped fiberglass applied to the buck.



Figure 9.6 - The main support structure added to the mold. Hemp, plaster and a tubular steel framework.



Figure 9.7 - The finished mold undergoing a final cleaning before the release agent is applied.

Because of the way C&D Zodiac made the molds and because we decided to layup the bulkhead with the tub instead of doing a post bond like originally planned, a plug had to be made that would effectively shorten the length of the mold and consequently the tub itself. The plug shape was made by making an extruded surface from the buck CAD. Pieces of MDF were laminated together and machined in the hangar on the TM1 using a 3D surfacing method with a ball end mill seen in Figure 9.8 below. Once the rough shape was made it was given a final fitment sanding to get it snugly into the mold. After the fit was correct, the pieces were removed and the surface that would be exposed to the layup was sanded sealed to keep the resin from soaking into the pores of the MDF. Finally the Frekote was removed from the mold where the plug would sit using MEK and the plug was glued in using high temp construction adhesive while under vacuum. Once the adhesive was dry, the edges between the mold and plug were sealed and filleted with high temp silicone shown in Figure 9.9 before being recoated with Frekote.

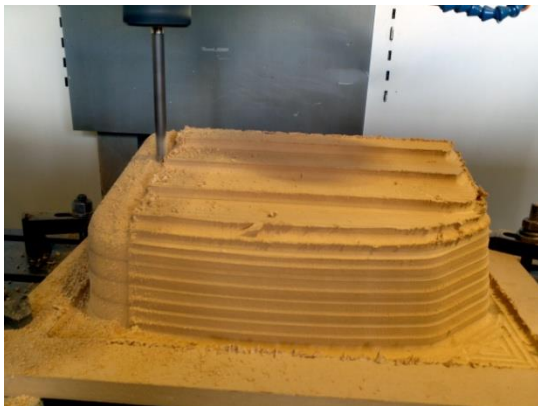


Figure 9.8 - Machining the front bulkhead plug from the MDF stock on the TM1.

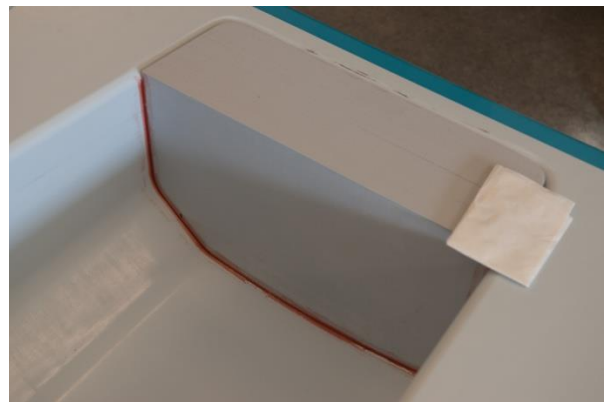


Figure 9.9 - The completed front bulkhead plug glued into the mold with the silicone fillet applied.

Prior to doing the actual layup of the tub, we ran a couple test layups to determine appropriate materials to use for the lap joint joggle and to validate the MDF plug that we had placed in the mold to form the front bulkhead. We also used these test layups to validate our cure cycle and check the temperatures of the composites during the cure.

The first test was to determine what material was best for creating the .040" step in the tub so that we had a recess to place the lap joint lay up in. We tested three separate materials: pipe tape, nylon plastic,

and delrin plastic. The pipe tape had adhesive already applied, so we used high temperature double sided stick tape to secure the delrin and nylon strips in the mold, laid carbon, core and carbon over them and baked it using our cure cycle. After curing, we discovered that the nylon and the delrin performed equally and better than the pipe tape but we ended up choosing the nylon as it was slightly cheaper and was the closest to the thickness we wanted.

Because we did not want to bake one mold more than the other, we did another short test with the second mold. For this test, we just wanted to make sure that the MDF plug we had installed in the front of the molds was properly sealed and the part was not going to glue itself to the porous MDF or wedge carbon past the silicone fillet we put at the edges. So we did what we called a “blob” layup which can be seen below in Figure 9.10. The “blob” layup was just us experimenting with laying carbon, honeycomb and balsa core and film adhesive to see how they draped, how they went around corners, how well the film adhesive stuck, etc. It was more of a trial run for doing the real layup and gave us an excuse to bake the second mold and validate our cure cycle. The “blob” released just fine and we were happy with the learning experience.

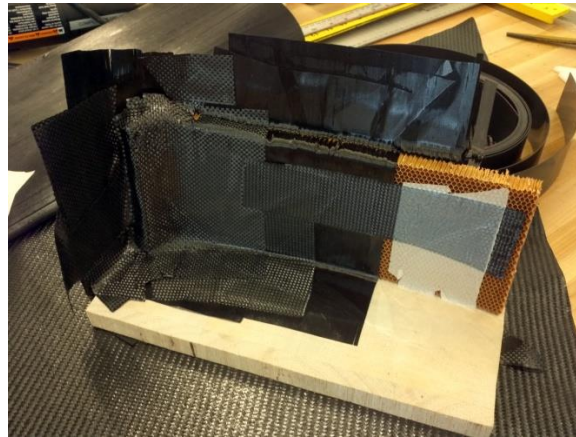


**Figure 9.10** - The experimental “blob” layup that was used to validate the cure cycle and see how the materials behaved while handling them.

The best lesson from these test layups was validating our cure cycle. The mass of the two molds was such that the parts would have never gotten to temperature. Our cure cycle was too fast. We needed to get the carbon and resin to 250F but with the cure cycle we had, we only reached 140F before it hit its cool down stage. We were able to pause the cool down period and keep pumping in heat to get the temp up, but the best we were able to achieve was 235F. So, it was back to the resin manufacturer's website to pull cure times and discovered that to cure at 235F, we needed to hold for three hours rather than the one hour required at 250F. This was a huge lesson that saved us and the actual tub.

### Layup and Cure

Before we did the layup, there was some preparation work that needed to be done first; small things like making our templates for cutting the material and making a game plan so we always knew what the next step was. We made cut templates as seen in Figure 9.11 and figured out how much material we had and laid out all of our cuts in an effort to minimize waste. We cut all of the bagging material we would need including peel ply, breather, and the vacuum bag. We made sure we had enough tacky tape and cleaned the molds as well as making sure all the vacuum fittings and thermocouples were working and the leads were long enough to reach wherever we needed them to in the oven. Finally, we used a sharp scribe to clean all the cast in scribe lines in the mold shown in Figure 9.12 to make sure they



imprinted well enough on the part to see. The last measure of business for the day was to place the nylon strip in the mold to create the step needed for the lap joint to later join the tub halves. High temperature double sided stick tape was applied to the mold surface and the nylon strap was placed over the tape as illustrated in Figure 9.13. For really tight corners, a heat gun was needed to help the plastic strap conform to the geometry. Once all of this was done, we called it an early night and went to bed so we could arrive really early the next day to begin the layup.



**Figure 9.11** - Using fabric store remnants to make patterns for cutting the carbon.



**Figure 9.12** - Using a sharp scribe to clean out the scribe lines in the mold.



**Figure 9.13** - Using high temperature double sided stick tape to place the two inch wide nylon strap for the lap joint step into the molds.

When we arrived the next morning, we did a quick cleaning of the room, work surfaces and the molds and pulled the carbon out of the freezer. The first layer was cut and the three most experienced team members placed the first layer in the first mold so that the younger members could see how the process went which is shown in Figure 9.14. We had quite a bit of trouble with the first layer as the carbon would not stick to the vertical sides of the mold due to the Frekote. So, the heat gun was brought out to get the resin a little warm so the cloth would drape better around the corners. Once we had the layer sitting where we wanted - with a little help from tape, we pulled out one of the premade vacuum bags and pulled a vacuum on the part. Pulling vacuum helped the cloth conform to the surface of the mold and get it to stay in place. After the younger members had seen how the first layer was done, we let

them dive in head first, placing the first layer in the second mold. This allowed the more experienced members to supervise, help when needed and constantly be ready with the next piece of cloth. Once again, after the first layer in the second mold was installed, we placed it under vacuum to debulk it and get it to stick to the mold surface a little better. After this we broke for a late lunch and let the first layer sit under vacuum for an hour.

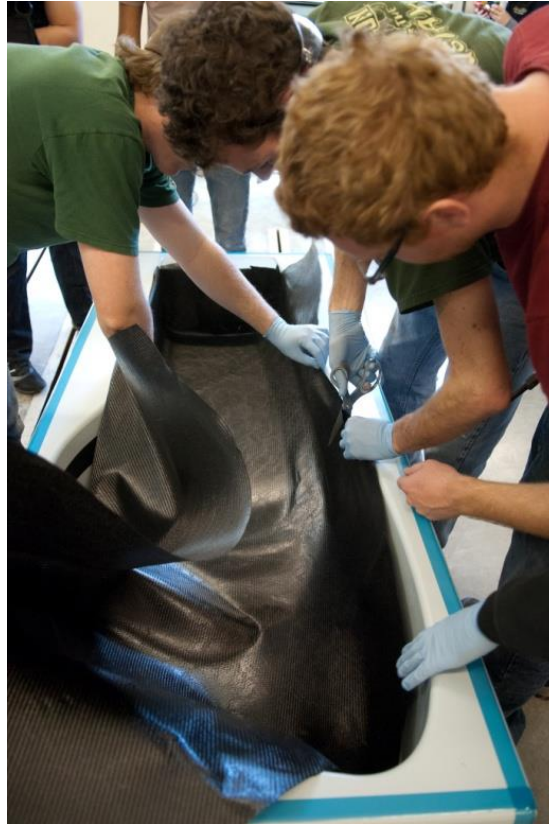


Figure 9.14 - Placing the first layer of carbon into the first mold

Upon returning from lunch, we stopped the vacuum pump and pulled off the vacuum bag. Then we started on the rest of the layers that make up the outer skin, letting everyone take part. We had one guy cutting and about 4 people per mold placing and smoothing layers. Hagan and Rappolt kept a close eye on things and lent a helping hand for complex and tight corners, ripples, and were always watching for bridging. After all the inner layers were installed, we placed the pre made front bulkhead in and again vacuum bagged the part. This time we pulled vacuum to debulk the part and left it overnight. Figure 9.15 through Figure 9.18 below shows the front bulkhead and the outer skin after debulking overnight.



Figure 9.15 - The premade front bulkhead skins.



Figure 9.16 - Installing the front bulkhead sub-assembly.



Figure 9.17 - The part under vacuum for one of the many debulking periods.



Figure 9.18 - The completed outer skin after an overnight debulk.

The next morning we came back to start placing the core in the mold. First a layer of film adhesive was placed in the mold to help the bond between the core and outer skin as seen in Figure 9.19. After a layer of film adhesive was placed in both molds and covering all of the skin, we started cutting sections of core and placing it in the molds which is shown below in Figure 9.20. We kept the core as continuous as possible, but it does not drape as well as carbon and we had to keep the ribbon direction of the nomex running along the car from the front to rear, not around the tub in the hoop direction. This was due to the core having different shear properties along the ribbon and transverse directions. In certain points of the chassis we cut the core out to insert end grain balsa. We placed end grain balsa at the front suspension mounts, front shock mounts, and underneath the pedal box as is seen in Figure 9.21 below. The most difficult part about placing the core and balsa was its thickness. When going around corners, the only way to get it to completely conform to the curve was to compress the core in the transverse direction. This kept the core from tearing, eliminated the saddling effect when you bend it, however, doing this also effectively increased the density of the core adding weight to the chassis. The proper way to fix this would be to increase the bend radii on the chassis and/or use a more flexible core such as over expanded cells or flex core.



**Figure 9.19** - Placing the film adhesive in the mold before the core goes in.



**Figure 9.20** - Placing the core in the mold. The white seams are film adhesive used to splice sections of core together.



**Figure 9.21** - Placing the end grain balsa inserts in for the lower front suspension mount and the pedal box.

While we were placing the core, we also placed film adhesive at all the seams where core needed to be spliced together. This can be seen as white lines inlaid in the core in Figure 9.20 and Figure 9.21 above. We were not sure if it was necessary - our initial tests were inconclusive - but we wanted to be safe rather than having the chassis fail in shear due to a discontinuity in the core. After the core was placed and the seams had film adhesive to promote core bonding, we debulked yet again. This time it was to get the core and film adhesive to conform to all of the curves and stay while the rest of the chassis layup was completed. We got the parts under vacuum and let them sit for a few hours while we had lunch, took a nap, and did a quick cleanup of the composites lab.

Next the inner skin had to be placed into the molds. We pulled the vacuum equipment and started placing a layer of film adhesive on top of the core in preparation for the inner carbon skins shown in Figure 9.22 below. Once the film adhesive had been applied and was as smooth as we could get it, we started placing the inner sheets of carbon in the mold. Again, one person cut the material, while the younger members placed the layers in the molds seen in Figure 9.23 below. Rappolt and Hagan kept a

close eye on the layup and made sure the correct layers were placed in the correct order. They were also there to lend a helping hand as the larger and more complicated plies of carbon were placed. Once the last layer of carbon was placed in the tub, preparation for final vacuum was started.



Figure 9.22 - The layer of film adhesive that was laid on the core in preparation for the inner skin.

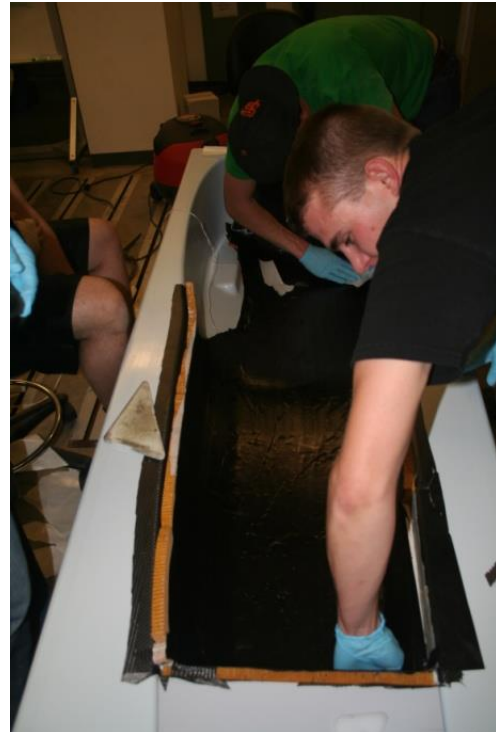


Figure 9.23 - The final layers of the inner skin going into the mold.

For the final vacuum bag, the first thing to place in the tub was the thermocouples make sure that the parts reached the required temperature to cure. Next was peel ply so that the breather would not cure with the carbon. After the peel ply was laid into the mold, it was followed by multiple layers of breather cloth to allow the air to escape. Finally was the vacuum quick connects and the vacuum bag. Once all of this was sealed, we place it under vacuum and checked for leaks. Once all the leaks were found and we had approximately 14 psi of vacuum we rolled the molds into the oven and allowed them to sit under vacuum only overnight to debulk and make sure our vacuum bag would not leak over a long period of time since the cure cycle was going to be 8 hours.

Unfortunately, and to our surprise, when we came back to check how our vacuum held up overnight, we discovered our vacuum was too good. The vacuum was pushing the ends of the core down into the part. The pressure from the vacuum was collapsing the cells of the core along the transverse section. If it had pushed the core too far down during the cure, there would be gaps when we were trying to bond the two halves. To remedy this problem, we stopped the vacuum and built some quick edge dams to keep the vacuum bag off of the core ends. The edge dam was just simple wooden block made by taking two 1"x2" pieces of wood and screwing them together in the shape of an 'L'. This dam was simply hooked over the edge of the mold underneath the vacuum bag to block it from putting pressure on the ends of the core. The edge dams can be seen below in Figure 9.24 After they were installed, the vacuum bag was resealed and the vacuum pump was turned on again.



Figure 9.24 - The edge dams that had to be installed to prevent the core from being crushed under vacuum.

After the overnight debulk period, and edge dams were installed, the cure recipe was uploaded to the oven. The first step was to perform a one minute, vacuum only step. The oven was placed in a manual hold to keep the recipe from advancing. The part's vacuum bag seal was inspected to ensure a proper seal, as shown in Figure 9.25 below. Once confirmed, the oven doors were closed and locked. The oven was then allowed to advance to the temperature ramp stage at a rate of 5 F/min. This stage had a quality check built into the program to make sure the oven did not advance if the temperature was too low. After the ramp, the next stage was a hold at 250 F for one hour. Due to mass effects, the part temperature only reached approximately 235 F. Because of this, the hold time was increased to 3 hours as per manufacturer's recommendation to allow for a complete cure. Once the cure cycle was complete, the oven was ramped down at a rate of 5 F/min. Once the oven temperature reached 105 F, the vacuum pump was shut down and the parts were ready to be pulled. In all, this process took approximately 10 hours to complete.



Figure 9.25 - The parts under vacuum and ready for the cure cycle to start.

Once the parts had cooled, the molds were taken out of the oven and the vacuum bag was pulled along with all of the breather, thermocouples, peel ply and vacuum line quick connects. To get the parts out of the molds, we started by carefully using wedges and plastic putty knives to pry all of the edges of the part away from the mold surface. Once we had a gone as deep into the part as the putty knives and wedges would allow, we used the leftover nylon strips that were used to create the joggle as a makeshift hoist. Since the two inch wide, nylon strips were only .030" thick, we were able to use them as wedges and work them all the way under the part. We could slide them down one side of the mold, underneath the part and then out the other side. We placed one nylon strip on each end and with two people, one grabbing each end; they both lifted straight up together pulling the part from the mold. The hardest part was lifting the parts out because of the vacuum created as air tries to make its way between the part and the mold. Two people were necessary because using only one person, the mold would wedge itself sideways in the mold getting stuck and you would have to start all over again. The finished parts can be seen below in Figures 9.26, 9.27, and 9.28.

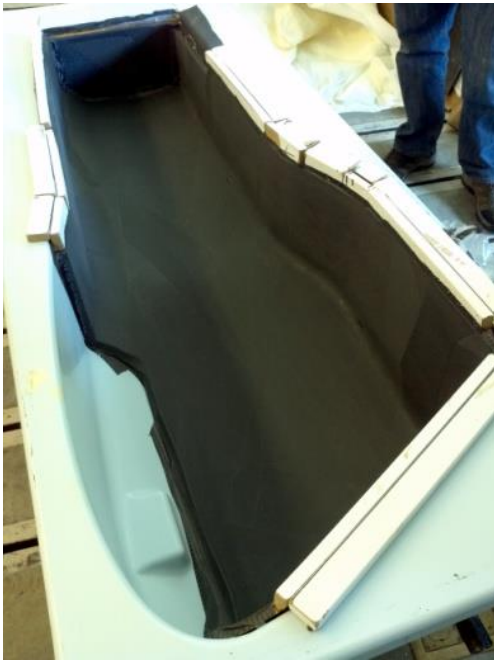


Figure 9.26 - The cured part after taking the vacuum bag off.



Figure 9.27 - The first part to be taken out of the mold.

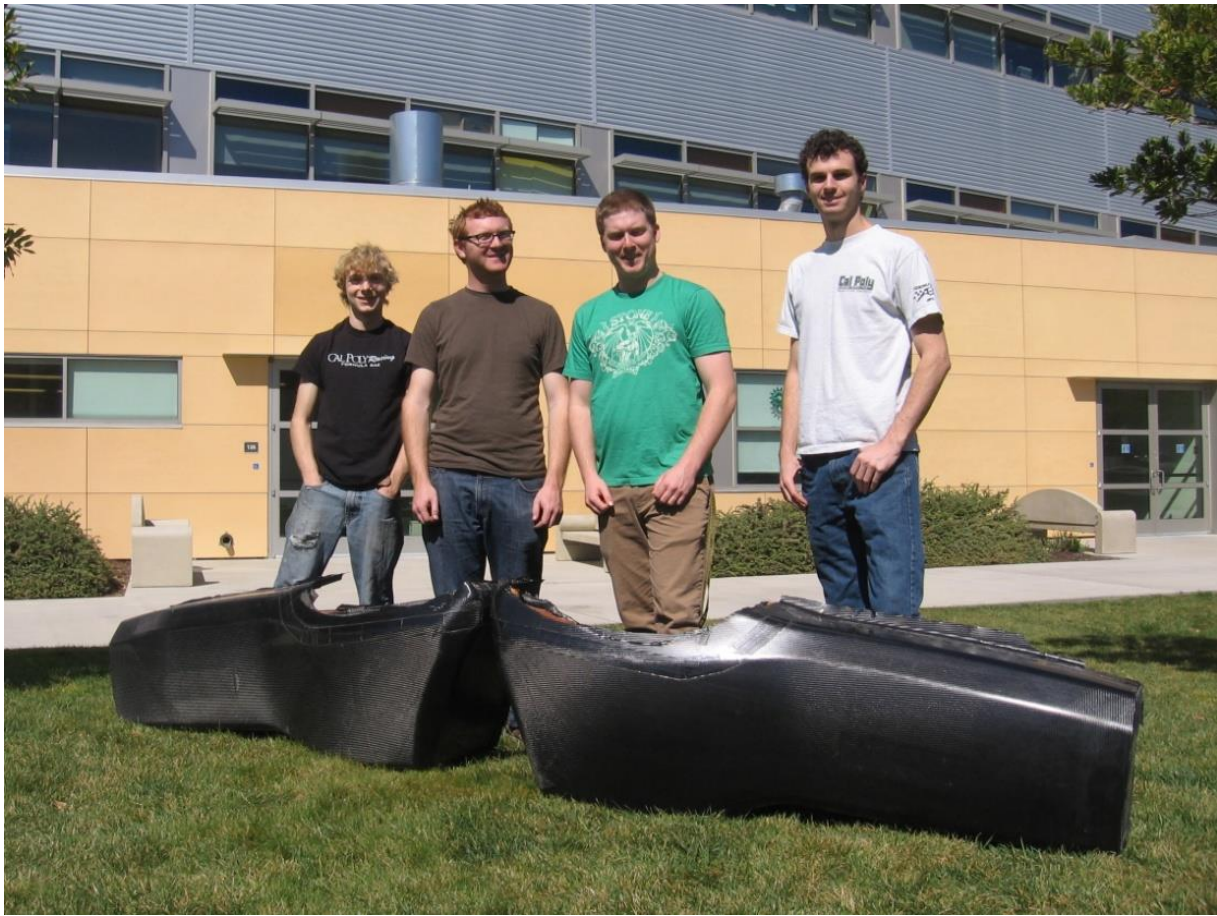


Figure 9.28 - The two completed monocoque halves and four happy team members.

### **Bond and Lap Joint**

After the parts were pulled from the molds, we needed to bond the two halves together. Using the scribe lines imprinted on the tub from the layup, we used a cutoff wheel in an air tool to trim a majority of the excess off of the edges as shown in Figure 9.29. After the rough trim, an air tool with a 80 grit sanding disk was used to get right up to the line on the tub half. For all of these processes we were wearing full tyvek suits, dust masks, and used a vacuum to catch as much of the carbon dust as possible. Once both halves were trimmed we taped sheets of sandpaper to the frame table and using two people we pushed and pulled the tub across the frame table using it to effectively deck the parts flat along the joint seen below in Figure 9.30. Once the two pieces were sanded flat, resin filled with microballoons (to a peanut butter consistency) was used to edge fill the core to make it a solid surface. After the epoxy dried, the parts were deck sanded again to get the parts a flat mating surface.





Figure 9.29 - Rough cutting the parts to prepare to bond the two halves together.



Figure 9.30 - Sanding the mating surfaces flat using a frame table.

Both surfaces were finally roughed up with 80 grit sandpaper and cleaned with MEK. Then we prepped another microballoon resin mixture (soft serve ice cream consistency) and coated both sides of the joint the epoxy mixture was allowed to set until tacky and then the two halves were mated together shown in Figure 9.31 below. After they were joined, the two halves were lined up and the front suspension jig was used to hold the two halves relative to each other. The whole assembly was then placed on the jig table relative to ride height and locked into the rear frame. This completely fixed the two halves together relative to each other. Finally ratchet straps and clamps were used to lock the two halves together and provide some compression to the joint and glue. It was allowed to cure overnight before the clamps and jigs were removed.

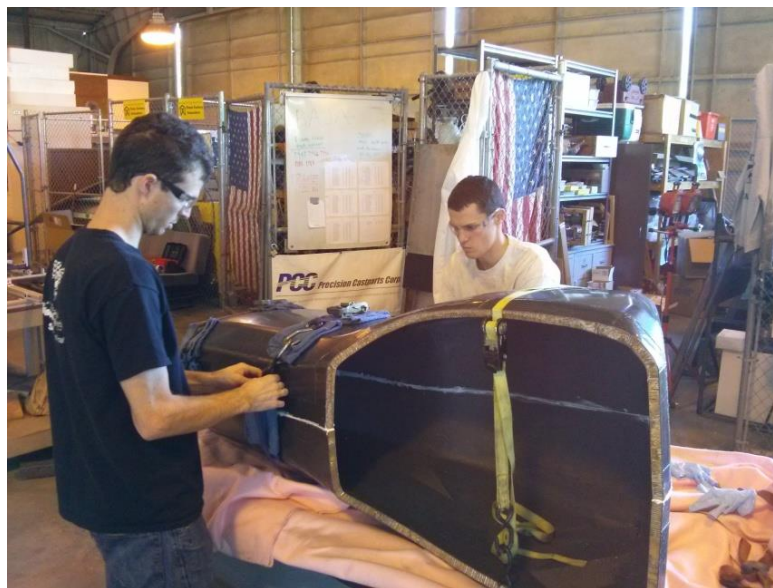


Figure 9.31 - Bonding and clamping the two halves together.

Once the tub was bonded together, we added a carbon lap joint to strengthen and better transfer the loads between the halves. The first task was to prep the surface and remove any resin and microballoons that oozed out during the bonding. This involved sanding the surface to remove any foreign debris and dirt. Once all of that was removed, it was cleaned with MEK. Following the cleaning, the surface was scratched up with some 80 grit sandpaper to give the epoxy resin on the post bond something to bite too. After scoring the surface, it was again cleaned with MEK to remove any dirt, dust, and oils left behind.

The fabric for the layup was then cut, weighed and placed in the proper order in a plastic sheathing. The resin was weighed and mixed and was poured over the fabric and spread evenly over the carbon cloth. After the carbon was completely wetted out, it was cut to a 4" width and one side of the plastic was peeled off. After the plastic cover was removed, the fabric was laid into the lap joint channel and positioned. The second layer of plastic was removed and the fabric was inspected and made sure that it was centered over the joint. After we were happy with the placement, peel ply, perforated bag, breather, and the vacuum bag were placed over the top as shown in Figure 9.32. The vacuum bag was tacky taped to the tub and vacuum was pulled overnight. This process was repeated for each side of the top and bottom of the bonded tub. One thing to note is that our vacuum bag and tacky tape were fairly old and were not sticking to the surface very well. We had a very tough time getting the tacky tape to seal as vacuum was pulled and had to watch each vacuum for a couple hours before we left it overnight. But we were able to get all the leaks sealed and all lap joints were able to cure under vacuum overnight. The finished lap joint can be seen below in Figure 9.33.



Figure 9.32 - The top lap joint lay up under vacuum.



Figure 9.33 - The completed top lap joint.

After the two halves were completely bonded together, we printed out templates to cut the hole for the steering shaft in the bottom of the tub shown in Figure 9.34 and the access hole for the pedal assembly in the front bulkhead. A drill was used to drill out the corners and a cutoff wheel was used to make the straight cuts. After the cutouts were made, we sanded the edges smooth to get rid of the carbon splinters and a resin and microballoon mixture was used to closeout and add strength the exposed core. Once the resin and microballoon mixture was dry, the two cutouts were sanded smooth and the steering shaft hole was painted black. The bulkhead cutout was left white so that the judges could see just how our bulkhead was constructed and how thick the face sheets were seen in Figure 9.35.



Figure 9.34 - The steering shaft cut out on the bottom of the tub.



Figure 9.35 - Front bulkhead cut out after it was filled with microballoons.

### Closeouts

Close outs were placed at the cockpit opening to create a continuous fiber shell around the core to carry the shear load effectively. Before the carbon closeouts can be added we edge filled the exposed core with resin and microballoons to make a solid edge. After the edge fill dried the corners were filleted by hand sanding so the carbon did not have to wrap around a sharp external corner, that never seems to work well and if that happened, the closeout would not be strong. Once the cockpit opening edge was shaped it was prepped in the same way as the lap joint. Sanding, MEK, roughing up the surface, MEK. After surface prep was done, the carbon was prepared - again, in the same way as the lap joint - cut, weighed, resin and final placement. The difference here was that once vacuum was pulled, we had people all the way around the tub pushing and working the fibers around the outside curve in an effort to keep the fiber from bunching up in the corners. Vacuum would be pulled, and then released. During releases we would work the carbon down and around the corners. Then the vacuum was reapplied as we held the carbon down. We repeated this process until we were satisfied that the cloth was not bunched up at any of the edges; we pulled a final vacuum and let it cure overnight. When we removed the vacuum and vacuum bag the next day, we were very pleased with the result, perfect corners with no bunched up material. Woo! The closeouts can be seen below in Figures 9.36 and 9.37.



Figure 9.36 - Making the cockpit opening closeouts.



Figure 9.37 - The finished cockpit opening closeouts.

## Inserts

### *Design*

In order to transfer load from a bolted joint to the composite monocoque, an insert is typically utilized to reduce the bearing stresses in the composite skin. For the purpose of the tub, the laminate thickness changes throughout the structure so various insert lengths needed to be procured. Additionally, there were several different bolt sizes to consider so different diameter inserts needed to be considered. In the interest of time and manufacturability, aluminum sleeve type inserts were chosen.

The aluminum sleeves would carry the compression loads to avoid compressing the core when tightening bolts. Also it allowed some clamping of face sheets for better friction and transfer of radial loads. The sleeve design reduced manufacturing time and effort as there were no flanges to machine that are typically found in inserts. The design also provided minimal insert weight compared with the steel inserts used in the past. The final weight for all aluminum inserts on the car was 0.37 lb compared to the project value of 1.10 lb if steel was utilized. Finally, the design allowed for minimal tub modification. The only process was to drill the appropriate hole and slip insert in with the ends sitting flush or just under the face sheet. The insert was not potted because the loads the chassis is subjected to are relatively low and the lifetime of the chassis is relatively short. By not utilizing a potting compound, the insert solution was able to save weight and allow for easy manufacturability.

### *Monocoque Preparation*

Once a hole was located on the monocoque a small indentation was made in the resin with a drill bit (by spinning it very slowly or by hand). A drill bit no larger than 1/4" was used to start a hole. It was drilled through the first face sheet, and then a guide was used to drill through the second face sheet, as shown in Figure 9.38, to ensure that the hole was normal to the surface. Drill sizes were stepped up only 1/8" at a time to avoid ripping fibers out of the matrix. Any drill bit larger than 1/2" also had a tendency to do this, and had to be spun slowly.



Figure 9.38 – Using a guide to drill a hole in the monocoque.

### **Manufacturing**

Aluminum tubing was purchased in two sizes: 3/8"x.065" for 1/4" fasteners and 7/16"x.065" for 5/16" fasteners. In both cases, drilling out the inner diameter for a tight clearance hole would result in a .060" wall thickness, with minimal material removal. First, the stock was parted slightly long on the lathe for an insert. With one insert parted, the tubing was pulled out of the chuck to part a new one. Once the stock material was depleted, each insert was placed in the chuck to drill out the holes. This was done in a single pass, and the part was deburred. This whole process took an average of about 1 minute per part.

For each region of the monocoque, inserts required slightly different lengths due to the different laminate thicknesses. A completed insert was placed in its hole and checked for flushness with the face sheets. It was filed or sanded until it was flush; if it was too long, compression on the face sheet would be too little to transfer load through friction, and if it was too short, the insert could slip under the face sheet and not transfer load. The hole in the monocoque was drilled out slightly if required, but not so much as to create a loose fit. The tight fit kept the insert in place without adhesive. If disassembly of a mounted component was required and the inserts slipped out, they were labeled such that they would return to the same holes. Figure 9.39 includes an image of an insert in its hole.



**Figure 9.39** - Aluminum insert in the monocoque.

### **Fit and Finish**

Once everything was fit and placed and the car was together, we tore it apart to clean and paint it. Before paint, we sketched out multiple ideas on paper and picked our favorite. The first thing to do was to get the shape of the tub smoothed out. Remember that the top of the tub had multiple steps in it from the draft, the recess for the lap joint, the lap joint itself, and the cockpit opening close out. However, bondo is too heavy to fill and profile the top of the tub the way we wanted it. So it was back to resin and microballoons. We cleaned, and prepped the top of the tub in the same way we did for bonding on the lap joints - sanding, MEK, scoring - and then mixed up the microballoons and resin to thicker than peanut butter. When we weighed the mixture, it was less than one third of a pound (the equivalent bondo would have been about 5 lb). We spread the makeshift body filler all over the top of the chassis and all around the sides of the cockpit opening. After letting it dry for 24 hours under heat lamps, we came back and started sanding until we had the profile we were after. The microballoon bondo can be seen below in Figure 9.40. We were very careful to put on more than we needed and sand carefully as we did not want to have to wait another 24 hours had we needed to apply more.



Figure 9.40 - The microballoon and resin surface (in white) and the glazing putty used to fill the pinholes.



Figure 9.41 - The tub after it had been primed.

After the profile we wanted was achieved, we used tiny amounts of bondo and glazing putty to take care of any pinholes in the resin/microballoon coat which can be seen above in Figure 9.40. Small amounts of bondo dry quickly and we were able to finish filling pinholes and sanding in less than a day. After the pinholes were filled and the block sanding was done, masked the paint outline, covered the rest with plastic and sprayed primer shown in Figure 9.41 above. We used an AutoZone rattle-can primer that was both high build (to fill in sanding scratches and pinholes in the carbon weave where there was no excess resin to fill in between the carbon weave) and sandable. It was an automotive primer that dried quickly so that we could primer, primer sand and paint in one day. We sprayed two heavy coats of primer to fill holes and scratches and then block sanded to 400 grit removing most of the primer we had just sprayed. Then it was two more light coats with a 600 grit sand to finish it off. Once the primer was sprayed, we went straight to color. We laid down four light coats of green Rustoleum rattle can until the car was completely covered. Then we let it cure. We wanted to clear coat it to protect the color, but did not have the time. We originally wanted a week to paint, but only had three days. After the paint had cured, we hand sanded the rest of the exposed carbon to 220 grit to get rid of the glossy finish from the resin to give it a satin or matte finish which we liked better. Finally, we went to an auto body supply store and bought a one half inch wide gold pinstripe tape and placed it over the line where the paint met the exposed carbon and then the sponsor stickers as seen in Figure 9.42 below.



Figure 9.42 - The finished green paint and gold pinstripe. There is a satin finish on the exposed carbon and all of the sponsor stickers have been placed.

## Frame and Attachments

### Jig

After all the design of the rear frame was completed, the first step is to set up a frame table and/or frame jig to make sure all the tubes end up in the correct place. We used the bigger frame table in the hangar and started by first drawing out the car's centerline on the table. To draw all of our lines on the table, we used dykem and a scribe. After the car centerline was drawn as shown below in Figure 9.43, the next step was to locate the front axle centerline and establish the car's zero point. The hardest part about the vehicle center line and the front axle centerline is making sure they are square to each other. Once these two lines are established, the layout for the rest of the car can be done.

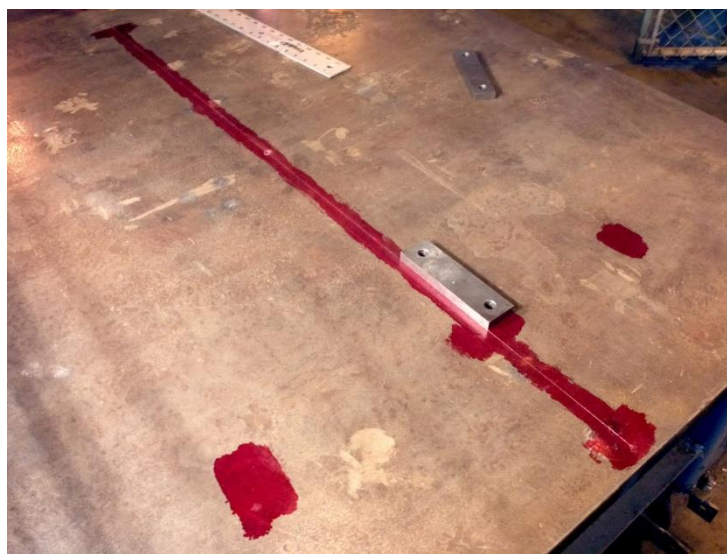


Figure 9.43 - The first layout line on the frame table representing the car centerline.

Next, all of the risers and limiting blocks were cut on a mill. The riser blocks are used to space tubes up off of the table. You draw your layout lines for each tube and then use the riser blocks which rise vertically from the frame table to a specified height to hold the tube at the correct height and in the correct location. Limiting blocks are just pieces of angle iron cut into about two inch long pieces that get welded to the table to provide a locating surface for tubes that are built in a flat plane directly on the table itself. Again, after drawing all of your layout lines, you weld the limiting blocks to the table in the correct place to give yourself another datum to hold the tube while you notch, test fit, and weld the frame together.

### Bulkhead and Box

The first main piece of the rear frame to be made was the bulkhead. This was arguably the most important piece of the rear frame as it was the main reference for the engine, differential, and rear suspension. After the layout for this individual bulkhead was done on the frame table, and the riser and limiting blocks were installed, construction began. The first step was to make the 2 main tubes - two rectangular tubes that served as the mount for the differential. These two tubes were notched, machined for clearance for the engine mount and reboxed before being placed in the jig. Once these two pieces were in, the perimeter box of one inch round tubing was notched and fit. Finally, the last piece to go in was the tube for the motor mount. Once all the pieces were in as seen in Figure 9.44 below, everything was given one final fit check and verification that it was all in the correct place after checking the final measurements. It was then tack welded on all sides, and fit checked one last time before it was fully welded. All of the welding that could take place while the bulkhead was fixed into its jig was done first, and the welding that required the part to be removed was finished.



Figure 9.44 - Using a frame jig to make and weld the bulkhead together.

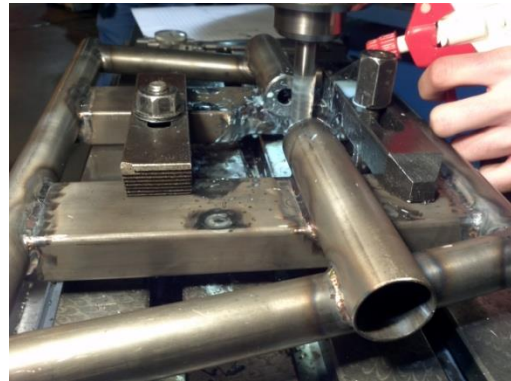


Figure 9.45 - The bulkhead on the mill for final post machining after welding.

After the bulkhead was completely welded up and everything looked good, it was taken to the mill and indexed on the table there for the first of two machining operations. In the first machining operation, the engine mount was machined to the correct width and used as the datum, the left upright was notched to provide more chain clearance, and the holes for the inserts for the differential mount were drilled. The bulkhead was removed from the mill, the engine fit was checked, and the inserts were welded into the previously drilled holes. Then the notches that were made for chain clearance were reboxed. After this final welding was done, it was put back on the mill for its final machining operation shown above in Figure 9.45. This operation was to drill out the inserts that were welded in to make sure the bolt pattern for the differential mounts - which was very critical - was located correctly. After the holes were all drilled, the final step was to mount the bulkhead into the main frame jig which was built earlier. We used risers with built in stops to locate it fore and aft, plumb bobs and layout lines to locate



it left to right, risers to get the correct elevation, and finally turnbuckles to make sure it was perpendicular to the frame table. Then we tack welded it into place.

The box was slightly easier. All that was needed for the box was a layout on the frame table and some limiting blocks as all the tubes for the box were located in the same plane. Once the jig was made, the tubes were notched and all fit into place before being tack welded together shown below in Figure 9.46. After everything was checked one last time, it was placed back in the jig for final welding. After it was completely welded, it was placed on the frame table just like the bulkhead: using risers, locating lines, plumb bobs, and turnbuckles to get it right where we wanted it before it was tacked into place.

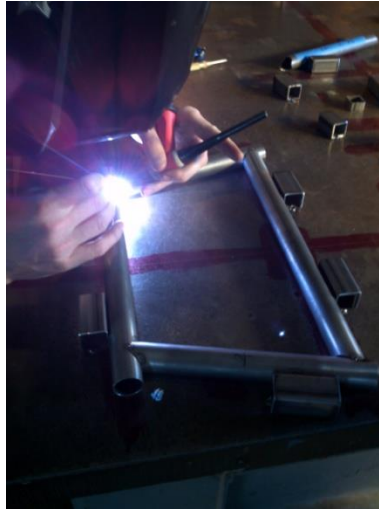


Figure 9.46 - Welding the box in its frame jig.

### Main Hoop

Once the bulkhead and box were in place, the main hoop needed to be bent and placed onto the frame table. Once this was located, all of the tubes connecting these 3 main sections could be added and the frame could be welded. To bend the main hoop, we needed a 1" diameter by 6" radius die for the tubing bender. However, we did not have a 1" diameter by 6" die; we had a 1.25" by 6" die. We could not get one sponsored and did not have enough money to buy a new die so we had to get creative. First, we bought a 1.25" by 0.125" wall tube. We then cut the tube in half on the band saw and then placed it around the 1" diameter tube we wanted to bend. This allowed us to bend both tubes at the same time shown in Figure 9.47 below, and then afterwards pull the 1.25" tube off and be left with the 1" tube and the bend we wanted at the radius we wanted. It took some trial and error, but eventually we used this method to make all three bends in our main roll hoop. The first bend was the easy part. The subsequent two bends had to be very carefully done because they were out of plane bends and being off in angle or placement would render the tube useless. To make sure we did not over bend, we made a representation of the back of the tub out of a cardboard skeleton and craft paper skin. This gave us a template to match the tube to so we could slowly approach the desired bend angle. By doing this, we were able to nail the complex out of plane bends on the first try. We did have to use a ratchet strap and tack weld a brace in to keep the spring back from the main bend from spreading the lower portion of the frame too far apart but we were only tweaking it about one half of one degree so we were ok with it. After the brace was placed on the roll hoop, it was located on the table and fore and aft, left and right and vertically using stop blocks, and again, turnbuckles and plumb bobs were used to get the angles just right as seen in Figure 9.48 below. Once it was where we wanted it, we used some beefy tack welds to hold it into place since this was the hardest part of the whole frame build.



Figure 9.47 - Getting ready to bend the main roll hoop. Both the one inch and 1.25 inch tubes can be seen.

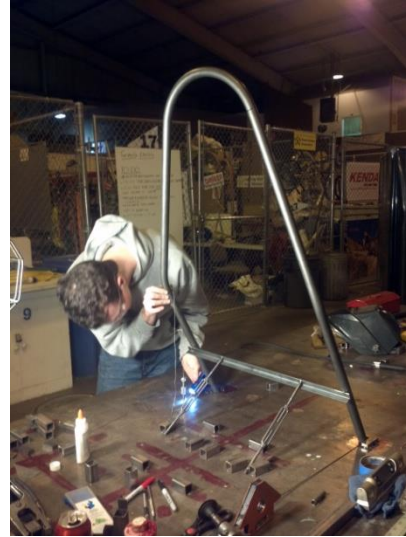


Figure 9.48 - Placing the completed main roll hoop onto the frame table in the correct position.

### Longitudinal Members

Once the above three main frame structures were made and located, the rest of the rear frame could be built. First, the box was joined to the bulkhead with all of the needed tubes as seen in Figure 9.49 below. Once all of the tubes were notched and fit, the differential cage was tack welded together and checked for fitment and final dimensions. Then as much welding as could be done on the box while it was in the jig was done before it was removed to access the rest of the welding. Once the rear box was completely welded, it was placed back on the frame table in its proper place and again tack welded to the frame table.

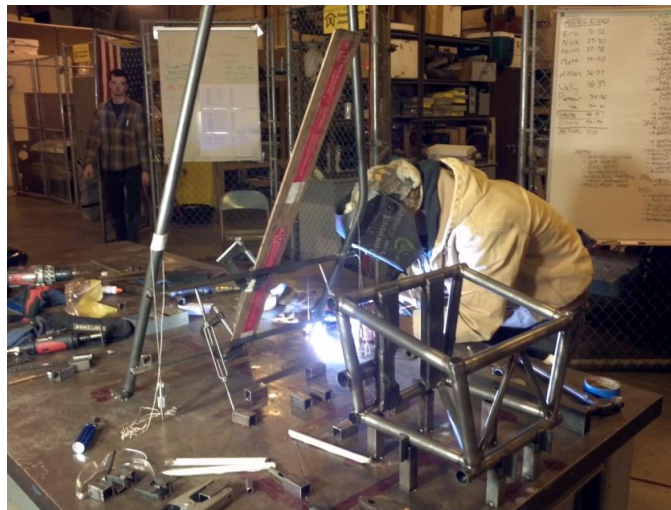


Figure 9.49 - Welding in the longitudinal members. The completed rear box can be seen.

Next the same process was used to attach the main hoop to the bulkhead and differential cage. But before the tubes were notched and fit, we placed the engine in the car and checked it for clearance issues. Just because it works in the model, doesn't mean it will work in reality. But thankfully after mounting the engine to the bulkhead and spacing it up off of the frame table so it was sitting at the correct angle, everything cleared. We even placed the cardboard representation of the back of the tub

on the table to make sure we had enough clearance to run the exhaust. Once all that was checked the process for building the differential cage was repeated and all the tubes were notched, fit, and welded. This completed the major structure of the frame and allowed us to start fitting all of the components that went in the rear of the car. The only things we left off were the main roll bar support braces (for better access), the front motor mount and the shoulder harness bar (both needed the tub on the table before they could be installed).

### Monocoque Attachment

The next step in the process was to attach the tub to the frame. First we located the finished tub on the frame table. this involved getting the centerline of the tub over the established centerline of the table, getting the nose at the right height so the back of the tub lined up correctly with the rear main roll hoop and getting the bottom of the tub the correct height off of the ground so that it would not scrape when the suspension was in full compression. To get the correct height, all we needed were spacers. To get the centerline in the correct place, we located the suspension jig on the table and then used that to hold the tub in the correct place. After all of this was accomplished, we clamped and strapped the tub to the table in an effort to keep it from moving while the attachment brackets were made.

To make the attachment brackets, first the appropriate perimeter shear area and the necessary weld length to meet the SES requirements were found and some brackets were drawn up by hand. These were then cut out of .080" thick sheet steel and hand formed to line up with the main roll hoop tube and the outer profile of the tub (it was a compound curved surface). This can be seen below in Figure 9.50. Once the four brackets were made and fit, they were tack welded onto the frame and mounting holes were drilled through the metal and tub at the same time while everything was clamped together. Then the through holes were transferred onto the corresponding backing plates that went on the inside of the tub to again provide the necessary perimeter shear area. These plates were also .080" thick steel that was hand formed to the inner contour of the chassis. Once all the holes were drilled, the four side plates were fully welded and bolted to the carbon chassis. The lower mounts had three bolts each and the uppers mounts had two. Once all of the mounts were made, the tub was removed to get the holes drilled out so inserts could be installed and the mounting plates on the rear frame got boxed in for added strength.



Figure 9.50 - Making the attachment plates to mount the monocoque to the rear frame.

Next, it was back to the frame for the final pieces. First the shoulder harness bar was installed. During the time the tub was on the table, the drivers sat in the car and the appropriate height for the shoulder harness bar was determined to keep the shoulder harnesses in the correct location and it was bent and welded in. After it was installed, gussets were added to the bottom of the tube since we had bends in it. We needed the bends so the bar wasn't so close to the driver's neck. Also, now that we had verified that the engine had enough clearance between it and the tub, it was mounted using the rear mount in the bulkhead and then spaced up off the table until it was at the correct angle for the oiling system. Then the front mount was fabricated and welded in. Again, this was just notching, fitting, and welding in more tubes. Also the main hoop bracing was installed and welded in and the main structure of the rear frame was completed.

### Suspension Attachment

Once all of the above was done and the major structures were both complete and located on the frame table, it was time to get the suspension ready. The suspension sub-team had created a jig that mounted to the frame table and located all of the suspension points in space. The only thing left to do was to drill the holes for the machined suspension mounts in the front of the tub and make the tabs that would span the gap from the spatial points to the rear frame. These two processes can be seen in Figure 9.51 and 9.52 below. For the front, only holes needed to be drilled and inserts installed, and the jig was used to locate the holes so that was pretty straight forward; use the drill guide that mounted to the jig and drill holes. For the rear, each of the eight nodes needed two custom tabs and that took the longest by far. Once all of the tabs were made and bolted to the jig, the jig held them in place while they were welded to the frame. Once this was completed, the suspension was bolted on and we had a rolling chassis with a motor installed.

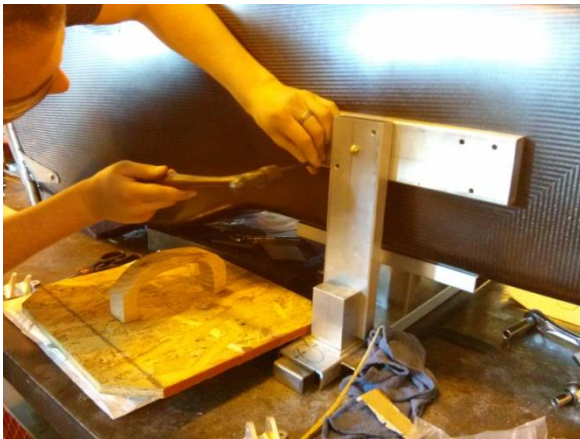


Figure 9.51 - Using the suspension jig to locate the holes for mounting the front suspension mounts.



Figure 9.52 - Using the suspension jig to locate the rear suspension mounting tabs.

### Fit and Finish

The last thing before the rear frame could go to paint was to get the rest of the mounting tabs welded on. This was done one at a time until all of the subsystem components had been placed in the car - radiators, shock mounts, catch cans, fuel tank, intake, exhaust, etc. After all of these components were placed, the tabs welded, and the car drove under its own power, it was all taken apart so the frame could be painted.

The hardest part about paint was the preparation work needed for the rear frame. Because of all the oil and grease and rust that had started to accumulate on the frame (the protective coating needs to be cleaned off of the tubes for welding leaving them exposed to the elements), paint prep was by far the

most time consuming part; although, it was still much less effort than prepping the tub for paint because the protective coating is removed from where welding takes place, which means the rust is in all the nooks and crannies of the frame - where all of the tubes come together at the nodes. So the better part of a day was spent with MEK and scotch brite pads to clean all of the oil, protective coatings, and rust off of the frame. Once the frame was clean, we used a primer that was self-etching and could paint over rust and stop it from spreading so that the spots we could not get too wouldn't ruin the paint. After 2 cans of primer - lots of overspray with space frames, we applied 3 coats of high temp roll bar chassis paint to make it look pretty. The paint was also resistant to scratches, dings, and solvents so that it would not get marked up too badly when it was hit with a wrench or gasoline was spilled while removing the fuel tank. We wanted to look good at comp. But again, since it's hard to paint a tubular space frame, we used 5 cans and it seemed like most of it ended up on the floor or getting sucked through the filters in the paint booth.

## Front Hoop

### Tubing

Once the model is created, we printed out a template and checked the fitment with the car. Once we had a template of the cross section where the front roll hoop was going and it cleared all of the templates and all the dimensions checked out, we started transferring measurements to the tube to be bent which can be seen in Figure 9.53 below. Because there were 5 bends and we were doing all of the layout by hand, we decided to bend the tube in two separate halves and then fit the halves into the tub and weld them back together. It would have been easy to fit the front roll hoop had we made it a bit too tall, but if it was too narrow or too wide, we would have had to start over. Rather than risk it - and because we were low on material - we decided to bend the front roll hoop in two separate pieces.



Figure 9.53 - Using the tubing bender to bend one half of the front roll hoop.

After each half was bent, we fit them into the chassis and kept trimming until both of the tubes fit close enough to the tub for the mounting plates to fit. Once all of the mounting plates were fit, the tubes were trimmed so they both fit and then it was tack welded together, shown in Figure 9.54. After another fit check, the tube was removed from the car and fully welded which is shown in Figure 9.55. There is nothing in the rules stating that the front roll hoop has to be one continuous tube, but just in case we

placed the seam directly under the biggest mounting plate that would serve to mount the roll hoop to the top of the tub, giving us much more surface area to spread the weld over.



Figure 9.54 - The front roll hoop fit into the tub and tack welded into place.



Figure 9.55 - The fully welded front roll hoop halves and steering mount.

### Monocoque Attachment

Once welded, the tube was placed back in the car and the mounting brackets were tacked on. After all of the mounting brackets were healthily tack welded on, holes were marked and drilled through the steel mounting plates and through the tub much in the same manner as the plates that joined the tub to the rear frame. After the holes were drilled through the tub, backing plates were made and drilled for the outside of the tub. Each of these plates was hand shaped to the outside profile of the tub and labeled so they didn't get mixed up. Once all of the plates were fit and the holes were drilled, the roll hoop was bolted in for one last check, shown in Figure 9.56 below. Everything looked good so we removed the front hoop, and installed the inserts into the tub while the front hoop was getting everything finish welded. It was then reinstalled in the car to await placement of the steering and cockpit controls.



Figure 9.56 - Showing how the front roll hoop attaches to the sides of the monocoque. There is an equally sized plate on the outside of the tub to spread the load out over a larger area.

## Cockpit Controls

We had to mount the engine kill switch, starter button, ECU power switch, fuel pump power switch, brake balance adjuster, and steering wheel display/controls connector. They would all be mounted to the front hoop via welded brackets, which would be stronger and simpler to manufacture than brackets fastened to the monocoque. The front hoop wouldn't be removed often, so the time to disconnect wires wasn't a concern. Overall, design was focused on minimizing the front hoop's profile to maximize room for the driver's legs and knees (this also minimized material usage and therefore weight). In doing so, driver egress time and risk of damage to the car during egress would be minimized. Originally, a dash panel fastened to the front hoop was conceived, but it wasted a lot of cockpit space above the driver's legs and made use of a lot of material. Most of the components would not be interacted with while driving the car, so pushing them to the far edges of the front hoop away from the driver's legs was prioritized over easy driver access (for example, allowing the driver to find controls without looking). However, it would be important to actuate the kill switch in the case of an emergency, so it was placed where the driver could quickly place their hand.

The front hoop was fastened in the monocoque and controls were mocked up. Room was found between the front hoop and monocoque on the right side for the kill switch and starter button, shown in Figure 9.57, and just below the hoop at the top for the ECU and fuel pump switches, shown in Figure 9.58. The connector was placed as high as possible on the steering shaft mount. Finally, the brake balance adjuster was placed low on the right side of the hoop, away from the driver and outside the template rules. With components located, steel sheet was cut, shaped, and tack-welded in place. Full welding was done with the hoop outside the monocoque. The hoop with completed mounting brackets is shown in Figure 9.59.



**Figure 9.57** - The starter button and kill switch at the side of the front hoop.



**Figure 9.58** - Engine switches in place near the top of the front hoop.



**Figure 9.59** - Front hoop with component mounting brackets.

## Fit and Finish

To finish the front roll hoop, we sent it out to a friend's shop to get powder coated. We cleaned it as much as we could at the shop and then the powder coat company did a final cleaning with a sand blaster. Afterwards it was coated in a transparent gold powder and baked at 400F for 30 minutes. We received it back from the powder coaters about a week later checked the front roll hoop off our to-do list.

## Nose Cone/Impact Attenuator

### Buck and Mold

To make the nose cone, we elected to machine our own buck and make a mold from it. We would have had C&D Zodiac make it for us just like the tub buck and molds, but we didn't finish the design or SES testing in time to have a finalized model. So, we did it ourselves. The only issue we had was that we had to make the buck in two halves as our CNC did not have the travel needed in the y-axis or the z-axis. To make the buck, we first split it down the center in CAD, and then programmed each half as a 3D surface using a half inch diameter ball end mill. After all the code was generated, we took a full sheet of high density foam and cut it down into pieces that were glued and screwed together to make our stock. The reason for the high density foam was that we thought the high density foam would be easier to seal and we would be less likely to over sand the buck during finish sanding as we had done on a previous attempt.

After the stock was made and code was written, the stock was loaded onto the CNC mill and cutting began. We used a rather large stepover (.020") when doing our finishing passes, but because foam is relatively easy to sand, we felt the increased hand sanding time was worth the decreased machine time. It took two setups to finish each buck half as the machine did not have the necessary y-axis travel. So, we had to machine half of the part, turn it around, find our origin again and machine the other half. It was a little time consuming, but by taking our time, you couldn't even tell it was done in two setups. After both buck halves were cut they were pulled off of the machine to be joined into one piece. The machining can be seen below in Figure 9.60 and 9.61.

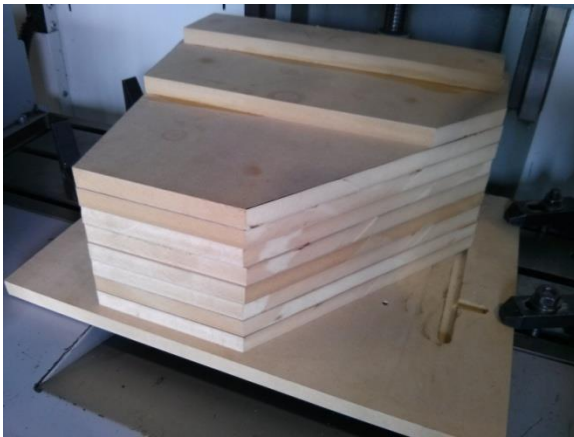


Figure 9.60 - The raw high density foam stock the nose buck was machined from



Figure 9.61 - The first operation in machining the nose cone buck.

We had machined an extra surface on the buck to give ourselves a flat reference to help mate the two halves into one piece so we could make the mold as seen below in Figure 9.62. The aft most surface of the buck (the face that mounts to the bulkhead) was machined and placed on a MDF base and screwed down. Next, and very carefully, the second half was placed on the same base and lined up by eye and by feel. Perhaps not the most accurate method to use, but close enough was all we cared about since we were going to hand sand out all of the ripples that were left by the ball end mill anyways. After the two halves were secured to the base, the seam where the two met was filled with bondo and the whole thing was sanded until smooth. After we were happy with the finish, we sealed the foam and got started on the mold. The original plan was to make a 350F prepreg mold so that we could use the 350F prepreg to do the part layup as well due to material shortages, but we instead elected to use the excess of



unidirectional fiber we had which cured at a much lower temperature allowing us to use a standard plaster mold. The plaster mold was made using the same process that was used to make the plaster molds for the tub and can be referenced above in the Buck and Mold section under Monocoque. For further information about the nose cone buck/mold process, see the Nose Cone section under Conclusions.

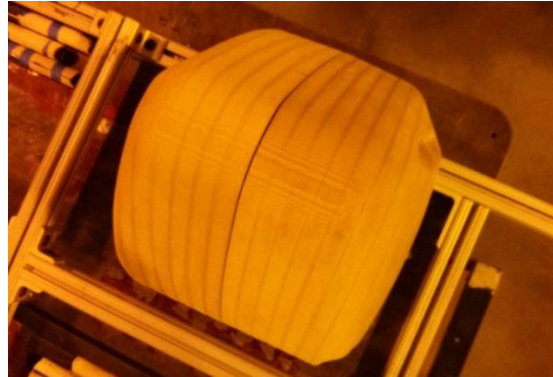


Figure 9.62 - The two nose cone buck halves getting test fit together.

### Layup

The first step in laying up the nosecone was to coat the mold with Frekote releasing agent. Next, the layers of carbon were placed into the mold according to the layup schedule, debulking once after five layers had been placed. Then, release film was placed on the inner skin of the nosecone, followed by breather material. Finally, Stretchlon vacuum bagging was installed to apply compression on the part. Stretchlon needed to be used because of the depth of the mold. The Stretchlon strains far greater than typical vacuum bag material and minimizes bridging the corners of the part.

Once the nose cone was vacuum bagged, the part was placed in the autoclave to cure. The autoclave was set to cure the part at 250 F for 1 hour with 5 F/min ramps. Additionally, the autoclave was pressurized to 20 psig for the duration of the ramps and hold. After the cure cycle was run, the nosecone was removed from the autoclave and pulled from the mold using wedges.

### Fit and Finish

After the nose cone was pulled from the mold, the nose needed to be trimmed and painted. To trim the nose cone, we first rough cut all of the excess fibers from the layup. After the rough cut was done, we sanded the end of the nose cone until we sanded all the way down to the flat mounting surfaces that would mount up against the anti-intrusion plate. Once all the trimming was done, the nose cone and Al plate were held together and the mounting hole pattern from the Al plate was transferred to the nose cone and the holes were drilled. Finally the nose and Al plate were both bolted to the car to check that everything fit how we wanted before we finished and painted the nose.

For paint, it really didn't take much work to get the nose ready. There was only some minor bridging at the tip of the nose, but other than that, the surface finish straight out of the mold was very good. So we decided to use a small amount of bondo to fix the bridging at the front and then primed the whole nose after a light scuff with a red scotch brite pad. We painted the nose while on the road to competition so we had to do all of the painting outside. First, we sprayed two coats of primer outside in the sun and used cardboard boxes to block the wind and keep dust out of the wet paint. The primer dried to the touch in about an hour and then we let it cure in the trailer overnight. The next day we gave it a light primer sand and then hit it with three coats of color and again using cardboard boxes to shield the wet

paint from the wind. We made sure the nose was always in the sun while it was out to try and get the paint to dry a little faster since the color took 4 hours to dry to the touch. Again, we let it cure overnight in the trailer before we finally mounted it to the car. The completed nosecone is shown in Figure 9.63 below installed on the car with anti-intrusion plate.



Figure 9.63 - Completed nosecone installed on the car. Anti-intrusion plate visible along base of the nosecone.

### Inserts

Calculations in the SES submission determined a 1/2" outer diameter for steel inserts to mount the Impact Attenuator to the Front Bulkhead. 4130 round stock was turned, drilled, and tapped through for the M8x1.25 fasteners. Metric fasteners were used to ensure that the grade was acceptable (Grade 8.8 was required by the rules). Holes were located in the bulkhead with the nose cone held in place, and drilled through the first bulkhead face sheet only. The inserts were butted up against the second face sheet, and shortened until they were flush. Originally, it was planned to shorten the inserts with a lathe, but it was forgotten that they were left long and this point of the process happened the night before the competition in a parking lot, so an angle grinder was used. The inserts were plugged on the back side with set screws, and potted into the bulkhead as displayed in Figure 9.64. The set screws also assisted with getting the inserts flush with the bulkhead face in case they were too short.



Figure 9.64 - Potted insert in front bulkhead.

## Anti-Intrusion Plate

### Design

The anti-intrusion (AI) plate prevents the impact attenuator from entering the driver cell and sits at the very front of the chassis behind the nosecone. The design chosen was that of a carbon fiber plate bolted between the chassis and the nosecone using the impact attenuator fasteners. This allowed for easy servicing of the pedal assembly and low fastener count. Additionally, utilizing carbon fiber was lighter than steel or aluminum. The layup schedule of [0c20] was determined in SES by adding layers to the laminate until all of the properties passed. For the carbon fiber prepreg, the limiting property was ultimate shear strength.

The weight of the AI plate was determined to be 2.59 lb. For comparison, if the AI plate were to be made from the minimum thickness steel or aluminum plate it would weigh 3.46 lb or 3.06 lb respectively; a weight savings of 25% over steel and 15% over aluminum. This illustrates the weight savings that carbon fiber composites brought to the AI plate. Further weight savings could be achieved by using a higher modulus carbon fiber thus increasing specific stiffness or incorporating core material into the layup.

### Manufacturing

The template for the AI plate was determined by tracing the cross section of the front bulkhead. The AI plate was then laid up on a flat aluminum plate tool with carbon fiber cloth with a layup schedule of [0c20]. Following a similar method as described in the Layup section under Nose Cone/Impact Attenuator above, the part was debulked, vacuum bagged and placed in the autoclave to cure. The autoclave was set for 5F/min ramps and a 1 hour hold at 250 F with 20 psig of pressure applied throughout the process. The part was then released, trimmed and drilled for mounting. The final product is shown in Figure 9.65.



Figure 9.65 - The anti-intrusion plate ready to mount to the car.

### Harness Mounting

A 6-point harness was used to comply with rules and provide driver safety. Shoulder belts were looped around the shoulder harness bar, while the lap belts and anti-sub belts had to be mounted inside the monocoque. To minimize weight, it was desired to integrate the lap belt mounts with the lower monocoque attachment backing plates in Figure 9.66, which were fastened with three fasteners instead

of two for this purpose. Drivers of various sizes were positioned in the monocoque and the angles of the lap belts when attached to these points were found to comply with the rules.

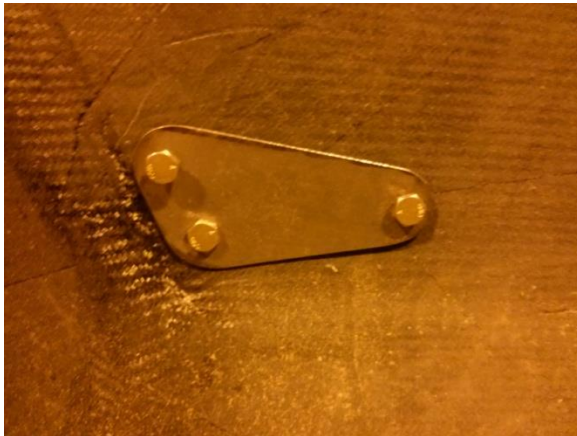


Figure 9.66 - Lower monocoque attachment backing plate.

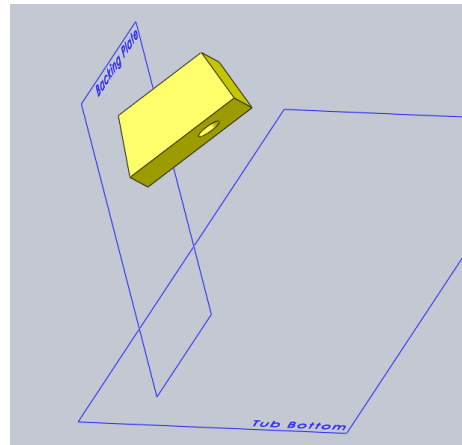


Figure 9.67 - Solid model of block for lap belt mounting tabs.

We planned to mount the belt buckle fastener in double shear, with fasteners as pins and two .063" steel tabs welded to each backing plate. These tabs would have to be oriented approximately parallel to and in the direction of the belt, to allow rotation of the belt with the driver strapped in and avoid loading the tabs in bending in an impact. Belt angle measurements were taken with drivers in the monocoque and the plane parallel and in-line with the belt was located in SolidWorks on one backing plate. The angle between this plane and the backing plate was found, and the block in Figure 9.67 was designed with two parallel faces at this angle relative to the backing plate face, spaced .7" apart to allow buckle movement. A hole was created to fasten the tabs in place on these faces. This part was machined on the mill: squared, drilled, and faced on an angled vice. Tabs for one belt were drilled and shaped using a grinding wheel, and were fastened to the block. The block was located and oriented on the backing plate, and the tabs were welded as shown in Figure 9.68. This process was repeated with the same block for the other backing plate, resulting in the final products in Figure 9.69.



Figure 9.68 - Lap belt mounting tabs being welded in place.



Figure 9.69 - Completed lap belt mounting brackets.

Eye bolts were purchased from Pegasus Auto Racing Supplies and fastened to the bottom of the monocoque near the lap belt points to attach the anti-sub belts. Aluminum inserts were used, and the threaded ends of the eye bolts were shortened to avoid contact with the ground during driving. With all mounting points in place, the seat was trimmed to accommodate belt routing.

## Head Rest/Firewall

A combination head rest mount and firewall was conceptualized. Starting from the top of the seat back (which acted as part of the firewall), a sheet of aluminum would be mounted to the main hoop and extend up to mount the head rest foam padding, in addition to blocking line-of-sight between the driver and the fluid systems. While adjustable padding was allowed to meet the rules, we decided to incorporate static padding for simplicity.

To define the geometry of the structure in SolidWorks, first the plane to which the foam would attach was located (parallel to the front plane), and a sketch of the foam pad's outline was made. It was located in all three directions by referencing the driver solid models. A boss was extruded to provide material which encompassed the final form. - which in front view overlapped the main hoop, in side view overlapped the main hoop, foam pad sketch, and top of the seat back, and in top view overlapped the main hoop and foam pad sketch. In the side view of Figure 9.70, a cut was made to remove the material below the line connecting the top of the seat back to the bottom of the foam pad sketch. The right and bottom edges shown formed the back and bottom surfaces of the head rest mount, respectively, locating the foam padding and keeping the mount behind the shoulder harness bar. A cut was also made to remove material forward of the main hoop. Next, the plane in Figure 9.71 was created on one side which was coincident with the line of the main hoop and the most extreme point of the foam pad sketch. Material toward the rear of the car from this plane was removed, offset to account for the main hoop tube size, and the feature was mirrored to the other side. The top and front surfaces were used to shell the part, which was then converted to a sheet metal part to be flattened. Cuts were also made to remove material to reduce weight and drag. The final model is shown in Figure 9.72.

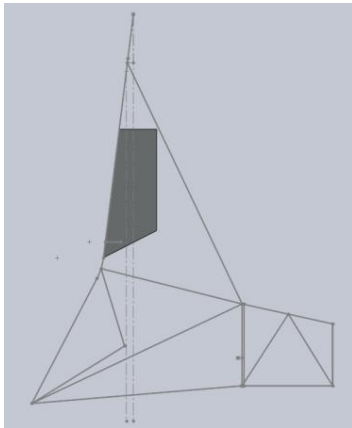


Figure 9.70 - Side view of head rest mount construction.

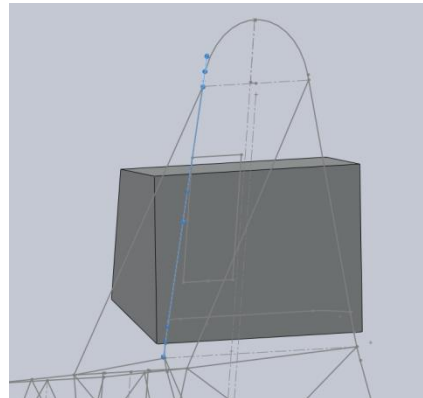


Figure 9.71 - Edge view of the plane for final shaping of the head rest mount boss. Material was removed to the left as shown.

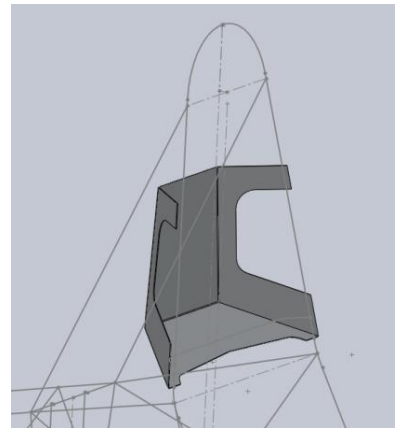


Figure 9.72 - Completed solid model of head rest mount.

The flattened shape was printed and used to outline the part on a piece of .063" aluminum sheet. Cuts were made using sheet metal tools and a cut-off wheel. The bends were then made on a break, shown in Figure 9.73, and the two seams were welded, shown in Figure 9.74. Holes were drilled for tabs which were welded to the main hoop, and material was removed for clearance to the seat back. The foam

padding was covered in gaffer tape and attached to the mount with Velcro before the assembly was fastened to the car as displayed in Figure 9.75.



Figure 9.73 - Bending the head rest mount.



Figure 9.74 - Welding the head rest mount.



Figure 9.75 - Head rest as assembled on the car.

## Electronics Cover

An electronics box cover was designed and manufactured to protect the onboard computers and data acquisition equipment. The cover was site right below the driver's thighs and was to remain flush with the floor of the chassis. The cover was made from a combination of prepreg carbon fiber sandwich structure and wet layups utilizing the "cut and fold" technique. First, a template was cut from cardboard to determine the shape of the cover and to locate where the bend would be placed. The cardboard template was located about half an inch from the computers.

Next, the template was used to cut eight layers of 0 degree carbon fiber prepreg cloth. The 0 degree fiber axis was parallel to the longitudinal axis of the vehicle. The layers were debulked in pairs, first debulking two layers, then debulking four layers to form each skin. Then, the entire laminate was debulked with a layup schedule of  $[0c4/(core)]_s$  where the core was a layer of 0.500 inch thick Nomex honeycomb. The part was cured on a flat aluminum plate tool for one hour at 250 F with 5 F/min ramps.

Once the part was pulled, the template was used to determine locate the seam of the fold. A cutoff wheel was used to remove a quarter of an inch of skin material on either side of the seam to allow the part to fold. Once angle was determined, a wooden jig was made to hold the part in shape. As shown in Figure 9.76, the cover was clamped to the jig and micro-balloons were applied to the removed inner skin. A wet layup using carbon cloth and epoxy resin was then placed over the micro-balloons. This layup held the cover in its folded shaped.



Figure 9.76 - Electronics cover undergoing cut and fold bend.



Figure 9.77 - The electronics cover seated in the car.

Finally, the part was trimmed and fitted to the chassis to ensure a flush finish. There was some difficulty in getting the part to fit nicely, as it was hard to estimate exactly what material needed to be removed. Despite this, the cover protected the electronic equipment from the elements and the driver, as shown in Figure 9.77.

## Seat

To make the seat for the driver, we decided to custom mold a bead seat to the driver. We chose this method because it would be easy to form the seat to the driver and to the chassis at the same time. We bought our bead seat as a kit from Bald Spot Sports and followed their instructions to make the seat. We first thoroughly mixed the resin and poured it into the plastic bag containing the beads. Once in the bag, we placed the bag on a soft surface and started to knead the beads and resin together as shown in Figure 9.76 until we had evenly coated all of the beads with resin. Then the bag was placed into the chassis and the driver sat on the bag displacing the beads and making it into a seat. While the driver sat in the seat we had three people working the beads around and moving them around to provide more support in key areas. We made sure that there was only a small amount of beads underneath the driver and pushed most of those beads up along the sides of the driver for lateral support. However, we did make sure to keep enough beads under the driver's thighs to support their legs. As for the beads behind the driver's back, we made sure to leave enough beads to make an inch thick padding between the back of the tub and the driver's spine in case of a rear impact. After all of this was accounted for, the leftover beads were placed around the driver's shoulders to again help with lateral support as shown in Figure 9.77. Once all of the beads were where we wanted them and the driver was comfortable, we brought out a venturi to pull a small vacuum so that the seat would keep its shape while the resin cured. Because we did not have a regulator, we could not turn the flow on the venturi down enough to keep the vacuum from crushing the bead seat. So we used a sharp pick and started poking holes all over the seat allowing air to leak in. We kept adding holes until the vacuum was approximately two inches of water. After we let the seat cure overnight which is shown in Figure 9.78, we pulled it out of the car and sanded all the rough edges off. The last step for the seat was to cut holes for the seatbelt and clearance for the anti-submarine belt.



Figure 9.78 - Mixing the resin with the beads.



Figure 9.79 - Working the beads down into the shoulder area.

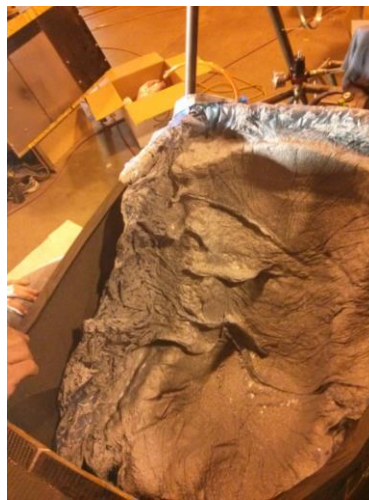


Figure 9.80 - The cured bead seat before trimming.

## 10. Mass Properties

Mass properties of the chassis subsystem for 2013 are included and compared to the 2012 subsystem in Table 10.1. Tables 10.2 and Table 10.3 include component details for the 2012 and 2013 subsystems, respectively.

Table 10.1 - Mass properties of the 2013 chassis subsystem, in comparison to the 2012 subsystem.

Category	2012 weight (lb)	2013 weight (lb)	Weight diff. (lb)	Weight diff. (%)
<b>Subsystem total</b>	<b>143.57</b>	<b>94.49</b>	<b>-49.08</b>	<b>-34%</b>
Chassis	121.80	81.67	-40.13	-33%
Harness	7.40	5.19	-2.21	-30%
Head Rest/Firewall/Padding	2.72	2.82	+0.09	+3%
Nose Cone/IA/AI Plate	11.65	4.81	-6.83	-59%



**Table 10.2** - Mass properties of the 2012 chassis subsystem components. Estimated weights are in parentheses, and are +/- 1 lb or +/- 10%, whichever is lower.

Category	Component	Weight (lb)
Chassis	Frame	(108.00)
	Floor	3.34
	Bodywork	6.91
	Seat back	3.54
Harness	Harness	(7.15)
	Hardware	(0.25)
Head Rest / Firewall / Padding	Sheet	1.84
	Foam	0.26
	Roll bar padding	(0.62)
Nose Cone / IA / AI Plate	Foam IA	1.50
	Nose cone	3.15
	AI Plate	3.80
	AI Plate bracing	(1.93)
	Hardware	1.26

**Table 10.3** - Mass properties of the 2013 chassis subsystem components. Estimated weights are in parentheses, and are +/- 1 lb or +/- 10%, whichever is lower. "H+BP" stands for "hardware and backing plates".

Category	Component	Weight (lb)
Chassis	Monocoque with inserts	(34.00)
	Frame	(35.00)
	Front hoop	5.39
	Suspension brackets	(0.92)
	Shock and rocker mounts	(0.67)
	Electronics cover	0.95
	Frame H+BP	1.65
	Front hoop H+BP	0.88
	Suspension brackets H+BP	(1.38)
	Shock and rocker mounts H+BP	(0.83)
	Harness	Harness
Hardware		0.67
Head Rest / Firewall / Padding	Mount and padding	2.33
	Roll bar padding	0.48
Nose Cone / IA / AI Plate	Nose cone	2.09
	AI Plate	2.59
	Hardware	0.14

It is important to note that the head rest in 2012 piggy-backed off a part of the chassis structure, so the difference in the Head Rest/Firewall/Padding category is not meaningful. Seat weight was ignored due to its variability for different driver sizes.

The 2013 chassis subsystem removed almost 50 lb from the car as compared to 2012. This weight reduction reflects the efforts put into the process from concept through manufacturing. The Chassis assembly was 33% lighter; at 82 lb. 11% of weight was removed as a result of integrating components into the structure, including the floor, seat back, and bodywork. The remaining reduction in the chassis structure was largely a result of improved use of material. The largest reduction on a percentage basis was found in the Nose Cone/IA/AI Plate assembly, which was almost 60% lighter: 22% from integrating the IA and aesthetic nose, 26% from improving load path, and 10% from changing AI Plate material. Weight was saved in the harness by using a modern design with a lighter quick release and avoiding use of a second anti-sub belt.

While weight was greatly reduced from 2012, requirements were not met. The total subsystem requirement of 69 lb was overshoot by 25 lb, or 37%. The accessories requirement of 19 lb was easily met with a weight of 13 lb, but the chassis structure was very heavy compared to its 50-lb requirement. This requirement was based on investigating the weights of previous Cal Poly chassis, which were underweight and would not meet today's rules as discussed in the Loading and Structural Equivalency section. Only the monocoques and frames were investigated: front hoop weight was ignored (5.4 lb in 2013), suspension mounts weren't considered (1.6 lb in 2013), and fastener and backing plate weights weren't accounted for (4.7 lb in 2013). As a result, the chassis weight requirement was very unrealistic. This contributed significantly to not meeting the expected weight for the 2013 car as a whole (overshoot by about 40 lb).

While it would be extremely difficult if not impossible to meet the 50-lb requirement for the chassis, we believe that the weight of our chassis concept could be reduced by approximately 15 lb with a year's-worth of development. This weight reduction would mostly come from reducing material usage in the monocoque, with no major design changes. See the Components section for further discussion.

Relevant mass properties for the entire 2013 car are included in Table 10.4.

Table 10.4 - Relevant vehicle mass properties.

Property	Value
Dry weight without driver	400 lb
Sprung weight	305 lb
Front weight dist. (driver-dependent)	44-45%

The weight distribution was slightly off what we originally designed the vehicle layout for (see the Vehicle Design section for the design process); we designed for 45-46%, but achieved 44-45%. Investigating the differences between the 2012 and 2013 cars and focusing on masses far from the CG, the 2012 car was approximately 7 lb heavier in the Nose Cone/IA/AI Plate assembly. The 2013 weight distribution was predicted assuming that the mass of this assembly would be a similar portion of the overall car weight. 7 lb removed at this location would shift the weight distribution rearward by 1.0%, so this difference at the nose was a contributor. Also, while most increases from weights at the time of the vehicle layout design were distributed fairly evenly around the car, the engine area's weight gains were distributed at the rear. These gains were likely significant. If these two factors had been accounted for, the weight distribution would have been predicted very accurately by the layout design.

## 11. Vehicle Performance

### Vehicle Testing

Once the chassis was assembled with the other subsystems of the car, the team put the car through series of dynamic tests, as shown in Figure 11.1. While no chassis-specific tests were run, some of the qualitative feedback from the drivers was important to consider. The drivers could consistently sense the balance of the car and its variance in respect to suspension adjustments. While performing suspension set-up testing, the vehicle behavior responded as expected to adjustments made with ARB and damper settings. This good response suggested that the chassis was adequately stiff.



Figure 11.1 - The car being driven during dynamic testing.

The ARB served to kill grip at the front to balance the car due to its rearward weight distribution. However, due to influences from the torque-biasing differential, the car handled best without the ARB. Although the weight distribution came out even further rearward than expected, it resulted in a balanced car considering these circumstances.

Additionally, no component of the chassis failed during operation of the vehicle. While this was a good result, it suggested that more aggressive designs could be utilized to save weight. Having a better understanding of the load paths and material properties would assist in reducing weight.

### Competition

The team competed at FSAE Lincoln in June 2013. It was the team's goal to place within the top 10 overall positions. The team did well in the Design Event, placing just below the finalists in 7<sup>th</sup> largely due to the team's design and manufacturing practices, led by this project. During dynamic events, the team struggled with what was later determined to be a wiring issue. The engine did not have adequate power and thus results were poor for Acceleration, Skidpad, and Autocross. During Lap 9 of the endurance race a hole was blown in the muffler from high exhaust gas temperatures and melted the wiring harness, causing the car to not finish. The Cal Poly group with the car in Lincoln is shown in Figure 11.2.

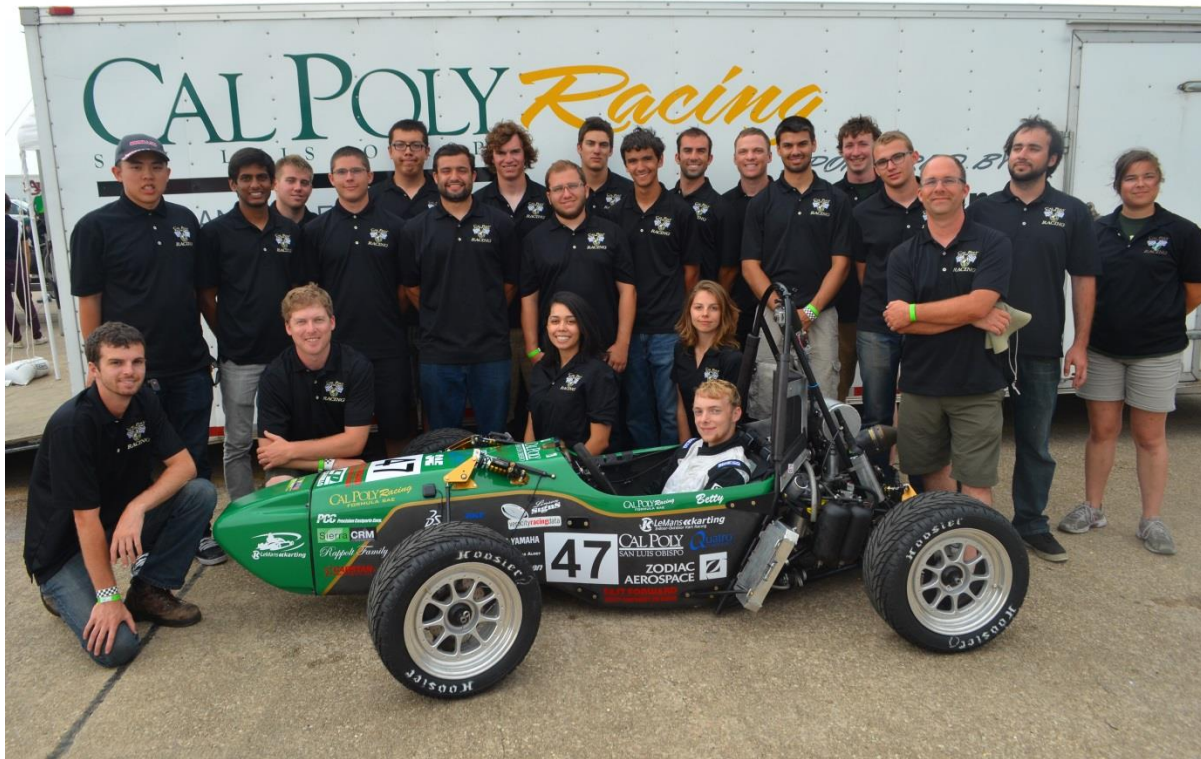


Figure 11.2 - The Cal Poly Formula SAE Team, Formula Electric team members, and advisor John Fabijanic at FSAE Lincoln.

Listed below are the takeaways for the chassis subsystem from competition:

- Tech Inspection
  - Scrutineers asked very few questions regarding composite structures (monocoque, impact attenuator, anti-intrusion plate)
    - Simply asked us to show approved reports, didn't check to see that car's components matched those reported
  - Almost ran into trouble with shoulder harness bar gussets, with special scrutineer walking around looking at SES issues
    - Apparently, were supposed to be same size tubing as shoulder harness bar
      - We used 0.5" tubing for easy notching and welding
    - We purposefully made our calculations vague, showed scrutineer that SAE approved us to use some form of gusset with no material properties specified, he let us go
  - Didn't know that shoulder harnesses had to be securely separated on shoulder harness bar
    - Scrutineers recommended welding pencil steel in a "U" so harnesses were captured, but they accepted cable ties securing cut pieces of radiator hose on either side
  - Thought we might have to install second anti-sub belt set due to "reclined" position of Percy, so had second a set on-hand
    - Realized late that Percy's back angle, not seat back angle, defined driver position and belts required

- Scrutineers didn't check Percy's back angle
- Lap belt angles were glanced at, not checked in-depth
- Harness spec (FIA) was different from that specified in rules
  - Had to pull up equivalent specs from online for proof
  - Need to explain stuff up front that's out of the ordinary
- Wiring in tub wasn't properly secured
  - Scrutineers wanted cable ties at all loose sections
- Line-of-sight to radiator cap and fuel cap wasn't blocked
  - Used gaffer tape to extend across gap in head rest sheet metal to block fuel cap, and used sheet metal fastened to radiator to block radiator cap
- Egress was fast, helped by room for knees and Camlok harness
  - 3.2 seconds, first try
- Overall, had smooth scrutineering process due to up-front work during design and manufacturing
  - 30 min. first round, 30 min. fixes, 15 min. second round
- Design Judging
  - Had trouble communicating information due to lack of prepared presentation materials
    - We knew this - we ran out of time to make nice posters for the whole team, and didn't bring the senior project poster
  - Perform detailed high-level analysis for decisions, ideally with points as the output
    - Including decision of chassis type
      - We had subjective criteria, not objective, and our work leading to the decision wasn't made explicit
    - Analyze cost and performance together
      - Don't let cost be a by-product of decisions
  - Explicitly present things that are out of the ordinary, or "stupid"
    - If something is different about our chassis, whether good or bad, explain why
    - Don't force the judges to ask or wonder
  - Tub was heavy relative to those of other teams
    - They complained that cost was also high relative to other teams, likely related to high weight
  - Present details behind obtaining torsional stiffness number, rather than just the number itself and why we chose it
    - Ideally, perform physical test to validate model
  - Present data behind impact attenuator numbers
    - Liked the concept but wanted a design with data backing it
      - We didn't have the time to pull up the data for them, and lacked design iterations with data
  - Pedal assembly was difficult to access
    - Luckily, we didn't have to move it during judging
  - Bead seat needed gaffer tape for sealing
    - Beads need containment in impact so they can absorb energy
      - Weren't aware of this
    - Didn't have time to tape it up after we finished trimming
  - Ergonomics judge (5'6", 160 lb, history in Indy racing) loved cockpit, said it was most ergonomical FSAE cockpit ever sat in
    - Liked that cockpit was designed specifically for our drivers, with meeting intent of rules being second priority

- Liked comfort
  - We assume he liked back, sides, and thigh support, and positioning of torso, arms, and legs
- Liked visibility
- Liked protection
  - Monocoque, and front axle centerline ahead of legs (liked engineering done to achieve this)
    - Result of wheelbase decision during vehicle design, and packaging
- Liked steering design
  - Liked low play from straight steering shaft, and fact that we managed to incorporate it without making the car a bus
    - Again, result of wheelbase decision during vehicle design, and packaging
  - We assume he liked positioning relative to driver, especially in context of straight shaft to floor, and room for thighs due to flat bottom
  - Liked paddle shifter actuation
  - Only criticism was that he wanted controls labeled
- Judges loved the manufacturing quality of our chassis and car
  - Reiterated by many teams we spoke with
  - Exemplified by fact that we were only team showing significant areas of raw carbon on our tub
- Overall, important to show off to judges what we like about our car and what engineering we're proud of, and make things organized
  - We attempted to show off the integration of systems due to how we made our top-level decisions and how those influenced system design, but failed to communicate it fully
    - Ergonomics judge got bits and pieces, but the judges didn't get the full story
  - Important to make it easy for judges to present and stand up for us when they're finalizing scores with other judges
- Cost report
  - Little cost savings potential in nose
  - No advantage to doing cut-and-fold (tooling cost low)
  - No advantage to non-structural nose
    - Decrease in material, cutting, and layup cost negated by cost of foam impact attenuator
  - Al plate cost can be eliminated by changing from composite to steel sheet (save almost \$300)
    - Significant weight increase, so "run" steel plate for cost event but composite for others
  - Tub cost
    - Practically eliminated if full steel tube frame is run (save almost \$4000)
    - Eliminate lap joint (save \$300-\$350)
    - Reduce cost by reducing material
      - Savings in material and cutting
      - Reduce size of tub
      - Optimize laminates (minimize cost for carbon and core)

- Only thing we forgot to include: paint
  - Knowingly left this out of report, were running out of time
- Overall, tub (and DAQ system) killed us in Cost
- Dynamic events
  - Tightest corner on Autcross and Endurance courses was much tighter than expected
    - Car had to tip-toe through corner at far end of endurance course, could have been much worse - keep turning radius in mind during future wheelbase decisions

## 12. Budget, Funding, and Sponsorship

This project cost the team approximately \$3,760 before monetary donations and discounts, and approximately \$3,300 after. A breakdown of expenditure is included in Table 12.1, and full accounting is included in Appendix F: Accounting.

Table 12.1 - Chassis subsystem costs.

Category	Expenditure
<b>Monocoque total</b>	<b>\$2,086.87</b>
Layup tooling	\$260.15
Layup material	\$1,511.52
Bulkhead tooling	\$79.74
Finishing tooling	\$59.21
Finishing material	\$176.25
<b>Frame and front hoop total</b>	<b>\$853.10</b>
Frame tooling	\$295.62
Frame material	\$303.59
Main hoop tooling	\$32.66
Main hoop material	\$179.55
Front hoop material	\$41.68
<b>Nose cone total</b>	<b>\$235.15</b>
Tooling	\$231.85
Hardware	\$3.30
<b>Testing total</b>	<b>\$322.13</b>
Laminate	\$56.18
Nose cone	\$119.70
Vehicle	\$146.25
<b>Accessories total</b>	<b>\$150.84</b>
Head rest material	\$35.11
Insert material	\$115.73

These costs do not include those shared with other subsystems, such as sheet metal and general car hardware. Sheet metal cost the team \$350, and about half of it was used for the chassis subsystem. Hardware cost \$400 for the whole car. Funding was provided by the team, which was sourced from Cal Poly's Instructionally Related Activities allocation to Cal Poly SAE and monetary donations from companies, families, and alumni.

The chassis subsystem cost was higher than originally expected, but was greatly helped by chassis-specific sponsorships. These are included in Table 12.2.

**Table 12.2** - Project sponsors with their contributions and their approximate values.

Sponsor	Contribution	Value
C&D Zodiac	Mold manufacturing services	\$20,000
Quatro Composites	Carbon fiber pre-preg	\$10,000
Simon Rowe	Welding services	\$1,500
ME Student Fee Allocation Committee	Money for monocoque material	\$150
AERO Student Fee Committee	Money for monocoque material	\$600
The Waldrop Family	Seats purchase	\$400
Tabak Law	Harness purchase	\$350
Texas Almet	Discount on monocoque material	\$400

## 13. Conclusions

Various conclusions from the project are included in this section. The purpose of these conclusions is to guide future chassis projects such that they may build from our results and understand how the process covered in this report can be improved.

### Requirements

- Weight requirements far from end result due to lack of knowledge and analysis
- Serviceability not addressed well
  - Need researched requirements considering time for removal/adjustment of important assemblies
    - Engine removal and installation
    - Diff removal and installation
    - Chain tension adjustment
    - Pedal assembly adjustment
    - Cable adjustment
    - Hypothesize time required for an appropriate scenario
      - To evaluate whether requirement met, calculate man-hours on basis of car position (ground/stands), count and accessibility and thread length of fasteners, and weight of assembly
- Some requirements chosen to be ignored
  - Front impact
    - Energy absorption not met
      - Test piece met SAE rules but not our energy requirement, no time to continue iteration or run test for higher displacement
  - Side impact
    - Impact structures abandoned
      - Not enough time to manufacture
      - Side impact unlikely
      - Side of tub very beefy - drivers felt safe
      - Finish at side of tub looked really good
  - Intrusion
    - Front suspension points



- Not enough time to test
  - Fuel tank
    - Protection deemed unnecessary
- Suspension alignment assistance
  - Not time-efficient given number of alignments expected
- Covering engine components
  - Not enough time to manufacture
  - Car looked cool with everything exposed
- Skid protection
  - Deemed unnecessary due to lack of risk, thickness of tub bottom at lap joint
- Thigh support
  - Potential to hinder egress
  - Sufficient support provided by electronics box cover

## Vehicle

- Understand section stiffnesses of chassis
  - Identify areas of excessive stiffness and insufficient stiffness
    - Maximize specific stiffness
  - Design suspension point location for chassis stiffness
- Design suspension and chassis together
  - Minimize material usage for both chassis and suspension through designing geometry to minimize loads/need for strength
  - For example, we had very high eccentric loads at front rockers due to changing direction of load (shock at 90 degrees from rod) - could have been designed better
- Chassis room was excessive
  - Difficult to reduce tub room at sides and top due to templates
    - Could be reduced if front roll hoop integrated into tub
  - Pedal assembly was long (forward master cylinders), and adjustment range was excessive (never used forward-most mounting position)
    - Shorten tub, reduce weight
  - Percy clearance to roll hoop line about 1 inch extra
    - Shorten main hoop, reduce weight and tube bending error
  - Drivers were not as close to roll hoop lines as expected (compare layout images to photos of drivers in car)
- Weight distribution excessively rearward - maybe?
  - In theory, had to kill grip at front with ARB to balance oversteer
    - Lower grip overall in cornering
  - In practice, removed ARB to balance car due to differential influences
    - No cornering grip sacrificed
  - 47% target with no differential considerations, maybe 45% good target with differential?
- Half-shaft angles huge
  - Move diff or rear axle - diff had room to move forward and up within existing frame
- Rear box low on space
  - Rear sprocket too small at first, limited room for larger sprocket in frame

- Lower box triangulation member, shocks
  - Diff insertion/extraction and chain tension shim installation difficult
    - Little hand room at sides (frame) and top (shocks)
- Diff and half-shaft fasteners difficult to access
- Engine assembly and servicing
  - Engine difficult to get into frame
    - More clearance with rectangular tubing for diff mounting would have made assembly easy
    - Complicated assembly process for engine alone (15 minutes, 2 people)
      - Bring straight up tilted forward
      - Slide back behind rear mount
      - Rotate front up
      - Slide forward to front mount
      - Drop rear mount in like its hot
  - Not enough room for socket at front mounts
    - Complicated fastening with allen wrench required
  - Not enough room for ratchet or full wrench rotation on head cover due to lack of clearance to head rest
  - Flywheel cover could barely come off without engine movement, would have required engine movement if there was the slightest bit less room
  - Lack of space in frame resulted in needing to move engine accessories to get to engine itself
    - Removed 2 to 3 inches of frame length in engine area as compared to Annie, to place driver farther rearward
      - Betty's engine components much more cramped
    - This is a race car, so maybe lack of space is something that just needs to be accepted
- Design for wrench clearances

## Components

### Monocoque and Attachments

- Mechanics
  - Reduce carbon weight
    - Increase core thickness (increase bending and shear strength/stiffness)
    - Optimize individual laminates (including bulkhead) for structural equivalency
    - Increase core strength/stiffness so core doesn't fail in compression, and core shear deformation is reduced, meaning less carbon needed
    - Reduce thickness of lap joint, or execute differently
      - Instead of bonding and wet layup, investigate whether bonding alone is possible
        - Keying to increase bonding area if needed
    - Improve templates to reduce buildup in tub layup
  - Reduce core weight
    - Use core with better bending ability (no compressing/crushing required)
      - Used twice as much core as expected due to compressing/crushing (about 5 lb extra)

- Optimize tub for shear strength
    - Use light core in most places and heavy core where strength required (some optimization with balsa)
- Reduce attachments weight
  - Increase shear strength at attachment points to reduce bracket and backing plate sizes, and optimize non-rules brackets and backing plates (suspension, etc.)
    - Bracket sizes dependent on carbon and core strength (mostly shear, some bending), which determine penetration load in test
    - Reduce fastener size/count for suspension points
  - Integrate front roll hoop into laminate
  - Strengthen harness attachment points to integrate lap and anti-sub points, if safety not a concern
  - Consider doublers and larger brackets as opposed to balsa
- Pay attention to core properties
  - Different cores can have very different properties, and both strength and stiffnesses have very large effects on laminate performance
- Manufacturing
  - Design and make patterns for layup beforehand (see note in Mechanics above)
  - Avoid uni-directional carbon fiber pre-preg
    - Fibers don't shift like in cloth to meet complex curvature
    - Solid sheet, unlike cloth, resulting in air bubbles which make layup difficult and require popping
  - Consider geometry and thickness of core in context of bending ability, to meet tub curvature (see note in Mechanics above)
    - Over-expanded, flex core, larger cells, thinner core
  - Investigate whether film adhesive required
    - Extra time for layup, and weight
    - Initial testing indicated it may not be required
  - Investigate whether peel ply required
    - Resin soaked up, but not too badly
      - Resin mass fraction went from 0.42 to 0.36 in single ply contacting peel ply
  - Use good vacuum bag
    - No Stretchlon, due to pulling plies into mold
      - We used pleated vacuum bag instead
    - Check temperature rating
  - Reduce work required for tub bonding
    - Investigate one-piece monocoque
      - Two-piece mold, bolted together
      - No bonding required (done in layup)
    - Improve design of joint (see note in Mechanics above)
  - Make molds perfect
    - Design bulkhead into mold, so plug isn't required
    - Do good mold finishing work, so minimal sanding, bondo, etc. required in part finishing (less time, less weight)
  - Size core/laminate thickness to make balsa and insert incorporation easy

- Paint important (tub got to above 160 F in sun, felt gooey at times)

## Frame

- Mechanics
  - Further optimize tubing geometry and sizing, especially around engine/diff/suspension bulkhead
  - Place engine to allow for tube in top view to triangulate engine region, on top or bottom
  - Design rear engine mount for clearance fit plus clamping mechanism, for ease of assembly and good engine constraint
- Manufacturing
  - Improve main roll hoop manufacturability (took 3 weeks and \$210)
    - Get the right die or outsource work
    - Reduce plane count for bends
  - Modify rear bulkhead design
    - Reduce number of processes/setups required
  - Build a planar frame. Almost every tube required 3 dimensions rather than planar setups. Planar setups are much easier - see if you can build the frame like you would a wall of a house: on a flat surface (no complex geometry), and then just effectively stand it up. Makes for a much quicker and easier process as the jigs are greatly simplified. Think about a planar main hoop versus all the extra work to get bends in multiple planes and how much time was invested in tools and jigs to get it right.
  - Improve tube notching/finishing processes
    - A few days with a few people to do rough notches, about 15 minutes per notch of very skilled labor to do finishing work
      - Finishing took longer as most rough notches were poor or the tubes were cut too short and would have to do them over from the start.
      - Another note, if you teach someone how to run the tubing notcher, it works really well, provided we have a 1" roller.
      - 15 minutes should be all it takes to final fit a tube. Otherwise, it's an hour to do it from the start for an experienced person.
    - Look into outsourcing to CNC notcher
      - Extra work up front (drawings, test runs), but could save a couple weeks of work for a few people
  - Have multiple dedicated welders/jiggers on-hand
    - We depended on Simon Rowe for most welding (especially difficult welds)
      - Depended on team members who had other things to do for rest of welding - caused much waiting and inefficient use of time
  - Make suspension tabs easier to manufacture
    - Boxing with separate pieces of sheet metal was time-consuming, both in shaping and welding
    - Perform analysis/testing to see if boxing is necessary, consider using notched rectangular tubing instead of four separate pieces of sheet

## Nose Cone

- Mechanics
  - Iterate laminate design to minimize weight and meet our energy absorption requirements

- Small amount of material absorbed energy in testing
  - Investigate whether there's a better energy absorption strategy than delamination
- Design and test for off-axis loading (only proven for head-on impact)
- Cap essentially didn't act as part of attenuation, but allowed us to meet acceleration rule
  - Loophole: have non-structural part start impact to increase length of attenuator
  - To meet spirit of acceleration requirement, should meet average acceleration for interval above defined acceleration level (e.g. 5 G)
- Manufacturing
  - Reduce depth of nose to simplify layup
  - Molds
    - Round 1
      - Intention to maybe work parts into final products, but mainly use parts for testing
        - Mounting not fully designed
      - C&D-style room-temp cure, high-temp, reusable mold
        - Foam buck
      - Difficulties encountered removing buck from mold due to waves in buck, not enough draft
        - Had to chip buck out
        - Ask C&D how they do this
      - Used mold to make parts for testing
    - Round 2
      - Mounting geometry included, intention was for this mold to be final
      - Carbon pre-preg mold so it wouldn't be totally rigid, be easier to remove buck and avoid issues from last time
        - MDF buck required to handle cure temperature
        - Plans abandoned and room-temp mold chosen again (we thought we could fix issues from last time), but MDF buck already in progress so we continued with MDF
      - Difficulties encountered removing buck from mold, because mounting hole geometry caused buck to wedge into mold
        - Also, no sealing wax used, not enough Frekote used
        - MDF buck was extremely difficult to chip out
      - Mold abandoned due to damaged incurred during removal
    - Round 3
      - Mounting geometry modified for draft in x, y, and z
      - Extended nose back, to give us more margin for error
        - Trim to fit tub
      - Room-temp cure mold, like Round 1
        - Foam buck used to avoid issues encountered with MDF
        - Sealing wax used (3-4 buffings), more Frekote used (4-5 coats)
          - Wax made a very obvious difference in surface finish
      - Difficulties encountered again, but solution found

- Chipped away center of buck to allow sides to flex in from mold wall
    - Air injected into gap, buck popped out
  - Used mold to make parts for car
- Layup
  - Deep geometry of the mold made laying in carbon fiber very difficult, especially the first few layers.
  - Unidirectional carbon fiber was difficult to work with for the first few layers, may want to consider using cloth.
  - Excessive bridging at the tip and mounting holes was experienced. May want to consider building nose on a male mold to make working with layup easier.

## Material Procurement

The obvious material choice for constructing a monocoque chassis is preimpregnated carbon fiber with a core material. The prepreg has a long out time so long layups can be done without the mess of doing a “wet” layup and the core provides stiffness with little weight. It is important to realize that in order to design a quality chassis, good material properties are needed for analysis. Carbon and core need to be procured early for testing so models (CLT) and manufacturing methods can be verified. This way, design can be done with high levels of confidence.

Testing requires a descent amount of material. To characterize the carbon fiber, three tests are needed: two tension tests and one shear test. Each of these tests requires at least five samples to establish any sort of statistical basis. Additionally, SAE requires testing for certain laminates and manufacturing solutions may also want to be tested. The important thing is to plan for this material usage when obtaining carbon in addition to the amount going into the chassis. Also include a safety factor so if additional testing is required, there will not be a material shortage.

For the 2013 chassis, the carbon fiber was not selected based on its properties. Rather it was selected because it was what was available to the team at low cost. While the FSAE team does operate on a tight budget, the properties of the carbon fiber should be taken into consideration. The ideal carbon fiber for the FSAE chassis is a medium strength, high modulus type. This will help meet stiffness requirements outlined in SES while reducing weight by using less plies. Additionally, a proper core splicing adhesive should be utilized. This will potentially reduce weight and allow for tidier core splicing.

The most promising sources for carbon fiber prepreg and core are aerospace companies. In the past, Quatro Composites, Lockheed Martin, and Boeing have been donors for prepreg. They usually have expired material that cannot be used in flight structures that they can give to the team at no cost. Sometimes these companies are willing to give you certified material at their cost, which is significantly lower than retail. This would be a good route to take if the team was well funded for the year and the chassis team was ambitious in composites engineering. It would give them the flexibility they need to pick the proper material and truly optimize the structure.

Finally, it is important to realize that prepreg needs to be kept in the freezer at all times to prevent it from curing prematurely. This is important when transporting and storing the material. Typically, the material can survive a long car ride if kept out of the sun and the car isn’t allowed to sit. The material should be placed in the freezer immediately after it has arrived at its destination. This requires some coordination at Cal Poly, since the freezer is shared with research and other student projects. The team should consider purchasing their own freezer, to make logistics in storing material easier.

## Analysis

### Structural Equivalency

Before a few years ago, the SES was called the “SEF”. This was a custom-formatted report which was submitted to SAE to prove structural equivalency. Because the format was customized, and SAE had to sort through a hundred such reports for each competition, it was very easy to deceive the officials. This resulted in very lightweight composite chassis which didn’t necessarily meet the rules.

Now, teams must submit the SES. This is a spreadsheet which is defined by SAE with equations which can’t be edited - all the teams can do is enter numbers and produce outputs. Most of the calculations are simply-supported beam calculations for the sake of being simple and conservative. Teams must test the Side Impact Structure (SIS) laminate to generate material properties; the face sheet is assumed to be isotropic with an elastic modulus, and the strength is interpreted. Now, any laminate of any structure is assigned this elastic modulus and strength, and its properties are calculated with these values and the core and face sheet thicknesses. To optimize, teams must test other laminates and generate their particular material properties.

In addition to generating properties, the SIS laminate is compared to steel tubes. The laminate of 19.7”x7.9” must show equivalency to a single steel tube. However, only the bending properties of the steel tube are accounted for. The SIS laminate undergoes both bending and shear deformation, so when it’s compared to the steel tube with only bending deformation it doesn’t stand a chance. SAE allows teams to test steel tubes themselves to calculate “rig compliance”. We did this, and calculated a “rig compliance” almost equal to the bending deformation of the tube - this was actually shear deformation in the tube. This compliance is subtracted from the SIS laminate data, resulting in an artificially stiff laminate to go against the bending-only tube - an even match-up. This new laminate property, with laminate compliance minus tube shear compliance, is also used for calculations with all the laminate structures.

On top of having to succeed in this test, the actual SIS dimensions as it appears on the car must be proven to be equivalent to the properties of three steel tubes. Unless the SIS is 24” tall (three times the width of the test piece), this is more difficult to meet than the test requirement itself.

While the stiffness requirements are difficult to meet, the energy requirements are incredibly easy. This is because all the deformation in the laminate, including bending and shear, is considered to be only bending deformation. Deflection due to bending constitutes significantly more energy than that due to shear, so the energy values are artificially high.

Overall, the SES is made too easy to fill out. It’s designed such that anyone with basic engineering experience can use it, at the cost that it is an inaccurate representation of reality and results in over-designed monocoques. Our project suffered because we couldn’t use our high level of composites knowledge to meet SAE’s rules through the SES. The only way to do this is through the use of FEA and the Alternative Frame rules.

### Finite Element Analysis

The best way to accurately represent the monocoque is to analyze the monocoque sections as part of the entire structure. This allows 3D geometry and accurate constraints to be considered, as opposed to treating everything as a simply-supported beam. The Alternative Frame rules, which are an alternative to the Structural Equivalency rules, allow the use of FEA in this manner. As a result, designs can be less

conservative and reduce weight in the chassis structure. Additionally, structures don't have to meet the shapes suggested by the Structural Equivalency rules.

We only used FEA for torsional stiffness analysis, but it should be applied to as much strength and stiffness analysis as possible, even beyond the Alternative Frame rules. This requires time, ability to use FEA programs, and validation of models. For validation, full material properties from testing are required and basic results such as those from simple beam models should be validated against real-life tests. Also, the torsional stiffness model should be validated through a torsional stiffness test. The easiest method of constraint of the car in real-life must be determined. A rig must be constructed and similar constraints must be applied to the finite element model for comparison purposes. Insights from this test may help with developing the model to account for complexities such as the monocoque/frame connection. With validated finite element models in general, analysis can be confidently performed for years to come to further reduce chassis weight.

### **Dynamic Loading**

One of the areas of the chassis and car that is not very well understood on the team is dynamic loading. Sources of dynamic loading come from suspension input loads and the engine. These loads cause the car to vibrate which could lead to premature failure due to fatigue. Understanding these vibrations will lead to a better design for the car. Some things to consider with regards to dynamic loading:

- The natural frequency of the chassis and suspension members is important. Making these members sufficiently stiff and not exciting their natural frequencies will make for a smoother ride. And a smoother is faster.
- Constraining the engine properly can result in a stiffer chassis. Currently, the engine is constrained by only 2 points (front and aft). Utilizing a third mounting point will help with dynamic load transfer from engine vibrations. Additionally, clamping the engine properly with these mounts is important. Any slop will result in the engine torquing itself around in the frame. This could cause premature damage from fatigue.

### **Bolted Connections**

The monocoque/frame connection is a key player in the chassis' torsional stiffness. Here, the twist of the chassis is supported by a handful of bolts so it is important to understand the mechanics of the system. To analyze this, FEA should be utilized. The bolted joints should be modeled as springs tied to the bolt holes of the frame and chassis. The springs' stiffness's can be tuned to match results from a physical torsional stiffness test or bolt shear stiffness's. Once the model is running, different bolt configurations can be tested to identify the optimal bolted connection that meets the chassis' torsional stiffness target.

Additionally, the suspension attachment points should be considered. By using a bolted connection for the attachment solution, heavy hardware and backing plates are utilized. A bonded type solution should be investigated. This incorporates a bracket that is bonded onto the monocoque with structural adhesive. Layers of carbon fiber are then post bonded on top of the base of the bracket thus sandwiching it. This solution may be better for load transfer to the monocoque (continuous versus discrete points) and may be lighter than the bolted solution.



## 14. Final Recommendations and Future Work

Following this project, our final recommendation regarding chassis type depends on any given Formula SAE team's plans. First, if a team is performing development of a chassis in a single year, a steel tube frame would be the ideal chassis type. Achieving high performance in a single year would be more likely with a steel tube frame than with a composite monocoque chassis because of the following tube-frame advantages:

- Low weight (for a single year's development)
- Short manufacturing time
- Low manufacturing skill required
- Ability to easily make changes during or after manufacturing
- Accessibility
- Low cost

However, if the team is willing to forego high performance for a year or two to focus on development, a monocoque chassis can perform very well and possibly better than a steel frame, for the following reasons:

- Low weight (following multiple years' development)
- High driver safety regarding intrusion
- Learning opportunity for composites and engineering in general

We believe that with one year's development following this project, Cal Poly's hybrid chassis could be at the same weight as the best steel tube frames through 15 lb of potential weight reduction. Weight could be further reduced through work to follow the Alternative Frame rules, or possibly through creation of a full monocoque using the processes developed and lessons learned from this project. In addition to reducing weight, the team can further develop chassis torsional stiffness analysis through testing to make the most of our work. Because this project was largely for the purpose of development and documentation for future years, and the facts that the chassis served the team well in 2013 and has large potential for improvement just one year out, the chassis type we developed was the right one for Cal Poly Formula SAE.

# Appendices

## Appendix A: Section Writers

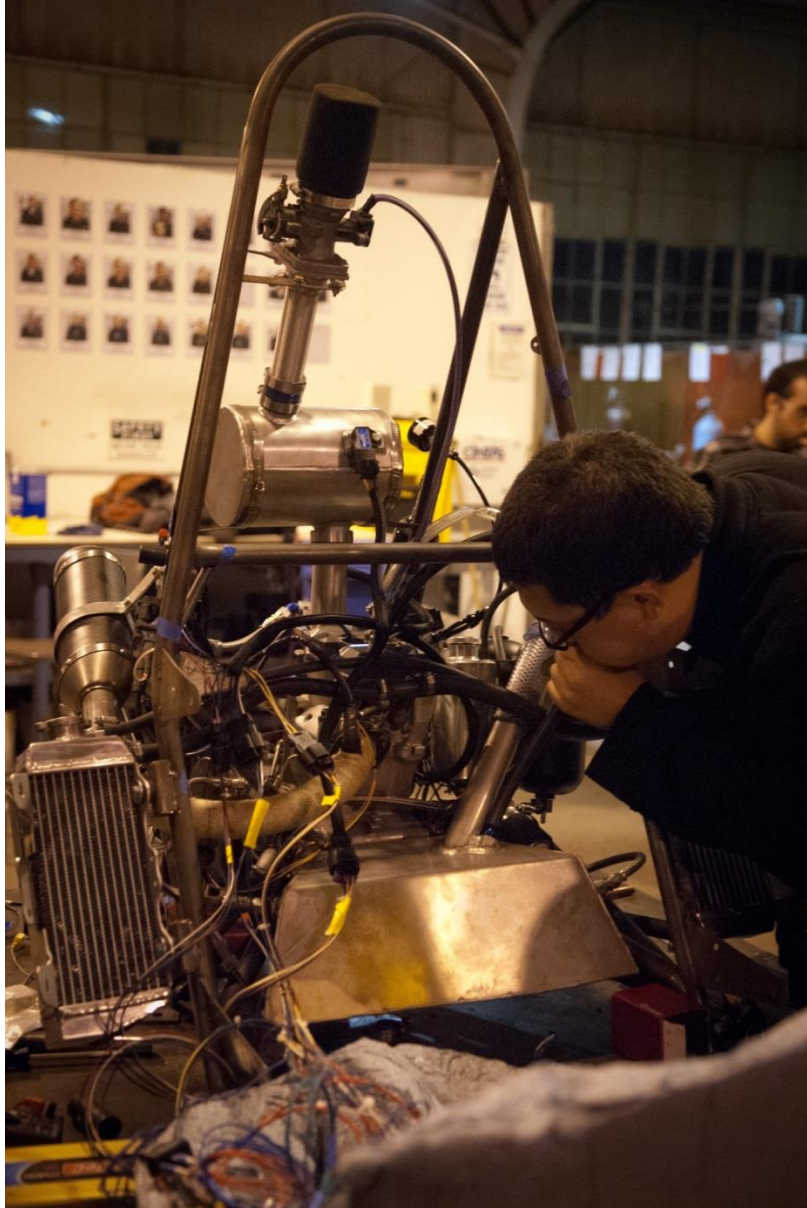
Executive Summary.....	John Rappolt/John Waldrop
1. Introduction .....	
Problem Statement.....	John Waldrop
Recent Team History.....	John Waldrop
Recent Chassis History .....	John Waldrop
Team Goals.....	John Waldrop
Project Goals .....	John Waldrop
Initial Project Direction .....	John Waldrop
2. Project Management .....	John Waldrop
3. Formula SAE Rules .....	John Waldrop
Structures.....	John Waldrop
Front Protection.....	John Waldrop
Templates.....	John Waldrop
Harness .....	John Waldrop
Miscellaneous .....	John Waldrop
4. Requirements.....	John Waldrop
Safety .....	John Waldrop
Impact .....	John Waldrop
Intrusion.....	John Waldrop
Torsional Stiffness.....	John Waldrop
Miscellaneous .....	John Waldrop
5. Vehicle Design.....	John Waldrop
6. Full Monocoque Chassis Design and Analysis.....	
Initial Material Selection .....	John Rappolt
Manufacturing Concept .....	John Waldrop
Geometry and Packaging Development .....	Nick Henderson/John Rappolt/John Waldrop
Analysis .....	
Mechanical.....	John Rappolt
Thermal.....	John Rappolt
Issues and Switch to Hybrid Chassis .....	John Waldrop
7. Hybrid Chassis Design and Analysis .....	John Waldrop
Loading Sources .....	John Rappolt
Monocoque.....	
Geometry .....	Matthew Hagan
Laminate Development.....	John Waldrop
Attachments.....	John Waldrop
Bond .....	John Waldrop
Frame and Front Hoop.....	
Attachments.....	John Waldrop
Initial Design.....	John Waldrop
Torsional Stiffness.....	John Waldrop
Final Construction .....	John Waldrop
Nose Cone/Impact Attenuator .....	John Waldrop
8. Laminate Testing and Data Analysis .....	John Rappolt
Material Properties Testing .....	John Rappolt

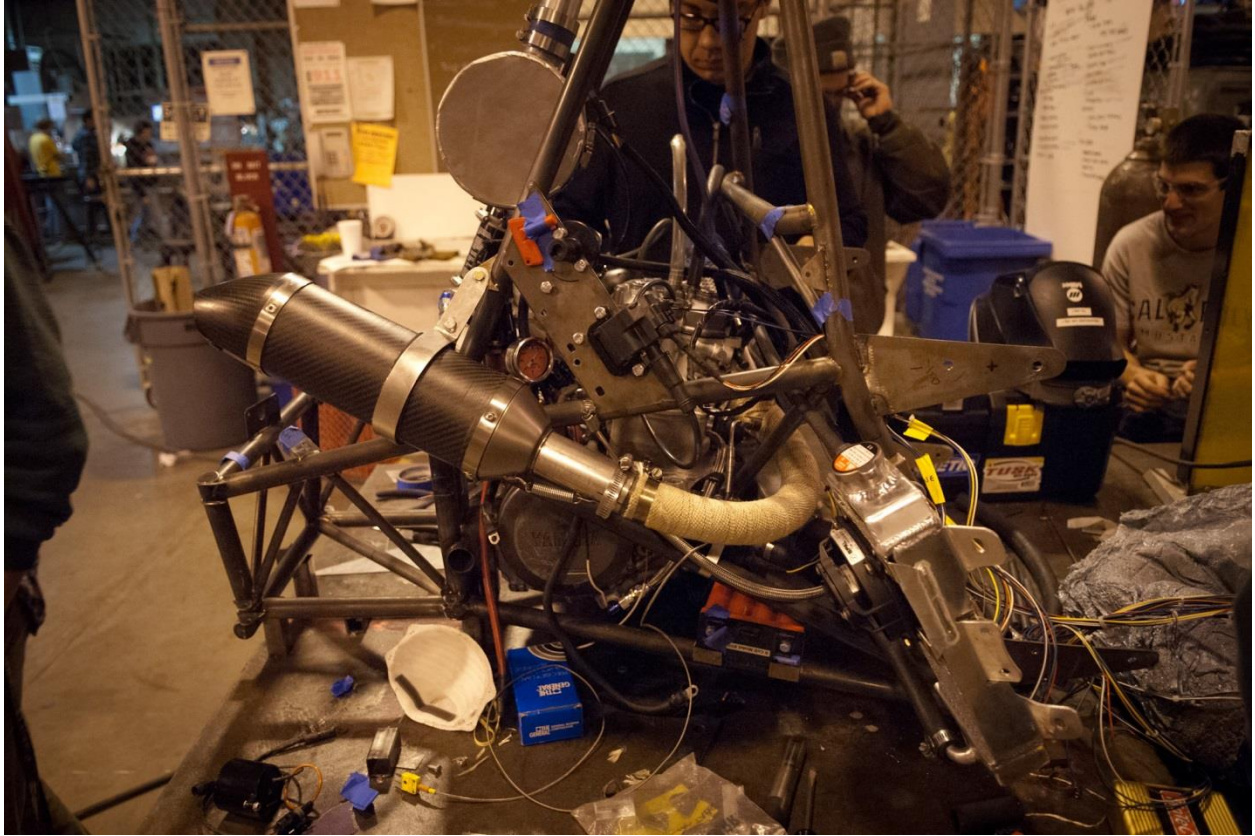
SAE Laminate Testing .....	John Rappolt
Suspension Attachment/Balsa Core .....	John Rappolt
Impact Attenuator Testing.....	John Rappolt
Conclusions .....	John Rappolt
9. Manufacturing and Vehicle Integration.....	John Waldrop
Monocoque.....	Matthew Hagan
Buck and Mold .....	Matthew Hagan
Layup and Cure .....	Matthew Hagan/John Rappolt
Bond and Lap Joint.....	Matthew Hagan
Closeouts.....	Matthew Hagan
Inserts.....	John Rappolt/John Waldrop
Fit and Finish .....	Matthew Hagan
Frame and Attachments .....	
Jig .....	Matthew Hagan
Bulkhead and Box.....	Matthew Hagan
Main Hoop .....	Matthew Hagan
Longitudinal Members .....	Matthew Hagan
Monocoque Attachment.....	Matthew Hagan
Suspension Attachment .....	Matthew Hagan
Fit and Finish .....	Matthew Hagan
Front Hoop.....	
Tubing .....	Matthew Hagan
Monocoque Attachment.....	Matthew Hagan
Cockpit Controls.....	John Waldrop
Fit and Finish .....	Matthew Hagan
Nose Cone/Impact Attenuator .....	
Buck and Mold .....	Matthew Hagan
Layup.....	John Rappolt
Fit and Finish .....	Matthew Hagan
Inserts.....	John Waldrop
Anti-Intrusion Plate .....	
Design.....	John Rappolt
Manufacturing .....	John Rappolt
Harness Mounting.....	John Waldrop
Head Rest/Firewall.....	John Waldrop
Electronics Cover.....	John Rappolt
Seat .....	Matthew Hagan
10. Mass Properties .....	John Waldrop
11. Vehicle Performance.....	
Vehicle Testing .....	John Rappolt/John Waldrop
Competition .....	John Rappolt/John Waldrop
12. Budget, Funding, and Sponsorship .....	John Waldrop
13. Conclusions .....	John Waldrop
Requirements.....	John Waldrop
Vehicle.....	John Waldrop
Components.....	
Monocoque and Attachments .....	Matthew Hagan/John Waldrop
Frame .....	Matthew Hagan/John Waldrop

	Nose .....	John Waldrop
	Material Procurement .....	John Rappolt
	Analysis .....	
	Structural Equivalency .....	John Waldrop
	Finite Element Analysis .....	John Waldrop
	Dynamic Loading .....	John Rappolt
	Bolted Connections .....	John Rappolt
14.	Final Recommendations and Future Work .....	John Waldrop

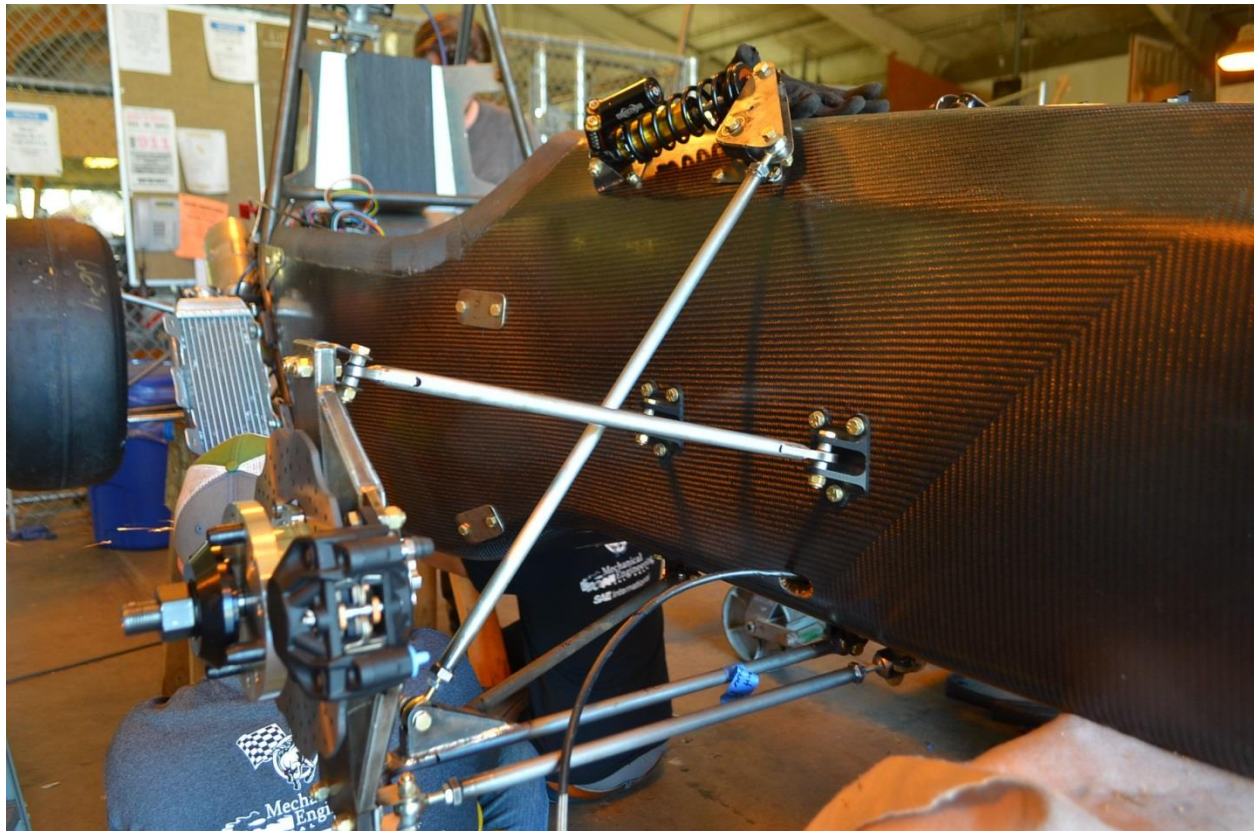
## Appendix B: Additional Photos

Relevant photos of the chassis subsystem which weren't appropriate for other sections of the report are included here. They span from car assembly to the competition, and provide further insight into the chassis' interaction with other subsystems.

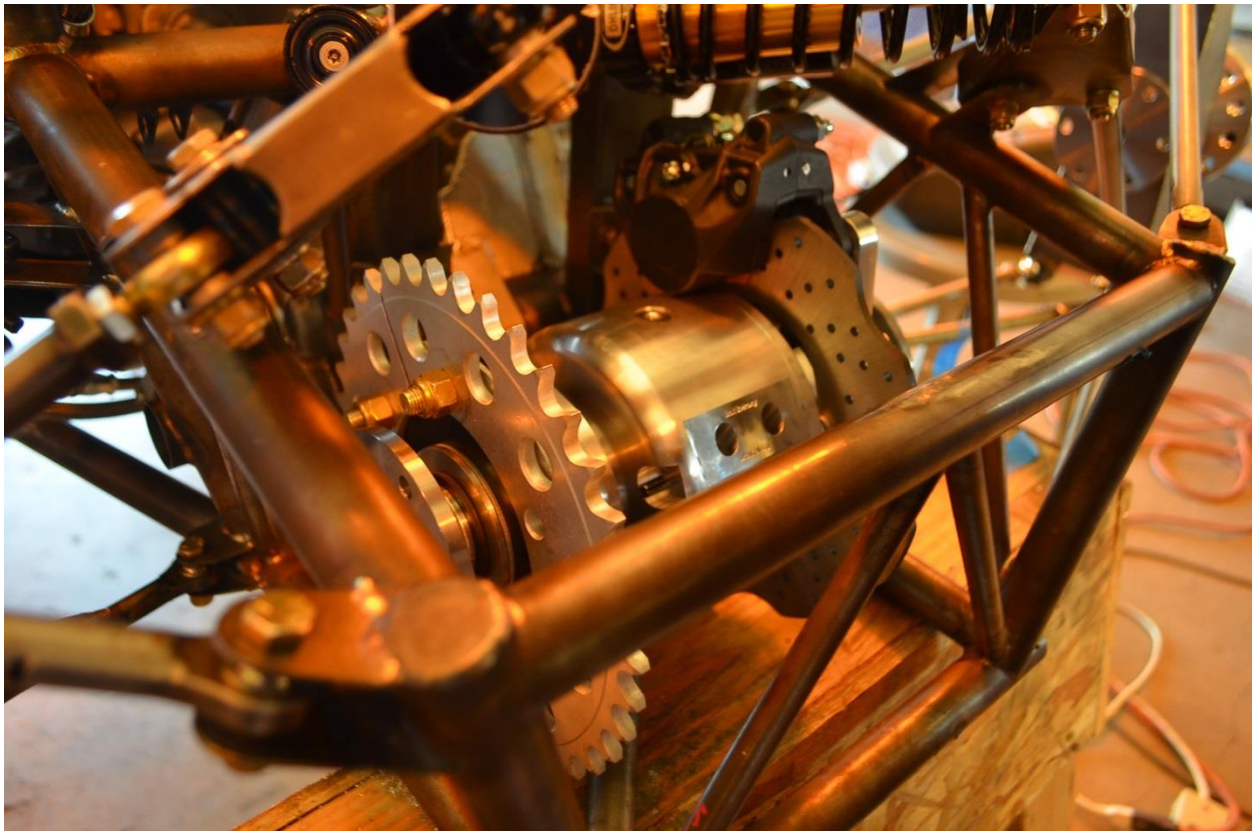
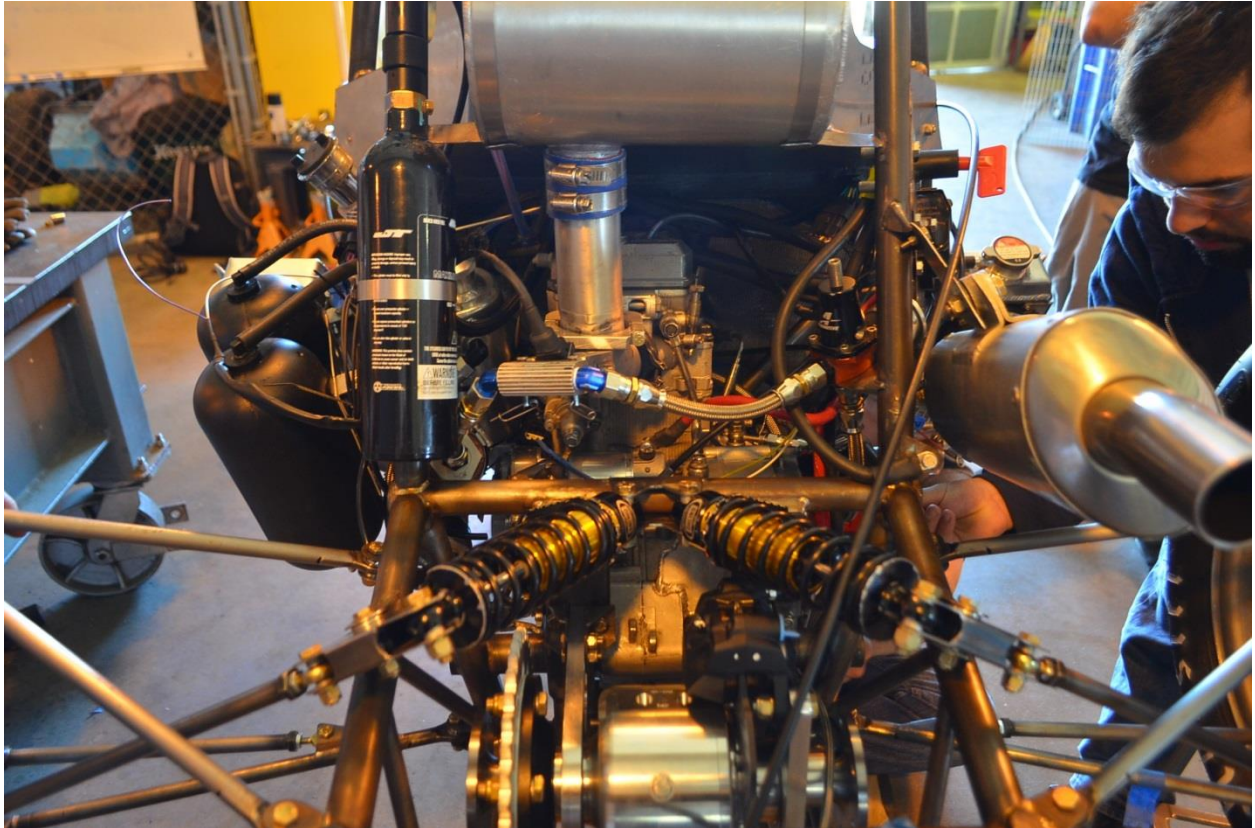


















## Appendix C: CLT Script

```
%% FORMULA CHASSIS WORKS - CLASSICAL LAMINATION THEORY
% John Waldrop
% (408) 504-6900
% johnwwaldrop@gmail.com

%% INSTRUCTIONS
% - Input material data, laminates, and loading cases (see USER INPUT
% indicators in script)
% - FI_n(a,b,i) is failure index, where n is laminate, a is loading case, b
% is ply tops and bottoms, i is 1 or 2 or 12 direction
% - squeeze(FI_n(a,.,:)) gives failure indices through laminate, where n is
% laminate, a is loading case
% - FI_max(n,a) gives maximum failure index, where n is laminate, a is
% loading case
% - FI_maxfib(n,a) gives maximum failure index in fiber direction, where n
% is laminate, a is loading case
% - squeeze(K(n,.,:)) gives stiffness matrix of laminate, where n is
% laminate
% - L_2(n,a) is failure load, where n is laminate, a is loading case
% - thick_mm is thicknesses used in SES
% - E_effPa is stiffness and strengths used in SES
% - uncomment lines at bottom of script to display results

%% CLEAN-UP

clear all
clc

%% MATERIALS & LAMINATES

% USER INPUT

% [ E11 E22 v12 G12 ] for materials
E = [
20.0e6 1.4e6 .30 .93e6 ; % 1 - carbon/epoxy, uni
9.4e6 9.4e6 .050 .77e6 ; % 2 - carbon/epoxy, cloth
1 1 .01 1 % 3 - core
];

% % for matrix failure
% E = [
% 1.0*20.0e6 .25*1.4e6 .15*.30 .20*.93e6 ; % 1 - carbon/epoxy, uni
% 9.4e6 9.4e6 .050 .77e6 ; % 2 - carbon/epoxy, cloth
% 1 1 .01 1 % 3 - core
% ];

% USER INPUT
% [ alpha11 alpha22 alpha12 ] for materials
CTE = [
-.5e-6 15e-6 0 ; % 1 - carbon/epoxy, uni
-.3e-6 -.3e-6 0 ; % 2 - carbon/epoxy, cloth
0 0 0 % 3 - core
```

```

];

req_T = [ 0 ; 0 ; 1 ; 1 ; 1 ; 1 ; 1 ; 1 ; 0 ; 0 ; 0 ];

% USER INPUT
% [ e11t e22t e11c e22c e12 ] for pseudo-A basis (80% of values)
e_max = .80*[
.014 .007 -.012 -.031 .0296 ; % 1 - carbon/epoxy, uni
.010 .010 -.010 -.010 .025 ; % 2 - carbon/epoxy, cloth
1 1 -1 -1 1 % 3 - core
];

% USER INPUT
% change in temperature
T_amb = 70; % ambient temperature
T_cure = 250; % cure temperature
T_delt = T_amb - T_cure; % change from cure temperature

% USER INPUT
% number of laminates
% must match number of laminates defined below, laminates called in
% following section
n_lam = 6;

% USER INPUT
% laminate schedule, top to bottom (outside to inside of chassis)

% Side impact structure

lam_1 = [
+45 .010 2 ;
+0 .010 2 ;
+0 .0052 1 ;
+0 .010 2 ;
+45 .010 2 ;
+0 .700 3 ;
+45 .010 2 ;
+0 .010 2 ;
+0 .0052 1 ;
+0 .010 2 ;
+45 .010 2
];

% USER INPUT
% strength requirements which apply to laminate, must match number of
% loading cases (1 for applies, 0 for doesn't apply)

req_L(1,:) = [ 1 ; 1 ; 0 ; 0 ; 0 ; 0 ; 0 ; 0 ];

% Front bulkhead support

lam_2 = [
+45 .010 2 ;
+0 .010 2 ;
+0 .0052 1 ;

```

```

+0 .010 2 ;
+45 .010 2 ;
+0 .700 3 ;
+45 .010 2 ;
+0 .010 2 ;
+0 .0052 1 ;
+0 .010 2 ;
+45 .010 2
];

req_L(2,:) = [ 1 ; 1 ; 1 ; 0 ; 1 ; 0 ; 0 ; 0 ];

% Front hoop bracing

lam_3 = [
+45 .010 2 ;
+0 .010 2 ;
+0 .0052 1 ;
+0 .700 3 ;
+0 .0052 1 ;
+0 .010 2 ;
+45 .010 2
];

req_L(3,:) = [ 1 ; 1 ; 1 ; 0 ; 0 ; 0 ; 0 ; 0 ];

% Cockpit floor

lam_4 = [
+45 .010 2 ;
+0 .010 2 ;
+45 .010 2 ;
+0 .700 3 ;
+45 .010 2 ;
+0 .010 2 ;
+45 .010 2
];

req_L(4,:) = [ 0 ; 0 ; 0 ; 0 ; 0 ; 0 ; 0 ; 1 ];

% Front floor

lam_5 = [
+45 .010 2 ;
+0 .010 2 ;
+0 .0052 1 ;
+0 .0052 1 ;
+0 .700 3 ;
+0 .0052 1 ;
+0 .0052 1 ;
+0 .010 2 ;
+45 .010 2
];

req_L(5,:) = [ 0 ; 0 ; 1 ; 0 ; 0 ; 1 ; 1 ; 0 ];

```

```

% Seat back

lam_6 = [
+0 .010 2 ;
+90 .0052 1 ;
+90 .0052 1 ;
+45 .010 2 ;
+0 .700 3 ;
+45 .010 2 ;
+90 .0052 1 ;
+90 .0052 1 ;
+0 .010 2
];

req_L(6,:) = [ 0 ; 0 ; 0 ; 1 ; 0 ; 0 ; 0 ; 0 ];

%% STIFFNESS, LOADING, FAILURE INDICES, FAILURE LOADS

thick = zeros(n_lam,3);

A_temp = zeros(3,3);
B_temp = zeros(3,3);
D_temp = zeros(3,3);

N_Ttemp = zeros(3,1);
M_Ttemp = zeros(3,1);

A = zeros(n_lam,3,3);
B = zeros(n_lam,3,3);
D = zeros(n_lam,3,3);
K = zeros(n_lam,6,6);

N_T = zeros(n_lam,3);
M_T = zeros(n_lam,3);

E_eff = zeros(n_lam,3);

N = zeros(6,size(req_L,2));
L_1 = zeros(n_lam,size(req_L,2));

L_2 = zeros(n_lam,size(req_L,2));
FI_max = zeros(n_lam,size(req_L,2));
FI_maxfib = zeros(n_lam,size(req_L,2));

% for each laminate
for n = 1:n_lam

    % USER INPUT
    switch n

        case 1

            lam = lam_1;

```



```

        disp('Laminate 1 loaded');

    case 2

        lam = lam_2;
        disp('Laminate 2 loaded');

    case 3

        lam = lam_3;
        disp('Laminate 3 loaded');

    case 4

        lam = lam_4;
        disp('Laminate 4 loaded');

    case 5

        lam = lam_5;
        disp('Laminate 5 loaded');

    case 6

        lam = lam_6;
        disp('Laminate 6 loaded');

    otherwise

        disp('WARNING: n_lam and laminate loading do not agree');

end

thick(n,1) = sum(lam(:,2)); % total laminate thickness (SES)
thick(n,2) = lam(round( length(lam) / 2 ),2); % thickness of core (SES)
thick(n,3) = ( thick(n,1) - thick(n,2) ) / 2; % thickness of face sheet
(SES)

% stiffness

z = zeros(( size(lam,1) + 1 ),1);

% locate bottom of laminate
z(1) = - sum(lam(:,2)) / 2;

% locate locations of each ply
for k = 2:( size(lam,1) + 1 )

    z(k) = z(k-1) + lam(k-1,2);

end

A_temp = 0;

```

```

B_temp = 0;
D_temp = 0;

N_Ttemp = 0;
M_Ttemp = 0;

% for each ply
for k = 1:size(lam,1)

    S = [ 1 / E(lam(k,3),1) , - E(lam(k,3),3) / E(lam(k,3),1) , 0 ;
          - E(lam(k,3),3) / E(lam(k,3),1) , 1 / E(lam(k,3),2) , 0 ;
          0 , 0 , 1 / E(lam(k,3),4) ];

    Q = inv(S);

    theta = lam(k,1)*( pi / 180 );

    T = [ cos(theta)^2 , sin(theta)^2 , 2*sin(theta)*cos(theta) ;
          sin(theta)^2 , cos(theta)^2 , - 2*sin(theta)*cos(theta) ;
          - sin(theta)*cos(theta) , sin(theta)*cos(theta) , cos(theta)^2 -
sin(theta)^2 ];

    R = [ 1 0 0 ; 0 1 0 ; 0 0 2 ];

    Qbar = inv(T)*Q*R*T*inv(R);

    % build up stiffness matrices
    A_temp = A_temp + Qbar*( z(k+1) - z(k) );
    B_temp = B_temp + ( 1 / 2 )*Qbar*( z(k+1)^2 - z(k)^2 );
    D_temp = D_temp + ( 1 / 3 )*Qbar*( z(k+1)^3 - z(k)^3 );

    % solve for thermal strains
    e_T1(n,k,:) = T_delt*[ CTE(lam(k,3),1) ; CTE(lam(k,3),2) ;
CTE(lam(k,3),3) ];
    e_Tx = R*inv(T)*inv(R)*squeeze(e_T1(n,k,:));

    % define thermal loads
    N_Ttemp = N_Ttemp + Qbar*e_Tx*( z(k+1) - z(k) );
    M_Ttemp = M_Ttemp + Qbar*e_Tx*( z(k+1)^2 - z(k)^2 );

end

% define stiffness matrices for laminate
A(n, :, :) = A_temp;
B(n, :, :) = B_temp;
D(n, :, :) = D_temp;
K(n, :, :) = [ A_temp B_temp ; B_temp D_temp ];

% define thermal loads
N_T(n, :) = N_Ttemp;
M_T(n, :) = M_Ttemp;

E_eff(n,1) = K(n,1,1) / ( 2*thick(n,3) ); % effective E for face sheet

```

```

% loading

% USER INPUT
% loading cases

% SES tensile failure

a = 1;

N_test = 1;

N(1,a) = req_L(n,a)*( N_test + req_T(a)*N_T(n,1) );
N(2,a) = req_T(a)*N_T(n,2);
N(3,a) = req_T(a)*N_T(n,3);
N(4,a) = req_T(a)*M_T(n,1);
N(5,a) = req_T(a)*M_T(n,2);
N(6,a) = req_T(a)*M_T(n,3);

L_1(n,a) = req_L(n,a)*N_test;

% SES shear failure

% loading case number
a = 2;

% load and dimensions
N_test = 1;

% line loads (made zero if loading case doesn't apply to laminate)
N(1,a) = req_T(a)*N_T(n,1);
N(2,a) = req_T(a)*N_T(n,2);
N(3,a) = req_L(n,a)*( N_test + req_T(a)*N_T(n,3) );
N(4,a) = req_T(a)*M_T(n,1);
N(5,a) = req_T(a)*M_T(n,2);
N(6,a) = req_T(a)*M_T(n,3);

% record input load
L_1(n,a) = req_L(n,a)*N_test;

% Front impact - x-dir in car x, z-dir into chassis

a = 3;

F = 20000;
p = 45; % front perimeter

N(1,a) = req_L(n,a)*( ( - F / p ) + req_T(a)*N_T(n,1) );
N(2,a) = req_T(a)*N_T(n,2);
N(3,a) = req_T(a)*N_T(n,3);
N(4,a) = req_T(a)*M_T(n,1);
N(5,a) = req_T(a)*M_T(n,2);
N(6,a) = req_T(a)*M_T(n,3);

L_1(n,a) = req_L(n,a)*F;

```

```

% Seat back - x-dir angled below car x, y-dir in car y, z-dir into
% chassis

a = 4;

P = 7000*cosd(30);
l = 15; % length (width in car)
b = 18; % width (height in car)

N(1,a) = req_T(a)*N_T(n,1);
N(2,a) = req_T(a)*N_T(n,2);
N(3,a) = req_T(a)*N_T(n,3);
N(4,a) = req_T(a)*M_T(n,1);
N(5,a) = req_L(n,a)*( ( P*l ) / ( 4*b ) + req_T(a)*M_T(n,1) );
N(6,a) = req_T(a)*M_T(n,3);

L_1(n,a) = req_L(n,a)*P;

% Front suspension, upper - x-dir in car x, y-dir in car z, z-dir
% into chassis

a = 5;

P = 300;
l = 12; % length (height of car side)
b = 8 + 3 + 3; % distance between suspension points plus a little

N(1,a) = req_T(a)*N_T(n,1);
N(2,a) = req_T(a)*N_T(n,2);
N(3,a) = req_T(a)*N_T(n,3);
N(4,a) = req_T(a)*M_T(n,1);
N(5,a) = req_L(n,a)*( ( P*l ) / ( 4*b ) + req_T(a)*M_T(n,2) );
N(6,a) = req_T(a)*M_T(n,3);

L_1(n,a) = req_L(n,a)*P;

% Front suspension, lower - x-dir in car x, y-dir in car y, z-dir
% into chassis

a = 6;

F = 900;
p = 9 + 3 + 3; % distance between suspension points plus a little
d = 1.3; % eccentricity

N(1,a) = req_T(a)*N_T(n,1);
N(2,a) = req_L(n,a)*( ( - F / p ) + req_T(a)*N_T(n,2) );
N(3,a) = req_T(a)*N_T(n,3);
N(4,a) = req_T(a)*M_T(n,1);
N(5,a) = req_L(n,a)*( ( ( F*d ) / b ) + req_T(a)*M_T(n,2) );
N(6,a) = req_T(a)*M_T(n,3);

L_1(7,a) = req_L(n,a)*F;

```

```

% Brake pedal effort - x-dir in car x, y-dir in car z, z-dir into
% chassis

a = 7;

F = 450; % maximum pedal effort
d = 8; % eccentricity
b = 6; % width of mount

N(1,a) = req_L(n,a)*( ( - F / b ) + req_T(a)*N_T(n,1) );
N(2,a) = req_T(a)*N_T(n,2);
N(3,a) = req_T(a)*N_T(n,3);
N(4,a) = req_L(n,a)*( ( F*d ) / b ) + req_T(a)*M_T(n,1) );
N(5,a) = req_T(a)*M_T(n,2);
N(6,a) = req_T(a)*M_T(n,3);

L_1(n,a) = req_L(n,a)*F;

% Driver launch out of car - x-dir in car x, y-dir in car y, z-dir
% into chassis

a = 8;

P = 500;
l = 30; % length (length of cockpit)
b = 20; % width of cockpit

N(1,a) = req_T(a)*N_T(n,1);
N(2,a) = req_T(a)*N_T(n,2);
N(3,a) = req_T(a)*N_T(n,3);
N(4,a) = req_L(n,a)*( ( P*l ) / ( 4*b ) + req_T(a)*M_T(n,1) );
N(5,a) = req_T(a)*M_T(n,2);
N(6,a) = req_T(a)*M_T(n,3);

L_1(n,a) = req_L(n,a)*P;

% failure indices

FI = zeros(size(N,2),2*size(lam,1),3);

% for each loading case
for a = 1:size(N,2)

    % mid-plane strains
    e_mid = inv(squeeze(K(n, :, :))) * N(:, a);

    z = zeros(( size(lam,1) + 1 ), 1);

    z(1) = - sum(lam(:,2)) / 2;

    for k = 2:( size(lam,1) + 1 )

```

```

        z(k) = z(k-1) + lam(k-1,2);

    end

    e_x = zeros(( size(lam,1) + 1 ),3);

    % for each ply top and bottom
    for b = 1:2*size(lam,1)

        % ply index
        k_1 = round( b / 2 );

        % z index
        k_2 = round( ( b + 1 ) / 2 );

        % strain in x coordinates
        e_x = [ e_mid(1) + z(k_2)*e_mid(4) ; e_mid(2) + z(k_2)*e_mid(5) ;
e_mid(3) + z(k_2)*e_mid(6) ];

        theta = lam(k_1,1)*( pi / 180 );

        T = [ cos(theta)^2 , sin(theta)^2 , 2*sin(theta)*cos(theta) ;
            sin(theta)^2 , cos(theta)^2 , - 2*sin(theta)*cos(theta) ;
            - sin(theta)*cos(theta) , sin(theta)*cos(theta) ,
cos(theta)^2 - sin(theta)^2 ];

        R = [ 1 0 0 ; 0 1 0 ; 0 0 2 ];

        % strain in l coordinates
        e_1 = R*T*inv(R)*e_x - squeeze(e_T1(n,k_1,:));

        % failure index in 1-dir
        FI(a,b,1) = max( e_1(1) / e_max(lam(k_1,3),1) , e_1(1) /
e_max(lam(k_1,3),3) );

        % failure index in 2-dir
        FI(a,b,2) = max( e_1(2) / e_max(lam(k_1,3),2) , e_1(2) /
e_max(lam(k_1,3),4) );

        % failure index in 12-dir
        FI(a,b,3) = abs( e_1(3) / e_max(lam(k_1,3),5) );

    end

end

end

% USER INPUT
% record failure indices
switch n

    case 1

        FI_1 = FI;

```

```

        disp('Laminate 1 failure indices recorded');

    case 2

        FI_2 = FI;
        disp('Laminate 2 failure indices recorded');

    case 3

        FI_3 = FI;
        disp('Laminate 3 failure indices recorded');

    case 4

        FI_4 = FI;
        disp('Laminate 4 failure indices recorded');

    case 5

        FI_5 = FI;
        disp('Laminate 5 failure indices recorded');

    case 6

        FI_6 = FI;
        disp('Laminate 6 failure indices recorded');

end

% failure loads

% for each loading case
for a = 1:size(N,2)

    % if loading case applies
    if req_L(n,a) == 1

        % define maximum failure index
        FI_max(n,a) = max(max(FI(a, :, :)));

        % define failure load
        L_2(n,a) = L_1(n,a) / FI_max(n,a);

        % define maximum failure index for fibers
        FI_maxfib(n,a) = max(max(FI(a, :, 1)));

    end

end

E_eff(n,2) = L_2(n,1) / ( 2*thick(n,3) ); % tensile strength (SES)
E_eff(n,3) = L_2(n,2) / ( 2*thick(n,3) ); % shear strength (SES)

```

```
end

%% UNIT CONVERSION FOR SES

thick_mm = thick*25.4; % convert thick to mm
E_effPa = E_eff*6895; % convert E_eff to Pa

%% RESULTS

% FI_n(a,b,i)
% squeeze(FI_n(a, :, :))
% FI_max
% FI_maxfib
% squeeze(K(n, :, :))
% L_2
% thick_mm
% E_effPa
```



## **Appendix D: Cockpit Opening Stiffness Analysis**

The report written for the Cal Poly ME 404: Applied Finite Element Analysis course and its appendices are included here from their original PDF file.

# The laminate design of a Formula SAE carbon-fiber composite monocoque chassis for torsional stiffness and minimization of weight

John Waldrop

## Abstract

The Cal Poly Formula SAE Team must choose laminates for its carbon-fiber composite monocoque chassis which provide a high torsional stiffness for the least amount of material. Models were created in Abaqus/Standard to assist with the laminate choice in the region immediate to the cockpit opening. 2D and 3D models showed that torsional stiffness is increased by fibers which connect the chassis around its circumference and limit its radial deformation. These findings will influence the laminate design of the 2013 chassis and allow the team to minimize weight while meeting its torsional stiffness goals.

## Introduction

The Cal Poly Formula SAE Team has contracted the Formula Chassis Works senior project group to design a carbon-fiber composite monocoque chassis for their 2013 car. This chassis will serve to meet the safety requirements set out by the team, namely that of intrusion protection for the driver. Additionally, the work performed and documented by the senior project group will provide a basis for future development of carbon-fiber composite chassis at Cal Poly.

One of the major properties of the chassis is its torsional stiffness. This stiffness, coupled with the stiffnesses of the front and rear suspensions in roll, helps to define the behavior of the car in transient cornering. Generally, a stiff chassis results in a car which responds to driver input on the track as well as to changes in suspension setup. These characteristics are desirable as they give the driver confidence and yield clear testing results, thereby resulting in quick lap times.

The design of the laminates around the chassis should therefore make the best use of material with regard to torsional stiffness. Considering a closed-section tube, the material must support the shear stress induced during torsion, which results in normal stresses when transformed 45 degrees as in Figure 1.

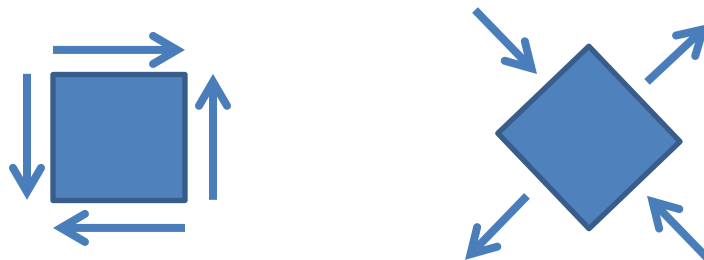


Figure 1. A stress block subjected to a shear load, transformed 45 degrees at right.

This stress situation calls for fibers in the  $\pm 45$ -degree directions, which will therefore make up the majority of the chassis. Where this theory breaks down is at the cockpit opening, where the chassis is no longer a closed-section tube.

The team expects the region of the chassis at the cockpit opening to be the governing compliance in the system. For this reason it is important to determine the most efficient use of material in this region so that the weight of the car may be minimized while torsional stiffness goals are met. Due to the complexity of the geometry, a finite element model is required.

## Model Development

The chassis involves very complex geometries in order to meet suspension points, house the driver, and package the engine and related components. It also undergoes complex loading during torsion, with the loads on the tires resulting themselves into the chassis through six suspension members of various orientations. This being the case, a simplified model which isolated the torsion and cockpit opening was chosen as the focus of analysis. Multiple models were created as intermediate steps to assist in model validation, mesh convergence studies, and obtaining initial results. These models were all based on parts created in Abaqus/Standard.

All models consisted of laminates of T700 carbon fibers in an epoxy resin and arbitrary core material. Material properties, thicknesses, and areal weights are given in Table 1.

Table 1. Materials used with models.

Material	$E_{11}$ (psi)	$E_{22}$ (psi)	$\nu_{12}$	$G_{12}$ (psi)	$G_{13}$ (psi)	$G_{23}$ (psi)	Thickness (in)	Areal weight (lb/in <sup>2</sup> )
Uni-directional tape (uni)	20e6	1.4e6	0.3	0.93e6	0.93e6	0.93e6	0.0052	0.00030
Plain-weave fabric (cloth)	9e6	9e6	0.05	0.80e6	0.80e6	0.80e6	0.010	0.00045
Honeycomb core (core)	1	1	0.5	1	2000	2000	0.460	0

The above material properties were entered into Abaqus as those for elastic laminae. The only important aspects of the core are its out-of-plane shear stiffness and thickness, as its only functions are to reduce shear deflection and space the composite face sheets for increased bending stiffness and strength. Composite layups of these materials were built up for the parts in Abaqus and assigned to the sections of the parts.

The first model (Model 1) consisted of a flat plate of length 34 inches subjected to an in-plane shear load of  $N_{xy} = 1$  pound/inch and allowed to deform in-plane. The deflection results would be compared to those found from classic lamination theory (CLT) in the MATLAB script in Appendix A to validate the Abaqus composite layup and loading. This plate represented an

un-wrapped tube of dimensions of the cockpit opening cross-section. A rectangular hole was then cut to represent the cockpit opening (Model 2). Models 1 and 2 are shown in Figure 2.

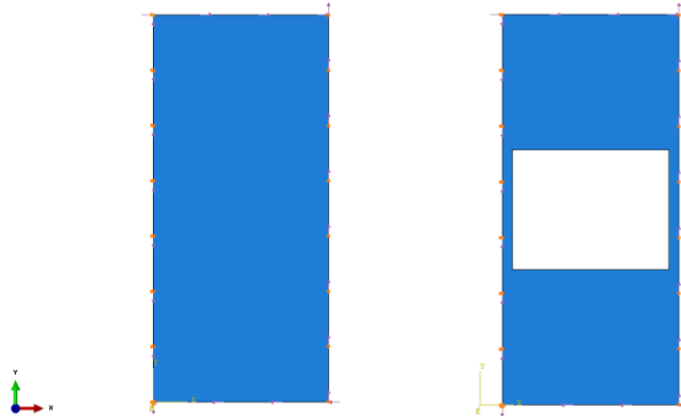


Figure 2. Model 1 (left) and Model 2 (right). The longitudinal axis of the car is in the x-direction.

Model 2 used the same loading as in Model 1 but with a boundary condition to keep the edges ahead and behind the cockpit parallel, as they would be constrained on the chassis itself. These edges naturally remained parallel in Model 1. This displacement boundary condition was modified for each analysis so that no longitudinal stress was induced. The inside corners of Model 2 were rounded to avoid excessive local shear deformation and better reflect the chassis geometry. Results of Model 2 were used to guide analysis of the final model, as was a mesh convergence study.

A tube was then created to represent the entire chassis in three dimensions, first with no cockpit opening (Model 3), then with a rectangular cockpit opening (Model 4), and finally with partitions surrounding the cockpit opening for more detailed layouts (Model 5). Diameter was 20 inches and length was 64 inches, equal to the wheelbase of the car. One end of the tube was constrained to radial displacement while the other end was subjected to a shear line load of  $N_{xy} = 0.159$  pound/inch. The boundary condition created non-linearity in the deflection results, so the tube was extended such that the region in question was unaffected. A mesh convergence study was run with Model 3 before a comparison to results from CLT. Model 4 underwent a mesh convergence study as well to finalize the approximate element size before results were obtained from Model 5. Models 3 through 5 are shown in Figure 3.

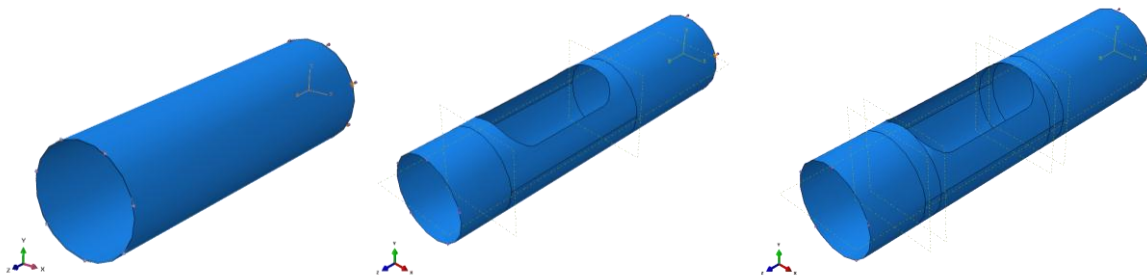


Figure 3. Models 3, 4, and 5. Models 4 and 5 are extended to the right, where the boundary condition is applied.

In Models 1 through 4 the laminate used was [ 45<sub>c</sub> / core / 45<sub>c</sub> ] ([ 45<sub>c</sub> / core ]<sub>s</sub>). This laminate was also used at the front and rear sections of Model 5, while the laminate in the middle section was varied.

### Mesh Development

The mesh type was determined based on the chassis geometry, loading, and the composites interface in Abaqus.

As a monocoque structure the chassis is essentially a skin, lending itself to shell elements. 3D shell parts were created in Abaqus to accommodate this. Edges of parts were seeded, with the partitions separating regions sometimes seeded as well to give cleaner meshes.

Linear quadrilateral elements were selected to fill the seeded regions. The sides of the quadrilaterals were mostly aligned with the longitudinal and transverse axes of the chassis, which made them ideal elements for the shear loading case. This replicated the untransformed stress block shown in Figure 1. The strain due to shear is linear, so linear elements were used.

The composite layup feature in Abaqus is useful only with shell elements, a fact which greatly influenced the element-type choice. This feature takes the shell as a mid-plane and builds the laminate from it. Composite layups are assigned in the “Parts” module. There are additional composite options available in the “Properties” module for both shell and solid elements, but these methods made creating layups and assigning loads difficult.

The meshes used are included in Appendix C. Details for each mesh are included in Table 2.

Table 2. Meshes used for each model.

Model	Element type	Seed size (in)	Element number	Degrees of freedom
1	Linear quadrilateral	5	75	370
2	Linear quadrilateral	1	2200	14000
3	Linear quadrilateral	2	1100	25000
4	Linear quadrilateral	0.5	18000	110000
5	Linear quadrilateral	0.5	18000	110000

The mesh size for Model 1 was chosen arbitrarily, with the loading and geometry yielding no difference in results between mesh sizes.

## Analysis

All models underwent static analysis in Abaqus/Standard with implicit integration. No errors were encountered. Model 2 was analyzed with various laminates to gain insight into the ideal laminates for specific stiffness, providing a starting point for laminates run with Model 5.

## Mesh Convergence

Meshes were converged for Models 2, 3, and 4 to ensure accurate results. No mesh convergence study was required for Model 1, which matched CLT for any mesh size due to its simplicity. The mesh convergence study from Model 4 was used to influence the mesh of Model 5. Images of final meshes are included in Appendix C, and deformed shapes with reference points are in Appendix D.

Model 2 began with a seed size of 5 inches, a large portion of its 34-inch length. Maximum transverse displacement was checked. The mesh was refined until the results had converged to within four significant figures. Results of the mesh convergence study are included in Figure 4.

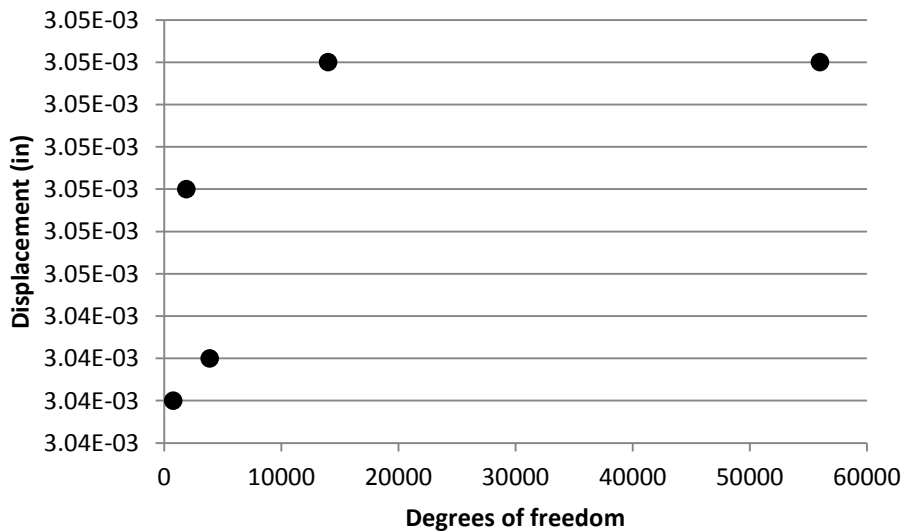


Figure 4. Mesh convergence study for Model 2.

While results were close with large seed sizes, the mesh was refined to achieve better results as computational time was not excessive. Final seed size was 2 inches, yielding 14,000 degrees of freedom (DOF).

Model 3 was much more sensitive to seed size due to its 3D geometry. Angular displacement about the longitudinal axis was checked at an area of the tube away from the boundary condition, where displacements were in the linear range. The mesh appeared to converge and then diverge, so CLT was used to determine the point of convergence. Results of the mesh convergence study are included in Figure 5.

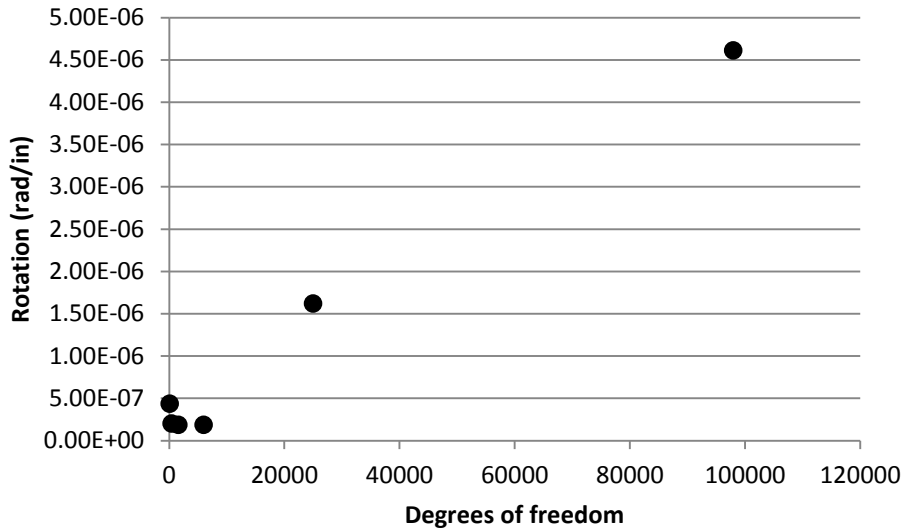


Figure 5. Mesh convergence study for Model 3.

With 25,000 DOF from a seed size of 2 inches the mesh had converged to replicate the results of CLT.

Model 4 began with a seed size of 4 inches following previous findings. Angular displacement about the longitudinal axis was measured between points ahead and behind the cockpit opening. Results of the mesh convergence study are included in Figure 6.

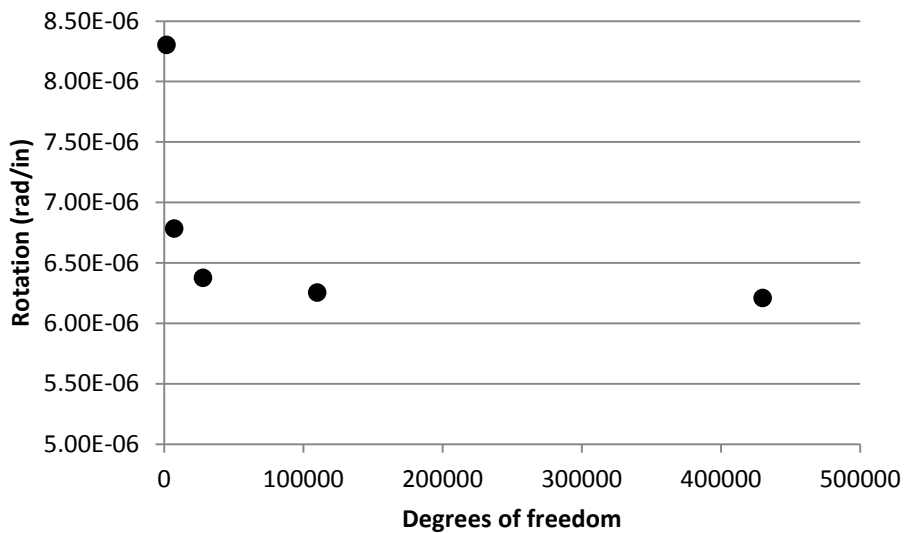


Figure 6. Mesh convergence study for Model 4.

A seed size of 0.5 inches was chosen, which yielded 110,000 DOF. The mesh continued to converge past this point, but increased computational time outweighed the improved accuracy.

The seed size for Model 5 was chosen to be 0.5 inches, as the model was the same as Model 4 in terms of geometry and points of interest.

## Results

Results from Abaqus were compared to results from CLT when possible. All hand calculations are found in Appendix B, and deformed shapes are found in Appendix D.

Shear strain found in Abaqus for Model 1 was compared to strain found using CLT, shown in Table 3. The strain was measured across the length of the part.

Table 3. Strain of Model 1.

Laminate	Analysis method	$\epsilon_{xy}$
[ 45 <sub>c</sub> / core ] <sub>s</sub>	Abaqus	9.72e-6
[ 45 <sub>c</sub> / core ] <sub>s</sub>	CLT	9.72e-6

The two values matched, as expected. This result validated the method of composites analysis in Abaqus and the boundary conditions used.

While the main purpose of Model 2 was to gain insight for Model 5, strain was first calculated to indicate the amount of stiffness lost when the cockpit opening was introduced, shown in Table 4.

Table 4. Strain of Model 2.

Laminate	Analysis method	$\epsilon_{xy}$
[ 45 <sub>c</sub> / core ] <sub>s</sub>	Abaqus	8.97e-5

This strain shows that the cockpit opening results in an 89% loss of stiffness. This confirms the team's suspicion that this region of the chassis would govern the overall stiffness. Various layups were then tested and specific stiffnesses were determined, as shown in Table 5. Maximum transverse displacement was measured at the end of the part.

Table 5. Specific stiffness of laminates in Model 2.

Laminate	Analysis method	Displacement (in)	Weight (lb)	Specific stiffness (1/in*lb)
[ 45 <sub>c</sub> ]	Abaqus	5.15e-3	0.045	4310
[ ±45 ] <sub>s</sub>	Abaqus	3.04e-3	0.120	2740
[ ±60 ] <sub>s</sub>	Abaqus	4.74e-3	0.120	1760
[ 45 <sub>c</sub> / 90 ] <sub>s</sub>	Abaqus	1.29e-3	0.150	5190
[ 45 <sub>c</sub> / 0 ] <sub>s</sub>	Abaqus	3.88e-3	0.150	1720



A layup of  $[45_c / 90]_s$  gave the highest specific stiffness, closely followed by a layup of  $[45_c]$ .

Model 3 was checked with CLT to validate loading of the tube. Results from Abaqus and CLT are shown in Table 6. Angular displacement was measured between two points 64 inches apart, in the linear range away from the boundary condition.

Table 6. Angular displacement of Model 3.

Laminate	Analysis method	$\phi$ (deg)
$[45_c / \text{core}]_s$	Abaqus	6.80e-4
$[45_c / \text{core}]_s$	CLT	6.82e-4

The two values differed by only 0.3%. This model validated the results given by Abaqus.

Following the mesh convergence study from Model 4, Model 5 was analyzed for specific stiffness with a wide variety of layups. Results are shown in Table 7. Region 1 indicates the region around the tube at the cockpit opening, while Regions 2 and 3 indicate the 4-inch long regions around the tube just ahead of the cockpit opening and just behind the cockpit opening, respectively. Angular displacement was measured between two points on the side of the chassis, from 4 inches ahead of the cockpit opening to 4 inches behind.

Table 7. Specific stiffness of laminates in Model 5.

Laminate		Analysis method	Disp. (rad)	Weight (lb)	Specific stiffness (1/rad*lb)
Region 1	Regions 2 & 3				
$[45_{2c} / \text{core}]_s$	Same as 1	Abaqus	3.09e-4	3.38	960
$[45_c / 0_c / \text{core}]_s$	Same as 1	Abaqus	2.52e-4	3.38	1180
$[45_{2c} / 0_c / \text{core}]_s$	Same as 1	Abaqus	2.07e-4	5.06	960
$[45_c / 0_{2c} / \text{core}]_s$	Same as 1	Abaqus	1.94e-4	5.06	1020
$[45_c / 90 / \text{core}]_s$	Same as 1	Abaqus	2.71e-4	2.81	1310
$[45_c / 0_c / 90 / \text{core}]_s$	Same as 1	Abaqus	2.16e-4	4.50	1030
$[45_c / \pm 60_c / \text{core}]_s$	Same as 1	Abaqus	2.20e-4	5.06	900
$[45_c / \pm 60 / \text{core}]_s$	Same as 1	Abaqus	2.72e-4	3.94	930
$[45_{2c} / \text{core}]_s$	$[45_c / 90 / \text{core}]_s$	Abaqus	3.10e-4	3.23	1000
$[45_c / \pm 60_c / \text{core}]_s$	$[45_c / 90 / \text{core}]_s$	Abaqus	2.41e-4	4.46	930

As in Model 2, a layup of  $[45_c / 90 / \text{core}]_s$  gave the highest specific stiffness. This was closely followed by a quasi-isotropic layup of  $[45_c / 0_c / \text{core}]_s$ .

## **Discussion**

The results for all models in Abaqus were clear, reasonable, and almost exactly equal to results from CLT where applicable. Importantly, close relationships between 2D models and 3D models were discovered. Displacement in a 3D tube (Model 3) was predicted well by 2D CLT, and the laminates which performed best for the 2D cockpit opening (Model 2) also performed best for the 3D cockpit opening (Model 5). These findings bode well for simplified analysis in this application, allowing time to be saved during future analyses.

The results regarding specific stiffness gave great indication of the laminate type to pursue. While 45-degree plies were a key aspect of stiffness as with a closed-section tube, 90-degree plies gave a notable increase in specific stiffness for both the 2D and 3D models. These plies in the hoop direction provided a solid connection around the circumference of chassis at either end of the cockpit opening, as opposed to angled plies which terminated in the opening. Also, a quasi-isotropic laminate performed very well in the 3D model. This is likely due to the fact that the open section at the cockpit opening induced the chassis to deform in the radial direction due to a lack of constraints. Plies in all directions helped to limit this outward expansion, thereby increasing torsional stiffness.

There are a number of ways to expand upon this analysis. First, an edge close-out should be incorporated with the cockpit opening. This would simulate plies wrapping around from the outside to the inside of the chassis at the cockpit opening edge, allowing for better load transfer in torsion. Such a close-out will be incorporated when the chassis is constructed. Second, the chassis should be modeled to better reflect the chassis of the 2013 car, the monocoque of which terminates at the back of the cockpit opening where it is connected to a frame which mounts the engine and suspension at the rear. Finally, loading from suspension should be modeled in detail to replicate the conditions of a real-life torsional stiffness test. This would allow for validation of the finite element model through testing.

## **Conclusion**

Models of increasing complexity were created in Abaqus/Standard to assist in determining the laminates of a carbon-fiber composite chassis with respect to torsional stiffness and weight. Comparisons were made to calculations using classic lamination theory, showing high similarity. Both 2D and 3D models gave a clear indication of the laminate type to use, which better connected the chassis around its circumference and limited radial deformation. Formula Chassis Works will incorporate a quasi-isotropic laminate around the cockpit opening of the Cal Poly Formula SAE Team's 2013 chassis, influenced mainly by the findings of this report.

```
% APPENDIX A
```

```
%% MATERIALS & LAMINATES
```

```
% USER INPUT
```

```
% [ E11 E22 v12 G12 ] for materials
```

```
E = [  
20.0e6 1.4e6 .30 .93e6 ; % 1 - carbon/epoxy, uni  
9.4e6 9.4e6 .050 .77e6 ; % 2 - carbon/epoxy, cloth  
1 1 .01 1 % 3 - core  
];
```

```
% USER INPUT
```

```
% [ alpha11 alpha22 alpha12 ] for materials
```

```
CTE = [  
-.5e-6 15e-6 0 ; % 1 - carbon/epoxy, uni  
-.3e-6 -.3e-6 0 ; % 2 - carbon/epoxy, cloth  
0 0 0 % 3 - core  
];
```

```
% USER INPUT
```

```
% change in temperature
```

```
T_amb = 70; % ambient temperature
```

```
T_cure = 250; % cure temperature
```

```
T_delt = T_amb - T_cure; % change from cure temperature
```

```
% USER INPUT
```

```
% number of laminates
```

```
% must match number of laminates defined below, laminates called in
```

```
% following section
```

```
n_lam = 1;
```

```
% USER INPUT
```

```
% laminate schedule, top to bottom (outside to inside of chassis)
```

```
% Side impact structure
```

```
lam_1 = [  
+45 .010 2 ;  
+0 .010 2 ;  
+0 .0052 1 ;  
+0 .010 2 ;  
+45 .010 2 ;  
+0 .700 3 ;  
+45 .010 2 ;  
+0 .010 2 ;  
+0 .0052 1 ;  
+0 .010 2 ;  
+45 .010 2
```

```
];

% USER INPUT
% strength requirements which apply to laminate, must match number of
% loading cases (1 for applies, 0 for doesn't apply)

req_L(1,:) = [ 1 ; 1 ; 0 ; 0 ; 0 ; 0 ; 0 ; 0 ];

%% STIFFNESS, LOADING, FAILURE INDICES, FAILURE LOADS

thick = zeros(n_lam,3);

A_temp = zeros(3,3);
B_temp = zeros(3,3);
D_temp = zeros(3,3);

N_Ttemp = zeros(3,1);
M_Ttemp = zeros(3,1);

A = zeros(n_lam,3,3);
B = zeros(n_lam,3,3);
D = zeros(n_lam,3,3);
K = zeros(n_lam,6,6);

N_T = zeros(n_lam,3);
M_T = zeros(n_lam,3);

E_eff = zeros(n_lam,3);

N = zeros(6,size(req_L,2));
L_1 = zeros(n_lam,size(req_L,2));

L_2 = zeros(n_lam,size(req_L,2));
FI_max = zeros(n_lam,size(req_L,2));
FI_maxfib = zeros(n_lam,size(req_L,2));

% for each laminate
for n = 1:n_lam

    % USER INPUT
    switch n

        case 1

            lam = lam_1;
            disp('Laminate 1 loaded');

        otherwise

            disp('WARNING: n_lam and laminate loading do not agree');
```

```

end

thick(n,1) = sum(lam(:,2)); % total laminate thickness (SES)
thick(n,2) = lam(round( length(lam) / 2 ),2); % thickness of core (SES)
thick(n,3) = ( thick(n,1) - thick(n,2) ) / 2; % thickness of face sheet (SES)

% stiffness

z = zeros(( size(lam,1) + 1 ),1);

% locate bottom of laminate
z(1) = - sum(lam(:,2)) / 2;

% locate locations of each ply
for k = 2:( size(lam,1) + 1 )

    z(k) = z(k-1) + lam(k-1,2);

end

A_temp = 0;
B_temp = 0;
D_temp = 0;

N_Ttemp = 0;
M_Ttemp = 0;

% for each ply
for k = 1:size(lam,1)

    S = [ 1 / E(lam(k,3),1) , - E(lam(k,3),3) / E(lam(k,3),1) , 0 ;
          - E(lam(k,3),3) / E(lam(k,3),1) , 1 / E(lam(k,3),2) , 0 ;
          0 , 0 , 1 / E(lam(k,3),4) ];

    Q = inv(S);

    theta = lam(k,1)*( pi / 180 );

    T = [ cos(theta)^2 , sin(theta)^2 , 2*sin(theta)*cos(theta) ;
          sin(theta)^2 , cos(theta)^2 , - 2*sin(theta)*cos(theta) ;
          - sin(theta)*cos(theta) , sin(theta)*cos(theta) , cos(theta)^2 - sin(theta)^2 ];

];

R = [ 1 0 0 ; 0 1 0 ; 0 0 2 ];

Qbar = inv(T)*Q*R*T*inv(R);

% build up stiffness matrices
A_temp = A_temp + Qbar*( z(k+1) - z(k) );
B_temp = B_temp + ( 1 / 2 )*Qbar*( z(k+1)^2 - z(k)^2 );
D_temp = D_temp + ( 1 / 3 )*Qbar*( z(k+1)^3 - z(k)^3 );

```

```
% solve for thermal strains
e_T1(n,k,:) = T_delt*[ CTE(lam(k,3),1) ; CTE(lam(k,3),2) ; CTE(lam(k,3),3) ];
e_Tx = R*inv(T)*inv(R)*squeeze(e_T1(n,k,:));
```

```
% define thermal loads
N_Ttemp = N_Ttemp + Qbar*e_Tx*( z(k+1) - z(k) );
M_Ttemp = M_Ttemp + Qbar*e_Tx*( z(k+1)^2 - z(k)^2 );
```

```
end
```

```
% define stiffness matrices for laminate
A(n,,:) = A_temp;
B(n,,:) = B_temp;
D(n,,:) = D_temp;
K(n,,:) = [ A_temp B_temp ; B_temp D_temp ];
```

```
% define thermal loads
N_T(n,:) = N_Ttemp;
M_T(n,:) = M_Ttemp;
```

```
E_eff(n,1) = K(n,1,1) / ( 2*thick(n,3) ); % effective E for face sheet
```

```
end
```

```
%% UNIT CONVERSION FOR SES
```

```
thick_mm = thick*25.4; % convert thick to mm
E_effPa = E_eff*6895; % convert E_eff to Pa
```

```
%% RESULTS
```

```
% squeeze(K(n,,:))
```

# APPENDIX B: HAND CALCULATIONS

## Model 1

Hand:  $N_{xy} = 1 \frac{\text{lb}}{\text{in}}$

$$A_{66} = 1.029e5 \frac{\text{lb}}{\text{in}} \quad (\text{from CLT})$$

$$\epsilon_{xy} = \frac{N_{xy}}{A_{66}} \Rightarrow \underline{\epsilon_{xy} = 9.72e-6}$$

Abaqus:  $a = 34 \text{ in}$  (length)

$$v_z = 3.306e-4 \text{ in} \quad (\text{maximum transverse disp.})$$

$$\epsilon_{xy} = \frac{v_z}{a} \Rightarrow \underline{\epsilon_{xy} = 9.72e-6}$$

## Model 2

Abaqus:  $a = 34 \text{ in}$

$$v_z = 3.050e-3 \text{ in}$$

$$\underline{\epsilon_{xy} = 8.97e-5}$$

## Model 3

Hand:  $N_{xy} = 0.159 \frac{\text{lb}}{\text{in}}$  (from  $T = 100 \text{ lb in}$ )

$$l = 64 \text{ in} \quad (\text{length})$$

$$d = 20 \text{ in} \quad (\text{diameter})$$

$$A_{66} = 8.571e4 \frac{\text{lb}}{\text{in}}$$

$$\epsilon_{xy} = 1.855e-6$$

$$x = \epsilon_{xy} l \Rightarrow x = 1.187e-4 \text{ in}$$

$$\phi = \frac{x}{\left(\frac{d}{2}\right)} \left(\frac{180}{\pi}\right) \Rightarrow \underline{\phi = 6.80e-4 \text{ deg}}$$

Abaqus:  $\frac{d\phi}{dl} = 1.86e-7 \frac{\text{rad}}{\text{in}}$

$$\phi = \frac{d\phi}{dl} \cdot l \Rightarrow \underline{\phi = 6.82e-4 \text{ deg}}$$

## Appendix C: Meshes

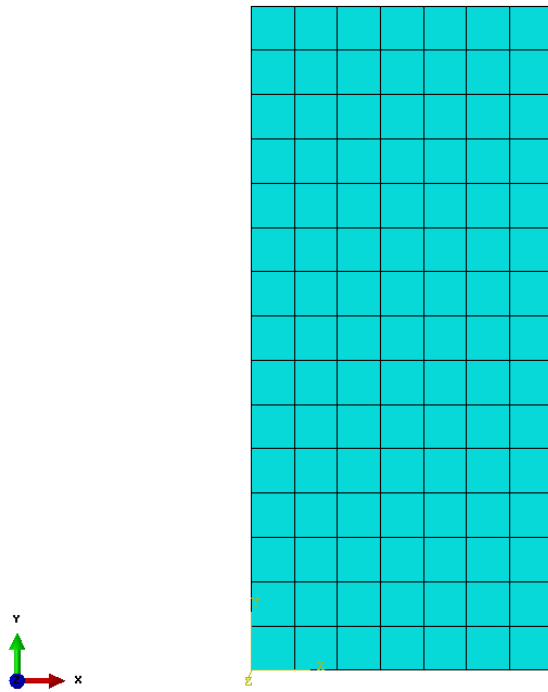


Figure 1. Model 1 mesh.

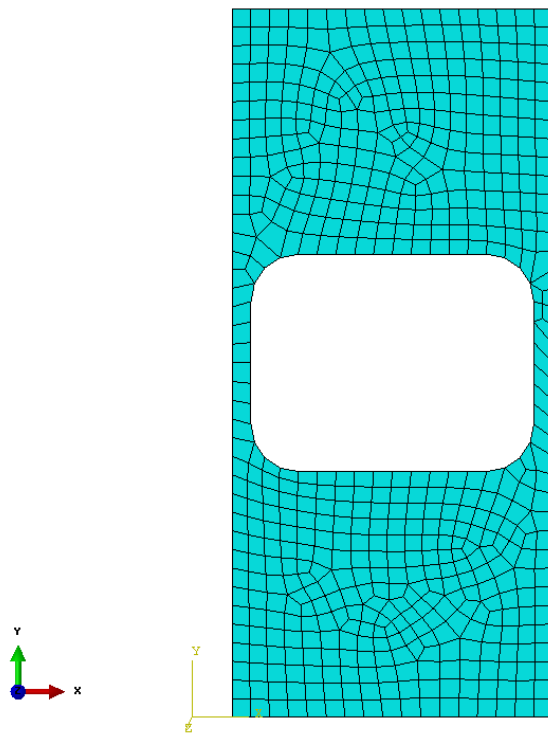


Figure 2. Model 2 mesh.



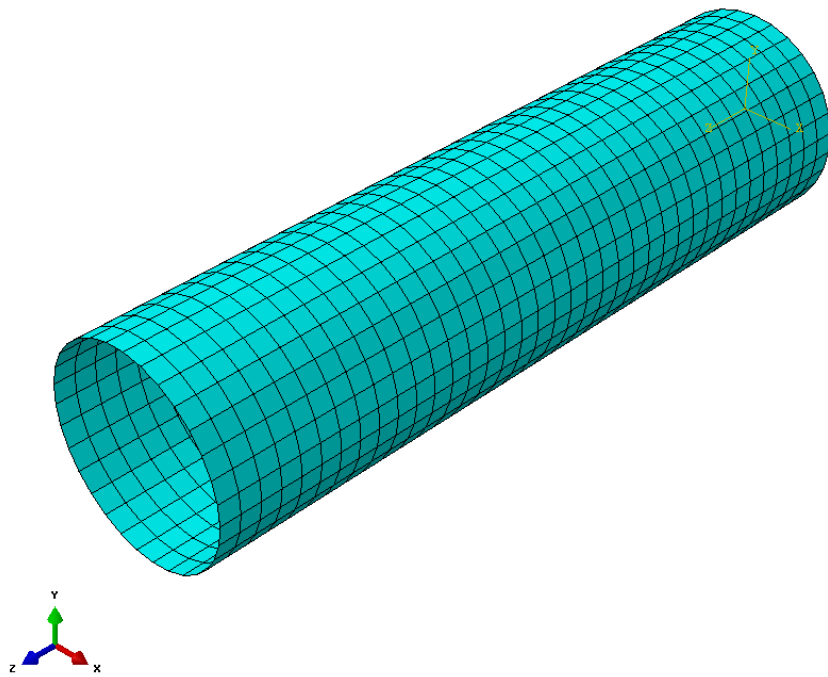


Figure 3. Model 3 mesh.

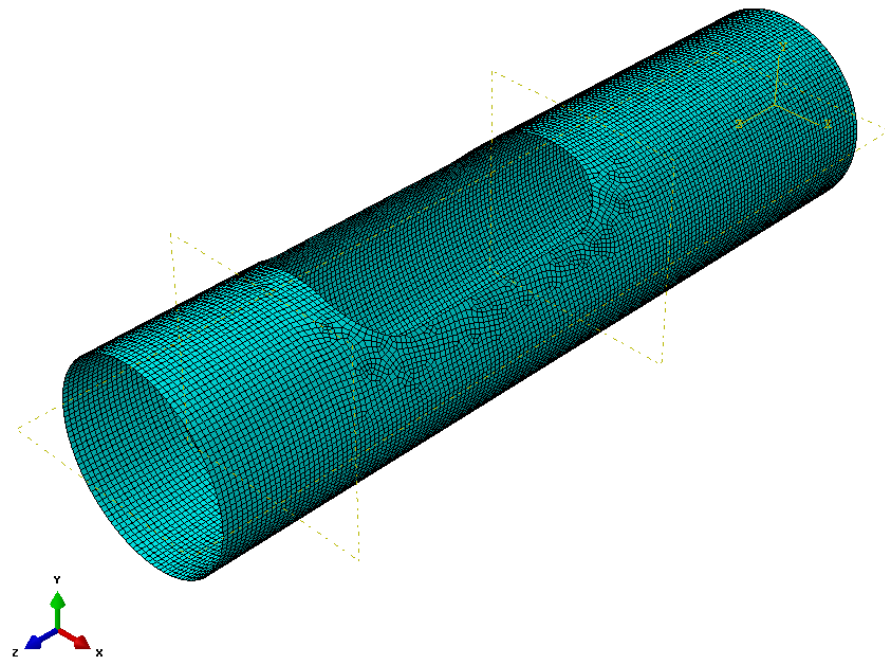


Figure 4. Model 4 mesh.

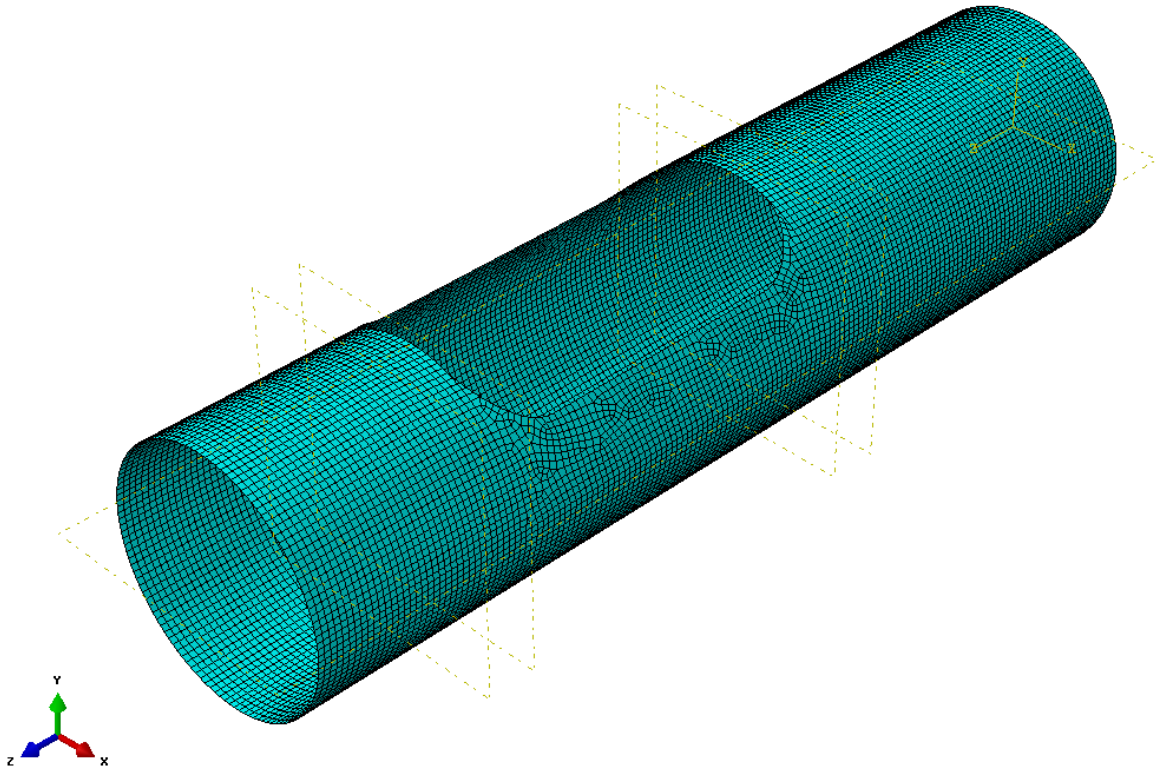


Figure 5. Model 5 mesh.

## Appendix D: Deformed Shapes

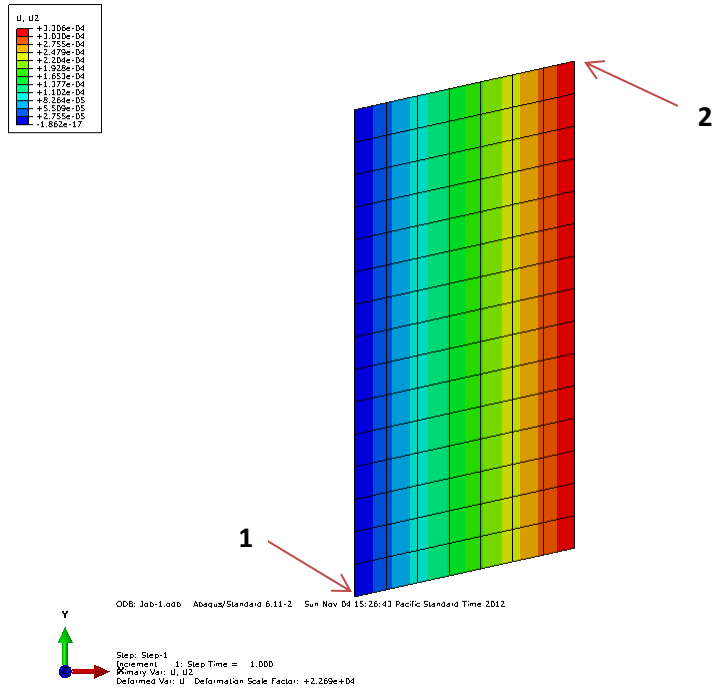


Figure 1. Model 1 deformed shape and reference points. Countours show displacement in y-direction.

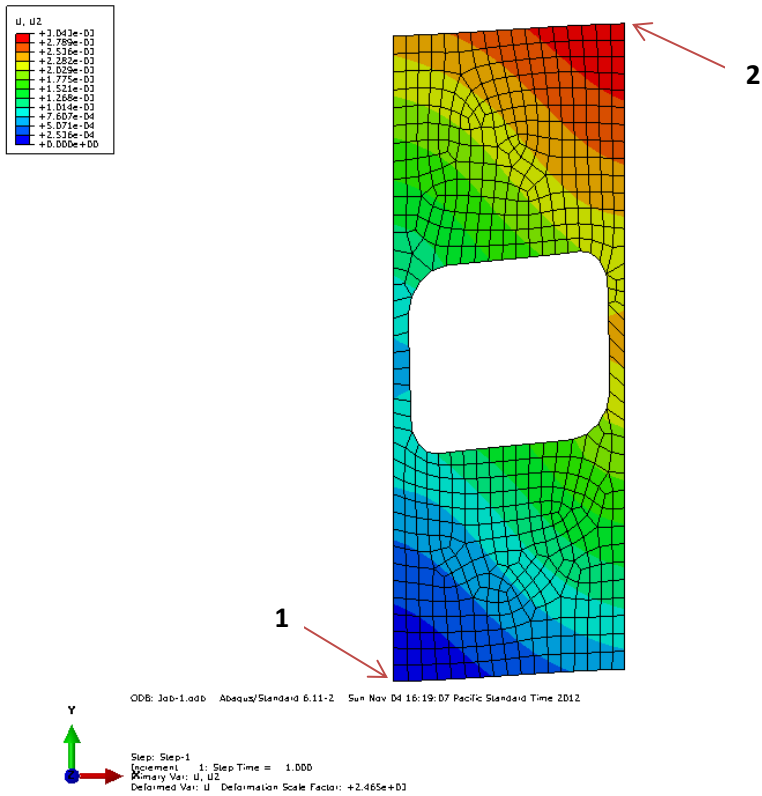


Figure 2. Model 2 deformed shape and reference points. Countours show displacement in y-direction.

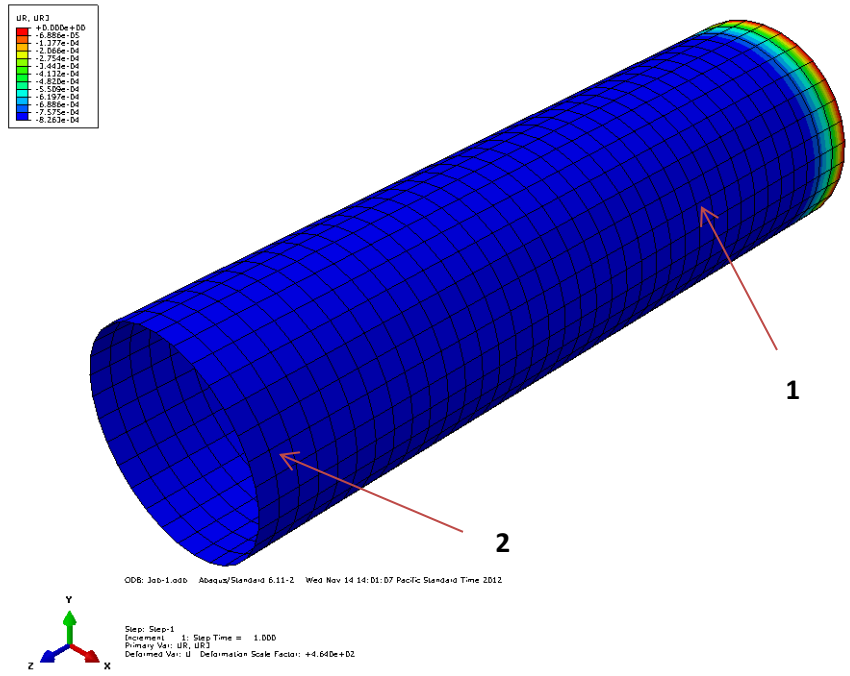


Figure 3. Model 3 deformed shape and reference points. Countours show rotation in z-direction. The non-linearity near the boundary condition is apparent.

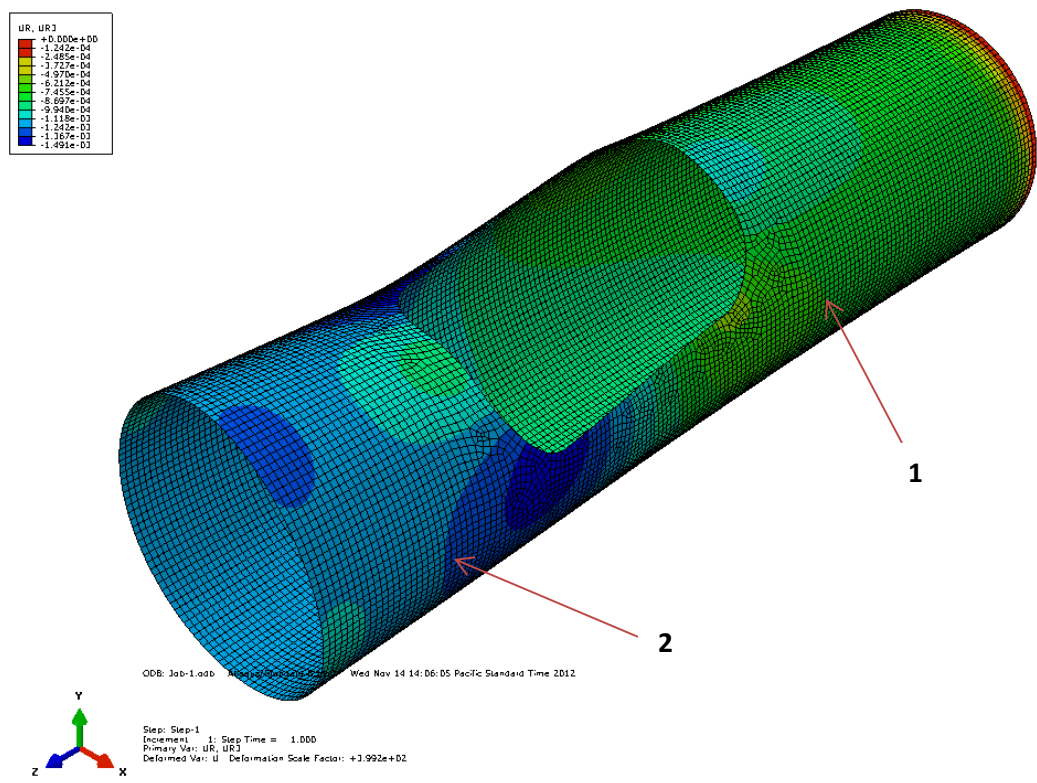


Figure 4. Model 4 deformed shape and reference points. Countours show rotation in z-direction.

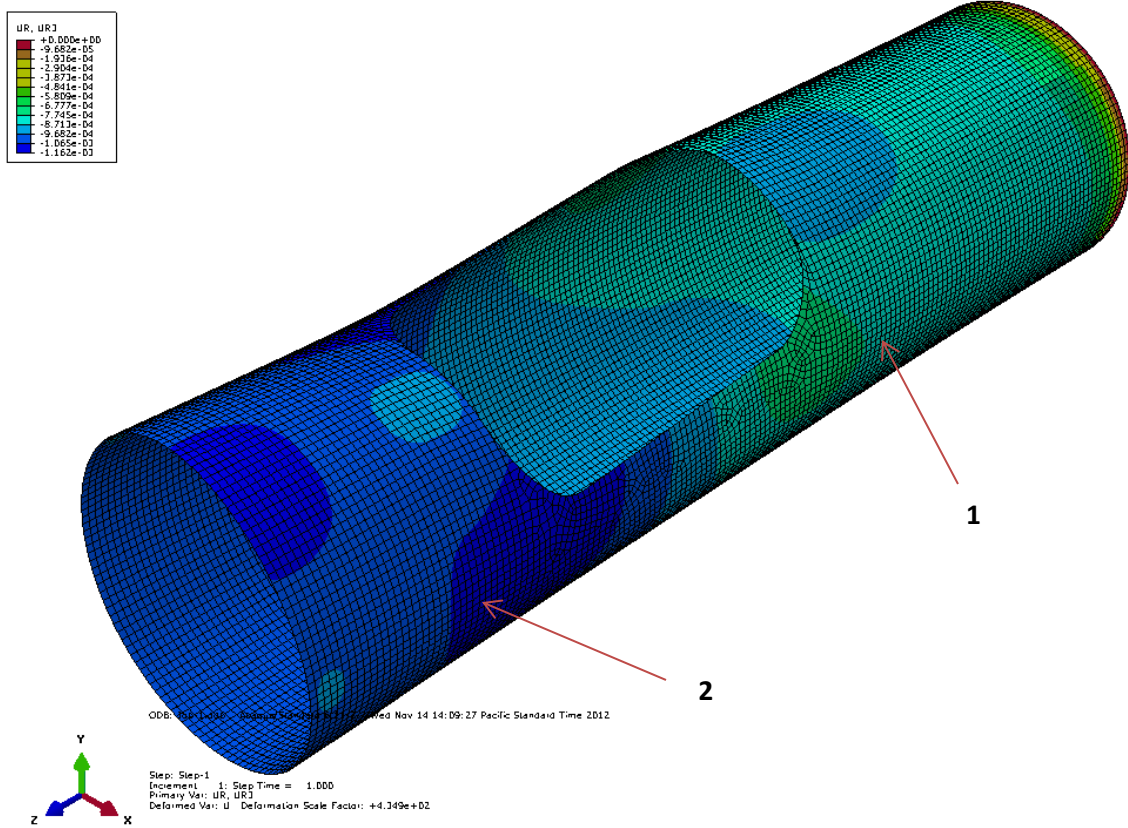


Figure 5. Model 5 deformed shape and reference points. Countours show rotation in z-direction.

## **Appendix E: Impact Attenuator Data**

The impact attenuator data report submitted to SAE is included here from its original PDF file.

**APPENDIX B-2**  
**2013 FSAE™ IMPACT ATTENUATOR DATA REPORT – Page 1 of 5**

This form must be completed and submitted by **all teams no later than the date specified in the Action Deadlines on specific event website**. The FSAE Technical Committee will review all submissions which deviate from the FSAE® rules and reply with a decision about the requested deviation. All requests will have a confirmation of receipt sent to the team. Impact Attenuator Data (IAD) and supporting calculations must be submitted electronically in Adobe Acrobat Format (\*.pdf). The submissions must be named as follows: schoolname\_IAD.pdf using the complete school name. **Submit the IAD report as instructed on the event website. For Michigan and California events submit through fsaeonline.com.**

**\*In the event that the FSAE Technical Committee requests additional information or calculations, teams have one week from the date of the request to submit the requested information or ask for a deadline extension.**

University Name: California Polytechnic State Univ - SLO Car Number(s) & Event(s): 047 FSAE Lincoln  
 Team Contact: John Waldrop E-mail Address: johnwwaldrop@gmail.com  
 Faculty Advisor: John Fabijanic E-mail Address: jfabijan@calpoly.edu

Material(s) Used	Unidirectional carbon fiber prepreg
Description of form/shape	Pyramidal skin
IA to Anti-Intrusion Plate mounting method	IA fastened using four (4) axial M8x1.25 Grade 8.8 bolts to Front Bulkhead (AI plate is clamped between IA and Front Bulkhead)
Anti-Intrusion Plate to Front Bulkhead mounting method	IA fastened using four (4) axial M8x1.25 Grade 8.8 bolts to Front Bulkhead (AI plate is clamped between IA and Front Bulkhead)
Peak deceleration ( $\leq 40$ g's)	31.3 g
Average deceleration ( $\leq 20$ g's)	17.0 g

Confirm that the attenuator contains the minimum volume 200mm wide x 100mm high x 200mm long  Yes

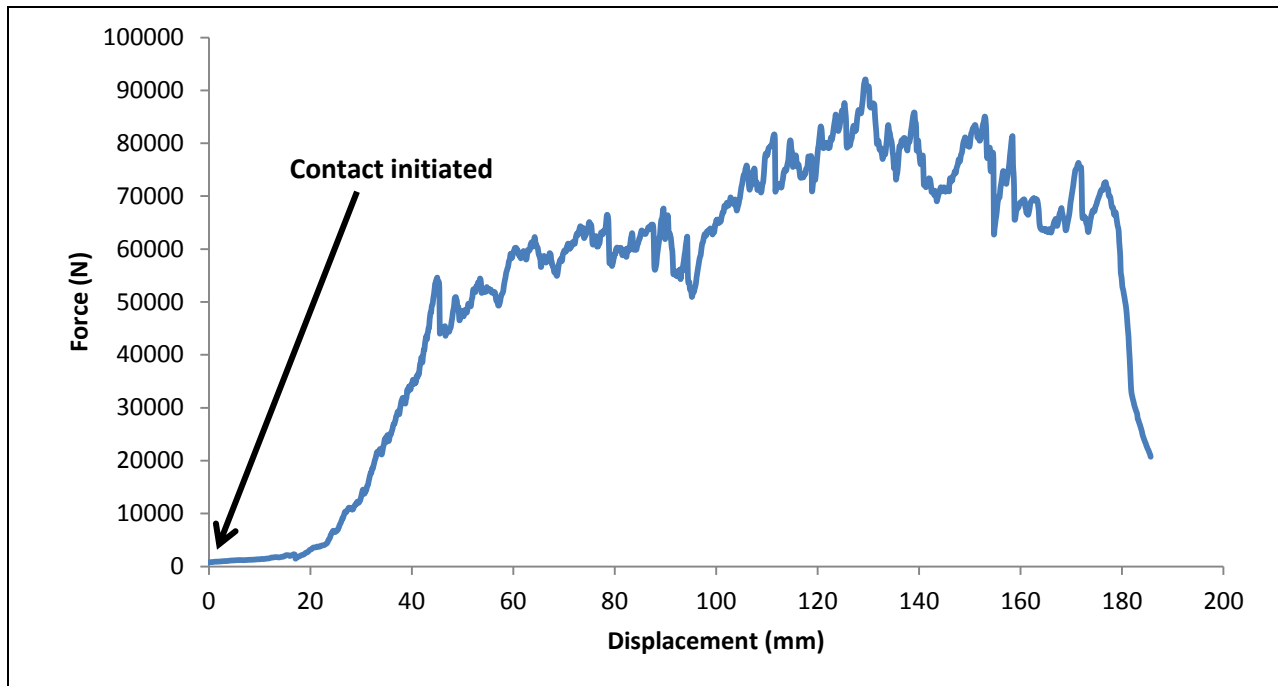


Figure 1: Force-Displacement Curve (dynamic tests must show displacement during collision and after the point  $v=0$  and until force becomes = 0)

**ATTACH PROOF OF EQUIVALENCY**  
**TECHNICAL COMMITTEE DECISION/COMMENTS**

Approved by \_\_\_\_\_ Date \_\_\_\_\_

**NOTE: THIS FORM AND THE APPROVED COPY OF THE SUBMISSION MUST BE PRESENTED AT TECHNICAL INSPECTION AT EVERY FORMULA SAE EVENT ENTERED**

**APPENDIX B-2**  
**2013 FSAE™ IMPACT ATTENUATOR DATA REPORT – Page 2 of 5**

University Name: California Polytechnic State Univ - SLO Car Number(s) & Event(s): 047 FSAE Lincoln

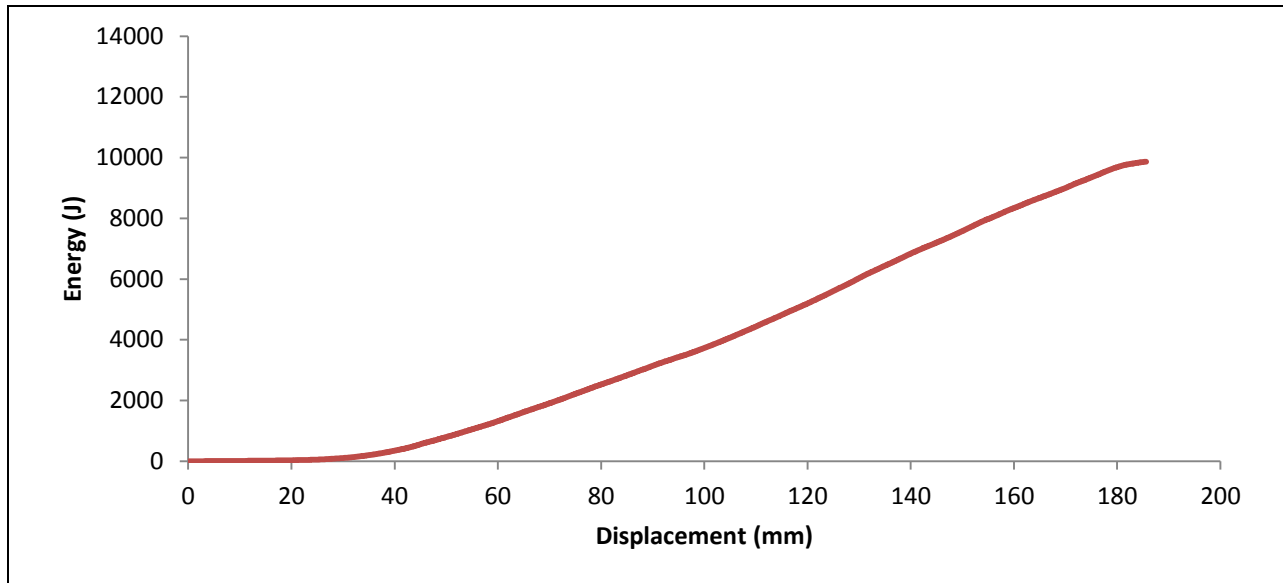


Figure 2: Energy-Displacement Curve (dynamic tests must show displacement during collision and after v=0)



Figure 3: Attenuator as Constructed



Figure 4: Attenuator after Impact  
(see attachment for AI plate)

Energy Absorbed (J): Must be $\geq 7350$ J	7350 J	Vehicle includes front wing in front of front bulkhead?	No
IA Crushed Displacement (mm):	147 mm	Wing structure included in test?	No
IA Post Crush Displacement - demonstrating any return (mm):	130 mm	Test Type: (e.g. barrier test, drop test, quasi-static crush)	Quasi-static crush
Anti-Intrusion Plate Deformation (mm)	0 mm	Test Site: (must be from approved test site list on website for dynamic tests)	Cal Poly Civil Engineering Dept.



**APPENDIX B-2**  
**2013 FSAE™ IMPACT ATTENUATOR DATA REPORT – Page 3 of 5**

University Name: California Polytechnic State Univ - SLO Car Number(s) & Event(s): 047 FSAE Lincoln

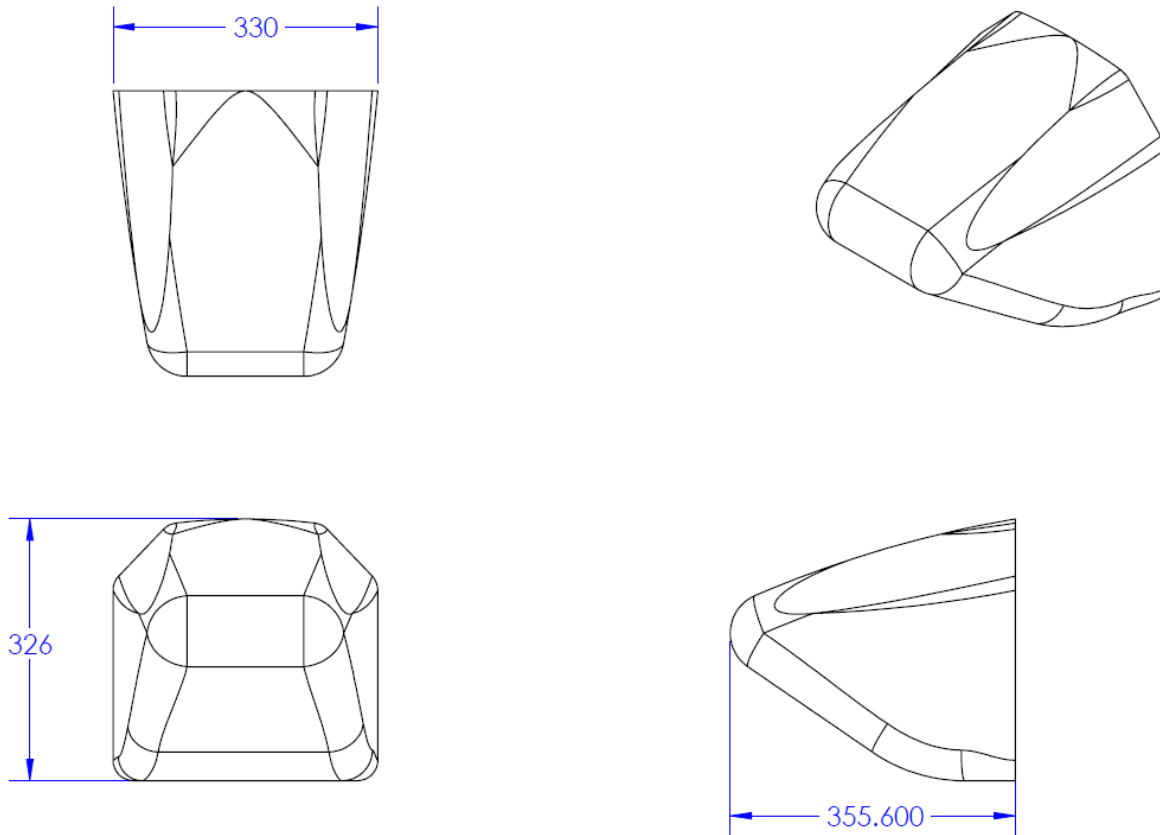


Figure 5: Design Drawings

Length (fore/aft direction): 355 mm ( $\geq 200$ mm)

Width (lateral direction): 330 mm ( $\geq 200$ mm)

Height (vertical direction): 326 mm ( $\geq 100$ mm)

Attenuator is at least 200mm wide by 100mm high for at least 200mm: Yes

***Attach additional information below this point and/or on additional sheets***

Test schematic, photos of test, design report including reasons for selection and advantages/disadvantages, etc.  
Additional information shall be kept concise and relevant.

**APPENDIX B-2**  
**2013 FSAE™ IMPACT ATTENUATOR DATA REPORT – Page 4 of 5**

University Name: California Polytechnic State Univ - SLO Car Number(s) & Event(s): 047 FSAE Lincoln



Figure 6: Anti-Intrusion Plate after test.

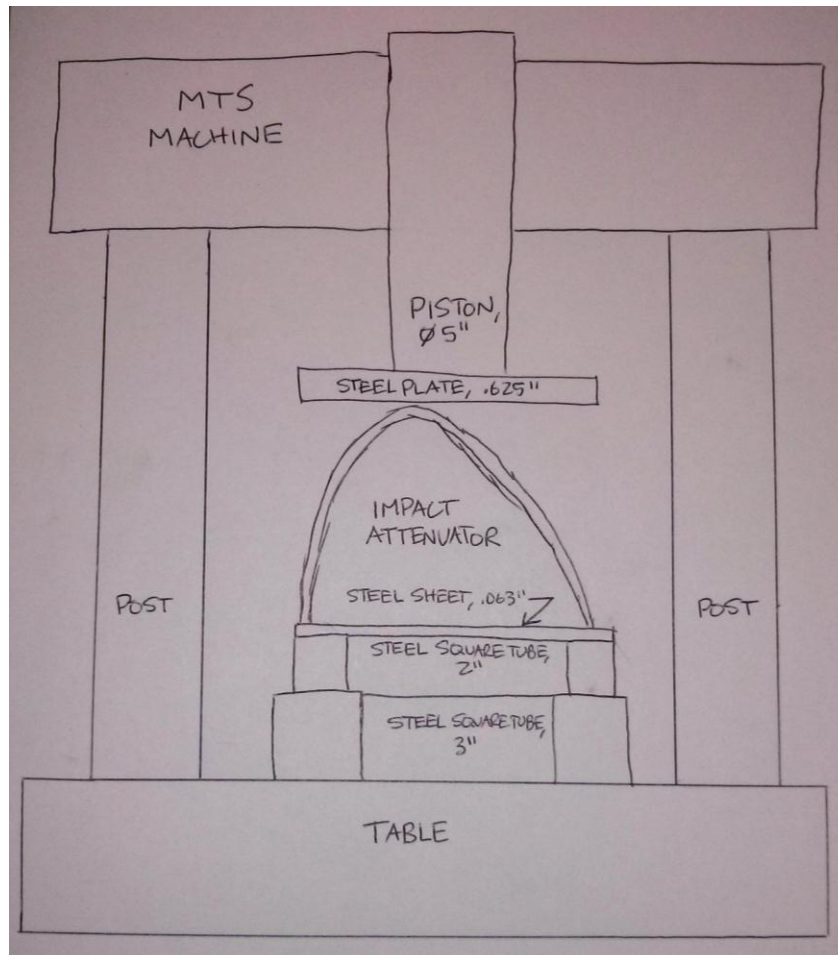


Figure 7: Test setup.

**APPENDIX B-2**  
**2013 FSAE™ IMPACT ATTENUATOR DATA REPORT – Page 5 of 5**

University Name: California Polytechnic State Univ - SLO Car Number(s) & Event(s): 047 FSAE Lincoln



Figure 8: Test procedure, from setup to end of test. A mid-test change to account for lack of piston travel is shown. This change occurs at 145 mm of displacement.

## Appendix F: Accounting

Date	Vendor	Disc.						
Item	Size	Qty	Use	Extra	Part no.	Price	Ext. cost	
11/29/2012	Cal Poly Supermileage	0.00%						
Duratec	1 gallon	1	Nose tooling	yes		\$70.00	\$70.00	
12/4/2012	Aircraft Spruce & Specialty Co.	0.00%						
4130 steel, round tube	.750" x .049" x 6' long	1	Frame material	yes	03-04400-6	\$23.70	\$23.70	
4130 steel, round tube	1" x .049" x 12' long	3	Frame material	yes	03-06200-12	\$40.20	\$120.60	
4130 steel, round tube	1" x .065" x 8' long	1	Frame material	yes	03-06400-8	\$32.80	\$32.80	
4130 steel, round tube	1" x .095" x 9' long	2	Frame material (main hoop)	yes	03-06500-9	\$35.91	\$71.82	
4130 steel, round tube	1.25" x .049" x 2' long	1	Frame material	yes	03-07600-2	\$10.50	\$10.50	
12/5/2012	McMaster-Carr	0.00%						
1018 steel, square tube	1" x .083" x 6' long	1	Frame tooling	yes	6527K22	\$21.72	\$21.72	
1018 steel, angle	.75" x .125" x 6' long	1	Frame tooling	yes	9017K42	\$12.28	\$12.28	
Carbide-Tipped Scriber		2	Frame tooling	yes	2157A11	\$5.79	\$11.58	
Carbide-Tipped Hole Saw	1" diameter	2	Frame tooling	yes	4192A16	\$9.38	\$18.76	
Carbide-Tipped Hole Saw	1.25" diameter	1	Frame tooling	no	4192A21	\$10.76	\$10.76	
Pistol-Grip Infrared Thermometer		1	Vehicle testing	no	9254T61	\$109.08	\$109.08	
Temp. Indicating Labels, 154-185 F		1	Vehicle testing	no	59485K25	\$15.09	\$15.09	
Temp. Indicating Labels, single		1	Vehicle testing	yes	5955K26	\$11.04	\$11.04	
Temp. Indicating Labels, single		1	Vehicle testing	yes	5955K27	\$11.04	\$11.04	
12/5/2012	McMaster-Carr	0.00%						
4130 steel, rect. tube	2" x 1" x .065" x 3' long	1	Frame material	yes	6566K563	\$65.61	\$65.61	
12/7/2012	Krayden	0.00%						
Frekote 700 NC aerosol	10.5 oz.	2	Nose tooling	yes	FK38428	\$8.86	\$17.72	
12/12/2012	McCarthy Steel	0.00%						
Steel, square tube	1" x .065" x 1' long	20	Frame tooling	yes		\$0.94	\$18.80	
12/12/2012	McMaster-Carr	0.00%						
4130 steel, round tube	1 1/4" x .120" x 6' long	1	Frame tooling	yes	89955K96	\$73.89	\$73.89	
12/13/2012	McMaster-Carr	0.00%						

Carbide-tipped drill bit	F	2	Frame tooling	yes	31575A516	\$17.79	\$35.58
Carbide end mill	1/4"	1	Frame tooling	no	8928A331	\$27.97	\$27.97
	12/14/2012	McMaster-Carr	0.00%				
Carbide-tipped drill bit	F	2	Frame tooling	yes	31575A516	\$17.79	\$35.58
	12/18/2012	Texas Almet	30.00%				
HRH-10-1/8-3.0	.700"x4"x8'	2	Tub material (layup)	yes		\$690.00	\$1,380.00
	1/2/2013	Aircraft Spruce & Specialty Co.	0.00%				
4130 steel, round tube	1" x .095" x 9' long	3	Frame material (main hoop)	yes	03-06500-9	\$35.91	\$107.73
4130 steel, round tube	1.25" x .120" x 4' long	1	Frame tooling (main hoop)	yes	03-08000-4	\$23.92	\$23.92
	1/12/2013	Cal Poly University Store	0.00%				
Chipboard		2	Frame tooling (main hoop)	no		\$1.75	\$3.50
Cardboard		1	Frame tooling (main hoop)	no		\$2.25	\$2.25
Envelope clasp		2	Frame tooling (main hoop)	no		\$0.40	\$0.80
	1/12/2013	The Home Depot	0.00%				
Acetone		1	Nose tooling	yes	30192018255	\$16.96	\$16.96
Maintenance coating		1	Nose tooling	yes	30192346303	\$8.98	\$8.98
Sandpaper, 80 grit		1	Nose tooling	yes	051141349695	\$3.97	\$3.97
Sandpaper, 220 grit		1	Nose tooling	yes	051141941004	\$3.97	\$3.97
	1/15/2013	Rite Aid Pharmacy	0.00%				
Glue		1	Frame tooling (main hoop)	yes		\$2.19	\$2.19
	1/15/2013	AutoZone	0.00%				
Bondo body filler	14 oz.	1	Nose tooling	yes		\$9.99	\$9.99
	1/16/2013	McMaster-Carr	0.00%				
Turnbuckles		2	Frame tooling	no	2996T15	\$14.35	\$28.70
	1/23/2013	Jamestown Distributors	0.00%				
ProBalsa Plus	3/4" x 2' x 4'	1	Tub material (NOT USED)	yes	COM-29306	\$46.51	\$46.51
	1/28/2013	Online Metals	5.00%				
6061 aluminum, round tube	.438" x .065" x 36" long	1	Insert material	yes		\$14.18	\$14.18
6061 aluminum, round tube	.438" x .065" x 10"-12" long	1	Insert material	yes		\$4.73	\$4.73
	2/2/2013	The Home Depot	0.00%				
Whitewood stud		5	Tub mold vehicle	no		\$2.93	\$14.65
Lumber		5	Tub mold vehicle	no		\$0.02	\$0.10
Caster wheel		10	Tub mold vehicle	no		\$3.97	\$39.70
Screws		1	Tub mold vehicle	no		\$8.47	\$8.47

2/4/2013	Specialized Balsa Wood	0.00%						
End grain balsa	3/4" x 12" x 12"	8	Tub material (layup)	yes			\$16.44	\$131.52
2/8/2013	Miner's ACE Hardware	0.00%						
Fasteners		4	Nose tooling	no			\$0.48	\$1.92
Fasteners		1	Nose tooling	no			\$0.26	\$0.26
Fasteners		2	Nose tooling	no			\$0.16	\$0.32
Fasteners		1	Nose tooling	no			\$0.55	\$0.55
Fasteners		1	Nose tooling	no			\$0.15	\$0.15
Fasteners		1	Nose tooling	no			\$1.50	\$1.50
Fasteners		1	Nose tooling	no			\$0.65	\$0.65
Fasteners		2	Nose tooling	no			\$0.11	\$0.22
2/8/2013	McCarthy Steel	0.00%						
Plate	1/8"	1	Laminate testing	no			\$8.04	\$8.04
Plate	1/4"	2	Laminate testing	no			\$13.75	\$27.50
Square tubing	2" x 2" x .120"	3	Laminate testing	no			\$3.48	\$10.44
Square tubing	1-1/2" x 1-1/2" x .120"	1	Laminate testing	no			\$2.57	\$2.57
Angle	1/4" x 1" x 1" x 20'	2.98	Laminate testing	yes			\$1.15	\$3.43
2/13/2013	Beverly's	0.00%						
Cloth	1 yd	5	Tub tooling (layup)	yes			\$3.97	\$19.85
2/13/2013	Online Metals	5.00%						
4130 steel, round tube	1" x .095" x 6' long	1	Front roll hoop material	yes			\$41.68	\$41.68
2/13/2013	McMaster-Carr	0.00%						
Drill bit	3/16	4	Insert material	yes	2901A119		\$2.09	\$8.36
Drill bit	3/8	3	Insert material	yes	2901A133		\$6.19	\$18.57
Drill bit	7/16	2	Insert material	yes	2901A137		\$8.20	\$16.40
Fiberglass-reinforced cloth tape	1/2" wide x 18 yards long	1	Tub tooling (layup)	yes	7577A1		\$21.32	\$21.32
High-temperature masking tape	1" wide x 60 yards long	1	Tub tooling (layup)	yes	7627A23		\$6.01	\$6.01
Nylon, bar by foot	.031" x 2"	5	Tub tooling (layup)	yes	8751K26		\$0.78	\$3.90
Delrin, bar by foot	.025" x 2"	5	Tub tooling (layup)	yes	8738K24		\$0.81	\$4.05
2/14/2013	Miner's ACE Hardware	0.00%						
Fastener		6	Laminate testing	no			\$0.40	\$2.40
Fastener		6	Laminate testing	no			\$0.30	\$1.80
2/15/2013	The Home Depot	0.00%						
MDF		1	Tub tooling (bulkhead)	no			\$5.67	\$5.67
Lumber fee		1	Tub tooling (bulkhead)	no			\$0.05	\$0.05

Wood glue		1	Tub tooling (bulkhead)	no		\$3.83	\$3.83	
	2/17/2013	The Home Depot	0.00%					
MDF		1	Tub tooling (bulkhead)	no		\$11.87	\$11.87	
Lumber fee		1	Tub tooling (bulkhead)	no		\$0.11	\$0.11	
	2/17/2013	Miner's ACE Hardware	0.00%					
Fasteners		2	Tub tooling (bulkhead)	no		\$0.15	\$0.30	
Fasteners		1	Tub tooling (bulkhead)	no		\$0.40	\$0.40	
Fasteners		1	Tub tooling (bulkhead)	no		\$1.49	\$1.49	
Threaded rod		1	Tub tooling (bulkhead)	no		\$2.59	\$2.59	
	2/19/2013	Online Metals	5.00%					
6061 aluminum, round tube		.375" x .065" x 36" long	1	Insert material	yes	\$9.70	\$9.70	
4130 steel, round tube		1" x .065" x 6' long	1	Frame material	yes	\$30.73	\$30.73	
	2/20/2013	The Home Depot	0.00%					
Drywall screws		1	Tub tooling (bulkhead)	yes		\$6.47	\$6.47	
Gorilla wood glue		1	Tub tooling (bulkhead)	yes		\$5.97	\$5.97	
Loctite		1	Tub tooling (bulkhead)	yes		\$4.57	\$4.57	
3M caulk		1	Tub tooling (bulkhead)	yes		\$11.47	\$11.47	
PVC		1	Tub tooling (bulkhead)	yes		\$0.99	\$0.99	
MDF		2	Tub tooling (bulkhead)	yes		\$11.87	\$23.74	
Lumber fee		2	Tub tooling (bulkhead)	yes		\$0.11	\$0.22	
	2/21/2013	McMaster-Carr	0.00%					
Fiberglass-reinforced cloth tape		1/2" wide x 18 yards long	1	Tub tooling (layup)	yes	7577A1	\$21.32	\$21.32
Nylon, bar by foot		.031" x 2"	50	Tub tooling (layup)	yes	8751K26	\$0.78	\$39.00
Blades for utility knives		.018"	1	Tub tooling (layup)	yes	3957A16	\$15.99	\$15.99
	2/21/2013	Beverly's	10.00%					
Fiskars titanium scissors		2	Tub tooling (layup)	no		\$16.99	\$33.98	
Paint pen		2	Tub tooling (layup)	no		\$3.99	\$7.98	
Sharpie		2	Tub tooling (layup)	no		\$1.99	\$3.98	
Tape measure		1	Tub tooling (layup)	no		\$1.99	\$1.99	
	2/22/2013	Beverly's	50.00%					
Fabric		7	Tub tooling (layup)	yes		\$6.99	\$48.93	
	2/24/2013	Miner's ACE Hardware	0.00%					
Nitrile gloves		2	Tub tooling (layup)	yes		\$12.99	\$25.98	
	2/25/2013	The Home Depot	0.00%					
Screws		1	Tub tooling (layup)	yes		\$4.29	\$4.29	

Shims		1	Tub tooling (layup)	yes		\$1.57	\$1.57
Lumber fee		1	Tub tooling (layup)	yes		\$0.01	\$0.01
	3/4/2013	McMaster-Carr	0.00%				
Drill bit	1/2	1	Nose tooling	no	2901A142	\$10.79	\$10.79
HSS hand tap, taper	M8x1.25, D3	1	Nose tooling	no	26015A167	\$12.16	\$12.16
	3/4/2013	Online Metals	5.00%				
6061 aluminum, sheet	.063" x 24" x 36"	1	Head rest material	no		\$35.11	\$35.11
6061 aluminum, round tube	.313" x .065" x 36" long	1	Insert material	yes		\$10.21	\$10.21
6061 aluminum, round tube	.375" x .065" x 36" long	2	Insert material	yes		\$9.70	\$19.40
6061 aluminum, round tube	.438" x .065" x 36" long	1	Insert material	yes		\$14.18	\$14.18
	3/6/2013	Fiberglass Supply	15.00%				
West System epoxy, B-6, 206B	1.2 gal	1	Tub material (finishing)	yes	G73-7534	\$136.57	\$136.57
3M glass bubbles	1 lb	1	Tub material (finishing)	yes	J05-1457	\$16.35	\$16.35
	3/7/2013	The Home Depot	0.00%				
MDF		1	Nose tooling	yes		\$31.74	\$31.74
Coveralls		1	Tub tooling (finishing)	no		\$10.98	\$10.98
	3/7/2013	Fastenal	0.00%				
Socket head cap screw, 8.8	M8x1.25 x 20mm	8	Nose hardware	yes	11103359	\$0.41	\$3.30
	3/8/2013	The Home Depot	0.00%				
Gorilla wood glue		1	Nose tooling	yes		\$5.97	\$5.97
Shop vac filter		1	Nose tooling	no		\$22.97	\$22.97
	3/11/2013	McCarthy Steel	0.00%				
Steel, square tube	2" x .188" x 6'	1	Nose testing	yes		\$29.52	\$29.52
Steel, sheet	.063"	1	Nose testing	yes		\$25.00	\$25.00
Cutting fee		1	Nose testing	N/A		\$5.00	\$5.00
	3/18/2013	McCarthy Steel	0.00%				
Steel, square tube	3" x .188" x 1' long	6	Nose testing	yes		\$7.86	\$47.16
	3/21/2013	Beverly's	30.00%				
Wood sticks		1	Tub tooling (finishing)	yes		\$5.49	\$5.49
	3/25/2013	The Home Depot	0.00%				
Threaded rod	1/2-13	2	Nose testing	no		\$4.71	\$9.42
Nut		9	Nose testing	yes		\$0.20	\$1.80
Washer		9	Nose testing	yes		\$0.20	\$1.80
	3/26/2013	Miner's ACE Hardware	0.00%				
Fiberglass spreaders		1	Tub tooling (finishing)	no		\$3.99	\$3.99



Barb tee		1	Tub tooling (finishing)	no		\$7.99	\$7.99
Barb tee		1	Tub tooling (finishing)	no		\$8.99	\$8.99
Brush		2	Tub tooling (finishing)	no		\$0.87	\$1.74
Brush		2	Tub tooling (finishing)	no		\$1.19	\$2.38
Tube		3	Tub tooling (finishing)	no		\$0.39	\$1.17
3/27/2013	Miner's ACE Hardware	0.00%					
Tube		8	Tub tooling (finishing)	no		\$0.39	\$3.12
Barb tee		1	Tub tooling (finishing)	no		\$7.99	\$7.99
Hose clamp		3	Tub tooling (finishing)	no		\$1.79	\$5.37
4/13/2013	Miner's ACE Hardware	0.00%					
Fasteners		1	Nose tooling	no		\$4.45	\$4.45
Fasteners		1	Nose tooling	no		\$4.73	\$4.73
Fasteners		4	Nose tooling	no		\$0.15	\$0.60
Fasteners		4	Nose tooling	no		\$0.15	\$0.60
Fasteners		4	Nose tooling	no		\$0.17	\$0.68
4/18/2013	McMaster-Carr	0.00%					
ABS, bar, black	3/8" x 1.5" x 2' long	1	Skid plate material (NOT USED)	yes	8712K146	\$7.04	\$7.04
6/10/2013	San Luis Auto Parts	0.00%					
Spray paint, gloss black roll bar		2	Frame material	yes		\$7.89	\$15.78
6/10/2013	The Home Depot	0.00%					
Spray paint, gloss meadow green		5	Tub material (finishing)	yes		\$3.87	\$19.35
Spray paint, orange		1	Frame material	no		\$3.87	\$3.87
Spray paint, auto primer		1	Tub material (finishing)	yes		\$3.98	\$3.98

## Appendix G: References

- 2012 Formula One Technical Regulations, FIA *et seq.* (2011). Print.
- 2013 Formula SAE Rules, SAE International *et seq.* (2012). Print.
- Agarwal, Bhagwan D., Lawrence J. Broutman, and K. Chandrashekhara. *Analysis and Performance of Fiber Composites*. 3rd ed. Hoboken, NJ: John Wiley, 2006. Print.
- ASTM Standard D3518, 2007, "Standard Test Method for In-Plane Shear Response of Polymer Matrix Composite Materials by Tensile Test of a  $\pm 45^\circ$  Laminate," ASTM International, Test Conshohocken, PA, 2007, DOI: 10.1520/D3518\_D3518M, www.astm.org
- ASTM Standard D790-10, 2010, "Standard Test Methods for Flexural Properties of Unreinforced and Reinforced Plastics and Electrical Insulating Materials," ASTM International, West Conshohocken, PA 2010, DOI: 10.1520/D0790-10, www.astm.org
- Bergman, T. L., and Frank P. Incropera. *Fundamentals of Heat and Mass Transfer*. Hoboken, NJ: Wiley, 2011. Print.
- Budynas, Richard G., and J. Keith. Nisbett. *Shigley's Mechanical Engineering Design*. 9th ed. New York: McGraw-Hill, 2011. Print.
- Cook, Robert Davis., and Warren C. Young. *Advanced Mechanics of Materials*. New York: Macmillan, 1985. Print.
- Henderson, Nick. *Cal Poly Formula SAE Monocoque Chassis Development*. California: Cal Poly, 2012. PDF.
- HexWeb Honeycomb Sandwich Design Technology*. Hexcel, 2000. Web. October 2012
- Milliken, William F., and Douglas L. Milliken. *Race Car Vehicle Dynamics*. Warrendale, PA, U.S.A.: SAE International, 1995. 673-76. Print.
- Riley, William B., and Albert R. George. "Design, Analysis and Testing of a Formula SAE Car Chassis." *SAE Technical Paper Series* (2002): n. pag. Web.
- Shur-Lok Design Manual: Fasteners for Sandwich Structure*. Shur-Lok Corporation, 1996. Web. October 2012
- Spark, Nick T. "The Ejection Site." *Ejection Site: Fastest Man on Earth- John Paul Stapp*. N.p., n.d. Web. 23 Aug. 2012.
- Young, Warren C., Richard G. Budynas, and Ali M. Sadegh. *Roark's Formulas for Stress and Strain*. New York: McGraw-Hill, 2012. Print.